CRANFIELD UNIVERSITY

BIOTECHNOLOGY CENTRE

PhD THESIS

Academic Years 1990-93

Mithran Somasundrum

Electrochemistry of metal complexes and their use in amperometric sensors

Supervisor: Prof. J.V. Bannister

February 1994

... because I too am Jewish, and she is not: I am the impurity that makes the zinc react, I am the grain of salt or mustard... and I had begun to be proud of being impure.

Primo Levi
The Periodic Table

Abstract

This thesis concerns the utilization of metal complexes in amperometric sensors. Chapter One provides a general introduction to the area. The electrochemical theories relating to the development and use of amperometric sensors, are described, and applications for such sensors are outlined. These include trace element analysis for environmental and clinical use and the determination of NADH for the detection of clinical analytes.

In Chapter Two, the electrochemical changes occurring in a ligand upon complexation, are examined as a possible method of selective metal ion detection. Screen-printing is used to produce disposable, single-use electrodes modified with the ligand bis-cyclohexanone oxaldihydrazone. At +250 mV vs SCE, the electrodes give a linear response to copper(II) across the range 30-300 μM ($r = 0.983$, $n = 13$). The effect on the electrode response of variations in pH, temperature, ligand content and storage time are outlined; as well as the effect of competing cations.

In Chapter Three, pre-formed metal complexes are used as electron-transfer mediators. Part I considers homogeneous mediation from the enzyme NADH oxidase, using the Ru(III/IV) redox couple. A scheme for enzyme amplification of the NADH response is outlined using alcohol dehydrogenase (ADH) and NADH oxidase. Additionally, ethanol determination is performed using an ADH/NADH oxidase bilayer.

In Part II, mediator immobilisation is examined using a novel ion-exchange/hydrogel composite (Nf/PVA). The structure of the composite is investigated by following the

diffusional characteristics of both hydrophobic and hydrophilic mediators, incorporated within the film. An analytical application of the Nf/PVA layer is illustrated following the co-immobilisation of a mediator with glucose oxidase. The effect of protein adsorption onto the composite is also examined.

Part III of Chapter Three considers a possible alternative to mediated electrocatalysis, by using an electro-deposited film of poly(indole-5-carboxylic acid) (PICA). The overpotential for the oxidation of ascorbate and NADH is lowered, apparently without the action of a redox mediating species. Strategies for the development of a PICA-based biosensor are outlined.

Chapter Four provides an overview and general discussion of the experimental results and suggests areas for further work. These include further improvements to the design of the screen-printed electrodes in Chapter 2; the preferable choice of mediator for the immobilisation matrix in Chapter 3 Part II, as well as possible methods of improving the biocompatability of the matrix; and a possible route to the immobilisation of NAD^+, for the PICA-based system described in Chapter 3 Part III.

Acknowledgements

I would like to thank my supervisor Prof. Joe Bannister for his guidance and encouragement during this project.

The NADH oxidase used in Chapter 3 Part I was extracted and purified by Mark Cassar and Genaro Ramino while at Cranfield.

This work was funded by the S.E.R.C. The studies in Chapter 3 received additional funding from an European Community BRIDGE programme.

Finally, I would like to thank the staff and students at the Biotechnology Centre (and especially the smokers' hut !) for their friendship and good humour over the last three years.

Contents

List of Figures

List of Tables

List of Abbreviations and Symbols

Abbreviations

AAS	Atomic Absorption Spectroscopy
ADH	Alcohol Dehydrogenase
ASV	Anodic Stripping Voltammetry
BCO	Bis-cyclohexanone Oxaldihydrazone
CE	Counter Electrode
CME	Chemically Modified Electrode
CV	Cyclic Voltammetry
FAD	Flavin Adenine Dinucleotide
$FADH_2$	Reduced Flavin Adenine Dinucleotide
GOD	Glucose Oxidase
IHP	Inner Helmholtz Plane
ISE	Ion-Selective Electrode
L	Ligand
mcp	Modified Carbon Paste
MB	Meldola Blue
MS	Mass Spectrometry
MV	Methyl Viologen
NAA	Neutron Activation Analysis
NAD^+	Nicotinamide Adenine Dinucleotide
NADH	Reduced Nicotinamide Adenine Dinucleotide
Nf	Nafion

OBLA	Onset of Blood Lactate Accumulation
OHP	Outer Helmholtz Plane
PI	Poly(Indole)
PICA	Poly(Indole-5-Carboxylic Acid)
PMS	Phenazine Methosulphate
PPy	Poly(Pyrrole)
PVA	Poly(Vinyl Alcohol)
RE	Reference Electrode
RMM	Relative Molecular Mass
RR	Ruthenium Red
SCE	Saturated Calomel Electrode
TEAFB	Tetraethylammonium Fluoroborate
Tris	Tris(Hydroxymethyl)Aminomethane
XRF	X-Ray Fluorescence
WE	Working Electrode

<u>Symbols</u>

A	electrode area (cm^{-2})
C_i	concentration of species i (mol dm^{-3})
C_o	concentration of oxidised species at electrode surface (mol dm^{-3})
C_R	concentration of reduced species at electrode surface (mol dm^{-3})
C_{obs}	experimentally observed capacitance (F)
C_{hl}	double layer capacitance (F)

C_{sc}	space charge region capacitance (F)
D_{et}	electron self-exchange diffusion coefficient (cm s^{-1})
D_{exp}	experimentally observed diffusion coefficient (cm s^{-1})
D_i	diffusion coefficient of species i (cm s^{-1})
D_o	physical diffusion coefficient (cm s^{-1})
E	potential vs a reference electrode (V)
E_e	equilibrium potential (V)
E_e°	standard potential (V)
E_a	activation energy (KJ mol^{-1})
$E_{1/2}$	half-wave potential (V)
E_{pk}	peak potential (V)
ΔE_p	peak to peak separation (V)
F	Faraday constant (9.6485 x 10^4 C mol^{-1})
i	current; subscripts $_A$ and $_C$ indicate anodic and cathodic currents respectively (A)
I	current density (A cm^{-2})
I_O	exchange-current density (A cm^{-2})
I_p	peak current density; superscripts ^{A} and ^{C} denote anodic and cathodic processes respectively (A cm^{-2})
I_{dl}	double layer charging current density (A cm^{-2})
$I_{faradaic}$	faradaic current density (A cm^{-2})
j	steady-state flux of reactant at electrode (mol cm^{-2} s^{-1})
k_{ex}	electron self-exchange rate constant (M^{-1} s^{-1})
k'_{ME}	heterogeneous rate constant for enzyme electrode (cm s^{-1})

k'_s	rate of diffusion of substrate through membrane (cm s^{-1})
K	equilibrium constant
K_M	Michaelis constant (mol dm^{-3})
K'_M	apparent Michaelis constant (mol dm^{-3})
K_{ME}	electrochemical Michaelis constant (mol dm^{-3})
Kr	reaction rate (A)
L	thickness of immobilised mediator layer (cm)
n	equivalents (moles) (eg. reactants, electrons etc.)
n_a	no. of electrons involved before and including rate determining step (dimensionless)
q	charge under redox peak of voltammogram (C)
Q	charge (C)
Q_{dl}	charge due to double layer (C)
R	Resistance (Ohms)
	or gas constant (8.314 J K^{-1} mol^{-1})
S	gradient of chronocoulometric plot (C $s^{-1/2}$)
	or concentration of substrate in bulk solution (mol dm^{-3})
t	time (s)
u_j	chemical potential of species j (J mol^{-1})
$\tilde{u}_j$	electrochemical potential of species j (J mol^{-1})
V_0	inital reaction velocity (A)
V_{max}	maximum reaction velocity (A)
x	distance from electrode (cm)
z_j	charge of species j (C)

α	transfer coefficient; subscripts $_A$ and $_C$ indicate anodic and cathodic processes respectively.
Γ	coverage of redox species (mol cm^{-2})
δ	diffusion layer thickness (cm) *or* distance between redox species at reaction (cm)
η	overpotential ($E - E_e$) (V)
ν	potential scan rate ($V\ s^{-1}$)
ρ	ratio of $[i/S] / [i/S]_0$ (dimensionless)
Φ	Galvani potential (V)

Chapter One

General Introduction

Theory of Amperometric Sensors

1.1 Introduction

In 1600 William Gilbert discovered a force between two charged objects, which he described as 'electric' and in 1791 Luigi Galvani found that electric charge could be conducted from a metal, into the nerve of a dissected frog. This lead Alessandro Volta of Pavia (in 1800) to develop the voltaic pile, in which silver and zinc electrodes separated by a salt solution, produced electrical energy. In the 1830s Michael Faraday's experiments provided a framework for electrochemistry and introduced terms such as anode, cathode and ion.

Modern electrochemistry has since stemmed largely from the semi-empirical equations produced by Tafel (1905), Butler (1924) and Edey Gruz & Volmer (1930); with the field of voltammetry being developed chiefly from the polarographic experiments of Heyrovsky (1960). Electroanalytical techniques have found a variety of applications, particularly in quantitative analysis. Their strengths are that they can achieve relatively high sensitivities using equipment which is easy to operate and maintain, and is of relatively low cost, while not being affected by the optical state of the sample matrix. In addition to this, relatively recent methods of electrode modification, have resulted in sensors with both improved sensitivity and selectivity, requiring minimal sample pre-treatment. The development of these methods is the subject of this thesis.

1.2 Principles of Electrochemistry

1.2.1 The Electrode - Solution Interface

The principles of electrochemistry are based around the idea of heterogeneity. The presence of an electrode in a solution leads to a phase boundary and allows us to differentiate between the previously homogeneous solute molecules. The species in solution can now be seen to form two separate components : those molecules which cannot feel the presence of the electrode and those molecules which are close enough to the electrode to participate in electrochemical reactions.

The region of solution interacting with the electrode is illustrated in Fig 1.1. This region can be viewed as consisting of three separate planes. Firstly, at the inner Helmholtz plane (IHP), the solute molecules are specifically adsorbed to the electrode surface and therefore cannot be fully hydrated by the solvent. Next, the outer Helmholtz plane (OHP) contains molecules carrying their primary hydration shell, separated from the electrode by a monolayer of solvent molecules. Finally, in the diffuse layer, the solute molecules experience an equilibrium between attraction to the ions in the OHP and the opposing random forces of thermal motion.

The potential experienced by these molecules decreases exponentially with distance from the electrode, until eventually in the bulk solution they are subject only to thermal motion.

The electrochemical equilibrium eventually reached across this phase boundary for a component (j), will be governed by it's chemical (u_j) and electrical potential ($z_jF\Phi$)

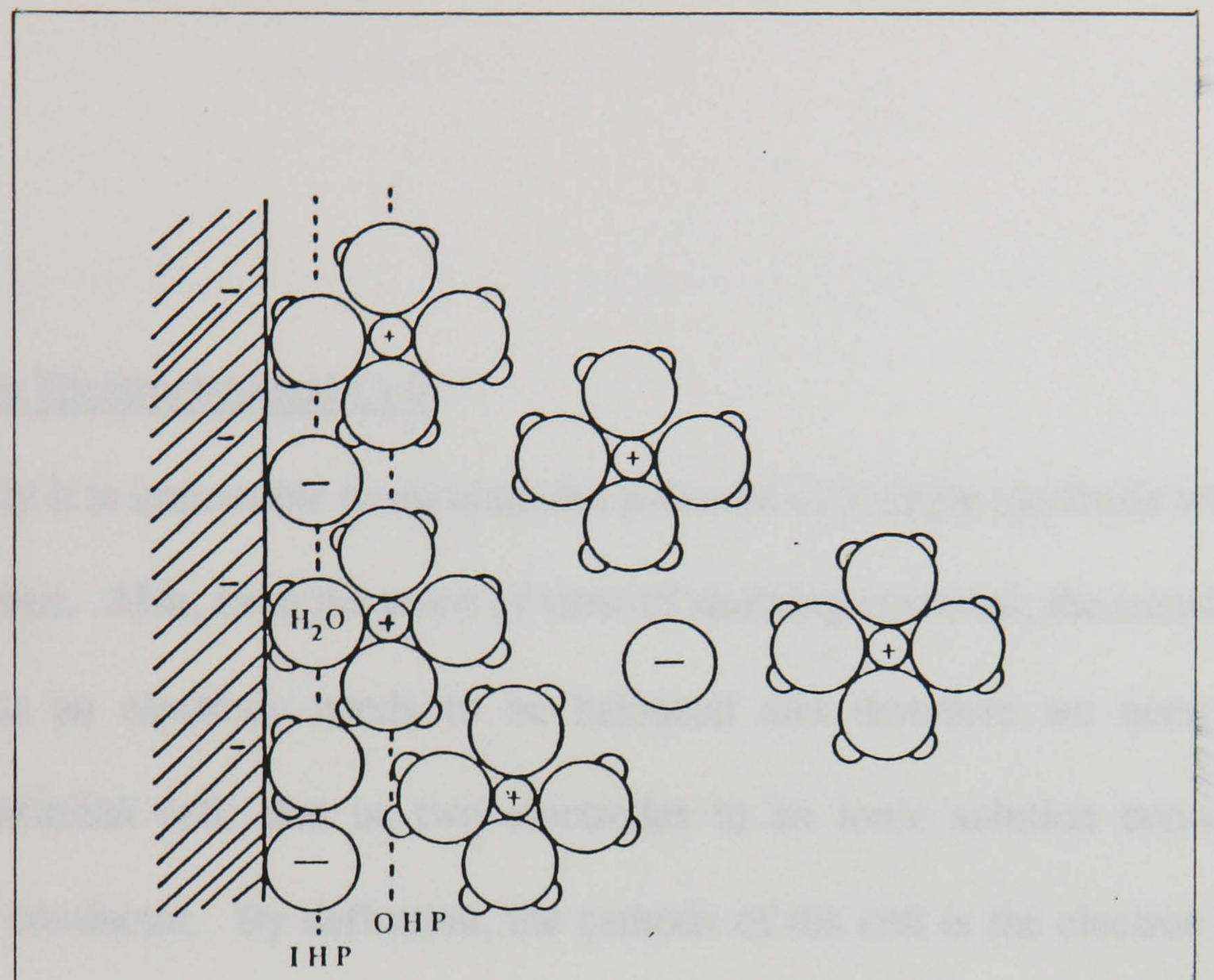

Fig. 1.1 Schematic representation of the electrode-solution interface.

and can be described by :

$$\tilde{u}_j = u_j + z_j F\Phi \qquad (1.1)$$

1.2.2 The Electrochemical Cell

Obviously it is impossible to measure the potential of a single electrode without a point of reference. Also, from the point of view of studying reactions, the transfer of electric charge at an electrode needs to be balanced and therefore we need to form an electrochemical cell; that is, two electrodes in an ionic solution connected via an external conductor. By definition, the cathode of the cell is the electron supplier and the anode is the electron sink.

Two types of cell are possible: A Galvanic cell converts the Gibbs free energy of a physical or chemical change into electrical energy, while in an electrolytic cell an external supply of electrical energy is required to bring about a physical or chemical change at the electrode surface.

Detection in amperometry depends on the imposition of conditions which will force a particular reaction to occur and is therefore concerned with electrolytic cells.

1.2.3 Reaction at the Electrode

During reaction at an electrode, the passage of a constant amount of electric charge, Q (Coulombs) will by Faraday's law, give a fixed amount of chemical change, Δn (moles):

$$\Delta n = Q/nF = It/nF \qquad (1.2)$$

where I is current, t is time, n is the number of electrons transfered in the overall reaction and F is Faraday's constant.

Meanwhile, the current through the external circuit is given by

$$i = AI \qquad (1.3)$$

Where A is the electrode area and I is the current density.

1.2.4 Reaction Requirements

The thermodynamic requirement for the cell reaction is that the overall Gibbs free energy change be negative. As previously stated, to meet this requirement in an electrolytic cell, energy is supplied to the system by applying a potential. Thus, the potential of the electrode is shifted from its equilibrium value (E_e) by an amount defined as the overpotential (η):

$$E = \eta + E_e \qquad (1.4)$$

The total voltage applied to the cell must also allow for the drop (iR) in the actual potential experienced by the electrode, due to the electrolyte solution having a resistance R.

1.2.5 Application of Potential

The potential applied to the electrode is referred to a benchmark (ie. a particular half-cell reaction) so that experimental conditions can be reproduced. This reference point is usually present as a third electrode as shown in Fig. 1.2. The potential is controlled between this and the working electrode, while the current is driven between the working and counter electrodes using circuitry in the potentiostat which prevents passage of current through the reference. This is to ensure that the potential of the reference half-cell remains stable and also that the contribution of iR drop to the measured potential is minimised.

1.2.6 Nature of Reference Electrode

The choice of appropriate half-cell for the reference is made by considering the rate of electron transfer across the resulting electrode. At equilibrium this will be the same in both directions and the exchange-current density (i_o) of the electrode is defined as being the current per unit area thus passed at equilibrium:

$$i_o = i_c = i_a \qquad (1.5)$$

For a reliable reference potential electrode/electrolyte systems utilized must have high exchange-current densities (described as being nonpolarizable). This is because

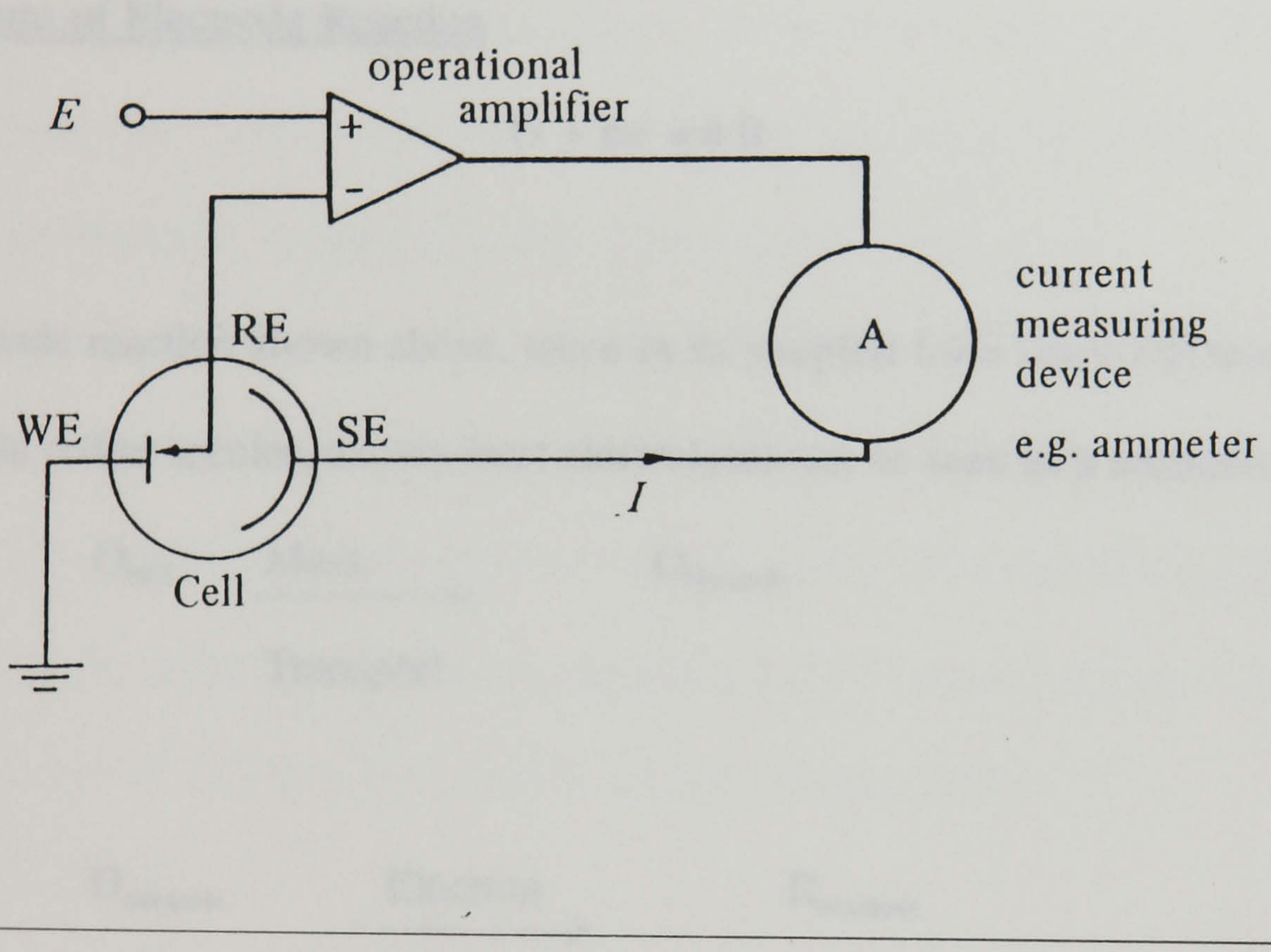

Fig. 1.2 Principle of operation of a three-electrode electrochemical cell.

a rapid rate of electron transfer to and from the electrode is required to ensure that charge does not build up on the electrode surface. Such an occurrence would change the potential difference across the inner and outer Helmholtz planes, altering the reference potential. Examples of non-polarizable electrodes are mercury/mercury chloride in saturated KCl and silver/silver chloride in 3.5 M KCl.

1.2.7 Nature of Electrode Reaction

$$O + ne^- \rightleftharpoons R \qquad (1.6)$$

The electrode reaction shown above, taken in its simplest form (inert electrodes, stable and soluble redox species, excess inert electrolyte) can be seen as a sequence of steps:

O_{bulk} —Mass Transport→ $O_{electrode}$

$O_{electrode}$ —Electron Transfer→ $R_{electrode}$

$R_{electrode}$ —Mass Transport→ R_{bulk}

Thus a description of the electrode reaction must consider two separate processes: mass transport and electron transfer.

1.2.8 Mass Transport

Mass transport to the electrode can be seen as consisting of three separate components:

i) *Convection* is the movement of species due to mechanical forces such as stirring or the use of a rotating disk electrode.

ii) *Migration* is movement due to a potential gradient and is the mechanism of conduction of charge through an electrolyte. As an electrostatic force, it acts on all ionic species in the solution and therefore if excess supporting electrolyte is present it will be responsible for transporting little of the redox species.

iii) *Diffusion* is the movement of a species down a concentration gradient and will occur when there is a chemical change at the electrode surface. In an unstirred solution with a supporting electrolyte, it is the most important form of mass transport. The process of diffusion can be characterised by Fick's laws (Moore, 1983) :

Fick's first law states that the flux of a component i through a plane parallel to the electrode, at a distance x from the electrode, will be proportional to the concentration gradient at that distance. ie.

$$\text{Flux (i)} = -D_i \, (dc_i/dx) \qquad (1.7)$$

Where the proportionality factor is the diffusion coefficient D_i.

Fick's second law describes the change in the concentration of i with time, due to diffusion into and out of the plane:

$$\partial C_i/\partial t = D_i(\partial^2 C_i/\partial x^2) \qquad (1.8)$$

To use this equation the particular conditions of the experiment need to be defined. For an unstirred solution containing excess supporting electrolyte, at a constant temperature, the current density I, at a planar electrode can thus be described by the Cottrell equation (Cottrell, 1902):

$$I = -nFD^{1/2}C_i/t^{1/2}\pi^{1/2} \qquad (1.9)$$

Where C_i is the concentration of i in bulk solution and the other symbols are as previously stated.

1.2.8 Electron Transfer

To consider the reaction outlined earlier (eq. 1.6):

$$O + ne^- \rightleftharpoons R$$

When the cell is in dynamic equilibrium (no net current flow) the potential of the working electrode will be given by the Nernst equation (Greef *et al.*, 1993):

$$E_e = E_e^\circ + RT/nF \ln[C_O/C_R] \qquad (1.10)$$

Where C_O and C_R are the concentrations of O and R at the electrode surface.

If a potential is then applied to the working electrode, the surface concentrations of O

and R will change to allow equilibrium to be re-established. Thus there will be a current flow through the electrode - solution interface.

The magnitude of this current will depend on the electrode kinetics. However, the rate constants for the anodic and cathodic processes will themselves vary with the applied electrode potential. Therefore, to describe the net current density I consideration must be given to the value of the overpotential, η. Also to be considered are the values for the exchange current density I_O, and the transfer coefficients α_A and α_C for the anodic and cathodic reactions. The transfer coefficient refers to the fraction of the electrical energy $zF\Delta\Phi$ used in lowering the activation energy of a particular electrode reaction, ie. the Gibbs's free energy of the reaction is lowered by an amount $\alpha zF\Delta\Phi$. For an ideally reversible process, potential energy will be supplied equally to both the oxidation and reduction reactions. Thus both transfer coefficients will be equal to 0.5.

Thus, the value for the net current density I is given by the Butler-Volmer equation (Greef *et al.*, 1993):

$$I = I_0 \{\exp(\alpha_A nF\eta/RT) - \exp(\alpha_C nF\eta/RT)\} \qquad (1.11)$$

In practice, this equation can be simplified to one of three limiting forms :

i) At high positive overpotentials, the second term can be ignored and the anodic current density is given by :

$$\ln I = \ln I_0 + \alpha_A nF\eta/RT \qquad (1.12)$$

ii) At high negative overpotentials, only the cathodic current density need be considered,

and is given by :

$$\ln -I = \ln I_0 - \alpha_c nF\eta/RT \qquad (1.13)$$

iii) At low values of η the current density can be described by the following equation:

$$I = I_0\, nF\eta/RT \qquad (1.14)$$

1.3 Voltammetric Techniques

The experiments in this thesis are based chiefly on the technique of voltammetry. That is, the measurement of current at an electrode (designated the Working Electrode) under conditions of controlled potential. Two methods of voltammetry have been used : cyclic voltammetry (CV) and amperometry. Additionally utilised, was a technique analogous to voltammetry, known as chronocoulometry.

1.3.1 Cyclic Voltammetry

In cyclic voltammetry, the potential applied between the working electrode and a reference point is scanned across a voltage range (E_i to E_f) and back again, at a constant rate; at least one full cycle being completed.

The main applications of cyclic voltammetry are qualitative. In its simplest use, CV provides an 'electrochemical spectrum' of the analyte solution, allowing the identification of the potentials at which redox reactions will occur. In addition to this,

the particular relationships between scan rate, peak potential and peak current, can be used to give information about processes such as diffusion, adsorption and coupled homogeneous reactions (Greef *et al.*, 1993). Under certain conditions, kinetic data such as heterogeneous and homogeneous rate constants can also be determined (Nicholson & Shain, 1964).

Redox Behaviour

The general form for redox behaviour in a cyclic voltammogram is illustrated in Fig. 1.3. As can be seen, the reduction of species O gives rise to an increased current flow through the external circuit. As the scan rate is increased, both an increase in the cathodic current and the formation of a peaked rather than plateau response are observed. These characteristics can be explained by considering the changes occurring in the concentration of O.

Under equilibrium conditions, concentrations in the bulk solution will be kept uniform by the forces of natural convection. However, in the region extending from the electrode surface to the outer limit of the diffuse layer (known as the Nernstian Diffusion Layer), concentration gradients exist, with the ratio of C^s_O/C^s_R governed by the Nernst equation (eq. 1.10). As the scan shifts the potential in a negative direction, C^s_O will decrease in a Nernstian manner, thus making the concentration gradient steeper. This will cause an increase in the flux of O at the electrode (from Fick's first law), and thus an increased current flow is observed. Eventually C^s_O will approach zero and the concentration gradient will be unable to change further. The flux to the electrode will now be constant, giving the plateau visible at low scan rates.

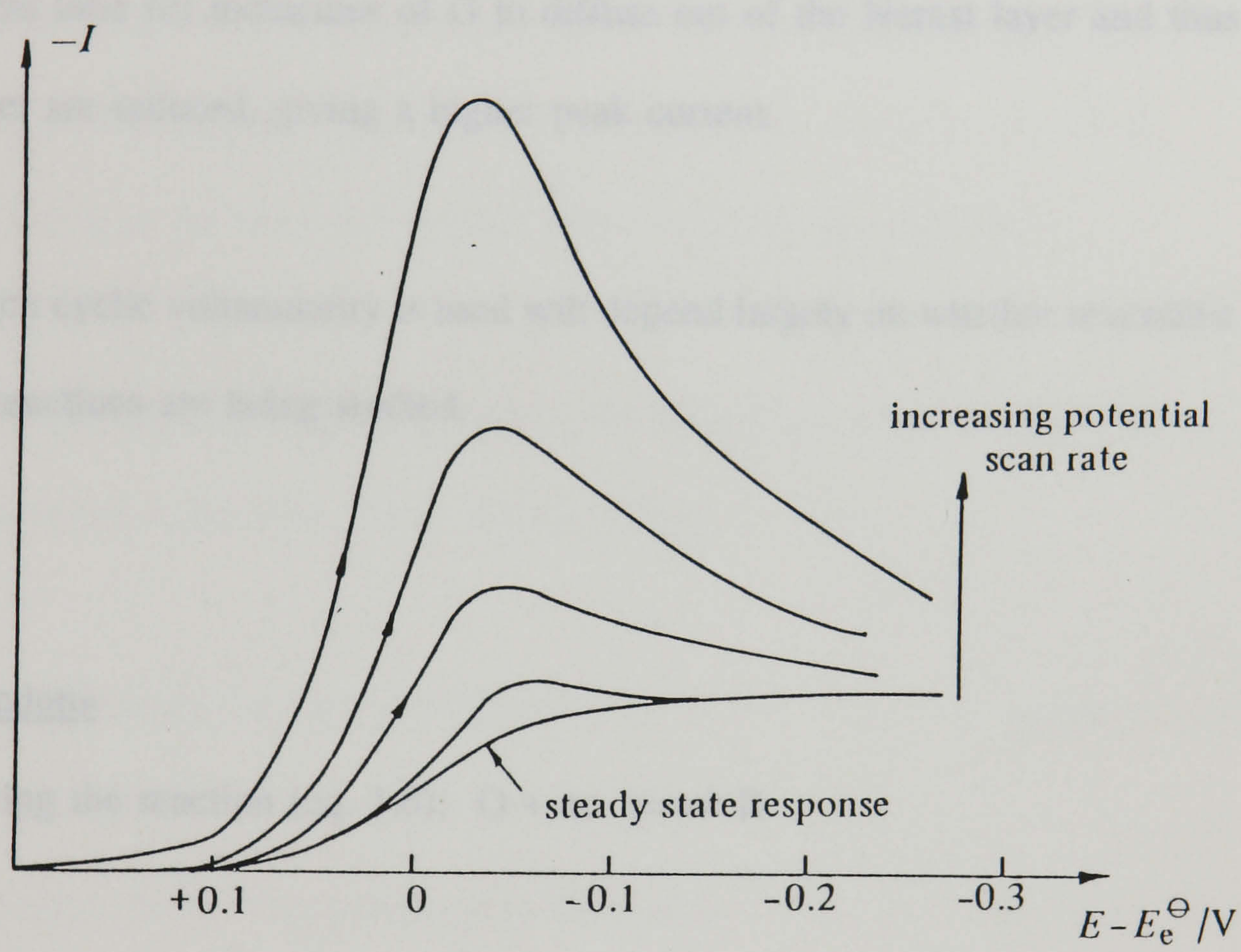

Fig. 1.3 A series of linear sweep voltammograms for the reaction

$O + ne^- \longrightarrow R$, at several potential scan rates.

The peak observed at faster scan rates can be understood by considering Fick's second law. From this, diffusion into and out of the plane at the Nernst Diffusion Layer is expected to occur, until equilibrium is reached. At faster scan rates the diffusion layer will not have enough time to relax to its equilibrium state and will therefore not extend far into the solution. Scanning 'empties' the layer of species O before O can diffuse in from the bulk solution and thus the current falls. If the scan rate is increased further there is even less time for molecules of O to diffuse out of the Nernst layer and thus a greater number are reduced, giving a higher peak current.

The way in which cyclic voltammetry is used will depend largely on whether reversible or irreversible reactions are being studied.

Reversible Reactions

Again, considering the reaction (eq. 1.6): $O + ne^- \rightleftharpoons R$

For this reaction to be reversible two conditions have to be met. Firstly, chemical reversibility requires that both O and R are stable in solution. Secondly, electrochemical reversibility requires that the rate of electron transfer is at all potentials considerably greater than the rate of mass transport. This is to ensure that the equilibrium at the electrode surface responds to concentration changes in a Nernstian manner.

To produce a mathematical description for a reversible cyclic voltammogram, Fick's second law must be solved for the appropriate conditions. Therefore the following

assumptions are made:

1. Initially only O is present.

2. The diffusion coefficients of O and R are equal.

3. At time zero: the concentration of O in bulk solution equals the concentration of O in the Nernst diffusion layer, and the concentration of R is zero.

4. At a time greater than zero: the rate of change in the concentration of O at the electrode is equal and opposite to the rate of change in the concentration of R.

5. The ratio of C_O/C_R at the electrode surface follows the Nernst equation.

Then for planar diffusion, the current density I_p at the electrode can be given by the Randles-Sevcik equation (Randles, 1948; Sevcik, 1958):

$$I_p = -0.4463nF(nF/RT)^{1/2}C^{bO}D^{1/2}\nu^{1/2} \qquad (1.15)$$

where ν is scan rate. At 25 °C this reduces to the form:

$$I_p = -(2.69 \times 10^5)n^{3/2}C_oD^{1/2}\nu^{1/2} \qquad (1.16)$$

Irreversible Reactions

Irreversibility can be brought about either because a reactant or product is chemically unstable (and thus reacts before the reverse cycle can be completed), or because the rate of electron transfer at the electrode is too slow to maintain a Nernstian equilibrium.

Slow rates of electron transfer can be identified by the effect of scan rate on peak separation. As the scan rate is increased, the rate of mass transport effectively increases (as less of O has time to diffuse away from the electrode). Eventually, the rate of mass transport approaches the rate of electron transfer and thus the peak separation increases above the Nernstian value (59/n mV).

The dependence of peak potential on scan rate for a totally irreversible system is given by:

$$E_p = E^o + RT/n_aF \{-0.78 + \ln K/D^{1/2} - \ln(n_aF\nu/RT)\} \qquad (1.17)$$

where n_a is the number of electrons transferred in the rate determining step of the electrode process.

The current for an irreversible reaction can be again derived from Fick's second law. At 25 °C the current density I_p is given by :

$$I_p = 2.99 \times 10^5 n(n_a)^{1/2}D^{1/2}C_o\nu^{1/2} \qquad (1.18)$$

In general, irreversible voltammograms give peaks which are broader and flatter than for the reversible case. This is because the slow rates of electron transfer will cause the concentration of O at the electrode surface to change more slowly with potential. Thus when the surface concentration of O approaches zero, the concentration gradient will be less steep than for a reversible system, giving a lower flux to the electrode.

1.3.2 Amperometry

Amperometry is a simpler form of voltammetry, used for quantitative measurement. Here, the potential of the working electrode is kept at a fixed value while the current flow through the electrode is measured as a function of time. Unlike in cyclic voltammetry, the solution undergoes constant stirring. Thus, convective transport of the redox species prevents the creation of a depletion layer at the electrode surface, producing a plateau response to the oxidation or reduction of the analyte. For the reaction :

$$O + ne^- \text{-----> } R$$

Where O and R are both stable and diffusion is rate determining, the current density I, can again be related to the concentration of O in bulk solution, C_o, by solving Fick's second law for the appropriate conditions.

$$I = -nFDC_o/\delta \qquad (1.19)$$

where δ is the diffusion layer thickness.

1.3.3 Chronocoulometry

In contrast to the previous methods, chronocoulometry involves the measurement of charge rather than current. It is described as a potential step technique, meaning that the potential of the working electrode is changed instantaneously, rather than scanned over a period of time. The potential step applied (from E_1 to E_2) is chosen such that, for the reaction

$$O + ne^- \rightleftharpoons R$$

at E_1 no reduction of O occurs and at E_2, O is reduced at a diffusion controlled rate (ie. the rate of electron transfer is significantly greater than the rate of mass transport). This is achieved by imposing a relatively high potential, while using an un-stirred solution containing a supporting electrolyte. Under these conditions, the charge passed (Q) can be described by the integrated form of the Cottrell equation (Anson *et al.*, 1967) :

$$Q = (2nFAD^{1/2}C_i t^{1/2} / \pi^{1/2}) + Q_{dl} + nFA\Gamma \qquad (1.20)$$

As can be seen, the total charge measured will include a component Q_{dl}, due to double layer capacitance (the re-distribution of charged or polar species at the electrode surface) and a component $nFA\Gamma$, due to the instantaneous reduction of adsorbed O. Neither of these quantities are time dependent and therefore rapidly decay to zero. The gradient of the linear portion of the curve can be used to calculate the observed diffusion coefficient of O, as illustrated in Chapter 3 Part II. The curve will remain linear until the effect of natural convection becomes apparent. Hence for a species in solution, a pulse lasting for a few seconds is usually possible. However, as seen in Chapter 3 Part II, for an immobilised compound the pulse width often needs to be considerably shorter, due to depletion of the species within the immobilised film.

It should be noted that current can also be measured following a potential step (chronoamperometry). But in this case, as seen in eq. 1.9, the x-axis is the reciprocal of $t^{1/2}$ and therefore at longer time data periods (when double layer charging has a minimal effect) the data points approach zero, making calculation of the correct gradient more difficult. Hence, chronocoulometry was the prefered technique for this thesis.

1.4 Advances in Voltammetry

1.4.1 Modified Electrodes

Until the mid 1970's, the range of analytes quantifiable by voltammetry had been severely restricted by the choice of available electrode materials. Namely, the mercury drop, bare solid metal or bare carbon. Hence, the advent of the chemically modified electrode (CME), was to have a profound effect on the field of electroanalytical chemistry, and was to considerably broaden its horizons.

The first deliberate modification of an electrode surface was carried out in 1973 by Lane and Hubbard, who chemisorbed functionalized alkenes onto a platinum electrode. They were thus able to incorporate a variety of electroactive and non-electroactive species such as hydroquinones and halides.

These experiments gave rise to much interest and in 1975 Miller's research group (Watkins *et al*, 1975) prepared a 'chiral electrode' by immobilising an asymmetric reagent (S(-)phenylalanine methyl ester), which when used in the electrolysis of 4-acetylpyridine, gave optically active products, illustrating that reactions at an electrode could be driven along a pre-determined pathway.

Also in 1975, Moses *et al* reacted hydroxyl groups on a tin dioxide electrode with an organosilane in dry benzene, to create an amine surface on the electrode available for complexation with a wide variety of redox species. This was the first time the term Chemically Modified Electrode appeared in literature.

Since then, CME's have been used for a variety of different electroanalytical applications and many comprehensive reviews exist (Murray, 1992). The purpose of CME research can be seen to fall broadly into two categories: sensitivity and selectivity, with some modifications being directed at both these goals.

One of the most important methods of increasing sensitivity via a CME is electrocatalysis. Most catalytic CME's function by utilizing a fast electron transfer mediator as shown in Fig. 1.4. As illustrated, an analyte molecule only slowly reduced (or oxidised) at a bare electrode can be detected at a lower potential, which will thus be less open to interference. Examples of successful mediators include cobalt phthalocyanine for carbohydrates (Tolbert & Baldwin, 1989), prussian blue for ascorbic acid (Dong & Wang, 1989) and ferricyanide (Cardosi *et al.*, 1988), Meldola's blue (Gorton, 1986) and phenazine methosulphate (Torstensson & Gorton, 1981) for NADH. These mediators have been adsorbed onto electrodes (Gorton, 1986) or entrapped in matricies such as conducting polymers (Khan *et al.*, 1992).

Recently, electrocatalysis has also been achieved using conducting polymers which contain no additionally immobilised mediators, but can still lower the activation energy for a particular redox reaction (Atta *et al.*, 1990). The mechanism for this process is still unclear and will be discussed more fully in Chapter 3 Part III. Other methods of CME electrocatalysis which have been investigated, are the use of adsorbed particles of metal oxide such as Al_2O_3, ZrO_2 or Cr_2O_3, for the oxidation of organic compounds (Dong & Kuwana, 1984) and metal particle CME's such as platinised carbon electrodes for the oxidation of hydrogen peroxide (Kao & Kuwana, 1984).

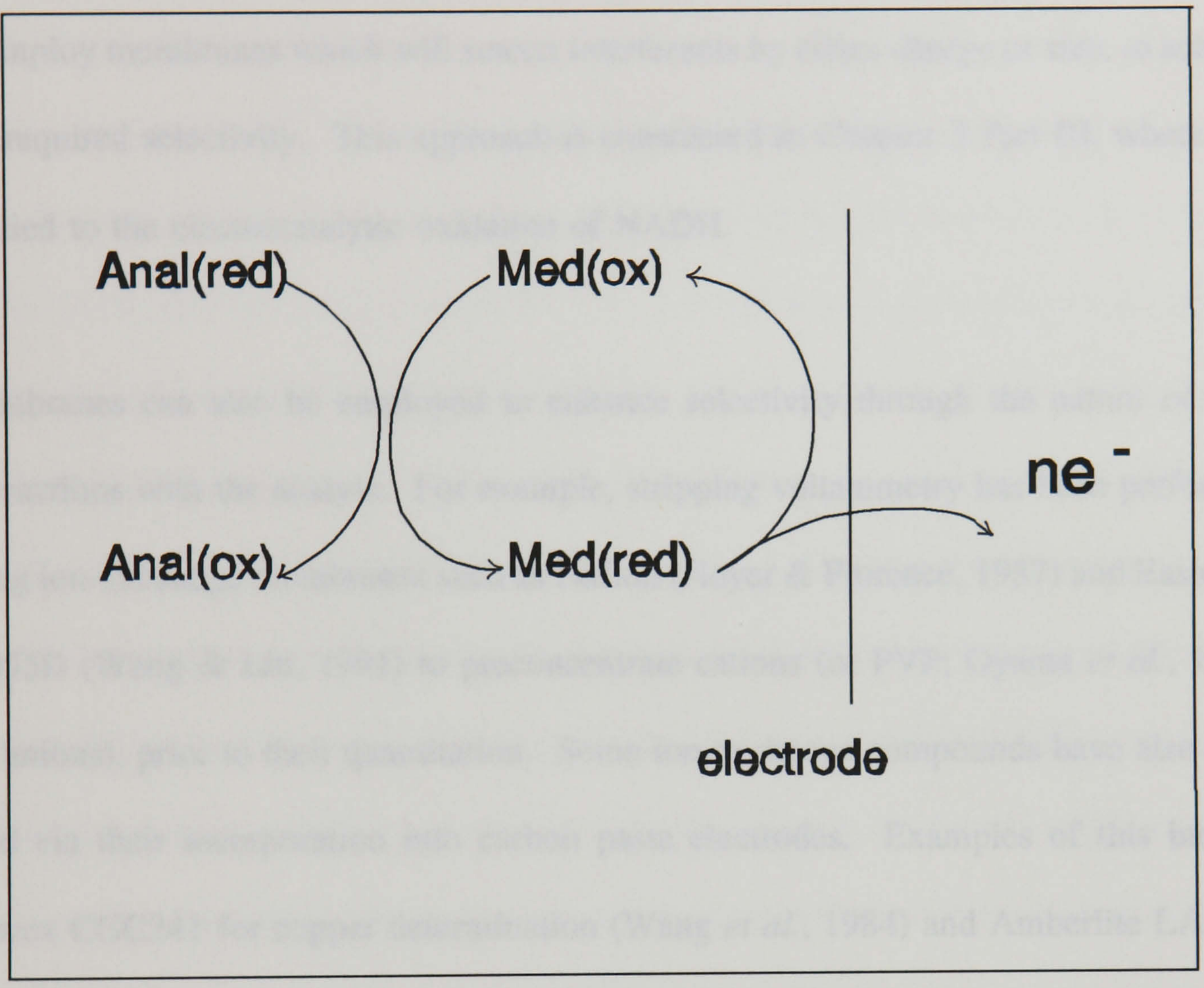

Fig. 1.4 Electrocatalysis by a fast electron-transfer mediator.

One problem sometimes associated with electrocatalysis, is that modification can also reduce the overpotential for the oxidation (or reduction) of other compounds present in the sample matrix. An increase in analyte sensitivity is obtained, but there is a need to employ membranes which will screen interferents by either charge or size, to achieve the required selectivity. This approach is considered in Chapter 3 Part III, where it is applied to the electrocatalytic oxidation of NADH.

Membranes can also be employed to enhance selectivity through the nature of their interactions with the analyte. For example, stripping voltammetry has been performed using ion-exchange membranes such as Nafion (Hoyer & Florence, 1987) and Eastman-AQ55D (Wang & Liu, 1991) to preconcentrate cations (or PVP; Oyama *et al.*, 1980) for anions), prior to their quantitation. Some ion-exchange compounds have also been used via their incorporation into carbon paste electrodes. Examples of this include Dowex CGC241 for copper determination (Wang *et al.*, 1984) and Amberlite LA2 for the determination of $AuBr^{4-}$ (Kalcher, 1985).

Chemical preconcentration can also be performed by complexation, using ligands which will selectively bond with the analyte. Complexing agents which have been examined include dimethylglyoxime for nickel (Baldwin *et al.*, 1986), adenosine-5'-monophosphate for iron(III) (Cox & Majda, 1980), 2,9-dimethyl-1,10-phenanthroline for copper(I) (Prabhu *et al.*, 1987) and trioctylphosphine oxide for uranium (Lubert *et al.*, 1982). The ligand can either be adsorbed onto the surface of the electrode (Cox & Majda, 1980), or incorporated into the electrode body, by methods such as entrappment within carbon paste (Baldwin *et al.*, 1986) or within a conducting polymer grown onto

the electrode surface (Hurrell & Abruna, 1988).

1.4.2 Electrochemical Biosensors

Another important and extensively researched method of electrode modification, has been the incorporation at the electrode surface of a biological component; the resulting device being described as a biosensor. This concept was first introduced in 1962 by Clark and Lyons, who suggested entrapping soluable glucose oxidase over a pH electrode, using a dialysis membrane. They showed that glucose could thus be detected selectively by monitoring the pH changes occurring during oxidation to gluconic acid. This 'enzyme electrode' (as it became known) was later used amperometrically by Updike and Hicks, who constructed a detection system by immobilising glucose oxidase in a polyacrylamide gel over a Clark pO_2 electrode. Hence, the drop in oxygen tension due to enzymic activity could be measured and related to the concentration of glucose.

Various biological components have since been incorporated into a variety of different electrode configurations. These include antibodies (Aizawa *et al.*, 1979), whole cells (Karube *et al.*, 1979) and plant tissues (Kuriyama & Rechnitz, 1981). Various texts have been written purely for the field of biosensors (Cass, 1990; Turner *et al.*, 1987) and the literature contains many reviews. Some of the most comprehensive are by Bartlett *et al* (1991), Saini *et al* (1991) and Brooks *et al* (1991).

1.5 Applications of Voltammetry

1.5.1 Trace Element Analysis

Clinical Applications

The trace elements in man are considered to be those present in concentrations of μg/g or less (Jacob, 1987), and can be seen as forming two types: essential and non-essential. An element is defined as being essential if its deficiency consistently produces an impairment that can only be allieviated by the element itself (Mertz, 1979). There are currently thought to be 10 elements which are essential to human health. A further 4 are consistently present in human tissues but are thought to be non-essential (Jacob, 1987). The clinical importance of trace element analysis (and the difficulties associated with it), can be understood by considering some of the general characteristics of trace element function.

Trace element action has been characterised as undergoing amplification (Mertz, 1979). This means that very small amounts of a trace element are neccessary for the optimal performance of an organism. This is due to these elements being constituents of, or interacting with, enzymes and hormones that regulate the metabolism of much larger amounts of biochemical substrate. As a result of this, the lack of even a small amount of an essential element can lead to disorders of great severity.

Also of great importance, is the phenomenon of trace metal interaction. Often, the occurrence of deficiencies or toxicities will depend on the interplay between two or more elements. These interactions can be positive or negative. Positive interaction refers to an element requiring the presence of another for efficient function. For

instance, copper deficiency is known to produce iron deficiency and anemia (Elvehjem & Sherman, 1932). Negative interaction (also known as 'antagonism') describes the impairment of one elements' function by the relative excess of another. This can, for example, be seen in the displacement of zinc from carboxypeptidase A by elements such as cobalt, nickel, iron or cadmium (Coleman & Vallee, 1961).

A further complication, is that trace element interaction can also be indirect, with the relationship between two elements affecting the concentration of a third (Kirchgessner *et al.*, 1982). Therefore, accurate diagnosis of the toxicity or deficiency of a particular element is difficult, and can only be reliably performed by a battery of quantitative tests on the same specimen.

Environmental Monitoring

While procedures exist for treating most forms of heavy metal poisoning, it is obviously far more preferable to try and prevent toxic exposures from occurring. Also, in cases where the uptake of a toxin occurs gradually over a long period of time, rather than in a high single dose, diagnosis of poisoning is likely to come too late. Environmental monitoring is therefore an important application of trace metal analysis. Viewed from an environmental standpoint, metals can be classified according to three types: non-critical, toxic but rare (or insoluble) and toxic and relatively accessible (Wood, 1974). The last category contains nineteen elements, the majority of which are transition metals, with the others coming chiefly from groups IV and V (lead, tin, arsenic etc.). Often, when toxic material enters the aquatic environment it will be accumulated in the food chain. One of the most disasterous examples of this was in Minamta Bay, Japan in the early 1950s, when a factory producing plastics discharged large amounts of a

mercury catalyst into the bay. This was converted by microorganisms into the more toxic monomethyl mercury and accumulated in fish and shellfish, leading to widespread neurological disorders and fatalities. The routes of entry into the environment for heavy metals are diverse and can be distinguished as six separate types (Forstner, 1979). These are, geologic weathering, mining effluents, industrial effluents, domestic effluents, inputs from rural areas and atmospheric sources.

The weathering of metal-containing rock formations provides a trace metal baseline. That is, the concentrations at which these metals would have been present in water sources in the absence of the activities of man. Although it should be remembered, that when metals are present in rocks at high concentrations they are usually mined, blurring the distinction between enrichment by natural and human activity.

Mining has been found to enrich the metal levels in both water and soil. This is due to the erosion and dissolution of mine soil heaps when exposed to rain, and also to the dispersion of fumes from smelters.

The disposal of industrial wastes results in a wide variety of heavy metals entering the aquatic environment. Some industries, such as textile mills, are responsble for the enrichment of a single metal (in this case chromium), while others such as steel works, are responsible for the entry of a wide spectrum of metals. A comprehensive list is given by Dean *et al* (1972).

Domestic effluents constitute the largest single source of elevated metal concentrations in rivers and lakes (Forstner, 1979), and can be from either untreated or mechanically

treated wastewaters, substances which have been biologically treated, or substances passsed over sewage outflows. The storm water runoff from urban areas (especially motorways) is also a source of contamination, usually of metals such as lead, zinc and copper. Studies in Lodi, New Jersey found the highest concentrations occurring within the first 30 minutes of the downpour (Whipple *et al.*, 1977). In rural areas, storm water runoff is also a contaminant, containing metals from fertilizers, pesticides and herbicides.

Finally, man-made processes have resulted in atmospheric metal-containing particles which eventually return to the lithosphere as precipitation. The most important process is the burning of fossil fuels, which contributes 11 toxic metals in appreciable quantities, the majority of which are transition elements. Values for these emissions in tons/year are given by Bertine and Goldberg (1971).

Methods of Trace Metal Analysis

The most popular techniques for the determination of trace metals are, atomic absorption spectroscopy (AAS), neutron activation analysis (NAA), x-ray fluorescence (XRF), mass spectrometry (MS) and electrochemical techniques such as anodic stripping voltammetry (ASV). The chief drawbacks to NAA, XRF and MS are the complexity and expense of the equipment needed and the high level of operator skill required. ASV is cheaper but still requires a skilled operator and has so far only been applied to a few metals. These constraints leave AAS as the most favoured alternative. Its strengths are that it has good sensitivity and specificity and is applicable to a wide range of metals. Its drawbacks are the cost of the equipment needed (albeit slightly less

less than that of its rivals), the need for some sample preparation, and the fact that the size and nature of the instrumentation makes transportation and on-site testing impractical.

1.5.2 Reduced Nicotinamide Adenine Dinucloetide Analysis

NAD^+ (shown in Fig. 1.5) functions as the coenzyme to a large number of oxido-reductases (Lehninger, 1975). In animal cells, most of these serve primarily in respiration; that is, in the transfer of electrons from substrates to oxygen. The role of NAD^+ during the catalytic cycle is to act as an electron acceptor, during the removal of two hydrogen atoms from the enzyme substrate. As shown in Fig. 1.5, one hydrogen atom is transferred as a hydride ion to the nicotinamide portion of NAD^+ (giving NADH), while the other enters solution as a proton. In general, the reactions catalysed by NAD^+-linked dehydrogenases are reversible, with the position of the equilibrium controlled by pH.

NAD^+-linked reactions can be followed by monitoring the changes in either NADH absorbance (340 nm) or fluorescence (460 nm), or the change in pH. Fluorescence though, can be prone to high levels of interference by quenching (Skoog & West, 1982), while changes in pH can often be non-specific. This usually leaves absorbance as the preffered form of measurement. However, because NAD^+ is non-covalently and relatively loosely bound to the dehydrogenase protein, the electrochemical oxidation of NADH could also be a possible form of measurement, assuming the problems of a high overpotential and electrode passivation, could be overcome. Circumvention of these problems will be disscussed in Chapter 3 Parts I and III. A wide range of NAD^+-linked

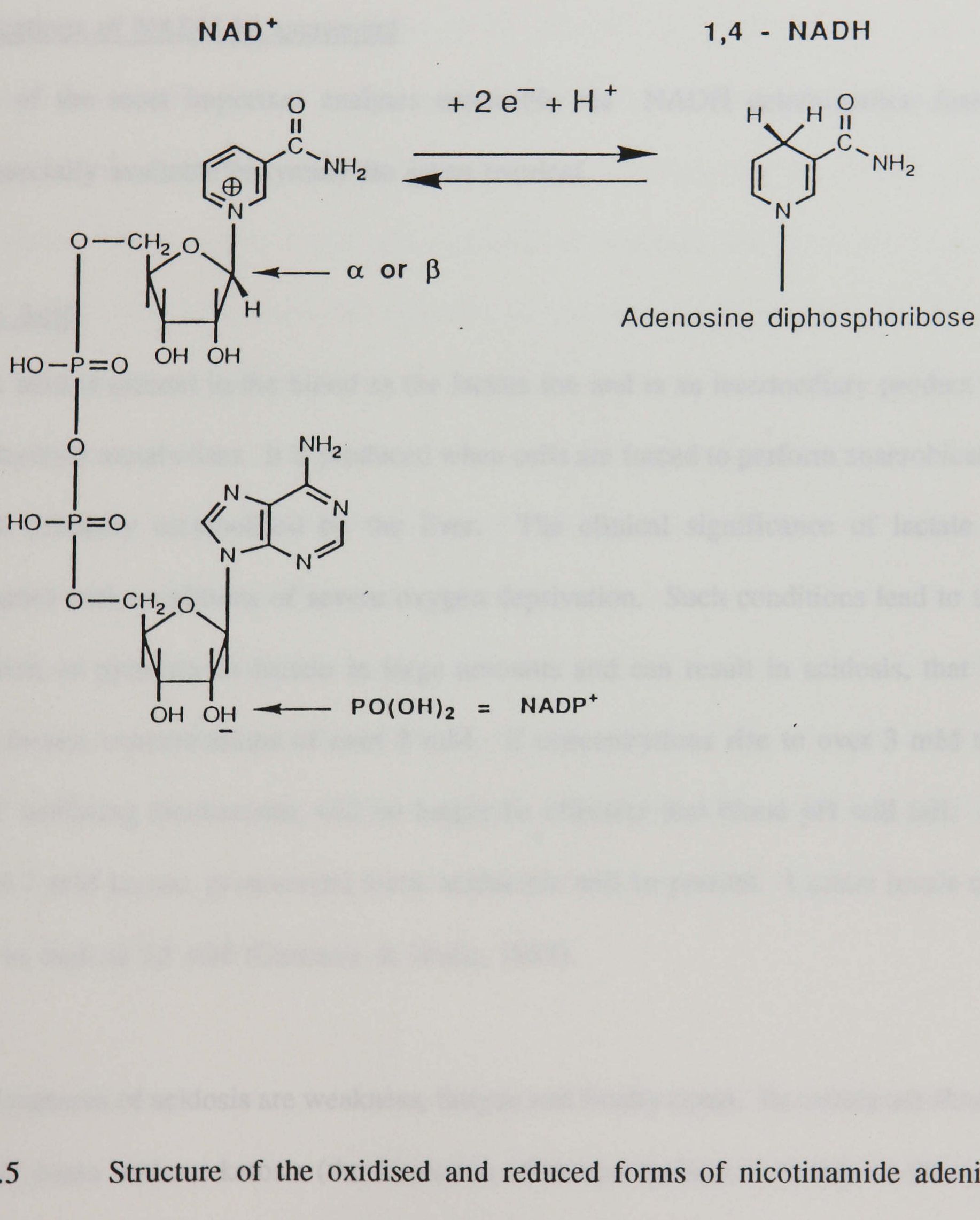

Fig. 1.5 Structure of the oxidised and reduced forms of nicotinamide adenine dinucleotide.

dehydrogenases are commercially available; which means that the measurement of NADH can provide us with a route to the quantitation of a variety of clinically important analytes.

Applications of NADH Measurement

Some of the most important analytes accessible via NADH determination (using commercially available enzymes) are given overleaf.

Lactic Acid

Lactic acid is present in the blood as the lactate ion and is an intermediary product of carbohydrate metabolism. It is produced when cells are forced to perform anaerobically and is normally metabolised by the liver. The clinical significance of lactate is associated with conditions of severe oxygen deprivation. Such conditions lead to the reduction of pyruvate to lactate in large amounts and can result in acidosis, that is, blood lactate concentrations of over 2 mM. If concentrations rise to over 3 mM the bodys' buffering mechanisms will no longer be effective and blood pH will fall. At around 7 mM lactate, pronounced lactic acidaemia will be present. Lactate levels can reach as high as 25 mM (Caraway & Watts, 1987).

The symptoms of acidosis are weakness, fatigue and finally coma. Its causes are shock, diabetic coma without ketosis (the formation of ketone bodies), a variety of illnesses in the terminal stage and liver damage. Lactate measurement can thus be applied to intensive-care and perinatal monitoring, as well as sports medicine, where the point of OBLA (onset of blood lactate) is a useful index of stamina.

Bile Acids

Bile acid metabolism is regulated by the liver and is the mechanism by which the liver maintains the cholesterol balance (Balistreri & Shaw, 1987). Cholesterol is synthesised by all tissues and is utilized in a variety of ways, including being a structural component of membranes and a precursor for hormone synthesis. A large amount of the cholesterol produced is converted in the liver to four primary and then two secondary, bile acids. These, because of their ampiphilic nature, solubilise additional cholesterol, thus providing the body with the most important method of cholesterol elimination. The transport of bile acids into the bile canaliculi also generates osmotic water flow, which influences the secretion of the other main components of bile (bilirubin and phospholipids).

The clinical significance of abnormal bile acid metabolism lies chiefly in the diagnosis of liver damage; with hepatitis and cirrhosis giving elevated serum bile levels. Obstruction of the gallbladder can also increase serum bile, while reduced bile acid concentrations can often be due to inflamation of the illeum. The clinically relevant range for total bile acid concentration is 0.74 to 5.64 μM (Balistreri & Shaw, 1987).

Glucose

Glucose is the major energy source of the human body and is produced as an intermediary in carbohydrate metabolism (Caraway & Watts, 1987). In this process, polysaccharides such as starch and glycogen, are digested first by salivary amylase and then by disaccharidases in the small intestine, to give glucose, galactose and fructose. These compounds are then absorbed into the portal vein and transported to the liver.

Galactose and fructose are phoshorylated and eventually enter the same pathway as glucose. This is to be initially either converted to glycogen and stored; metabolised immediately to carbon dioxide and water to provide energy; converted to keto acids, amino acids and proteins; or converted to fat and stored in adipose tissue. The interactions of these processes supply the regulation of blood glucose concentration. Also important in the control of glucose levels are various hormones. Insulin has the effect of lowering blood glucose, while 'counterregulatory' hormones such as glucagon, cortisol and epinephirne have the opposite effect.

The clinical significance of glucose measurement lies in the diagnosis and monitoring of abnormalities in carbohydrate metabolism. These can be due to either a deficiency of one or more of the enzymes involved in intermediary carbohydrate metabolism, or due to diabetes mellitus causing hyperglycemia. Diabetes mellitus, as it is currently understood, is thought to be more than a single disorder and various different classes of hyperglycemia have been defined (National Diabetes Data Group, 1979). In all cases, it is brought about by a deficiency of insulin secretion or action and is a result of impaired insulin production in the B cells of the pancreas.

<u>Ethanol</u>

The clinical significance of ethanol is in its importance as an analyte in toxicology laboratories. Analytical toxicology is an essential part of the diagnosis and treatment of chronic and acute poisoning. It usually consists of three separate components: clinical assesment of the patients symptoms in the light of patient history; qualitative screening tests and specific quantitative assays; and the co-ordination of toxicology data,

correlating the patients clinical state with existing information on toxic substances.

Ethanol is the most commonly encountered toxic substance in hospital laboratories (Blanke & Deker, 1987) and in cases of coma needs to be determined prior to diagnosis. Blood ethanol is toxic at concentrations of 11-22 mM. Depression of the central nervous system occurs at above 21.7 mM, with fatalities being reported at above 86.8 mM (Blanke & Deker, 1987).

1.6 Aims of Project

The objective of this research was to examine the possible use of metal complexes for the construction of selective amperometric sensors. Two approaches were taken: The first objective of the work, was to see whether the electrochemical change exhibited by a ligand upon complexation, could be used to detect the presence of the metal undergoing binding. Ligands were to be chosen which would undergo complexation with a degree of selectivity; the aim being to produce a selective metal ion response.

The second objective, was to use pre-formed metal complexes to mediate electron-transfer from oxidase enzymes. The aim of the work was to examine new mediator/enzyme configurations and to develop improved methods of enzyme and mediator immobilisation.

Chapter Two

Sensors Utilizing the Formation of a Metal Complex : Application to Trace Metal Analysis

2.1 Introduction

As previously described in Chapter 1 (Section 1.5.1), the main electrochemical technique for trace metal analysis is anodic stripping voltammetry (ASV). This is a two-step process involving the reduction and re-oxidation of the analyte. The first step consists of reductively depositing the metal ions in the sample solution onto a mercury electrode (either a hanging drop or a thin film), to form a mercury/metal amalgam:

$$M^n + ne^- + Hg \rightleftharpoons M(Hg) \qquad (2.1)$$

The second step is to then sweep the electrode potential in a positive direction, measuring the current flow as the metals return to an ionic form.

The position of the oxidation potential gives qualitative information about the ions being produced; while the size of the oxidation current can be related to the analyte concentration. The first step (known as preconcentration) is responsible for the sensitivity of the technique, with longer preconcentration times giving higher oxidative currents. However, some metals are unfortunately inaccessible via electrolytic preconcentration. This can be due either to a metal exhibiting irreversible reduction, the failure of a metal to form amalgams with mercury, or the formation of intermetallic compounds between species which have been co-deposited (Vydra *et al.*, 1976).

A way of circumventing these problems has been to utilise ligand-modified electrodes, that enable preconcentration to proceed by purely chemical means, as shown overleaf.

Preconcentration $M^n + L \rightleftharpoons M^nL \qquad (2.2)$

Quantitation $M^nL + xe^- \rightleftharpoons M^{n-x}L$ (2.3)

This concept was first illustrated by Cheek and Nelson (1978), who used carbon paste electrodes containing an ethylenediamine-functionalised organosilane, to preconcentrate silver ions prior to their reduction. These experiments were followed by several other research groups and many metals have been quantified this way, including nickel (Baldwin *et al.*, 1986), copper (Prabhu *et al.*, 1987) and bismuth (Kalcher, 1987). An up-to-date review is given by Forster and Vos (1992).

While this type of preconcentration step also gives additional selectivity (through the specific nature of the ligand/metal ion binding), the quantitative step can still be prey to interference, as the reduction potential of the metal could fall into a region where other sample species would be electroactive. Therefore, a possible improvement to the technique, would be to use a ligand which exhibits a change in redox behaviour on binding to the metal, rather than examining the redox potential of the metal itself:

$$M^n + L^m \rightleftharpoons M^nL^m \quad (2.4)$$

then $M^nL^m \rightleftharpoons M^nL^{m+x} + xe^-$ (2.5)

or $M^nL^m + xe^- \rightleftharpoons M^nL^{m-x}$ (2.6)

A judicious choice of ligand could enable quantitation to proceed at potentials of relatively low interference; whereas the redox potential of the metal would not be open to manipulation.

A judicious choice of ligand could enable quantitation to proceed at potentials of relatively low interference; whereas the redox potential of the metal would not be open to manipulation.

This method was first used by Flores *et al* (1984) for the determination of iron (II) via a nitroso salt and involved using the relevant ligand in solution, while monitoring the change in redox behaviour using cyclic voltammetry. It was latter followed by methods for determining iron (III) via ferron (Picon *et al.*, 1987), desferrioxamine B (Compagnone *et al.*, 1991) and 3-hydroxy-1-methylpyridine-4-one (Compagnone *et al.*, 1992). Copper (II) and mercury have also been examined (Compagnone *et al.*, 1992). Alkali metals have been determined by various groups using crown ethers bound either to nitrobenzenes (Miller *et al.*, 1988) or ferrocene derivatives (Beer, 1989a; Beer *et al.*, 1989b).

A further progression has been made by Abruna's research group, who have immobilised the necessary ligands by ion-exchange. The inital cationic polymer layer required for this, was grown onto the surface of a glassy carbon electrode by electrolytically initiated polymerisation. Sensors for nickel (McCracken *et al.*, 1987), calcium (Hurrell & Abruna, 1988) and copper (Cha *et al.*, 1991) have been reported.

The advantage of this approach is that it does not require the addition of any external reagents to the sensor system. However, there are further possible advantages which have so far not been examined. Previous methods of analysis have all been analogous to ASV, in that a preconcentration step is followed by quantitation via sweeping the

electrode potential. A quicker and simpler method of analysis, given a fast enough reaction between metal and ligand, would be amperometry, with the CME poised at the relevant redox potential, thus eliciting a 'real-time' response. In addition to this, alternative methods of fabrication could be used to improve upon the practical drawbacks of ASV, ie. the need for a skilled operator, and the fact that the complex and expensive equipment required makes transportation and on-site testing impractical. The manufacture of 'one-shot' disposable electrodes, by screen printing technology, would make CMEs amenable to use in hand-held amperometric sensors of the type used for glucose measurment (Hill & Sanghera, 1990). In this chapter the viability of this approach is examined.

The electrochemistry of a series of ligands in this chapter has been examined by cyclic voltammetry. Each ligand was known to bind to a particular metal with a high degree of selectivity. Ligands were chosen either from manufactures' data or from literature involving selective colorimetric metal determinations. Although slightly outside the scope of this thesis, compounds for the determination of phosphate using the same method, were also examined. The manufacture and characterisation of screen-printed CMEs is illustrated using a ligand selective to copper.

2.2 Experimental

2.2.1 Reagents

All reagents were supplied by Sigma/Aldrich (Dorset, UK) or BDH (BDH Ltd., Poole, UK) and were of reagent grade or better. The chelators were all commercial preparations, with the exception of desferrioxamine B, which was provided by Prof. Barry Halliwell of Kings College, University of London. All chelators were used without further purification and were stored as required by the manufacturer (either at room temperature or below 4 °C). The buffer used for inital investigations was 50 mM Tris-HCl, pH 7.0 with the exception of experiments involving, glyoxal-bis(2-hydroxyanil) (0.2 M NaOH-KCl, pH 12.6), alizarin red (50 mM borate-HCl, pH 6.6), eriochrome cyanine (0.1 M citric acid-Na_2HPO_4, pH 3.5) and murexide (0.2 M NaOH-KCl, pH 12.0). The experiments involving screen-printed electrodes were performed using 50 mM Tris-HCl, pH 8.0 unless otherwise stated. Metal ion solutions were prepared by dissolving the relevant metal salt in the working buffer at an inital concentration of 10 mM. The salts used were either sulphates or chlorides and were of analytical grade. All water was purified by reverse osmosis and ion-exchange.

2.2.2 Apparatus

All electrochemical experiments were carried out using a three-electrode cell of volume 25 ml. The reference was a saturated calomel electrode (Russell, Auchtermuchty, UK), the counter was a platinum flag electrode of approximate area 80 mm^2 and the working electrode, for inital experiments with desferrioxamine, was glassy carbon and for all other experiments was carbon paste. Carbon paste electrodes were either made

individually using glass tubes or screen printed in bulk onto PVC substrates. Methods of fabrication are given below. Cyclic voltammetry and amperometry experiments were performed using an Autolab electrochemical analyser (Windsor Scientific, Windsor, UK) interfaced to a DSL personal computer and Epson LX-400 printer. Voltammograms have been presented by importing data from the Autolab software (GPES2) into a graphics package (Sigmaplot, Jandel Corporation, USA). Potentials have been quoted without regard to the liquid/liquid junction potential. For temperature profile experiments the electrochemical cell was used with a water-jacket connected to a thermostated water-bath. All other measurements were made at room temperature (approx. 18-22 ℃). Absorbance measurements were made using a Beckman DU-8 single beam spectrophotometer.

2.2.3 Fabrication of Individual Electrodes

For inital experiments carbon paste electrodes were made individually by forming a slurry containing 55% graphite powder (T 10, Morganite, Swansea, UK) and 45% liquid paraffin (Spectrosol, BDH) which was then pushed into glass tubes of internal diameter 2 mm (Gallenkamp, Leicesteershire, UK). The surface of each electrode was smoothed by rubbing the head of the electrode over a piece of flat plastic. Insulated wire made contact with the external circuit. Modified electrodes were made by the same procedure, this time using a slurry into which the relevant ligand had been mixed. The ligand to graphite ratio was 1:2 unless otherwise stated.

2.2.4 Fabrication of Screen-Printed Electrodes

Screen-printed electrodes were fabricated using a model 245 screen printer (DEK, Weymouth, UK). In this process, eight-electrode arrays were printed by consecutively applying four different layers into 60 by 90 mm PVC substrates (Sericol, London, UK). These were, in order, a silver conducting track, a carbon overlay pad, a UV-cured insulation shroud and then the modified carbon paste. The first three layers were commercial printing inks (Acheson Colloids, Michigan, USA) and were inks Electrodag 477 SS RFU, Electrodag 423 SS and Product No. 451 respectively. The modified carbon paste was made by mixing graphite powder (2 g) and ligand (2 g) with a printing solution (5 ml); both organic and aqueous printing solutions having been examined. These were respectively, 2-butoxyethylacetate containing 3 % wt/vol ethyl cellulose and de-ionized water containing 2 % wt/vol hydroxyethyl cellulose and 6 % wt/vol ethylene glycol. The layers were printed using nylon screens obtained from DEK, with 200 counts in^{-1} screens used for the carbon and silver inks and 390 counts in^{-1} screens used for the insulating ink. After the printing of both the conducting tracks and the carbon overlay pads, the substrates were dried in a 30 °C oven for 20 min. After printing the insulation shroud, the substrates were cured by exposure to a UV source (power output 7.0 $mW.cm^{-2}$, 302 nm) under nitrogen for 3 min. After application of the modified carbon paste the substrates were left to dry at room temperature and then stored below 4 °C. The final configuration as shown in Fig. 2.1 gave an electrode of length 27 mm with an exposed electrical contact (6 mm^2) at one end and a modified working layer (14 mm^2) at the other. Electrodes were cut and used from the array as required.

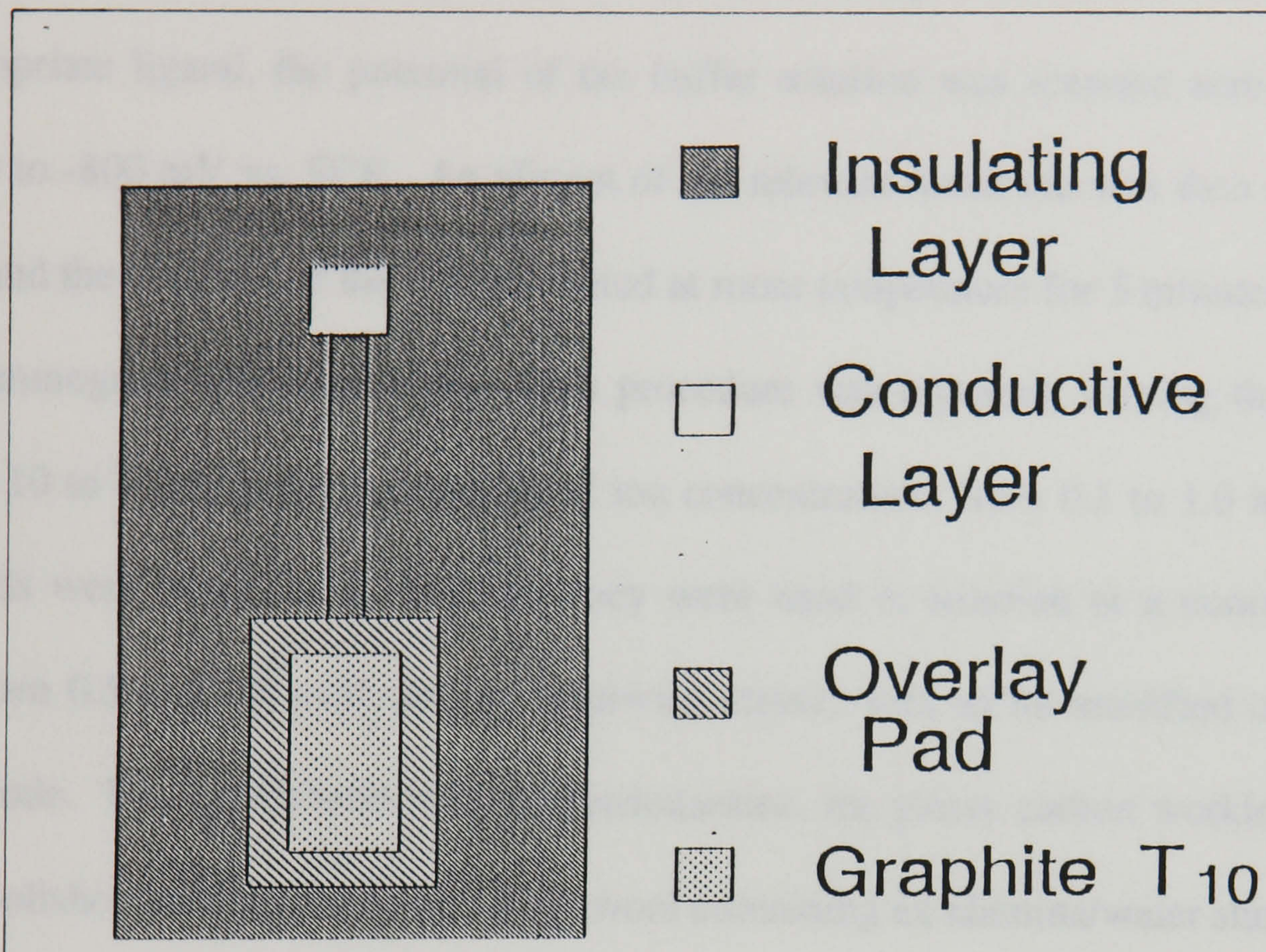

Fig. 2.1 Schematic representation of screen-printed electrode, not shown to scale.

Reproduced from Lafis (1992).

2.2.5 Procedures

Inital Investigations : Using a carbon paste working electrode, modified with the appropriate ligand, the potential of the buffer solution was scanned across the range +800 to -800 mV vs. SCE. An aliquot of the relevant metal ion was then added to the cell and the contents of the cell incubated at room temperature for 5 minutes. A second voltammogram was then taken. This procedure was repeated, varying the scan rates from 10 to 200 mV/sec and the metal ion concentrations from 0.1 to 1.0 mM. Where ligands were highly water soluble, they were used in solution at a concentration of between 0.5 and 1.0 mM (unless otherwise stated) with an un-modified carbon paste electrode. For experiments with desferrioxamine, the glassy carbon working electrode was polished between scans on cotton wool containing an alumina/water slurry (particle size 0.03 μm). Control experiments were performed by taking voltammograms of the metal ions in the absence of ligand and by noting the change in ligand electrochemistry upon the addition of de-ionized water.

Characterisation of Screen-Printed Electrodes : Copper (II) determinations were performed using amperometry; the working electrodes having been poised at +250 mV vs. SCE. The working electrodes were removed from the fridge 10 minutes prior to the start of the assay, to allow them to attain room temperature. Each electrode was used once only.

2.3 Results and Discussion

2.3.1 Initial Investigations

.1 Calcium Determination

Hydroxy Napthol Blue

In buffer solution the modified electrodes gave oxidation and reduction peaks at 0 and -100mV respectively. There was no change in electrochemistry on complexation with calcium.

Calcein Blue

The chelator when used in solution, showed no electrochemistry either before or after complexation with calcium.

Fura 2 AM

The chelator was examined in buffer at a concentration of 0.2 mg/ml. It showed no electrochemistry either before or after complexation with calcium.

Glyoxal-bis(2-hydroxyanil)

When used in solution the chelator exhibited oxidation and reduction peaks at -50 mV and -600 mV respectively. Addition of calcium lowered the oxidative peak height as shown in Fig. 2.2. However the same effect was seen upon addition of buffer.

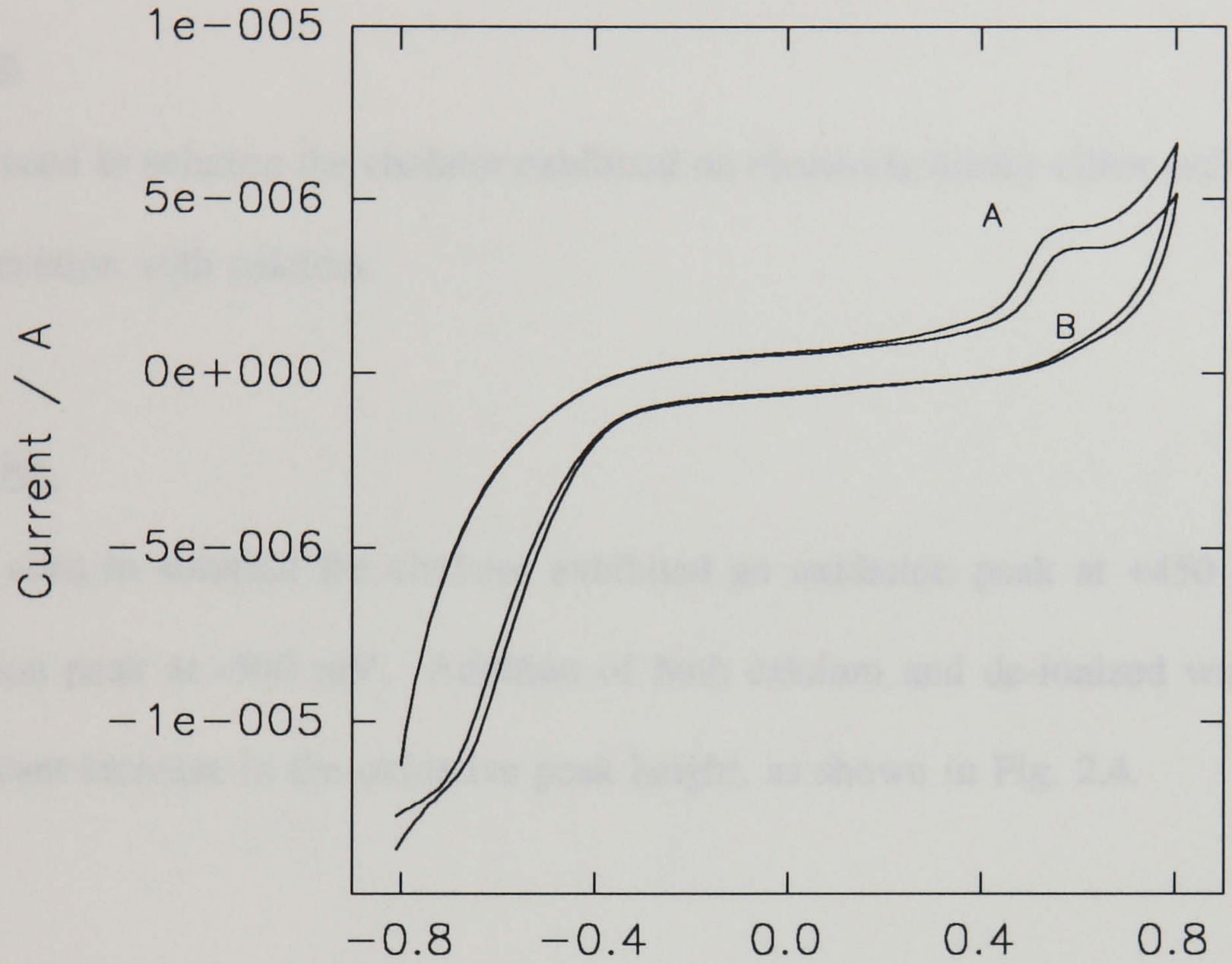

Fig. 2.2 (A) Typical voltammogram for a 0.5 mM solution of glyoxal-bis(hydroxyanil) at a carbon paste electrode. (B) was taken following the addition of Ca^{2+} to the cell at a final concentration of 3.33 mM. A similar effect was observed upon the addition of H_2O.

Scan rate = 50 mV/s.

Arsenazo III

When present in modified electrodes, the chelator showed a reduction peak at +100 mV and an oxidation peak at +600 mV. Addition of both calcium and de-ionized water gave an increase in the peak heights, as shown in Fig. 2.3.

Calcion

When used in solution the chelator exhibited no electrochemistry either before or after complexation with calcium.

Murexide

When used in solution the chelator exhibited an oxidation peak at +450 mV and a reduction peak at -500 mV. Addition of both calcium and de-ionized water gave a significant increase in the oxidative peak height, as shown in Fig. 2.4.

2.3.1.2 Lead Determination

Carminic Acid

When used in buffer solution the modified electrodes gave a reduction peak at +300 mV. There was no change in electrochemistry on complexation with lead.

Gallocyanine

Used in modified electrodes, the chelator showed no electrochemistry either before or after complexation with lead.

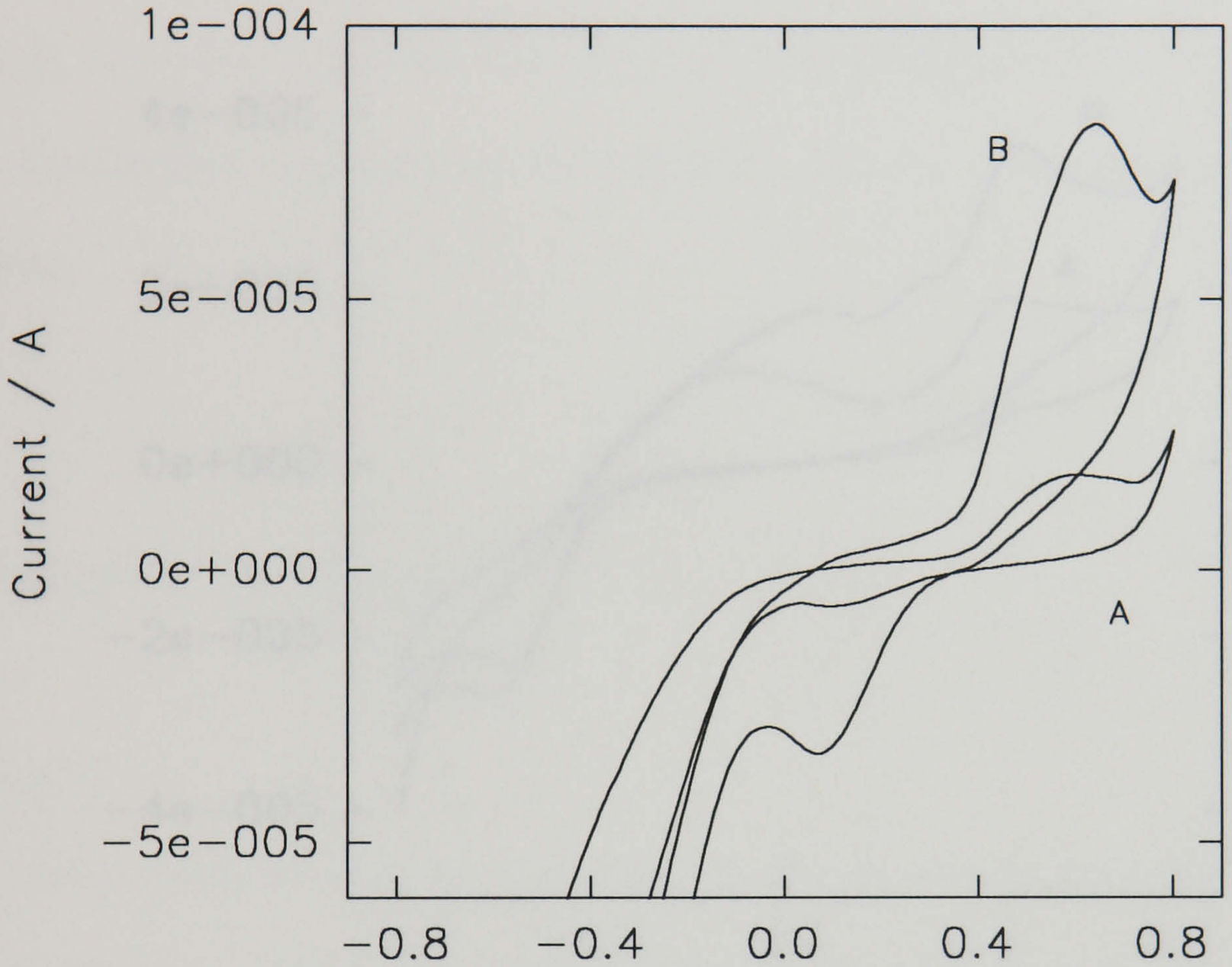

Fig. 2.3 (A) Typical voltammogram for arsenazo III-modified carbon paste electrode. (B) represents the addition to the cell of Ca^{2+} at a final concentration of 0.49 mM. A similar increase in peak heights was observed on addition of aliquots of de-ionized water.

Scan rate = 50 mV/s.

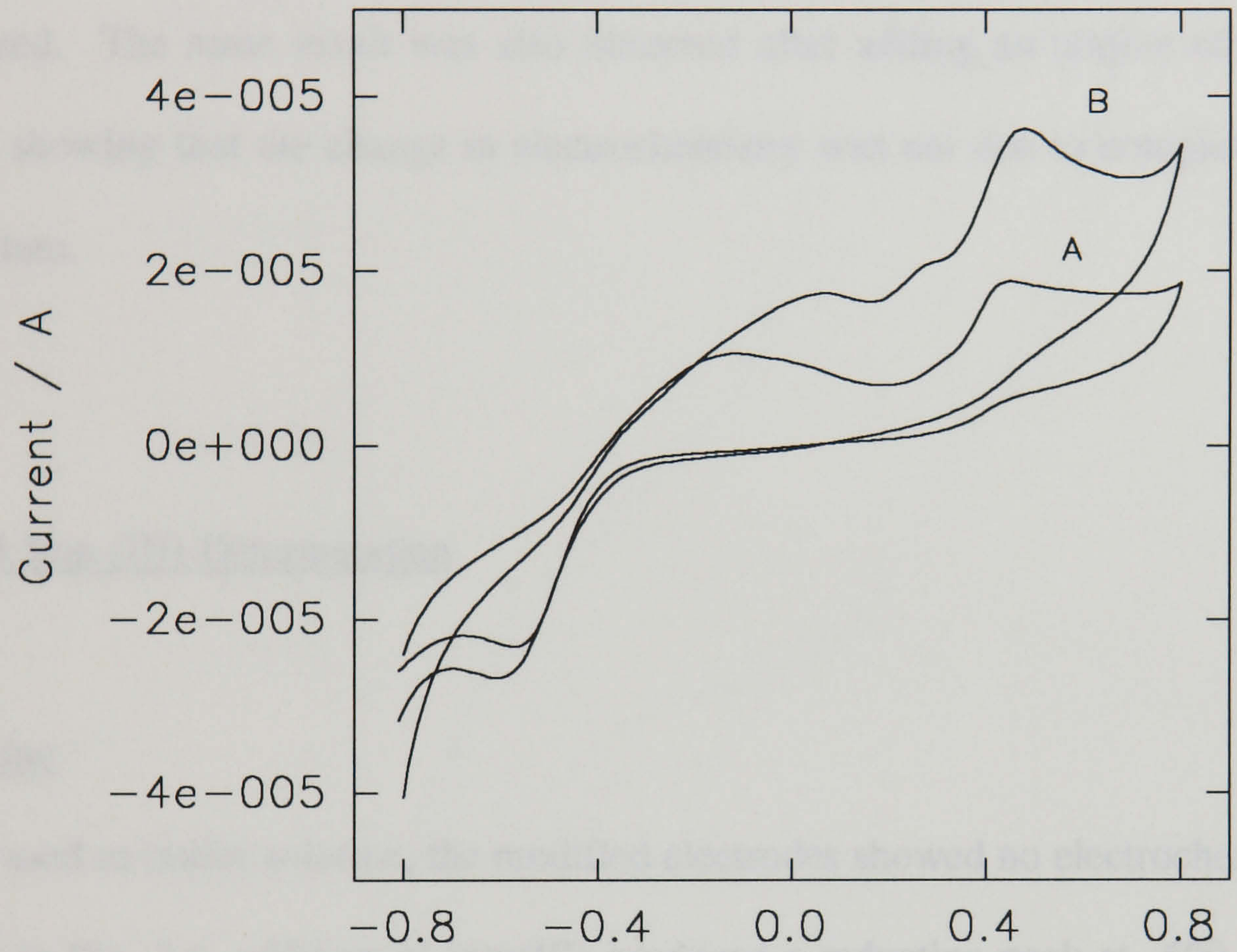

Fig. 2.4 (A) Typical voltammogram of a 1 mM solution of murexide at a carbon paste electrode. (B) represents the addition to the cell of Ca^{2+} at a final concentration of 1.82 mM. A similar change in electrochemistry was observed upon the addition of de-ionized H_2O. Scan rate = 50 mV/s.

2.3.1.3 Chromium (III) Determination

Orcinol Monohydrate

When used with buffer solution, the modified electrodes exhibited an oxidation peak at approx. +100 mV, as seen in Fig. 2.5. On addition of chromium (III) the peak height increased. The same result was also observed after adding an aliquot of de-ionized water, showing that the change in electrochemistry was not due to complexation with chromium.

2.3.1.4 Iron (III) Determination

Ferrozine

When used in buffer solution, the modified electrodes showed no electrochemistry. As shown in Fig. 2.6, addition of iron(III) produced a reduction peak at -600 mV. This was reproduced using a plain carbon paste electrode, showing that it was due to the reduction of the iron.

Desferrioxamine

When used in buffer solution at a concentration of 0.2 mM, the chelator showed an oxidation peak at +430 mV. Addition of iron (III) produced a reduction in the peak current. Adding corresponding aliquots of de-ionized water to a fresh chelator solution produced no significant change, showing that the effect was due to complexation with the iron. See Fig. 2.7 for examples of the voltammograms.

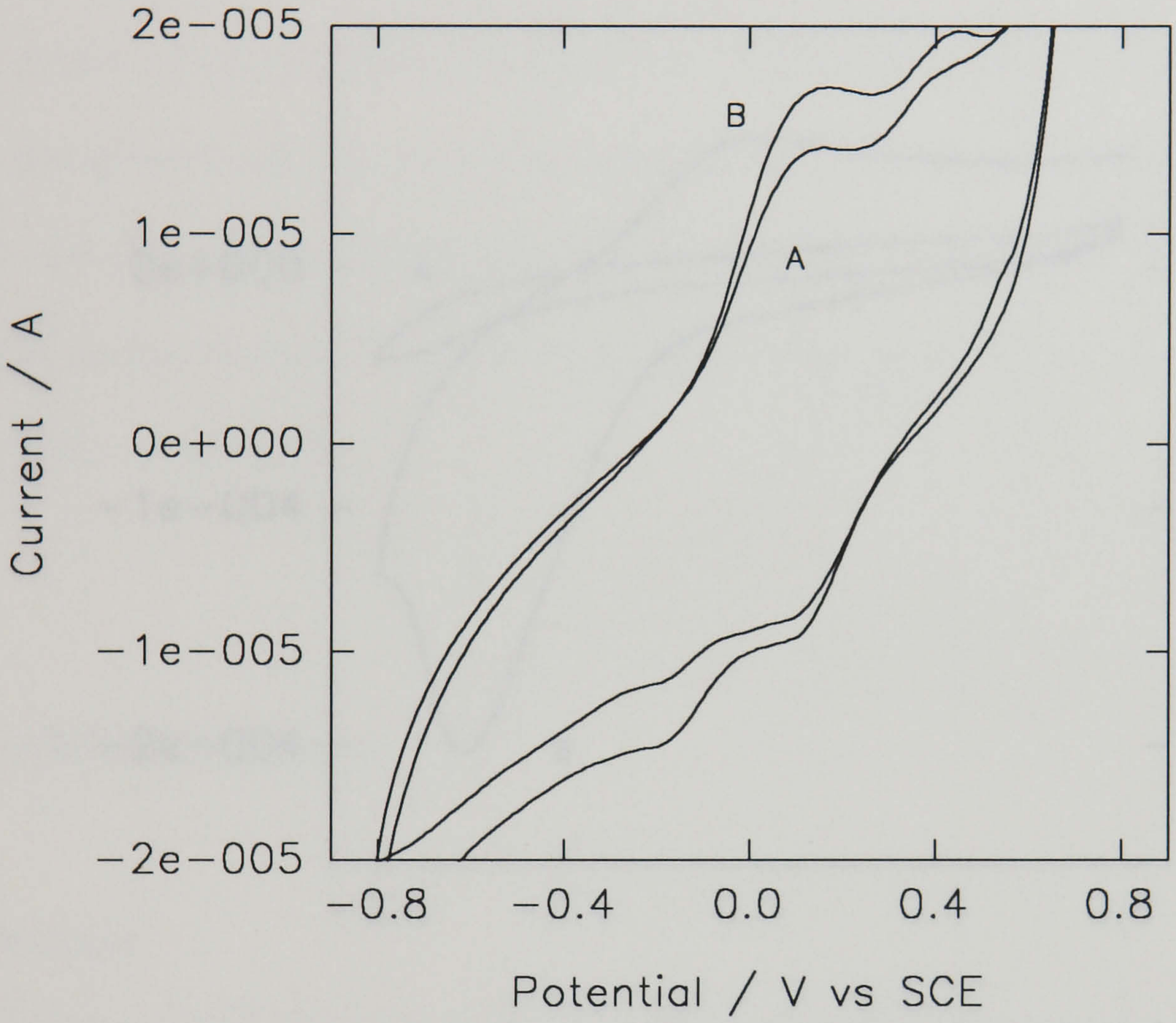

Fig. 2.5 Typical voltammogram for an orcinol monohydrate-modified carbon paste electrode in buffer solution. (B) represents the addition to the cell of Cr^{3+} at a concentration of 0.1 M. The same effect was observed on addition of aliquots of de-ionized H_2O. Scan rate = 20 mV/s.

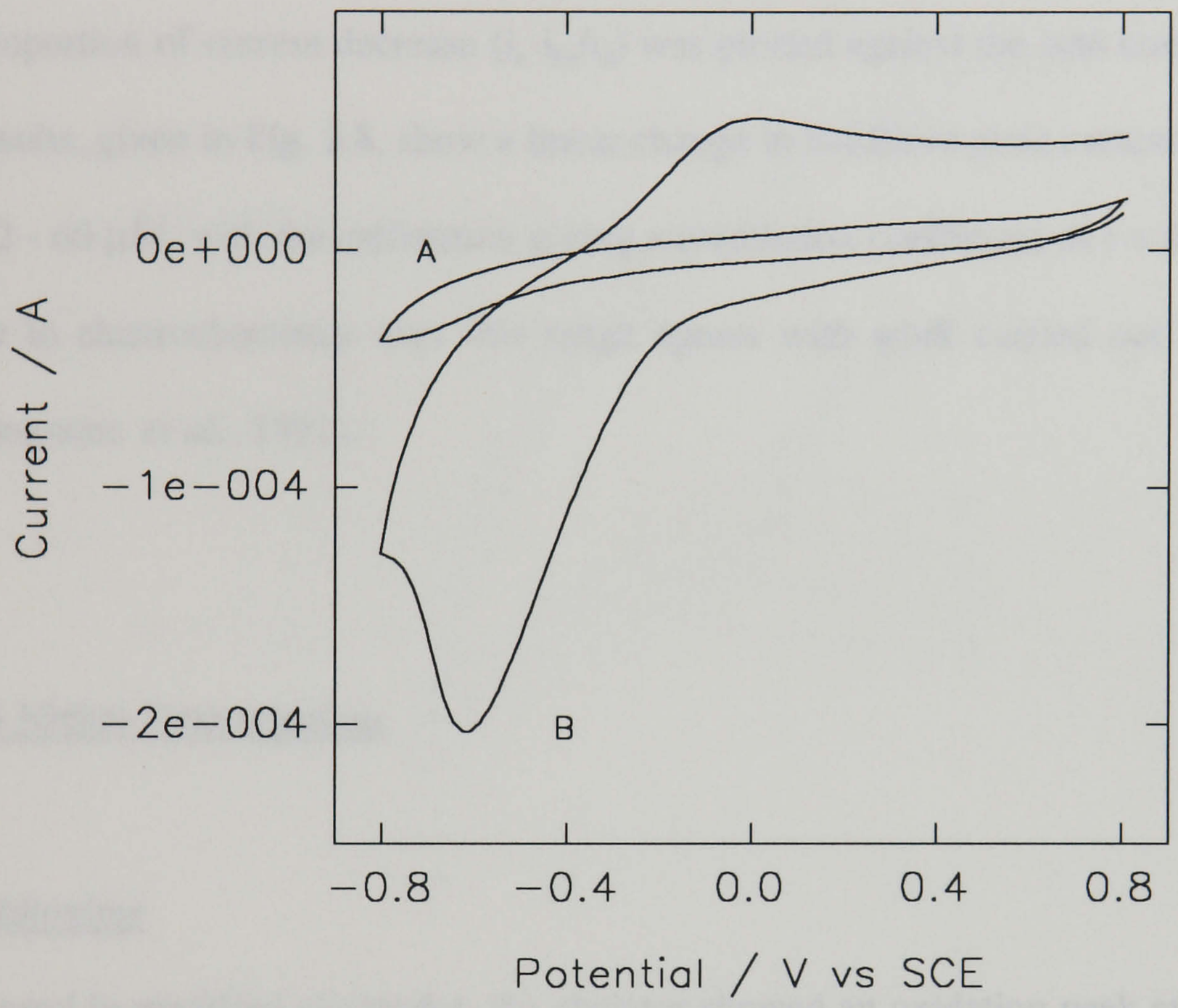

Fig. 2.6 Typical voltammogram of a ferrozine-modified carbon paste electrode in buffer solution. (B) represents the addition of Fe^{3+} to the solution to the cell at a final concentration of 0.5 M. The same redox behaviour was observed at a plain carbon paste electrode, suggesting it was due to the reduction of Fe^{3+}. Scan rate = 50 mV/s.

An inital calibration was performed with the chelator in solution at this concentration, using cyclic voltammetry. The peak current at +430 mV was measured at a scan rate of 20 mV/sec before (i_o) and after (i_{Fe}) the addition of an aliquot of a stock solution of 2 mM iron (III). A fresh chelator solution was used each time. Blank determinations were carried out by repeating the procedure with equal volumes of de-ionized water. The proportion of current decrease (i_o-i_{Fe}/i_o) was plotted against the iron concentration. The results, given in Fig. 2.8, show a linear change in oxidative peak current across the range 2 - 60 μM, with the calibration giving a correlation coefficient of r = 0.988. The change in electrochemistry over this range agrees with work carried out previously (Compagnone *et al.*, 1991).

2.3.1.5 Nickel Determination

α-Furildioxime

When used in modified electrodes, the chelator showed an oxidation peak at +600 mV in buffer. There was no change in electrochemistry on complexation.

2.3.1.6 Aluminium Determination

Eriochrome Cyanine

When used in modified electrodes, the chelator exhibited an oxidation peak at +540 mV. The peak current increased upon the addition of aluminium. However the same effect was seen upon the addition of de-ionized water.

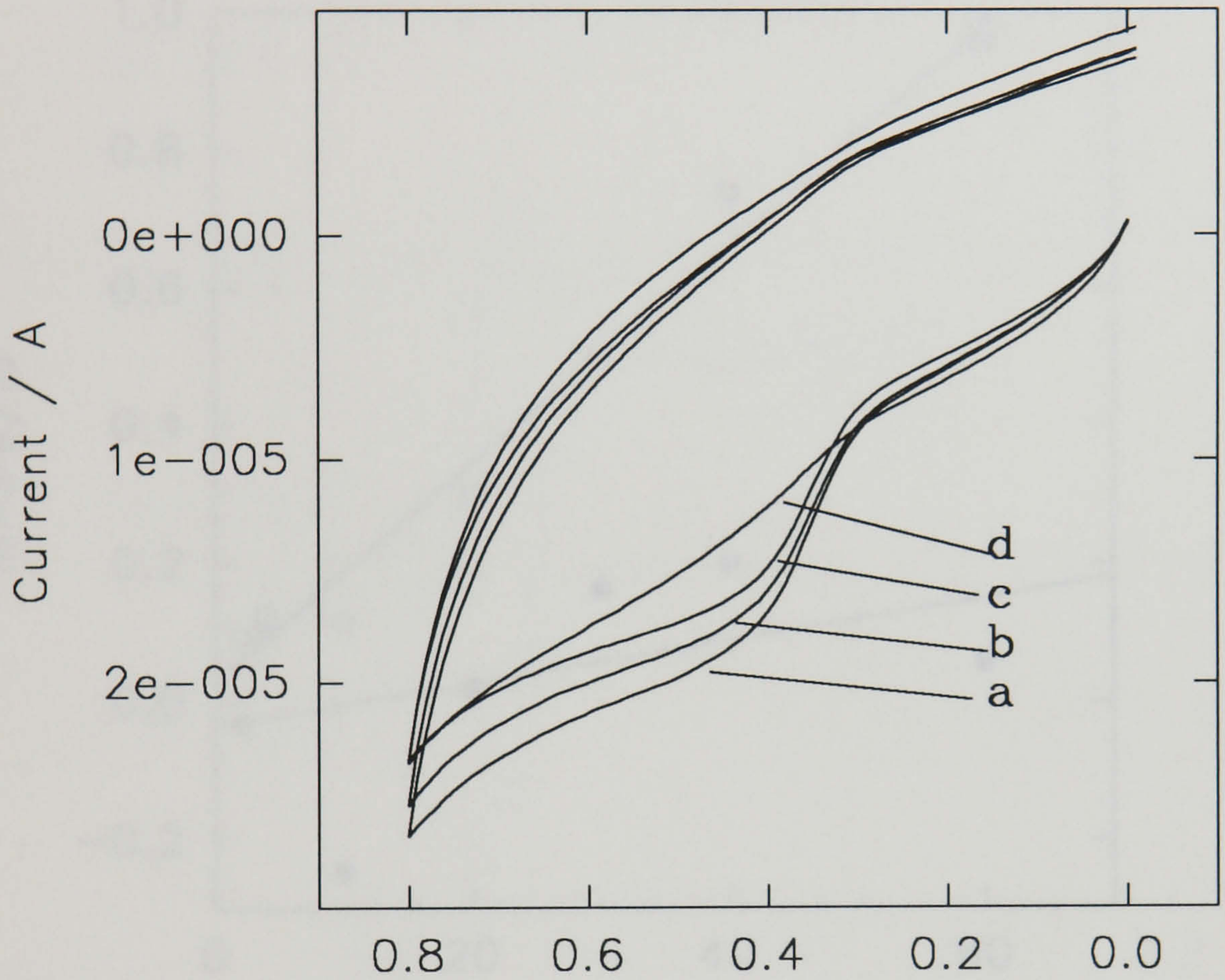

Fig. 2.7 Cyclic voltammograms of 0.2 mM desferrioxamine in buffer solution (50 mM Tris-HCl, pH 7.0). Initial voltammogram (a) and after additions of 10 μM (b), 30 μM (c) and 60 μM (d) of iron(III). Scan rate = 20 mV/s.

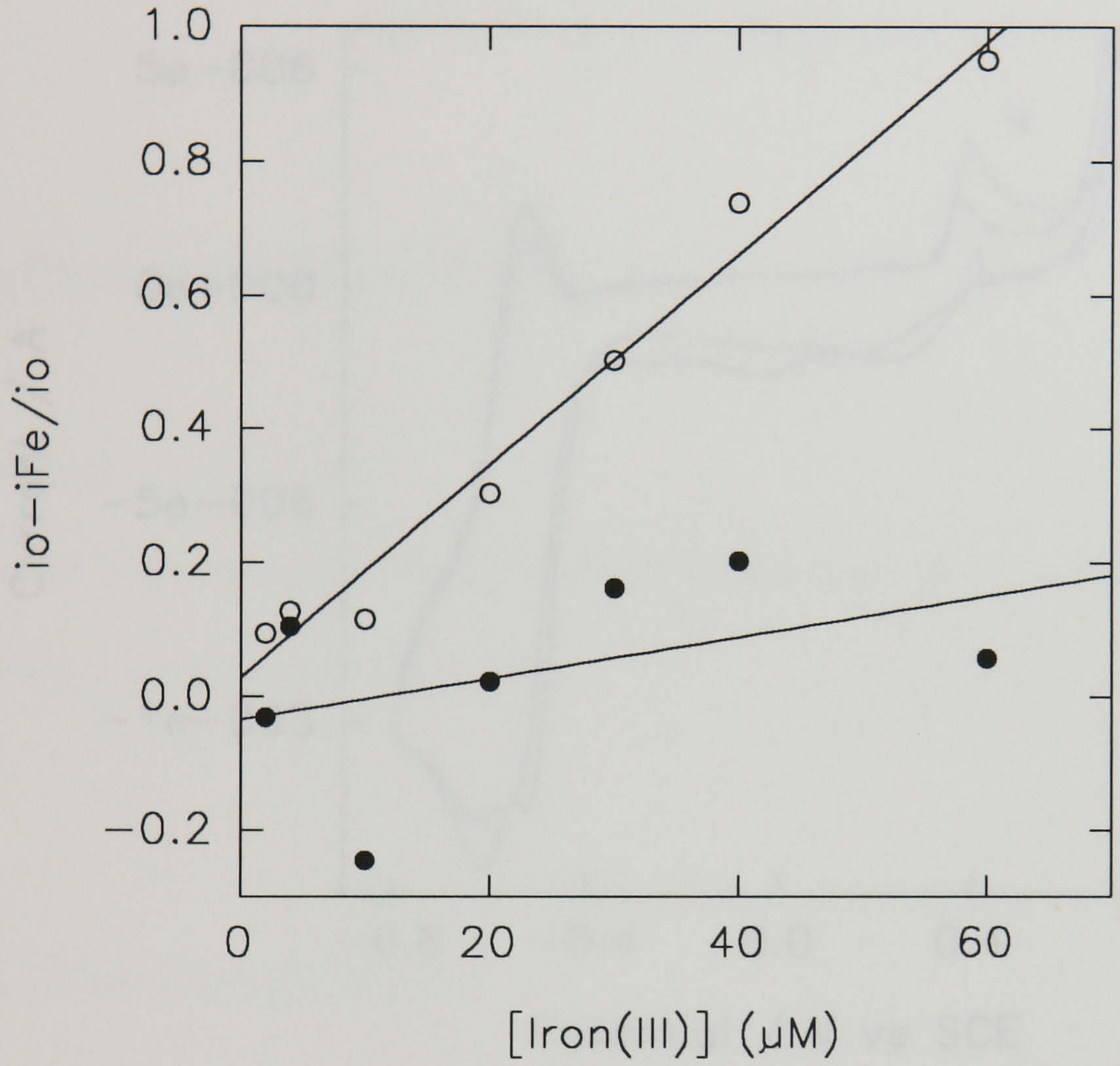

Fig. 2.8 Calibration of iron(III) by cyclic voltammetry, using desferrioxamine. The peak current at +430 mV was measured before (i_o) and after (i_{Fe}) the addition of iron(III). The proportion of current decrease (i_o-i_{Fe}/i_o) was plotted against iron(III) concentration (○) and against additions of an equal volume of de-ionized H_2O (●).

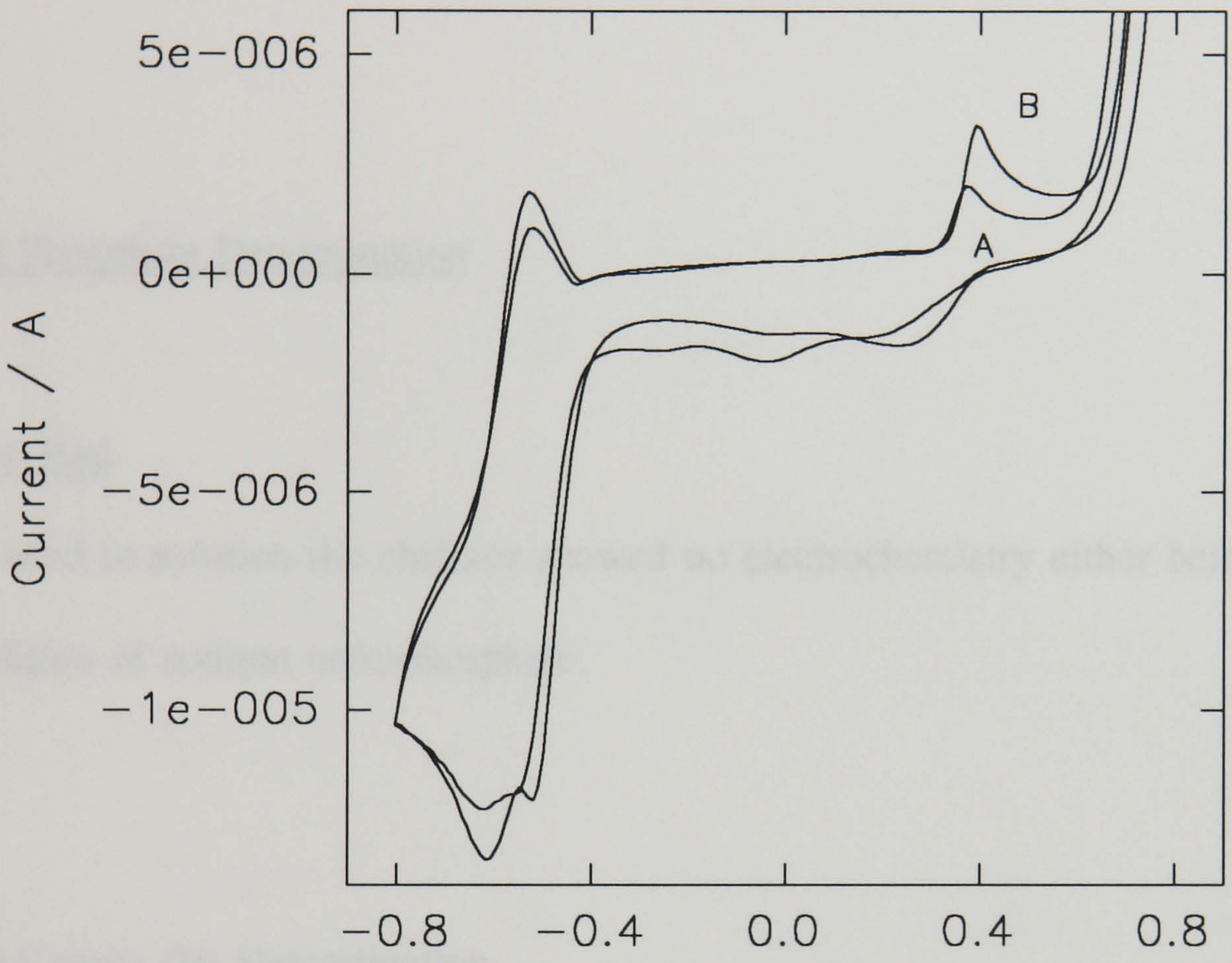

Fig. 2.9 Typical voltammogram of a 5 mM eriochrome cyanine solution at a carbon paste electrode. (B) represents the addition of Al^{3+} to the cell at a final concentration of 73 μM. Similar changes in electrochemistry were observed upon addition of de-ionized H_2O.

2.3.1.7 Cadmium Determination

Rhodamine B

When used in solution the chelator showed no electrochemistry, either before or after the addition of cadmium.

2.3.1.8 Phosphate Determination

Alizarin Red

When used in solution the chelator showed no electrochemistry either before or after the addition of sodium orthophosphate.

2.3.1.9 Copper (II) Determination

bis-Cyclohexanone Oxaldihydrazone

The modified electrodes showed no electrochemistry in buffer solution. As shown in Fig.2.10, complexation with copper gave rise to oxidation peaks at +235 and -100mV. The cyclic voltammogram of copper at an untreated carbon paste electrode (Fig. 2.11), demonstrated that the -100 mV peak could be ascribed to the electrochemistry of the copper; thus indicating that the peak at +235 mV was due to the oxidation of the ligand. This value is notably lower than the value reported by Compagnone *et al* (1991) (+350 mV) when using the ligand in solution with a glassy carbon working electrode.

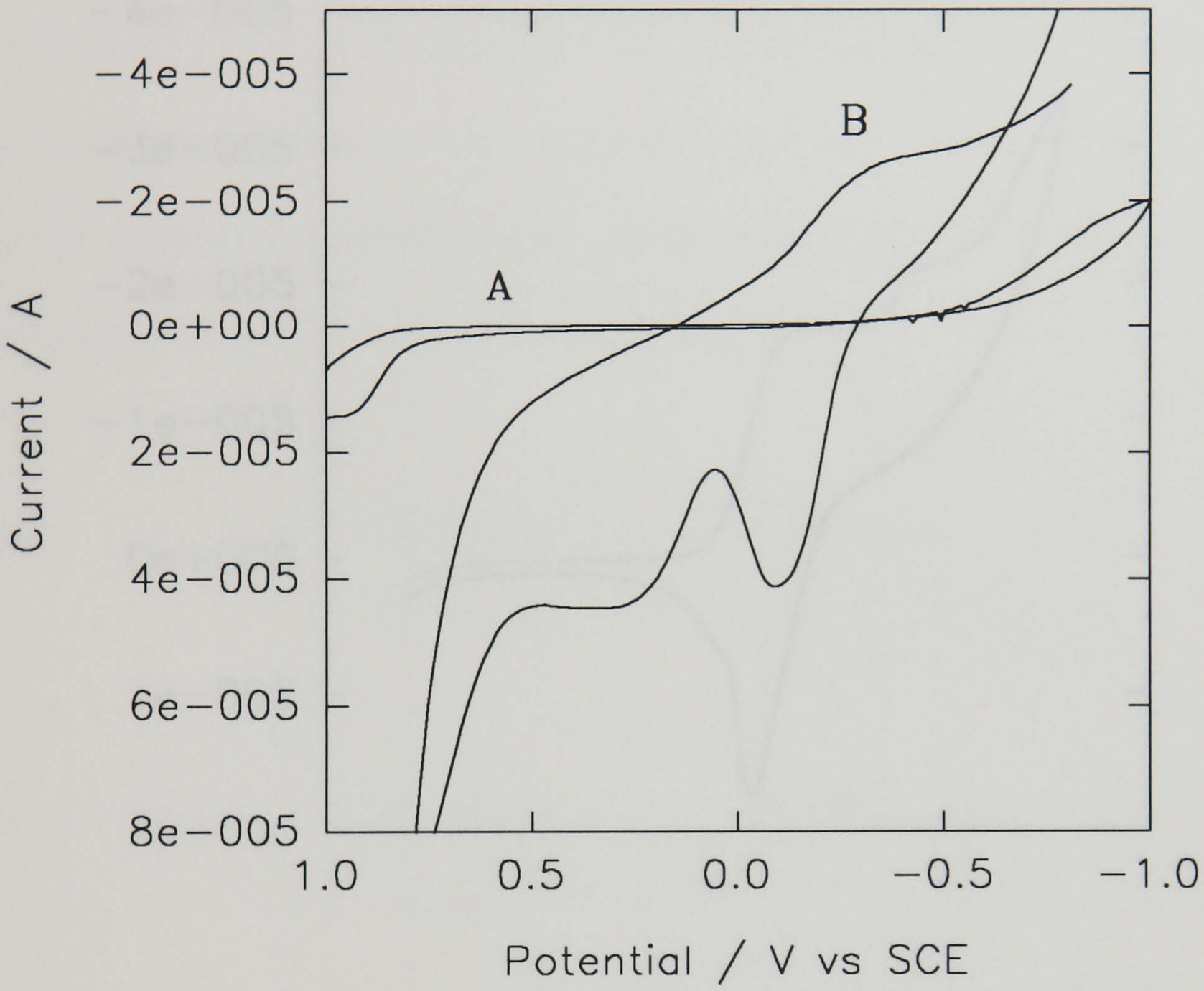

Fig. 2.10 Voltammograms of a bis-cyclohexanone oxaldihydrazone-modified carbon paste electrode in the absence (A) and presence (B) of a 2 mM copper (II) solution. Scan rate = 50 mV/s.

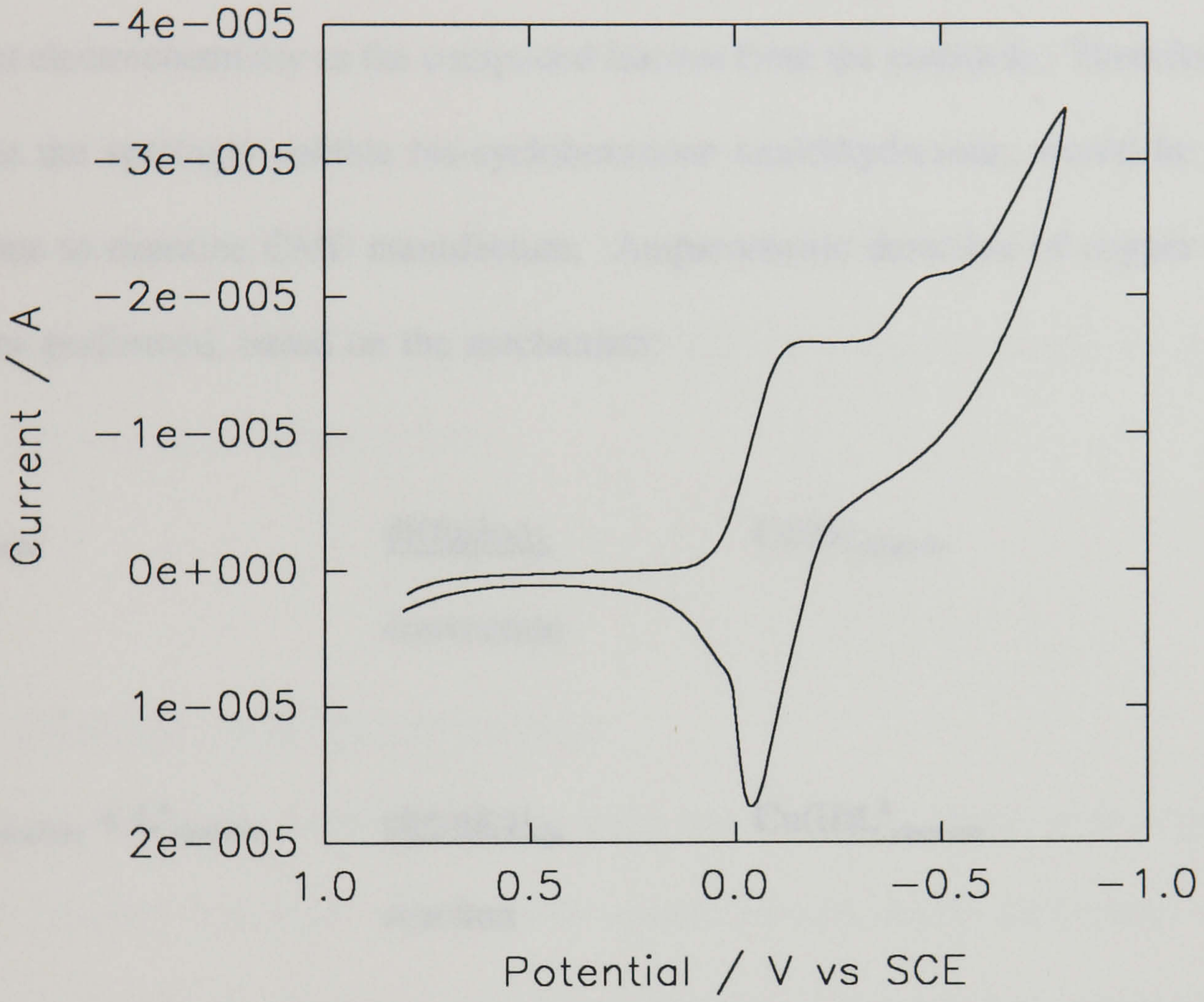

Fig. 2.11 Voltammogram of a 2 mM copper (II) solution at an un-modified carbon paste electrode. Scan rate = 50 mV/s.

2.3.2 Characterisation of Screen Printed CMEs

Both desferrioxamine and bis-cyclohexanone were examined for incorporation into screen printed CMEs. However, individually made carbon paste electrodes containing desferrioxamine showed unstable electrochemistry, with the +430 mV oxidation peak decreasing over time in buffered solution. This is likely to be due to changes in chelator electrochemistry as the compound leaches from the electrode. Therefore it was felt that the sparingly soluble bis-cyclohexanone oxaldihydrazone, would be a better candidate to examine CME manufacture. Amperometric detection of copper at +250 mV was performed, based on the mechanism:

$$Cu(II)_{bulk} \xrightarrow[\text{convection}]{\text{diffusion}} Cu(II)_{electrode}$$

$$Cu(II)_{electrode} + L^{x}_{electrode} \xrightarrow[\text{reaction}]{\text{chemical}} Cu(II)L^{x}_{electrode}$$

$$Cu(II)L^{x}_{electrode} \xrightarrow[\text{transfer}]{\text{electron}} Cu(II)L^{x+n}_{electrode} + ne^{-}$$

2.3.2.1 Ligand Concentration

Individually made modified electrodes were used to examine the effects of carbon paste composition on the amperometric copper response. Nine different graphite:ligand ratios were examined, ranging from 10:1 to 1:10. For each ratio, the steady-state current produced by a copper concentration of 0.2 mM was measured. Five electrodes were

employed in each case. The results, given in Fig. 2.12, show that initially the response increased with increasing ligand content. This is to be expected, as a higher ligand concentration will mean a greater number of ligand molecules present at the electrode surface, available for complexation. Maximium copper response was obtained using a ligand content of 50%. Above this concentration, electrodes gave lower activities with the 90% ligand electrodes giving a zero response. This is likely to be due to the high ligand concentrations lowering the conductivity of the carbon paste and also reflects the fact that at higher ligand concentrations, slightly more liquid paraffin was needed to hold the paste together. Screen printed electrodes were therefore made using carbon paste with a ligand content of 50%.

2.3.2.2 Fabrication of Working Electrodes

Screen printing of the modified carbon paste was attempted, using both organic and aqueous printing solutions. The organic system proved clearly unsuitable, with the graphite and solvent separating out during printing. The aqueous system gave an adequate print quality and was therefore used for all further electrode fabrication.

2.3.2.3 pH Profile

The assay pH was varied from 7.0 to 9.0 using 50 mM Tris-HCl. At each pH the response of five screen-printed electrodes to a 0.1 mM copper solution was measured. The results, given in Fig.2.13, show a maximum copper response at pH 8.0. All further experiments were performed at this pH. Peterson and Bollier (1955), when using the ligand for colorimetric determinations, found a pH-independent response from pH 7.0

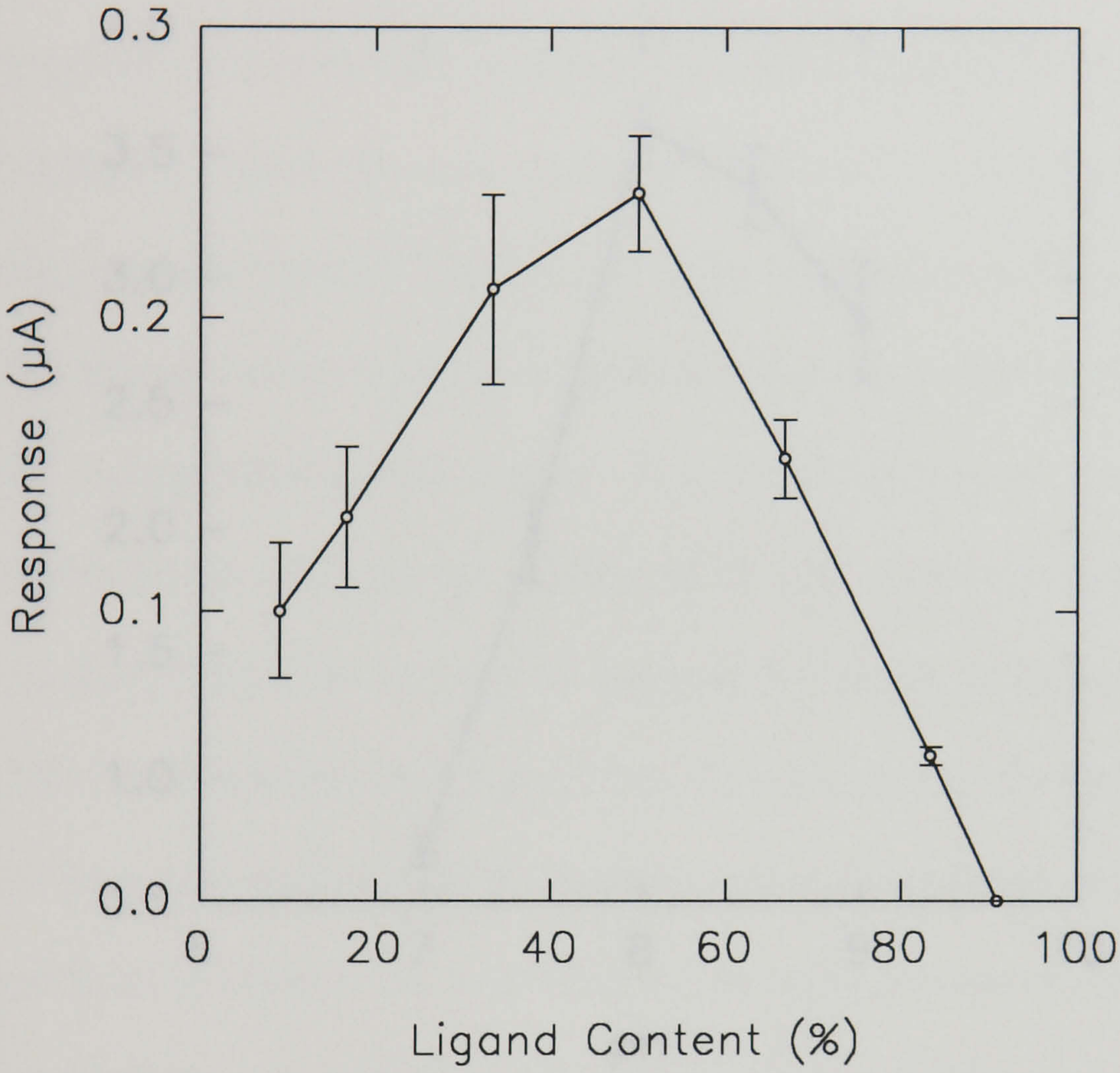

Fig. 2.12 Effect of ligand concentration on response of modified electrodes to 0.2 mM copper. Error bars give S.E.M. (n = 5).

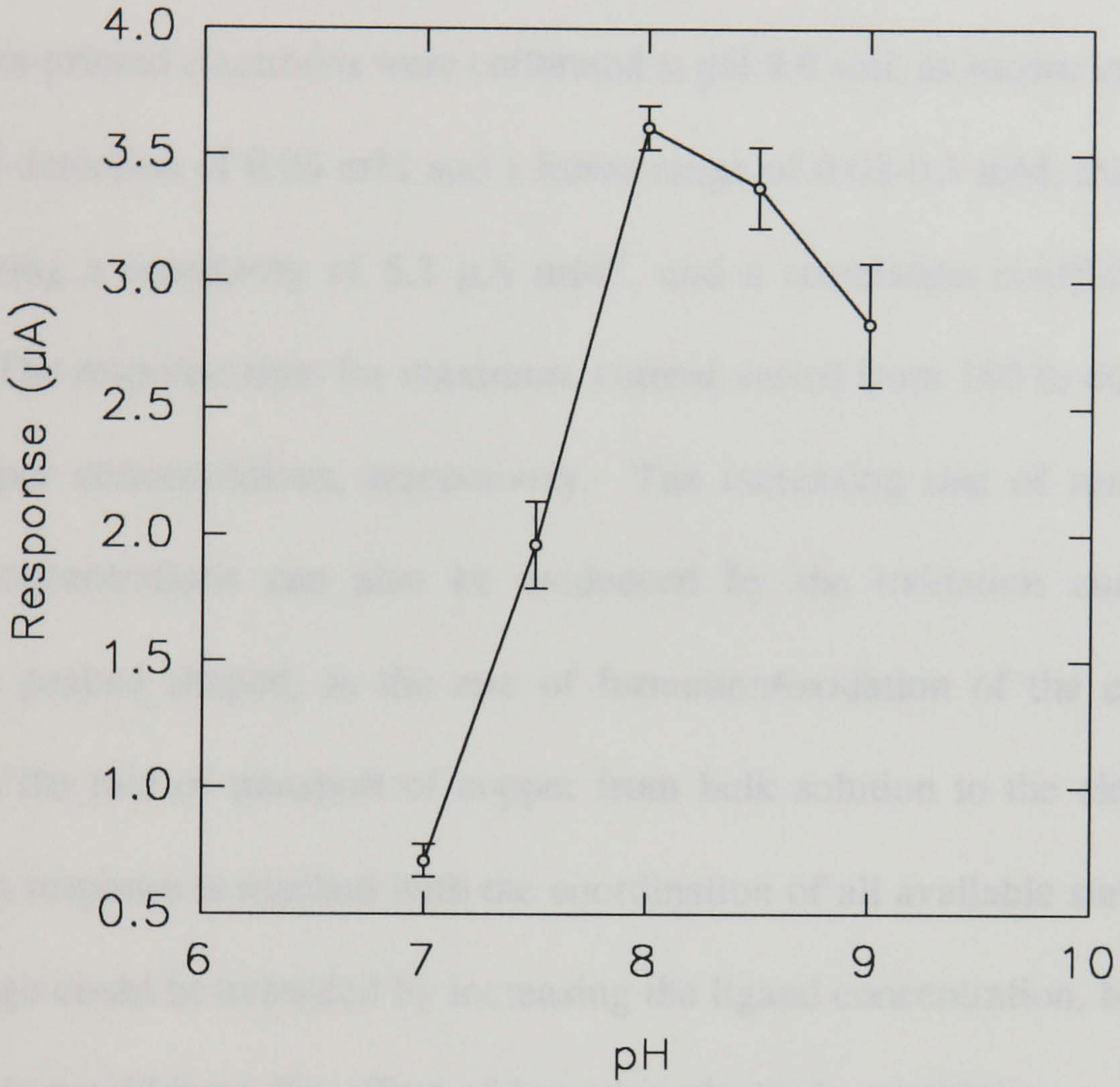

Fig. 2.13 Effect of pH on response of modified electrodes to 0.1 mM copper. Error bars give S.E.M. (n = 5).

to 9.5. This suggests these results reflect the pH sensitivity of the oxidation of the copper complex, rather than its formation.

2.3.2.4 Calibration of Copper Response

The screen-printed electrodes were calibrated at pH 8.0 and, as shown in Fig. 2.14, gave a limit of detection of 0.03 mM and a linear range of 0.03-0.3 mM, this portion of the curve giving a sensitivity of 5.2 μA mM^{-1}. and a correlation coefficient of r=0.983 (n=13). The response time for maximum current varied from 180 to 40 sec. for low to high copper concentrations, respectively. The increasing rate of reaction at higher copper concentrations can also be evidenced by the oxidation current becoming gradually peaked shaped, as the rate of formation/oxidation of the copper complex overtakes the rate of transport of copper from bulk solution to the electrode surface. Saturation response is reached with the coordination of all available surface sites. The linear range could be extended by increasing the ligand concentration, but as illustrated earlier, this would have the effect of lowering electrode sensitivity.

2.3.2.5 Precision of Copper Response

The coefficient of variance of the copper response (10 determinations) was measured at low (0.05 mM), medium (0.15 mM) and high (0.3 mM) concentrations and was found to be 9.3, 7.4 and 5.8% respectively. Full results are given in Table 2.1.

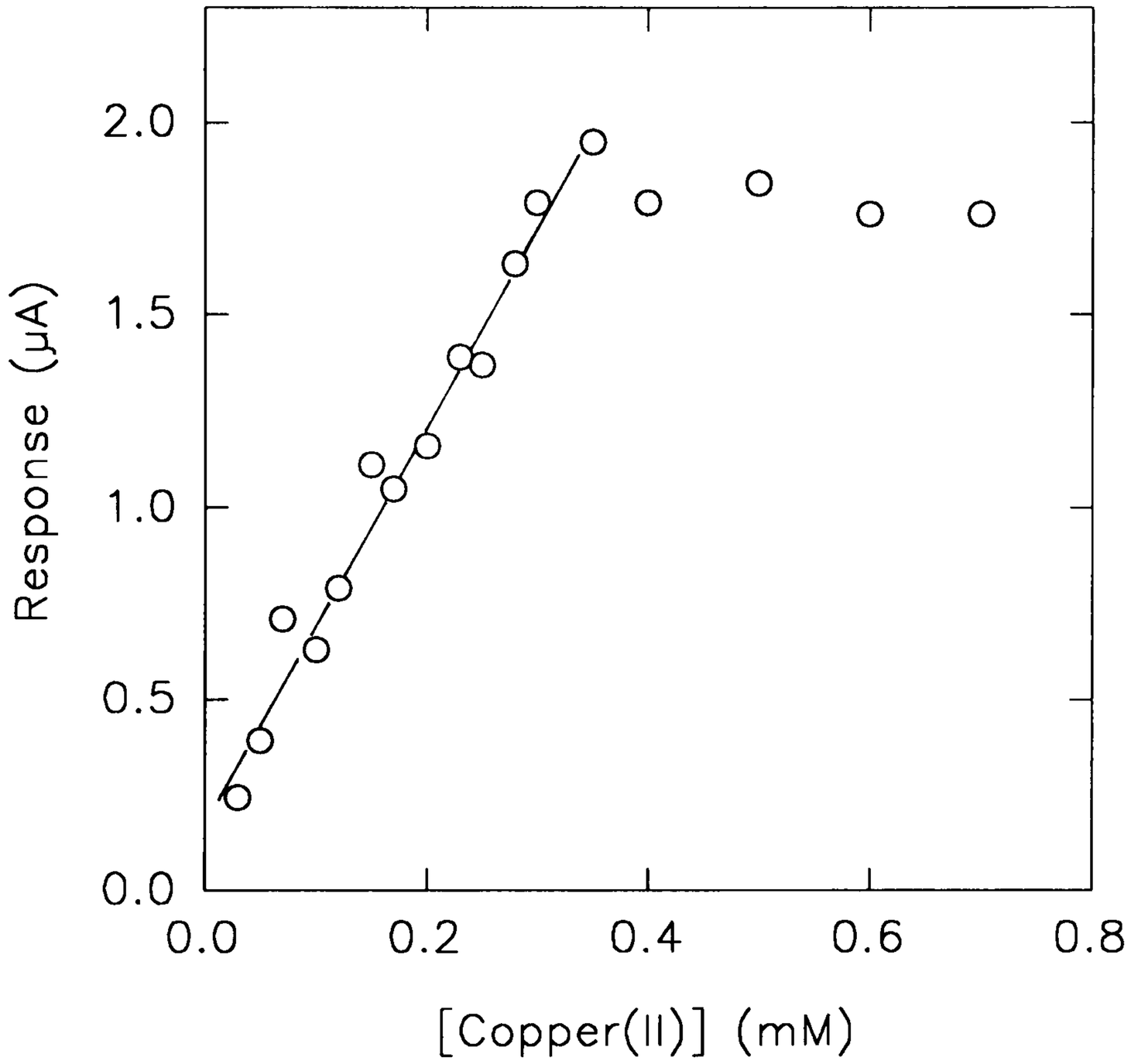

Fig. 2.14 Calibration of copper(II) at +250 mV vs SCE, pH 8.0, using bis-cyclohexanone-modified electrodes. Linear portion of curve gives $r = 0.983$, $n = 13$.

Table 2.1 Precision of copper(II) response at varying copper concentrations.

0.05 mM Cu^{2+}	0.15 mM Cu^{2+}	0.30 mM Cu^{2+}
Response (μA)	Response (μA)	Response (μA)
0.47	1.84	2.89
0.47	1.74	2.95
0.53	1.71	2.92
0.47	1.63	2.92
0.43	1.79	3.34
0.46	1.84	3.13
0.47	1.47	3.32
0.50	1.74	3.13
0.58	1.92	3.32
0.55	1.84	3.08
C.V. 9.3 %	7.4 %	5.8 %

2.3.2.6 Stability of Response

After fabrication in bulk, the electrodes were stored at below 4 °C for a period of 62 days. During this time they were removed in batches and used to construct calibration curves. The sensitivity, linear range and correlation coefficient of the plots were noted. The results, summarized in Table 2.2, show the sensitivity of the electrodes to have almost doubled in the first 10 days following printing. This is likely to be due to the remaining printing solution evaporating over this period. Such an effect would increase the porosity of the working layer, thus increasing the available surface area. The sensitivity of the electrodes remained approximately constant for up to 34 days, at a mean value of 9.8 ± 0.8 $\mu A.mM^{-1}$. The electrodes tested at 62 days showed a decrease in both sensitivity and precision (Table 2.2). However, the linearity of the electrodes remained constant throughout this period.

2.3.2.7 Temperature Profile

The copper response of the electrodes was measured at temperatures ranging from 25 to 75°C. At each temperature the oxidative current produced by 0.1 and 0.2 mM copper was noted; each concentration being assayed in duplicate. As shown in Fig. 2.15, the copper response continued to increase with temperature up to 75 °C. At above 45 °C, the oxidative current was in the form of a peak rather than the usual plateau response. This is again likely to be due to the rate of formation/oxidation of the copper complex overtaking the rate of mass transport. It is also possibly due to the breakdown of the chelator, which in a solid form needs to be stored at below 4 °C. The results of the temperature profile were used to calculate the activation energy of the overall electrode reaction (chemical followed by electrochemical) using the Arrhenius equation, given

Table 2.2 Long term stability of screen-printed, ligand-modified electrodes. Electrodes were stored dry, below 4 °C prior to measurement.

Time (Days)	Sensitivity ($\mu A\ mM^{-1}$)	Correlation Coefficient (r)
1	5.2	0.983
10	10.5	0.990
15	9.2	0.936
22	9.3	0.981
34	10.0	0.952
62	7.8	0.866

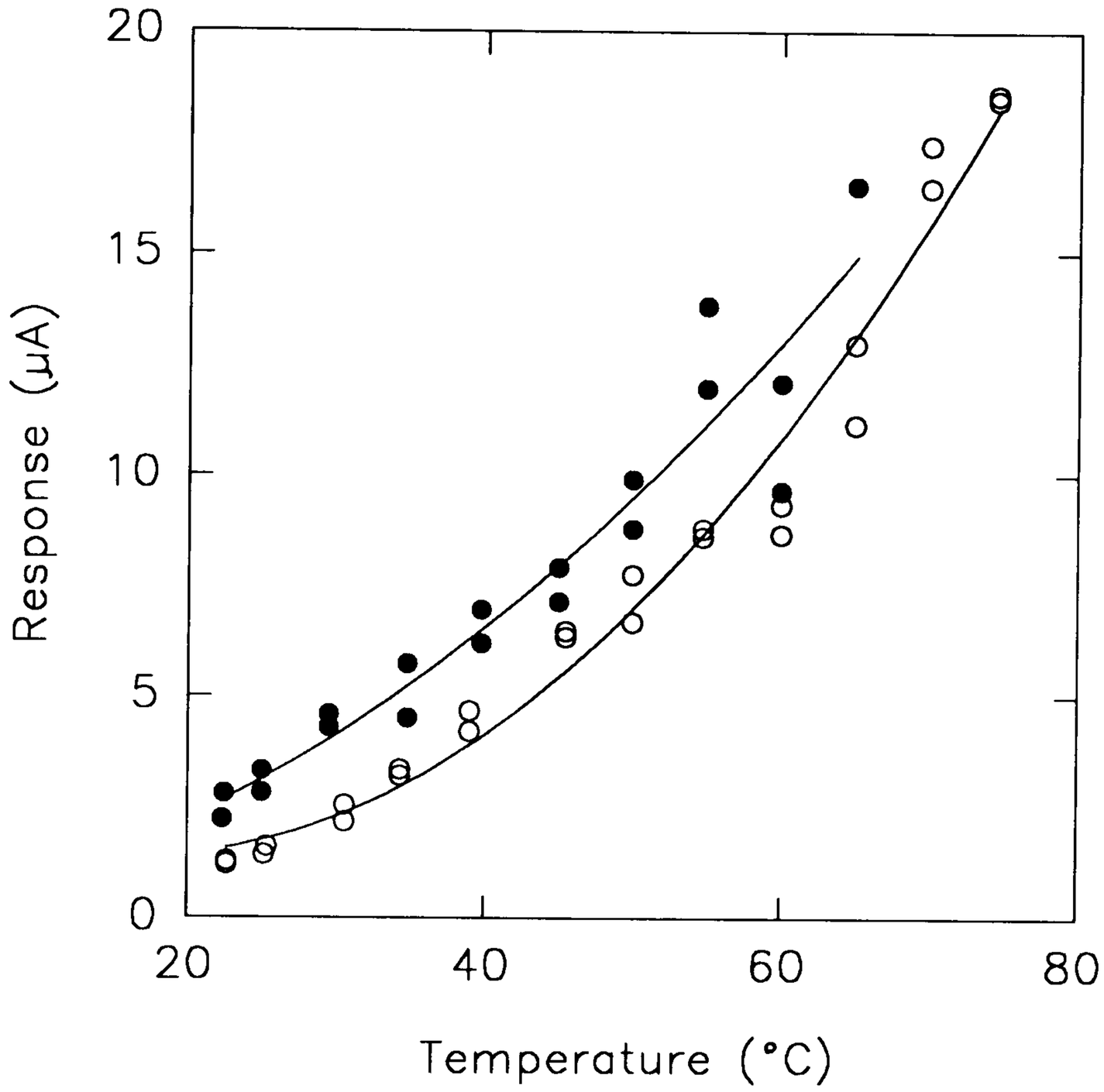

Fig. 2.15 Effect of temperature on the response of screen-printed modified electrodes to 0.1 mM (○) and 0.2 mM (●) copper.

below:

$$Kr = A \exp(-Ea/RT) \qquad (2.7)$$

Where Kr is the reaction rate in Amps and Ea is the activation energy in KJ mol^{-1}.

Plots of ln Kr against 1/T for both copper concentrations (Fig. 2.15.1 & 2.15.2), gave a mean activation energy of 36 $\pm$ 3 $KJ.mol^{-1}$.

2.3.2.8 Interferents

The effect of competing cations on the formation of the copper-ligand complex was examined. The steady-state current produced by 0.1 mM copper was measured five times in the absence of interferents and five times in the presence of increasing concentrations of another cation. As illustrated in Figs. 2.16.1 to 2.16.8 , the copper response was unaffected by the presence of magnesium, barium, calcium or cobalt ions in concentrations of up to 1.6 mM and ammonium ion concentrations of up to 3.2 mM. Nickel, zinc and iron (III) all had the effect of lowering the copper response with increasing interferent concentration. This suggests that these metals undergo complexation with bis-cyclohexanone oxaldihydrazone, but unlike copper (II), do not effect the electrochemistry of the chelator. Nickel began to cause a decrease in copper response at concentrations of approximately 0.2 mM. The exact point of interference for zinc and iron(III) is harder to determine as the copper response in the absence of these ions also goes down to equally low values. This is likely to be due to contamination caused by these ions adsorbing strongly to the inner walls of the electrochemical cell following measurement and thus lowering the response to subsequent copper additions.

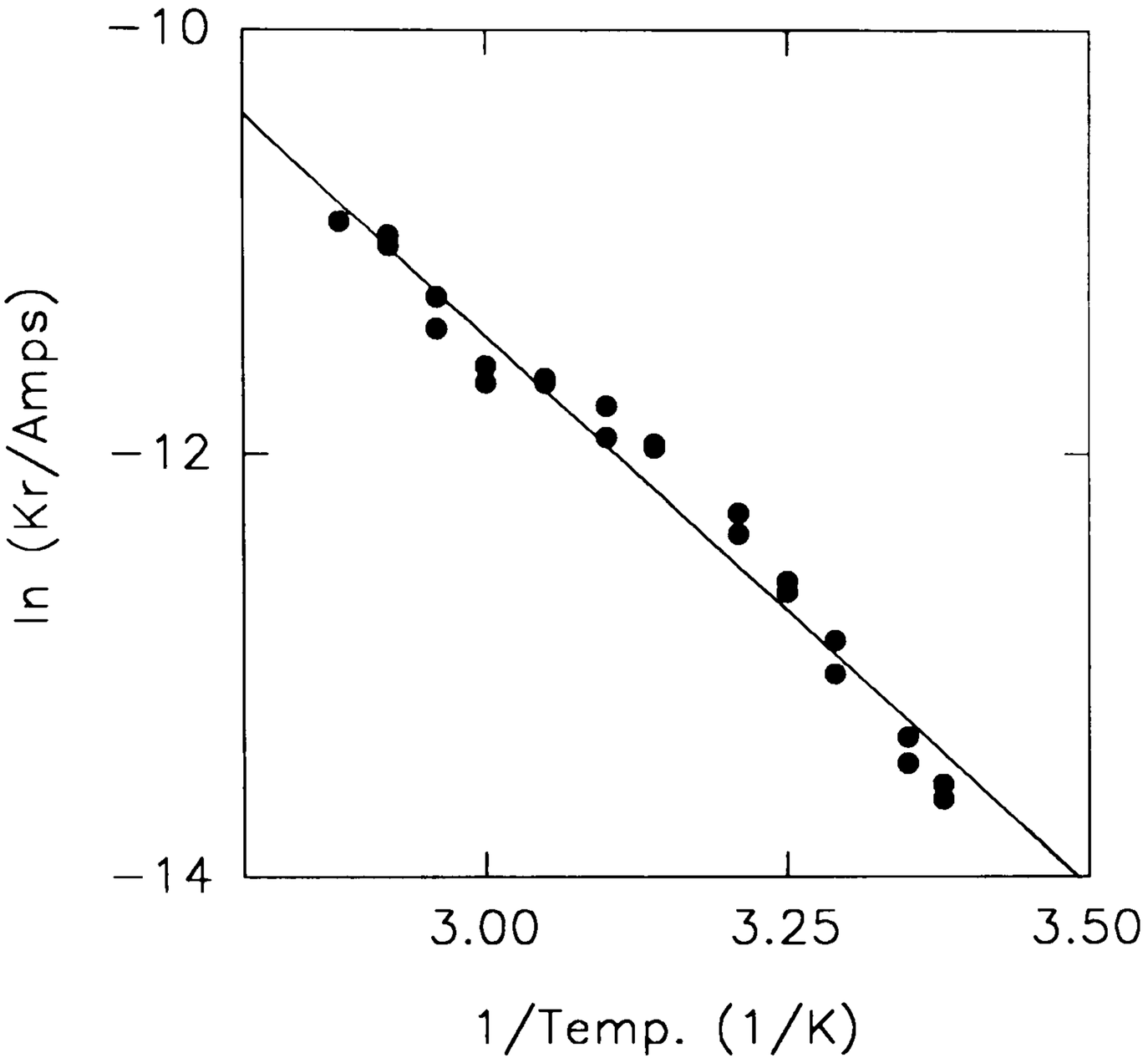

Fig. 2.15.1 Arrhenius plot for the response of modified electrodes to 0.1 mM copper

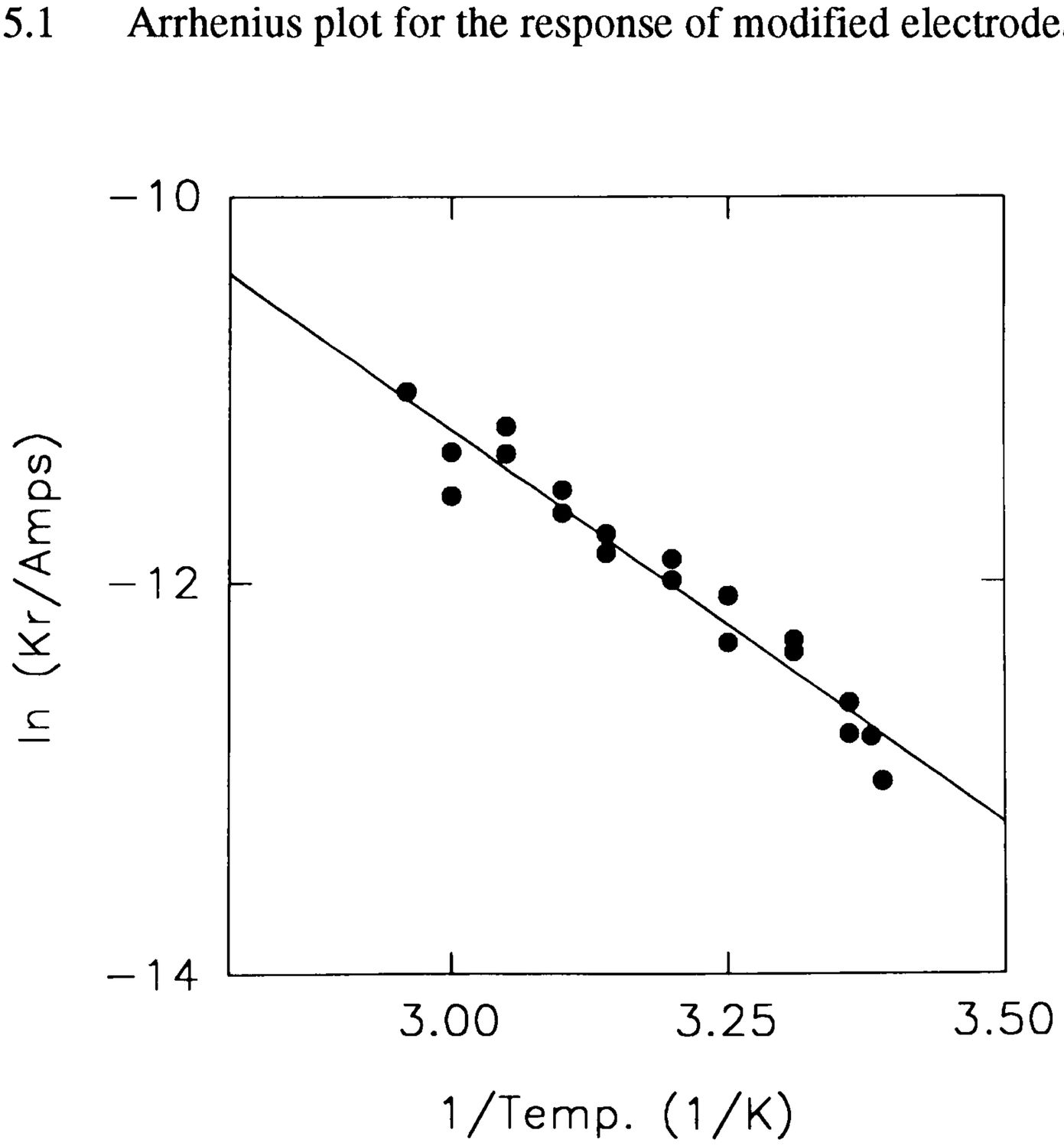

Fig. 2.15.2 Arrhenius plot for the response of modified electrodes to 0.2 mM copper.

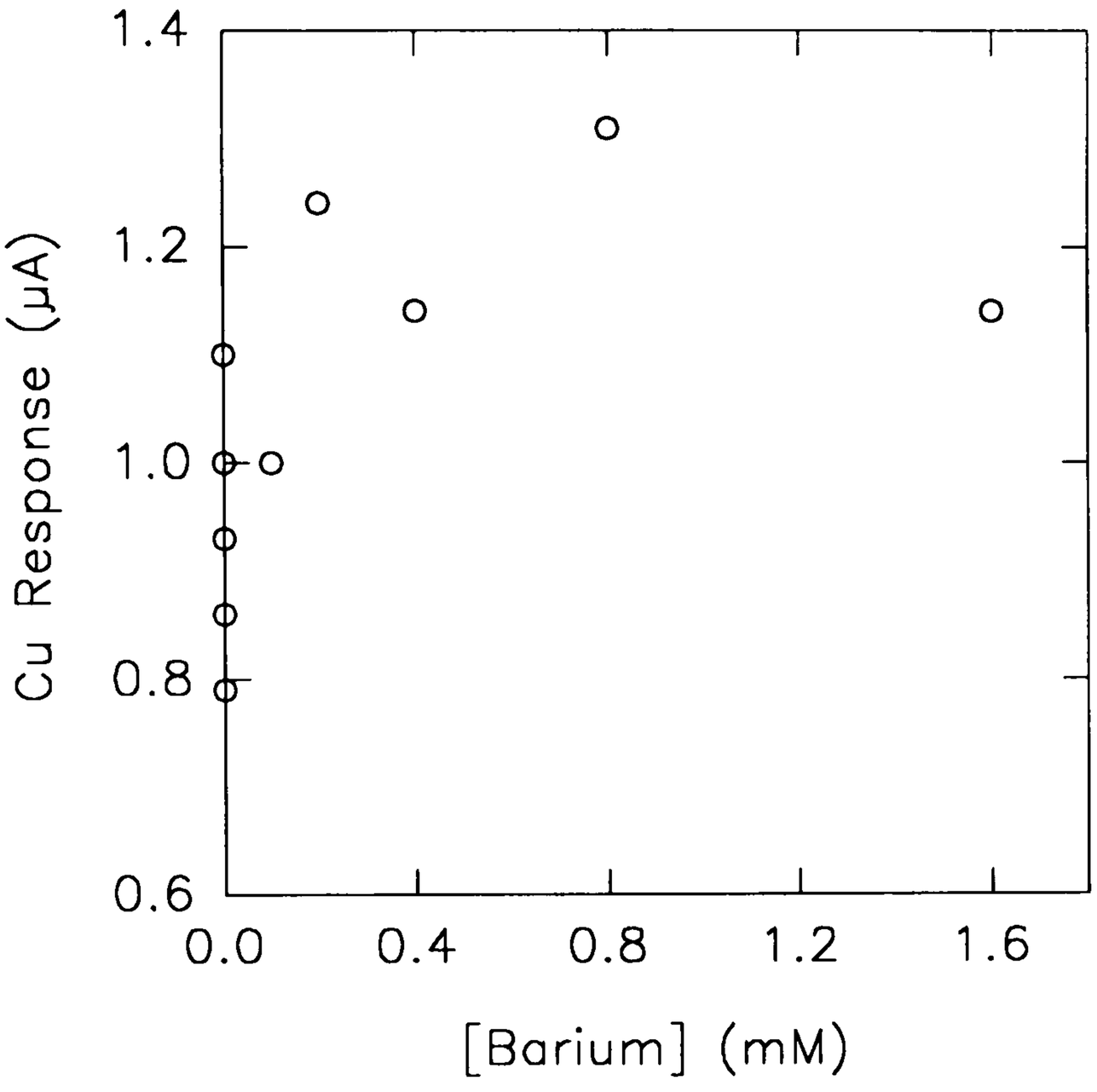

Fig. 2.16.1 Effect of barium on the response of modified electrodes to 0.1 mM copper.

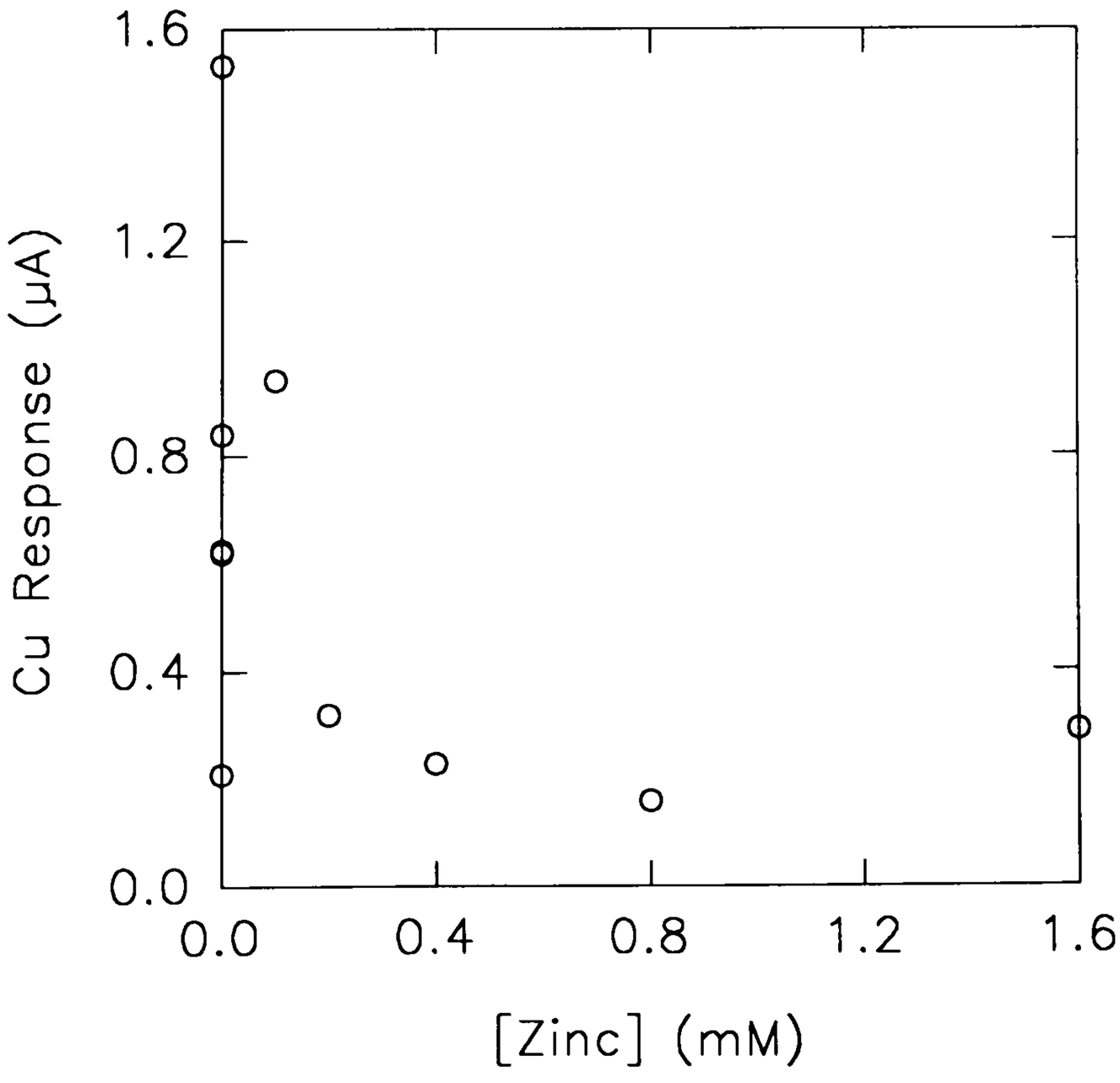

Fig. 2.16.2 Effect of zinc on the response of modified electrodes to 0.1 mM copper.

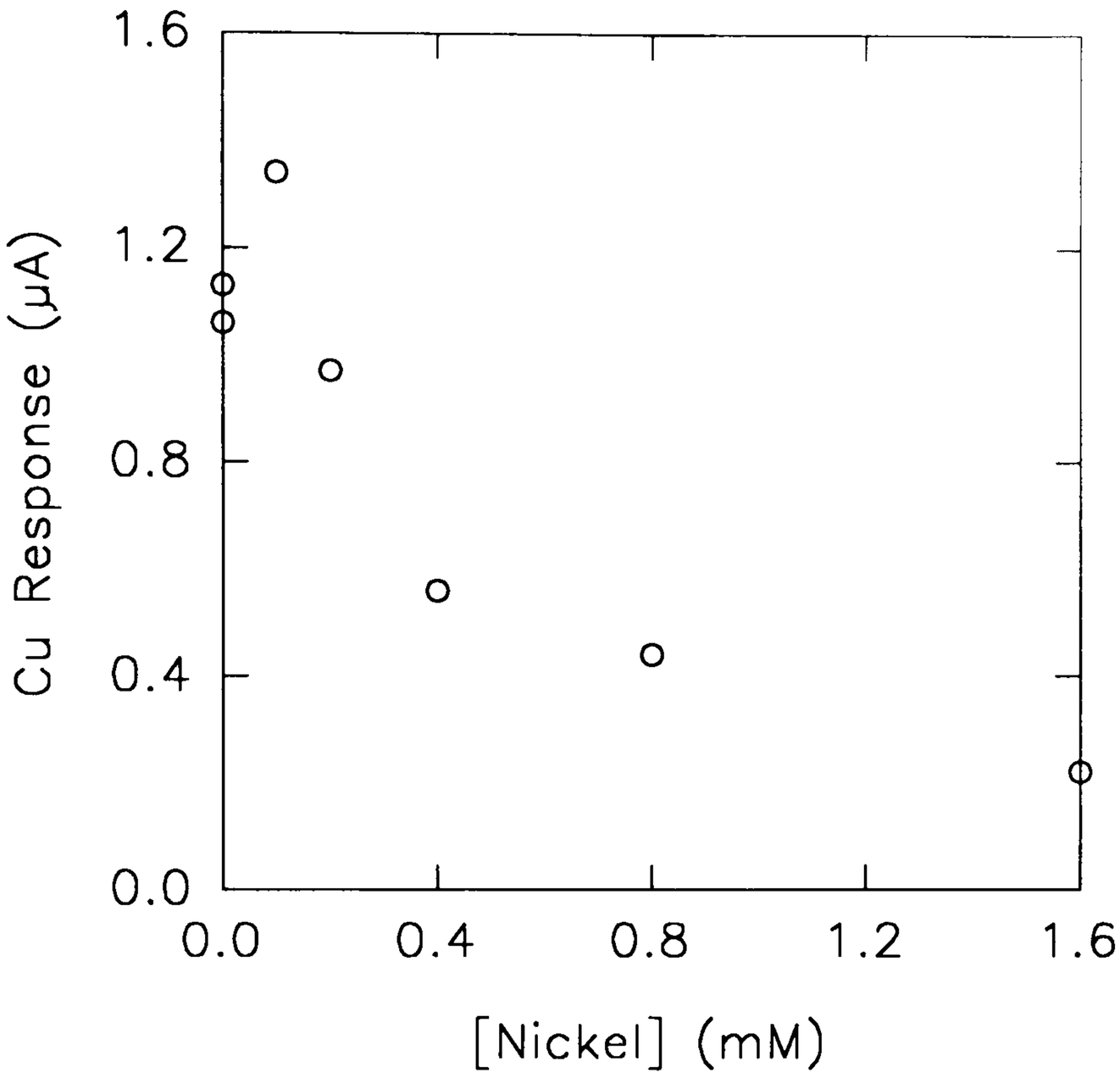

Fig. 2.16.3 Effect of nickel on the response of modified electrodes to 0.1 mM copper.

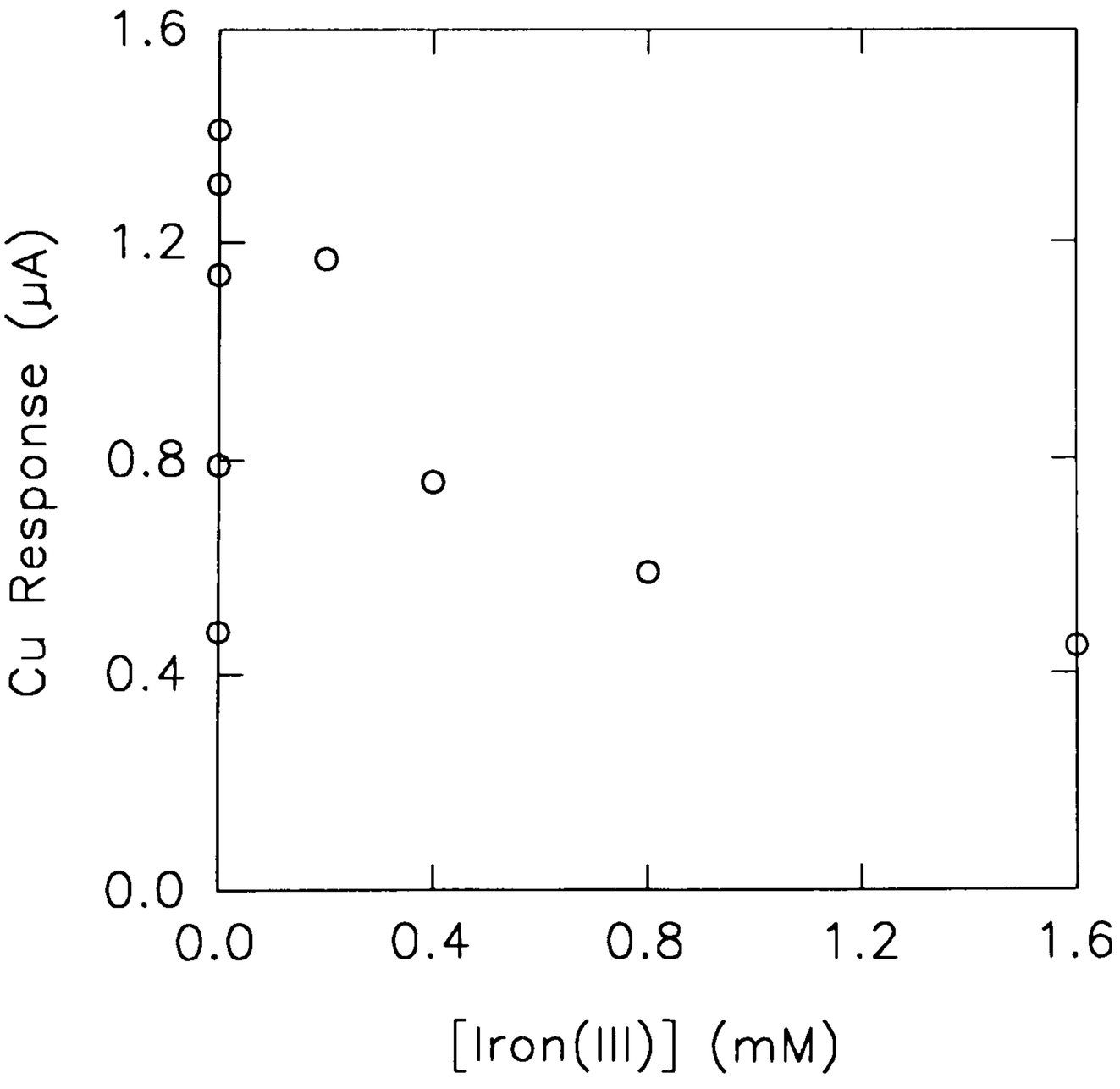

Fig. 2.16.4 Effect of iron(III) on the response of modified electrodes to 0.1 mM copper.

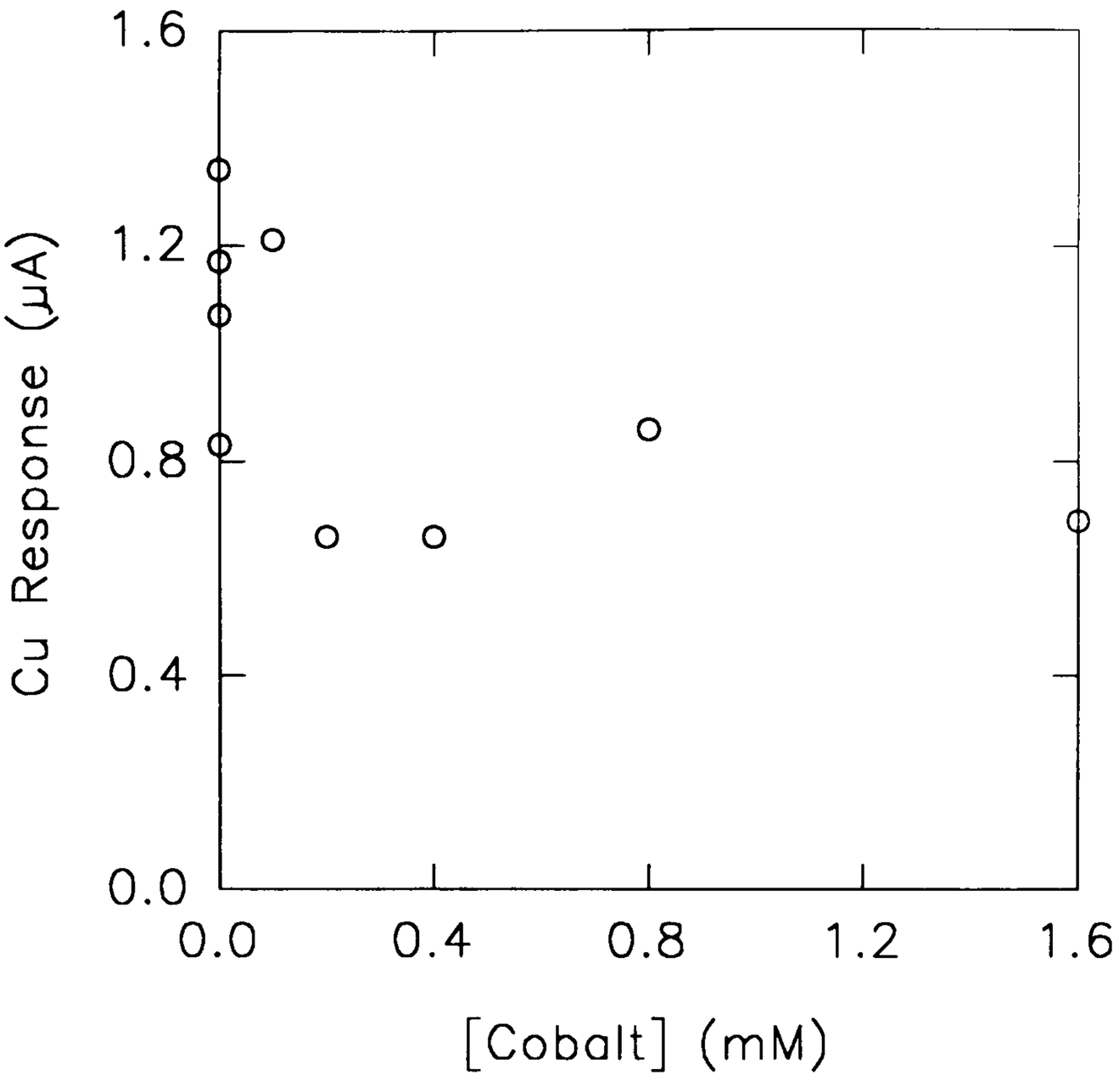

Fig. 2.16.5 Effect of cobalt on the response of modified electrodes to 0.1 mM copper.

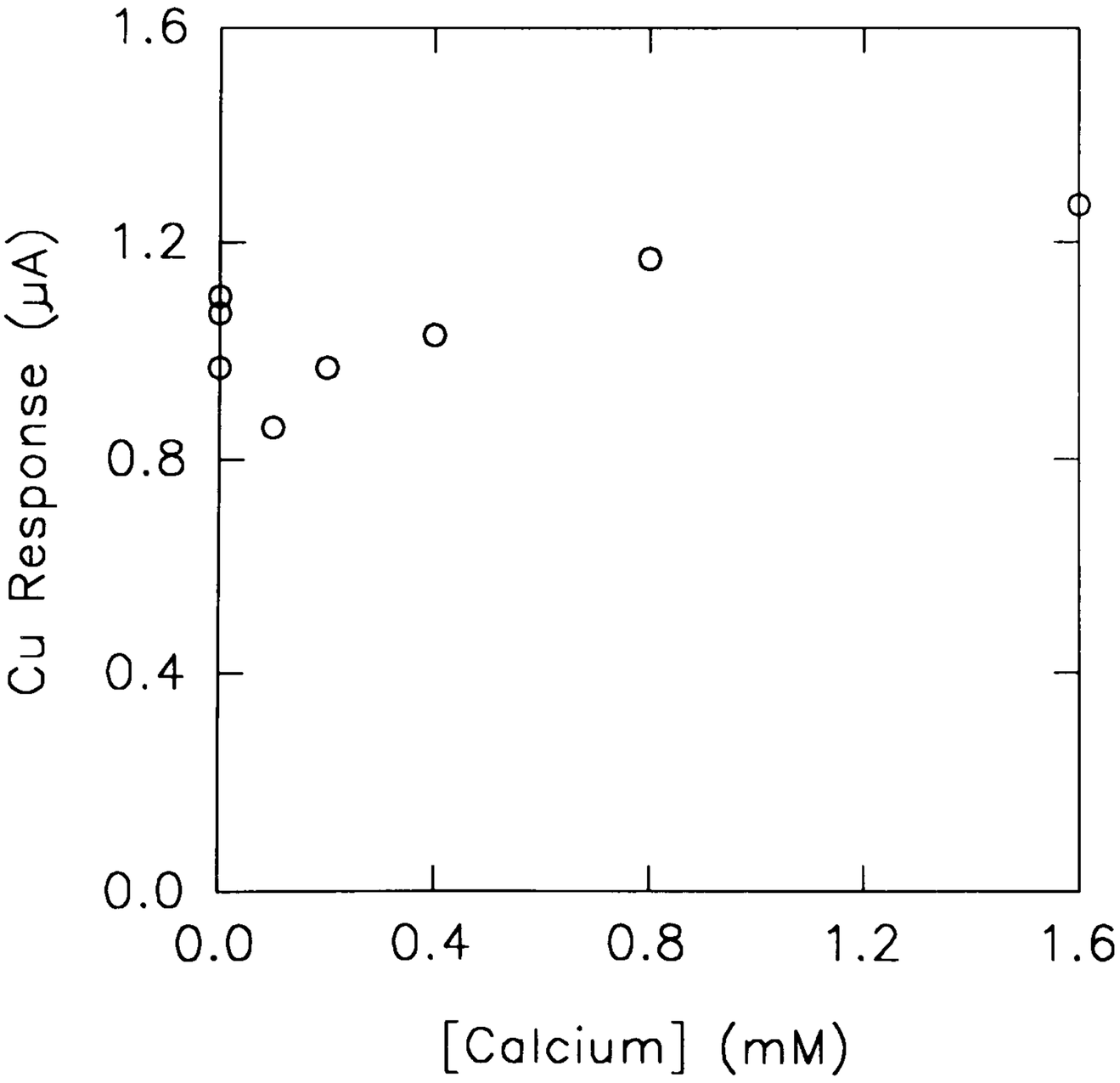

Fig. 2.16.6 Effect of calcium on the response of modified electrodes to 0.1 mM copper.

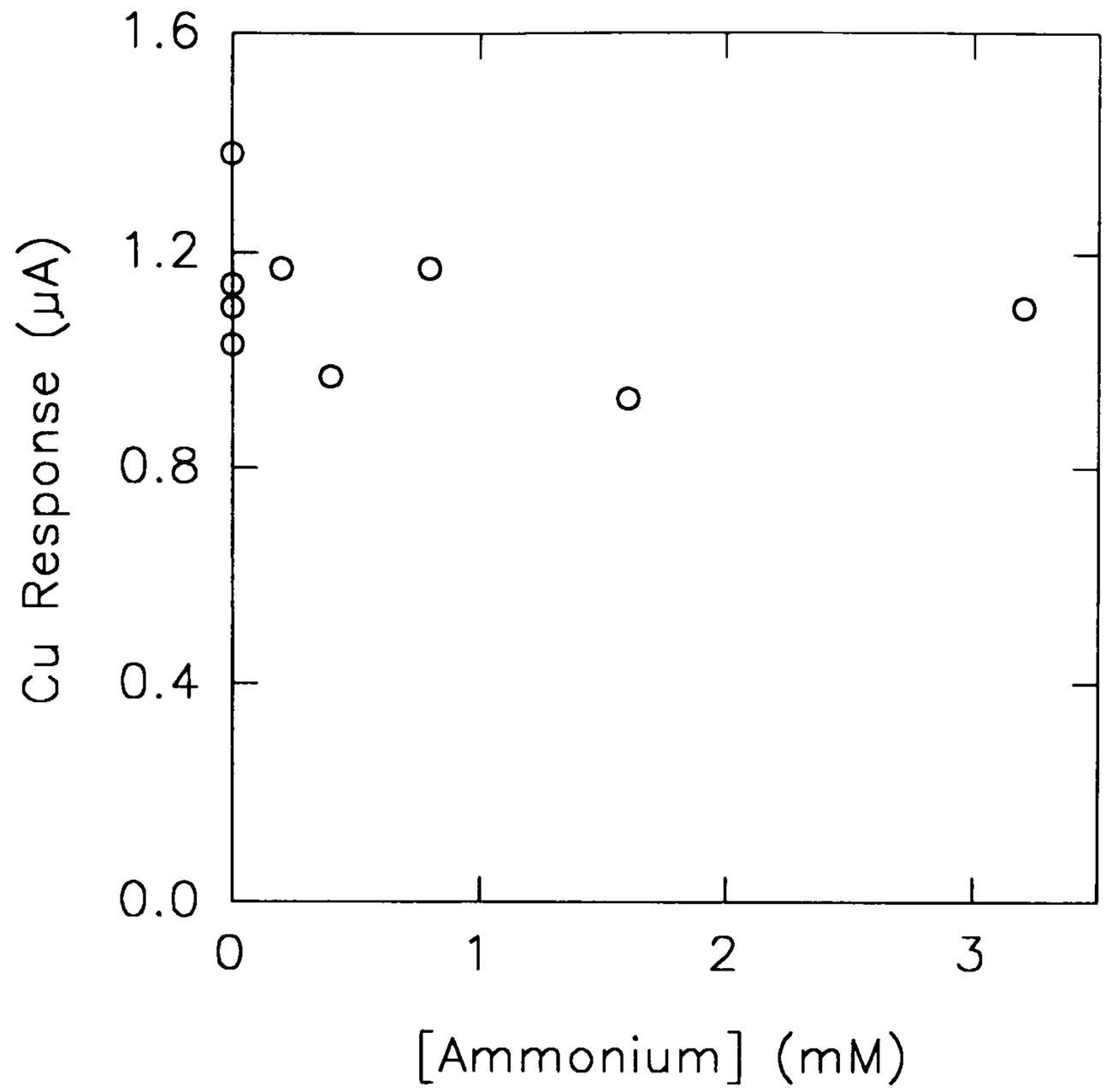

Fig. 2.16.7 Effect of ammonium ions on the response of modified electrodes to 0.1 mM copper.

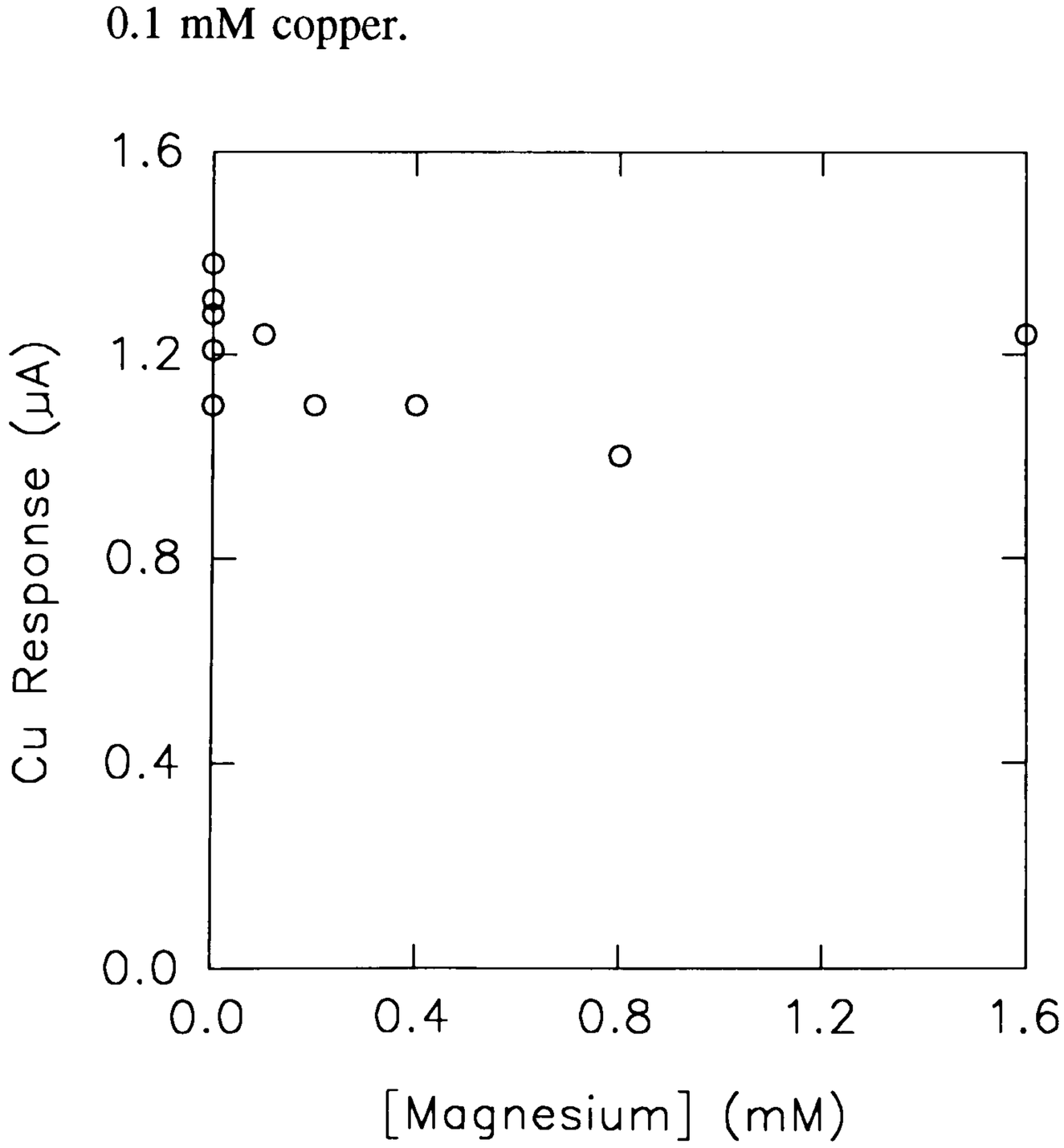

Fig. 2.16.8 Effect of magnesium on the response of modified electrodes to 0.1 mM copper.

2.3.3 Nature of bis-Cyclohexanone oxaldihydrazone-Cu Complex

In aqueous solution copper(II) exists within a distorted octahedral of the form $[Cu(H_2O)_6]^{2+}$. Addition of a stronger ligand to the solution will bring about subsequent displacement of the water molecules. The structure of bis-cyclohexanone oxaldihydrazone, as given in Fig.2.17, shows both amine and carbonyl groups in relatively unhindered positions and therefore available as electron donors. Complexation of copper by the ligand results in an increase in absorbance at 600 nm, relative to the hexaquo complex, as first described by Bollier and Peterson (1955). This suggests bonding to a species which produces a stronger ligand field than H_2O. Thus it is likely that the complex includes amine --> Cu bonds, as most known carbonyl groups (CH_3COO^-, $C_2O_4^{2-}$ etc.) are below H_2O in the spectrochemical series (Nicholls, 1974) and will therefore produce a *lower* crystal field split.

The stoichiometry of the complex was examined using the method of continuous variations (Hartley *et al.*, 1980). A series of solutions were prepared such that the total metal and total ligand concentration remained constant at 0.5 mM, while varying the molar ratio of ligand : Cu from 1:9 to 9:1. The solutions were prepared in the absence of Tris-HCl to avoid the possible effect of complexation of copper by the buffer. The absorbance of each solution was measured at 600 nm and was plotted as a function of the molar ratio, as shown in Fig. 2.18. The Cu : ligand ratio appeared to be either 2:1 or 3:2. The most likely structures for the complex from these observations, are shown in Fig. 2.17. Form II, involving the formation of a six-membered ring, would perhaps be the most stable.

2.3.4 Nature of Electrochemical Change

Desferrioxamine

The electrochemical change exhibited by desferrioxamine upon complexation, is of a similar nature to that found by previous workers, when applying other ligands to this method of analysis (ie. those mentioned in the introduction to this chapter, Compagnone *et al*, 1992; McCracken *et al*, 1987 etc.). That is, the presence of the cation causes the ligand oxidation peak to be either suppressed, or shifted to a more positive potential. This can be viewed as an electrostatic effect, in which the attractive force of the cation shifts the electron density of the redox active part of the ligand, so that either greater energy is required to remove these electrons, or in cases like desferrioxamine, the electrons can no longer be removed. This perturbation can either occur through space (if complexing and redox sites are close enough, Miller *et al*, 1988), or can be conducted through an appropriate linkage, such as the conjugated π electron system used by Beer *et al* (1990a). This view of the cations' effect is supported by Beers' (1990b) results, which show the positive shift of the ferrocene redox couple increasing with cations of increasing charge/size ratio.

Bis-Cyclohexanone Oxaldihydrazone (BCO)

Unlike desferrioxamine, the electrochemical change exhibited by BCO is in contradiction to the previous results obtained in this field. The explanation for this is currently unclear and would probably require, as a first step, the full elucidation of the copper-ligand complex. This could perhaps be achieved using X-ray crystallography. However, such studies were considered beyond the scope of this thesis.

I

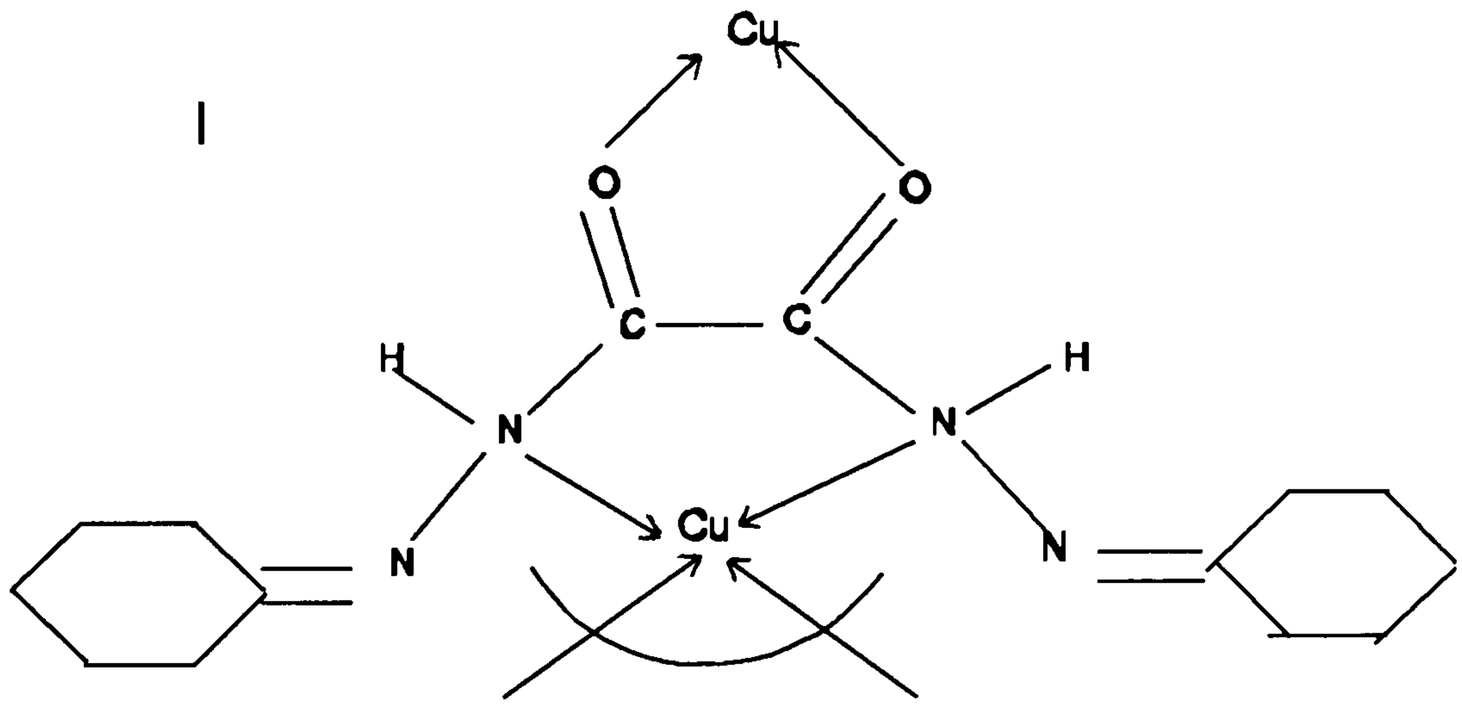

2nd Cu-Complex

II

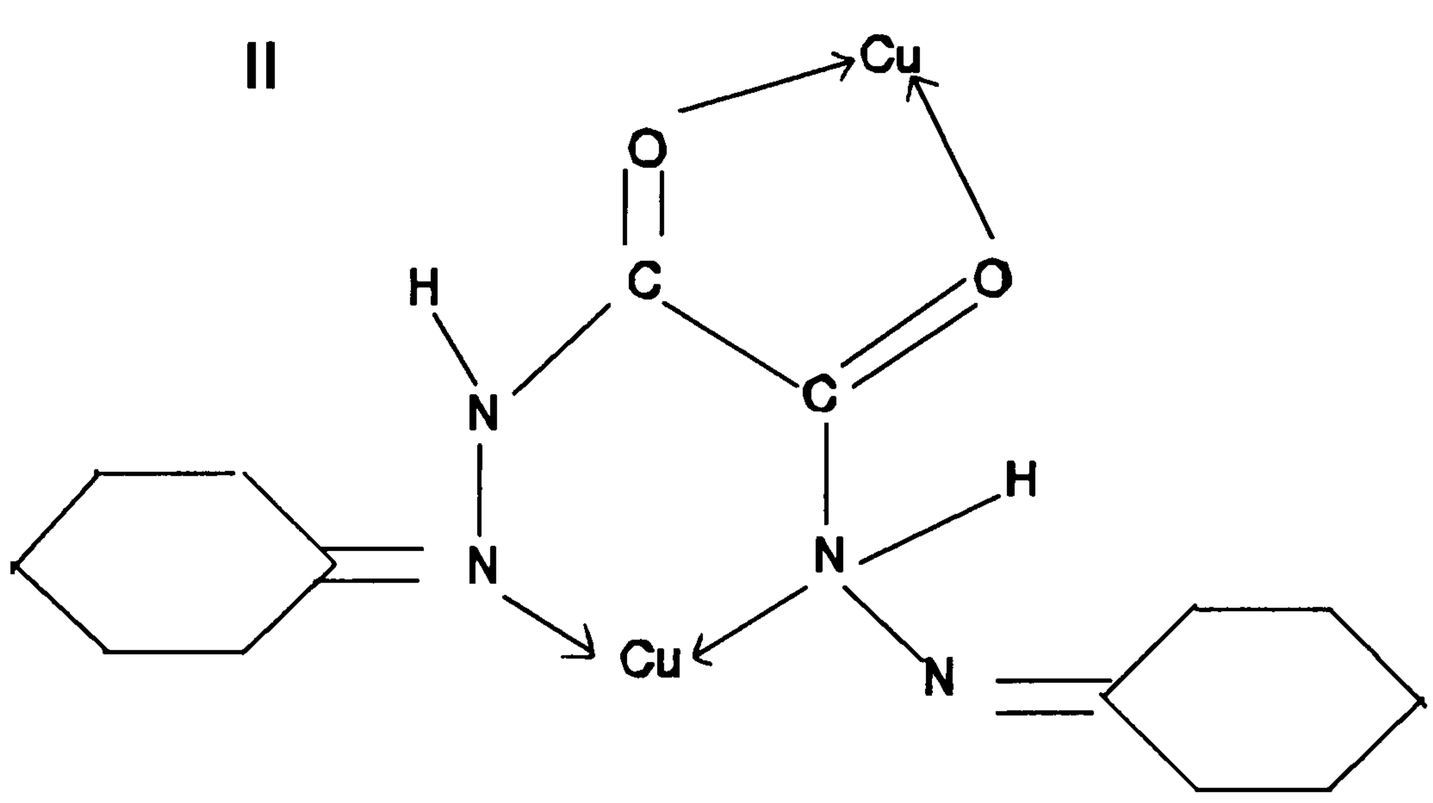

Fig. 2.17 Possible structures for the bis-cyclohexanone oxaldihydrazone-Cu complex, assuming a Cu:ligand ratio of 2:1. A ratio of 3:2 would involve similar bonding, with a central four co-ordinated Cu atom bound to a second Cu-ligand complex, as illustrated for structure I.

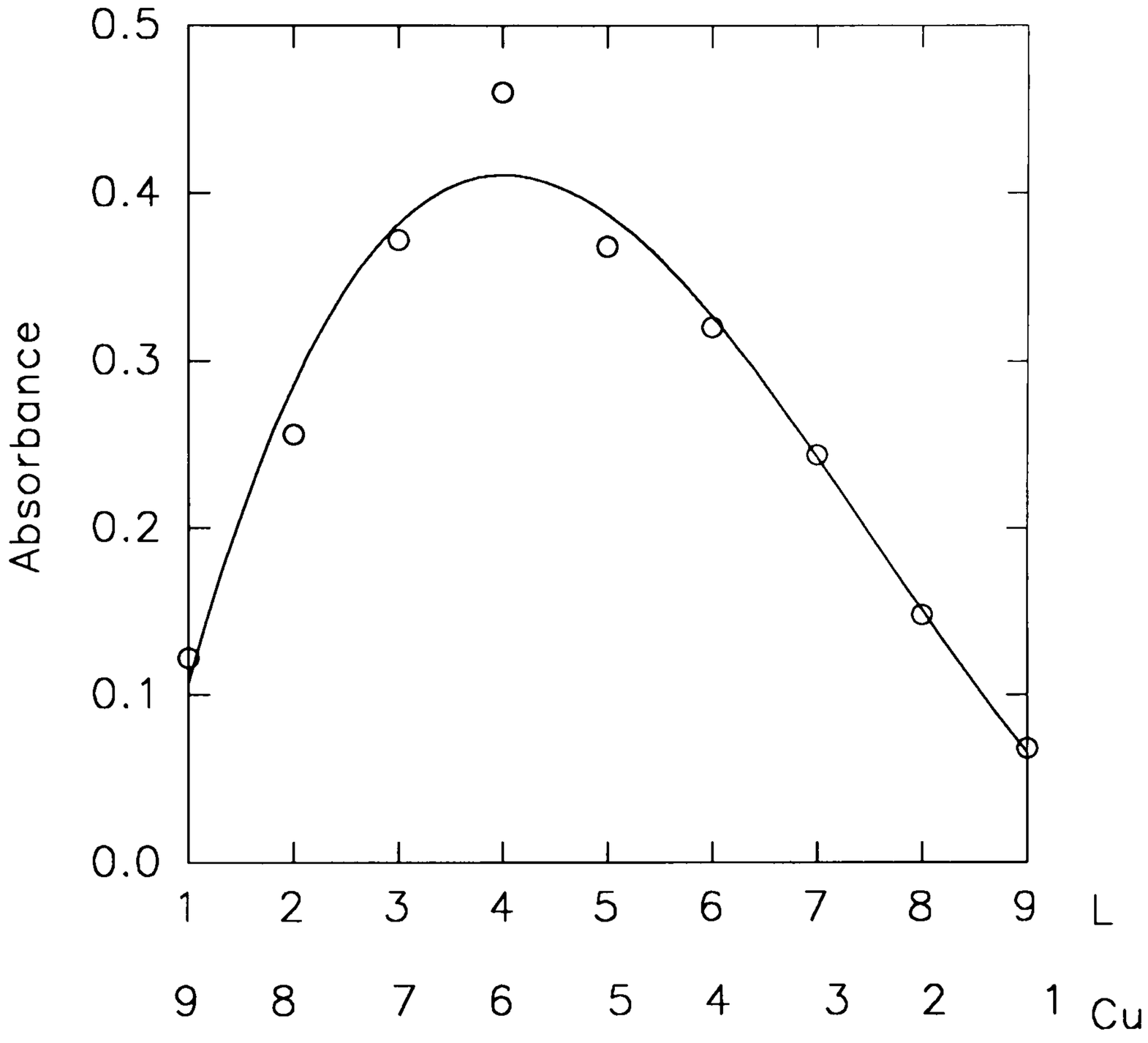

Fig. 2.18 Determination of stoichiometry of Cu - bis-cyclohexanone oxaldihydrazone complex by method of continuous variations. Absorbance measurements were made at λ = 600 nm.

Chapter Three

Sensors Utilizing a Pre-Formed Metal Complex as an Electron-Transfer Mediator: Using a Mediator in Bulk Solution

3.1 Introduction

As described in the General Introduction (Section 1.4.1), the purpose of an electron-transfer mediator is to lower the required overpotential for a redox reaction. As shown in Fig. 1.4, an analyte which exhibits slow reaction rates at a bare electrode, can interact with a mediator which is then oxidised or reduced at the electrode much more rapidly. Detection of the analyte through this more favourable route requires the application of a lower thermodynamic driving force, enabling the electrode to function at a lower potential and therefore reducing the risk of interference.

Possible mediators can be divided into three categories: organic, inorganic and organo-metallic. Organic compounds which have been utilised include dyes such as phenazine methosulphate (PMS), 2,6-dichlorophenolindophenol (DCIP) and N,N,N',N'-tetramethyl-4-phenylenediammine (TMPD) (Aleksandrovskii *et al.*, 1981). However, problems in the use of these compounds include their poor stability and the pH dependence of their redox potentials (Bartlett *et al.*, 1991). Far more stable electrochemistry has been found in inorganic metal complexes such as octacyanomolybdate (Taniguchi *et al.*, 1988) or hexacyanoruthenate (Crumbliss *et al.*, 1986) and organo-metallic complexes such as the ferrocenes (Cass *et al.*, 1984). The aims of Parts I and II of this chapter are therefore to examine the utilisation of metal complexes as mediators in biosensors.

The two most commonly used classes of enzyme in biosensors are dehydrogenases and oxidases, functioning via the two electron redox couples NAD^+/NADH and FAD/$FADH_2$, respectively. In the case of dehydrogenase-based biosensors, the prosthetic group is loosely held by the enzyme and can therefore be re-oxidised at an

electrode. However, this direct oxidation requires a high overpotential (+560 mV vs SCE; Elving *et al.*, 1982) and at NADH concentrations of above 0.5 mM, involves the formation of dimeric products which lead to electrode poisoning (Gorton, 1986). Thus, mediated electron transfer is the preferred technique. Oxidation via both organic and inorganic species has been examined, including catechols (Tse & Kuwana, 1978), redox dyes (Torstensson & Gorton, 1981), conducting organic salts (Kulys, 1986) and ferrocene derivatives (Matsue *et al.*, 1987). A problem with this approach has often been found to be poor selectivity, with many of the compounds electrocatalytic to NADH also increasing the electrode response to other analytes present in real samples, such as ascorbic acid, uric acid or glutathione (Hajizadeh *et al.*, 1991; Kulys & D'Costa, 1991).

A more selective route to NADH determination, would be to utilize an NADH specific enzyme. NADH oxidases have previously been isolated from *Bacillus megaterium* (Saeki *et al.*, 1985), *Streptococus faecalis* (Hoskins *et al.*, 1962), *Thermus aquaticus* YT-1 (Cocco *et al.*, 1988) and *Thermus thermophilus* (Park *et al.*, 1992). The enzyme from *S. faecalis* oxidises NADH to NAD^+ with the concomitant four-electron reduction of oxygen to water. The enzymes from the other three organisms reduce oxygen to hydrogen peroxide; which is of more interest from the viewpoint of biosensor research. Also of importance to biosensor development, is the issue of enzyme stability. The high stability of proteins isolated from thermophilic organisms (Daniel *et al.*, 1982), makes them ideal components for biosensor research. The enzymes from both *T. aquaticus* and *T. thermophilus* show activity at elevated temperatures (80 and 95 °C respectively). However, the oxidase from *T. thermophilus* shows peak activity at pH

5.0 (Park *et al.*, 1992), whilst the activity of the *T. aquaticus* oxidase is pH independent from pH 5.5-9.5 (McNeil *et al.*, 1989). This would enable it to be coupled with a wider range of dehydrogenases.

The prosthetic group in most oxidase enzymes is tightly bound deep within the protein and cannot therefore be influenced by the electrode. Instead, the natural oxidase electron acceptor, oxygen, has been detected following its reduction to hydrogen peroxide (Updike & Hicks, 1967). However, the oxidation of enzyme-generated hydrogen peroxide is not the most preferable method of analysis. The overpotential required (+650 mV vs SCE) would cause the oxidation of other species present in most real sample matrices and the electrode response of the resulting sensor would vary with any fluctuations in the concentration of ambient oxygen. A better alternative would be to replace oxygen with an artificial electron acceptor, capable of being re-oxidised at a lower potential. This was first illustrated by Cass *et al* (1984) for glucose oxidase, using ferrocene derivatives. Since then, the coupling of oxidase enzymes with mediators has been studied extensively. A thorough review is given by Bartlett *et al* (1991).

In the case of NADH oxidase from *T. aquaticus*, mediated electron transfer has previously been examined using ferrocene derivatives and 1',3-dimethylferroceneethanolamine has been shown to couple with the enzyme (McNeil *et al.*, 1989). However, the second order rate constant for the mediated reaction (8.10 x 10^4 $M^{-1}s^{-1}$) was significantly lower than that for oxygen (3 x 10^6 $M^{-1}s^{-1}$). Although applications for NADH determination were also illustrated, they involved hydrogen

peroxide detection and did not progress to mediated systems. This was due to concern about the possible interactions between the ferrocene derivative and the coupled dehydrogenase. Also, these studies did not include enzyme immobilisation. The NADH oxidase from *B. megaterium* has been immobilised for L-malate and L-lactate determination (Mizutani *et al.*, 1991), but again only using oxygen as the electron acceptor.

In Part I of this chapter, the construction of a dehydrogenase/NADH oxidase detection system is described, using mediators present in bulk solution. The possibility of using mediators which have low electrocatalytic activity to NADH and to interferents such as ascorbate, is examined.

3.2 Experimental

3.2.1 Reagents

All reagents were supplied by Sigma Chemical Co. (Dorset, UK) unless otherwise stated. NADH (disodium salt), NAD^+ and glutaraldehyde were of grade I purity. Alcohol dehydrogenase (ADH) from bakers yeast (alcohol:NAD^+ oxidoreductase, EC 1.1.1.1) was specified as being suitable for micro-recycling of NADH and contained < 0.005 moles of β-NAD^+ and β-NADH per mole ADH. Ruthenium red was purchased from Aldrich (Dorset, UK). Ruthenium (III) hexaamine was obtained from Johnson Matthey (Royston, UK). All solutions were prepared using de-ionized water. (1-cyclohexyl-3-(2-morpholino-ethyl)carbodiimide metho-p-toluene sulphonate was used

in 100 mM citric acid-sodium citrate, pH 5.5. For electrochemical experiments involving ADH, the buffer used was 50 mM Tris-HCl, pH 8.8 containing KCl as supporting electrolyte. For all other electrochemical studies this buffer and electrolyte were used at pH 7.0. All reagents were prepared fresh in the working buffer and were stored on ice during the course of each experiment.

3.2.2 Apparatus

A single compartment three-electrode cell of volume 10 ml was used for all experiments. The working electrode was a glassy carbon disc of 3 mm diameter. The reference and counter electrodes were a saturated calomel electrode (SCE) and a platinum wire respectively. Before recording each voltammogram or amperometric trace, the working electrode was polished on cotton wool containing an alumina-water slurry (particle size 0.3 μm) sonicated in de-ionized water for 3 mins, rinsed with acetone and then left to air-dry.

Cyclic voltammetry experiments were performed and presented as described in Section 1.2.2. Amperometric experiments were performed using a Ministat potentiostat (H.B. Thompson & Associates, Newcastle-upon-Tyne, UK), with current-time curves recorded on a BBC Goerz chart recorder, via a JJ Junior resistance bridge. Where required, anaerobic conditions were created by passing nitrogen through the cell for 20 mins and then maintaining a nitrogen blanket over the solution during the electrochemical measurement.

For amperometric NADH determinations, FAD was added to the cell to a final concentration of 0.2 mM, in order to ensure the enzyme was fully active. When used in solution, NADH oxidase was present at a concentration of 4 μg/ml, unless otherwise stated. Enzyme amplification experiments used ADH and ethanol at final cell concentrations of 9 U/ml and 2 % (v/v) respectively. When required, mediators were present at a final concentration of 0.4 mM unless otherwise stated. All experiments were performed at room temperature (18 - 22 °C).

3.2.3 Enzyme Immobilisation

Covalent immobilisation of NADH oxidase was based on the carbodiimide method of Bourdillon *et al* (1980). Carboxylic acid groups were generated on the electrode surface by exposure to a solution of 10 % HNO_3 and 2.5 % $K_2Cr_2O_7$ for 30 s at 1.1 V. These were then activated by incubation in a 20 mg/ml carbodiimide solution for 90 mins at room temperature. A 40 μl aliquot of enzyme solution (56 μg of enzyme) was then transferred to the electrode and left for 90 mins at room temperature to allow amide bonds to form. The electrode was then washed with de-ionized water and stored in the working buffer at < 4 °C.

Immobilisation by physical adsorption was performed via cross-linking with glutaraldehyde. The same mass of enzyme as above was transferred to the electrode and was left to stand (approx. 1 hr) to allow partial evaporation of the buffer solution. A 10 μl aliquot of glutaraldehyde (2.5 %) was then deposited onto the electrode surface and the mixture was left (1/2 hr) to allow cross-linking to occur. The electrode was washed and stored in the working buffer at < 4 °C.

Immobilisation of an ADH/NADH oxidase bilayer was also performed using glutaraldehyde. NADH oxidase was immobilised as described and following amperometric confirmation of enzyme activity, a 10 µl aliquot of ADH (19 U) was deposited on the electrode and was cross-linked with glutaraldehyde as described above.

3.3 Results and Discussion

3.3.1 Electrochemistry of FAD

In contrast to most oxidase enzymes, the prosthetic group from NADH oxidase is labile (McNeil *et al.*, 1989) and can therefore interact directly with the electrode. Before attempting to measure a mediated oxidation current from the enzyme, the scale and nature of this direct interaction would need to be examined. In anticipation of this, the electrochemistry of 2 mM FAD was examined in buffer solution by cyclic voltammetry. As shown in Fig. 3.1, two-electron transfer from the molecule is observed as a single set of redox peaks ($E_{1/2}$ = -515 mV). At slow scan rates ($\leq$ 5 mV/s) addition of the first electron (ie. reduction to the semi-quinone state) is visible as a shoulder in the peak. The electrochemistry of FAD can be considered overall to be quasi-reversible, with a value of ΔE_P (54 mV) greater than the predicted Nernstian value (59/n mV) and, as can be seen in the inset to Fig. 3.1, with values of $i_{pk}/v^{1/2}$ scan rate dependent above 15 mV/s.

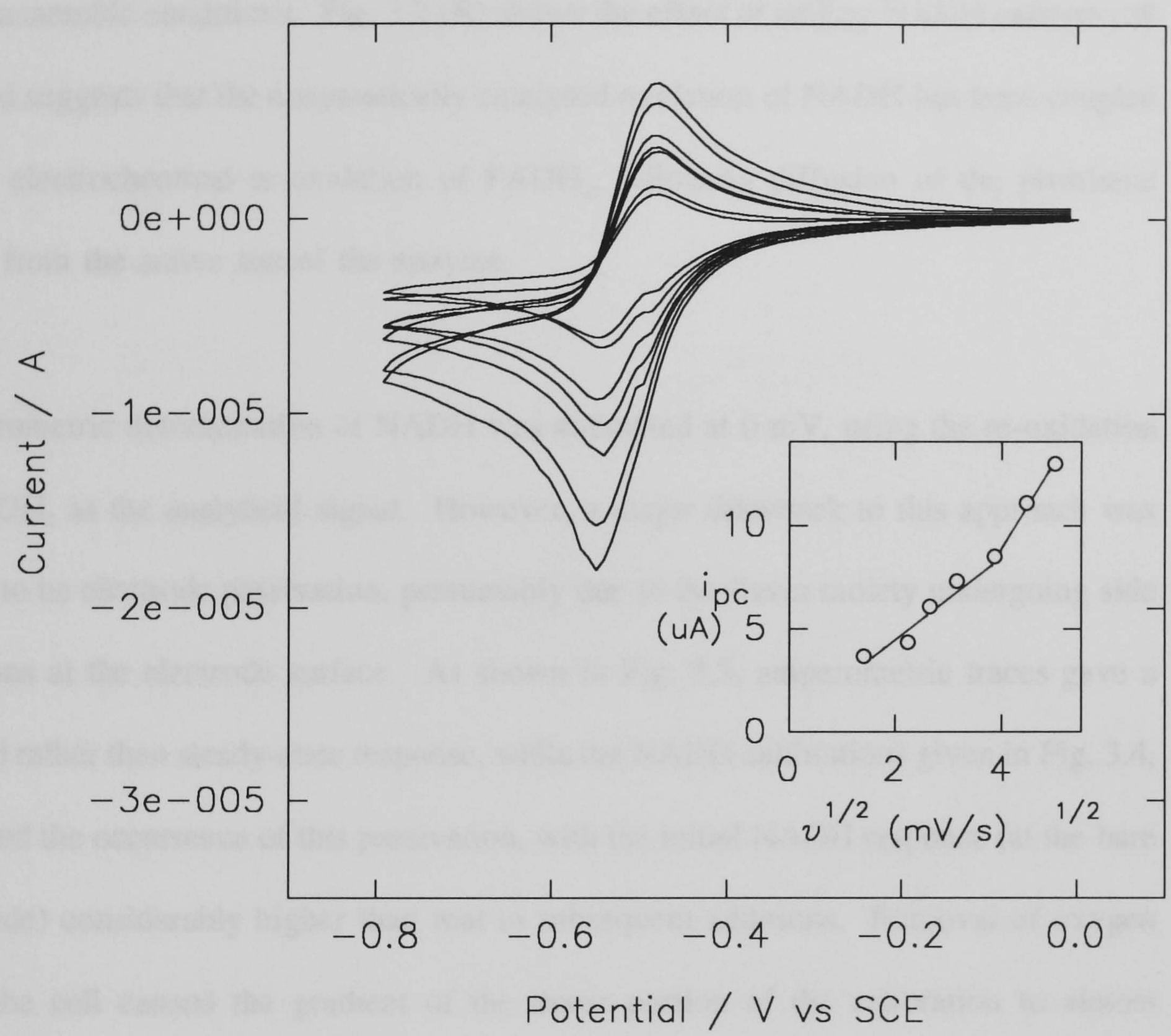

Fig. 3.1 Electrochemistry of 2 mM FAD in buffer solution (pH 7.0). Cyclic voltammograms were recorded at scan rates of 2,5,7,10,20 and 25 mV/s. Redox peak heights are seen increasing with subsequent scans. *Inset:* Cathodic peak current shown as a function of (scan rate)$^{1/2}$.

3.3.2 Lability of FAD

The lability of FAD was examined by slow scan rate cyclic voltammetry (2 mV/s). Fig. 3.2 (A) shows the voltammogram of 0.2 mM FAD in the presence of 3.3 mM NADH under anaerobic conditions. Fig. 3.2 (B) shows the effect of adding NADH oxidase (28 μg) and suggests that the enzymatically catalysed oxidation of NADH has been coupled to the electrochemical re-oxidation of $FADH_2$, following diffusion of the prosthetic group from the active site of the enzyme.

Amperometric determination of NADH was attempted at 0 mV, using the re-oxidation of $FADH_2$ as the analytical signal. However, a major drawback to this approach was found to be electrode passivation, presumably due to the flavin moiety undergoing side reactions at the electrode surface. As shown in Fig. 3.3, amperometric traces gave a peaked rather than steady-state response, while the NADH calibrations given in Fig. 3.4, reflected the occurrence of this passivation, with the initial NADH response (at the bare electrode) considerably higher than that to subsequent additions. Removal of oxygen from the cell caused the gradient of the linear portion of the calibration to almost double (from 0.17 to 0.42 nA μM^{-1}), suggesting that to a large extent $FADH_2$ is re-oxidised by ambient oxygen, before it can reach the electrode. These drawbacks suggest that NADH determination by this method would be unrealistic and that mediating electron transfer through a more cleanly oxidised species, would be preferable.

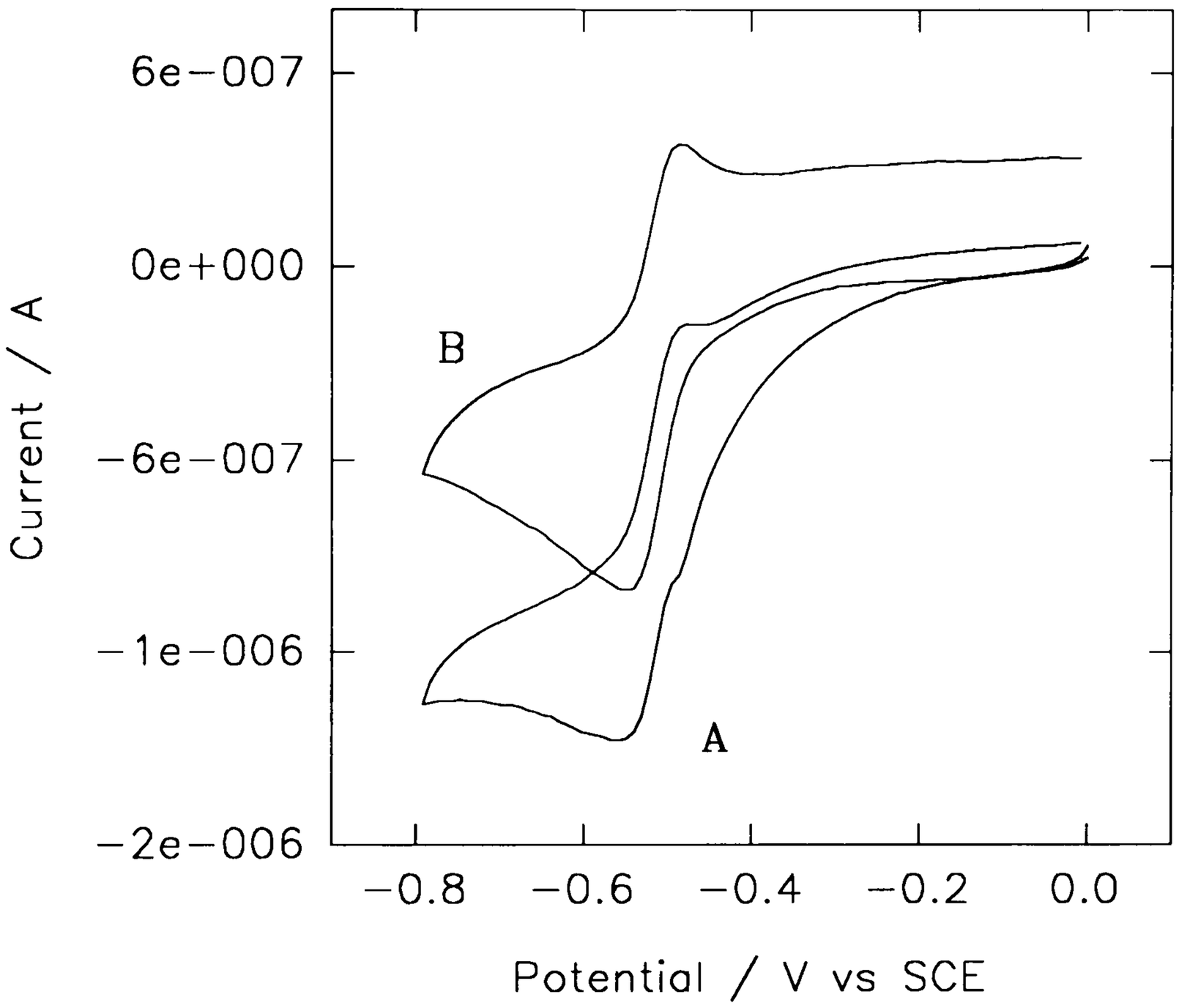

Fig. 3.2 (A) Cyclic voltammogram of FAD (0.2 mM) in the presence of NADH (3.3 mM) under anaerobic conditions. (B) as for (A) but following the addition of 28 μg NADH oxidase. In both cases scan rate = 2 mV/s.

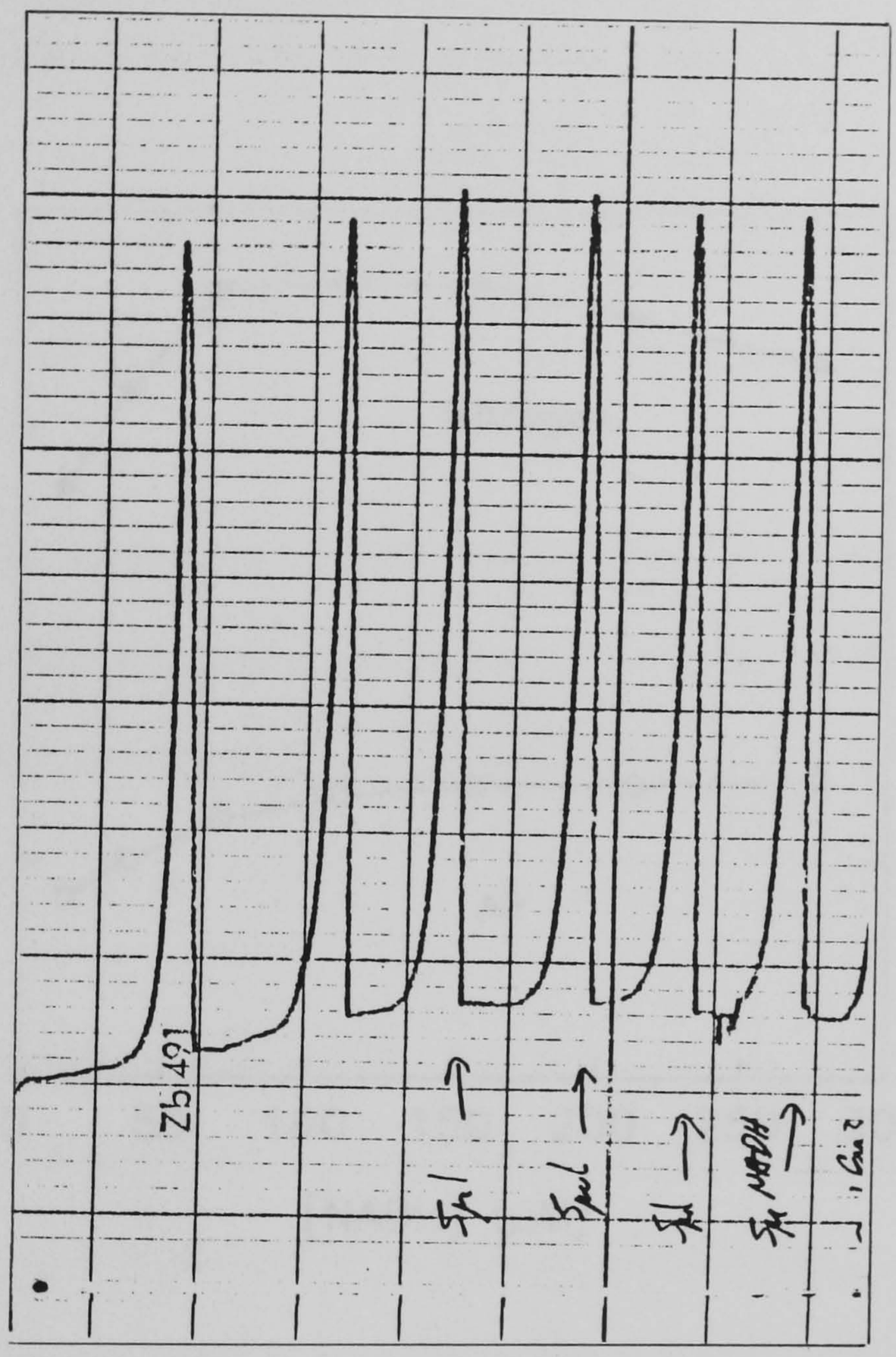

Fig. 3.3 Amperometric traces for the determination of NADH *via* the re-oxidation of $FADH_2$, illustrating the effect of electrode passivation. The cell contained 3 ml Tris-HCl (pH 7.0), 100 µl FAD (10 mM stock solution) and 10 µg NADH oxidase. The responses correspond to the addition of 5 µl aliquots of NADH (10 mM stock solution).

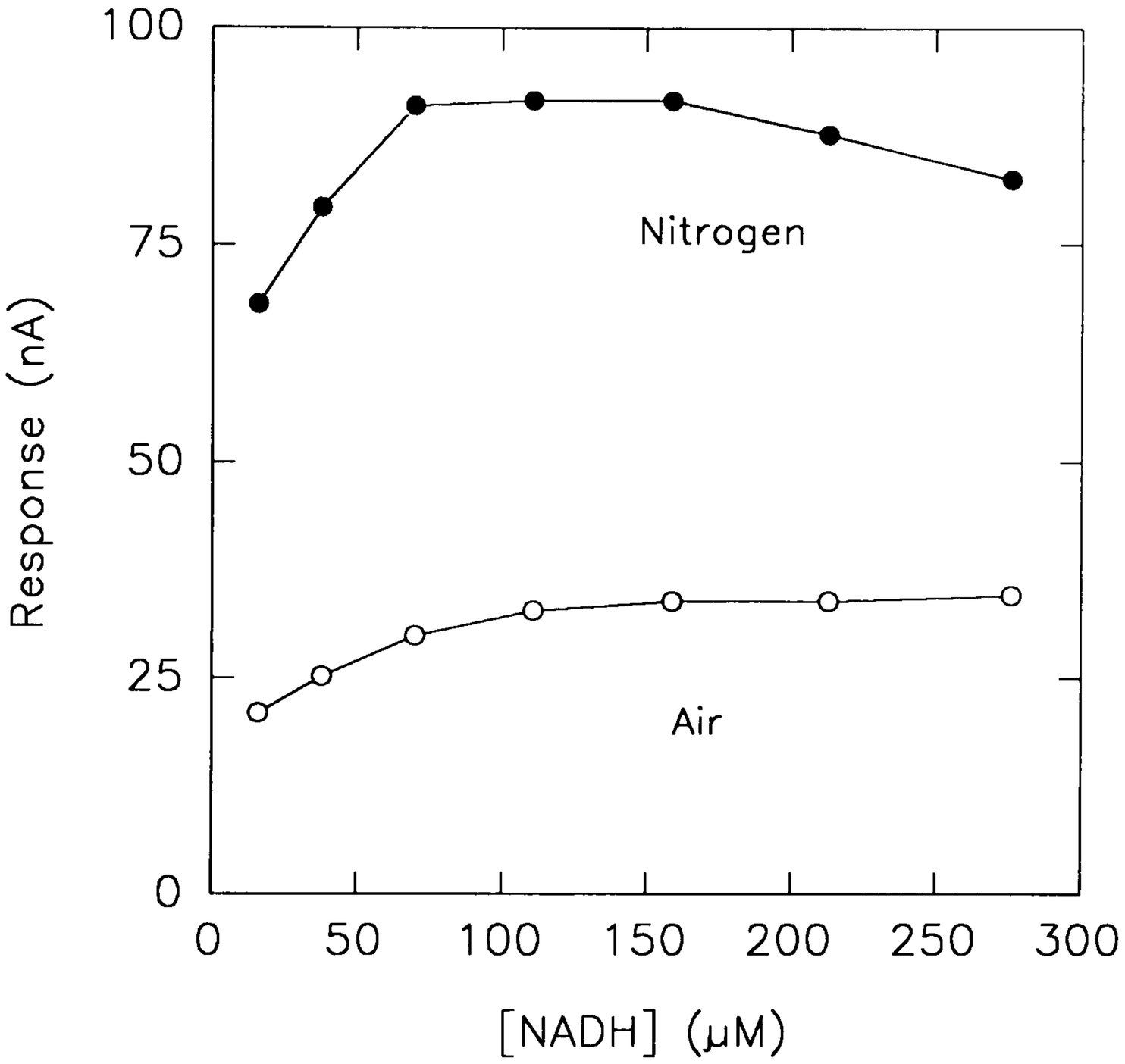

Fig. 3.4 Amperometric determination of NADH at 0 mV using the re-oxidation of $FADH_2$ as the analytical signal. Calibrations were made under ambient and anaerobic conditions.

3.3.3 Mediated Electron Transfer - Criteria

As noted in Section 3.1, the direct oxidation of NADH causes poisoning of the electrode surface and would thus need to be kept to a minimum for a sensor to function effectively. Therefore when choosing possible mediators, the resulting operating potential of the electrode should be considered. The oxidation potential of NADH was determined to be approximately +560 mV at bare glassy carbon and hence mediators which could be re-oxidised at below +200 mV were regarded as acceptable.

Also to be considered, is the possible electrocatalytic effect of the mediator to NADH. A mediator directly oxidising NADH, at a lower rate than the oxidase would cause a decrease in the total analyte signal.

3.3.4 Electrocatalytic Oxidation of NADH

The electrochemistry of nine quasi-reversible, transition metal complexes was examined by cyclic voltammetry. The observed $E_{1/2}$ values are given in Table 3.1. The possible electrocatalytic activity to NADH, of each mediator and of un-bound FAD, was examined using amperometry. Determinations were made at the foreseen working potential of the sensor, that is, at least 100 mV positive of the oxidation potential of the complex. To record the maximum electrocatalytic activity expected, solution concentrations of the components were set at slightly higher values than would be used for the working sensor. Hence, mediators were present at 0.61 mM and FAD at 0.41 mM. the response was measured to 0.82 mM NADH. All determinations were made in duplicate.

Table 3.1 Half-wave potentials for the one-electron redox couples examined for mediation with NADH oxidase. All compounds were present at a concentration of 2 mM in Tris-HCl buffer, pH 7.0. Voltammograms were recorded at a scan rate of 50 mV/s.

Mediator	$E_{1/2}$ (mV)	ΔE_P (mV)
$Ru(NH_3)_6^{3+}$	-175	80
$RuCl_6^{2-}$	-80	155
RR	-190	60
Ru(III)acac	-524	63
Cu(II)acac	-282	332
Ir(III)acac	-360	234
Fe(II)acac	-272	312
$OsCl_6^{2-}$	-4	69
Co(III)sep	-570	88

RR = ruthenium red

acac = acetylacetonate

sep = sepulchrate trichloride

The mediator and mediator/enzyme systems which showed an interaction with NADH are given in Table 3.2. As can be seen, ferric acetylacetonate was directly electrocatalytic to NADH and was therefore rejected as unsuitable for use with NADH oxidase. Three other mediators when combined with FAD showed some degree of electrocatalysis. These were ruthenium red, ruthenium(III) hexaamine and ruthenium (IV) hexachloride. Miyawaki and Wingard (1985) have previously reported that when immobilised on glassy carbon, FAD lowered the overpotential for NADH oxidation by 195 mV. Hence, the electrocatalysis reported here is likely to be a solution form of this electron-transfer, facilitated by the metal complexes' interaction with the electrode:

$$NADH + FAD \rightleftharpoons NAD^+ + FADH_2 \qquad (3.1)$$

$$FADH_2 + 2(RuL)_{ox} \rightleftharpoons FAD + 2(RuL)_{red} \qquad (3.2)$$

$$2(RuL)_{red} \rightleftharpoons 2(RuL)_{ox} + 2e^- \quad \text{at electrode} \qquad (3.3)$$

This reaction sequence is supported by the fact that steady-state rather than peaked responses were obtained. As seen earlier, this would not be the case if $FADH_2$ was directly re-oxidised at the electrode. The electrocatalytic current by FAD/$Ru(NH_3)_6^{3+}$ (220 nA) was considerably greater than the un-catalysed, background value for direct NADH oxidation (18 nA) and $Ru(NH_3)_6^{3+}$ was therefore also rejected. The remaining mediators were examined for coupling with NADH oxidase.

Table 3.2 The mediator and mediator/enzyme combinations which showed some interaction with NADH. Mediators were present at 0.61 mM and FAD at 0.41 mM. The response was measured to 0.82 mM NADH. All determinations were made in duplicate.

Potential (mV)	Oxidant	Current (nA)
0	none	18
"	FAD	-
"	RR	-
"	$Ru(NH_3)_6^{3+}$	-
"	RR/FAD	40
"	$Ru(NH_3)_6^{3+}$/FAD	220
"	RR/FAD/Enz.	432
	Fe(III)acac	621
150	none	79
"	FAD	-
"	$RuCl_6^{2-}$	-
"	$RuCl_6^{2-}$/FAD	108
"	$RuCl_6^{2-}$/FAD/Enz.	437

- = no current increase

3.3.5 Mediated Electron Transfer from NADH Oxidase

Coupling with the enzyme in the presence of ambient oxygen, was examined using amperometry; the working electrode having been poised positive of the oxidation potential of each mediator (+150 mV for $RuCl_6^{2-}$, +50 mV for $OsCl_6^{2-}$ and 0 mV for the remaining mediators). The final cell concentrations of enzyme mediator and FAD are those given in the experimental section.

NADH (final concentration 0.82 mM) was added to a cell containing mediator and FAD. After the electrocatalytic oxidation current had reached a steady-state, NADH oxidase was added. As seen in Table 3.1, for ruthenium red and $RuCl_6^{2-}$, this produced a significant current increase. The same concentrations of mediator and FAD gave no response to approx. 770 mM H_2O_2. This suggests that these current increases were not due to electrocatalysis of H_2O_2 oxidation, but instead to the ruthenium complexes replacing oxygen as oxidant to the reduced form of NADH oxidase. This seems reasonable in light of the fact that both compounds showed some facility for interacting with un-bound FAD.

Both compounds apparently mediate electron transfer through the Ru(III/IV) redox couple. It should be noted that once formed, $RuCl_6^{3-}$ will undergo aquation over a period of time, with a rate of substitution for the first Cl^- in the order of seconds (Cotton & Wilkinson, 1980). Hence, the actual structure of the mediating species is unclear and for the timescale of these experiments, would probably be $[RuCl_5H_2O]^{2-}$. Ruthenium red is a trinuclear amine complex of the form (Ru^{III}-Ru^{IV}-Ru^{III}) and has been shown to undergo a series of one-electron-transfer reactions, leading to the formation of (Ru^{V}-Ru^{V}-Ru^{V}) (Ramaraj *et al.*, 1987). It has been used in its higher oxidation states

for water splitting (Ramaraj & Kaneko, 1993). Its oxidation here, at 0 mV, will correspond to the first redox couple of the molecule, leading to the formation of ruthenium brown (Ru^{IV}-Ru^{III}-Ru^{IV}).

It is interesting to note that while the Ru(II/III) couple has been used previously to mediated with enzymes such as glucose oxidase (Morris *et al.*, 1992), sulphite oxidase (Coury *et al.*, 1990) and horseradish peroxidase (Frew *et al.*, 1986), this is, to the best of our knowledge, the first reported use of the Ru(III/IV) couple with an enzyme. The first redox peak exhibited by ruthenium red was very similar to the $Ru(NH_3)_6^{3+/2+}$ couple and mediation between ruthenium red and glucose oxidase was attempted using amperometry as before. Glucose (final concentration 83.7 mM) was added to a cell containing 0.63 mM ruthenium red in buffer solution (pH 7.0). No electrocatalytic oxidation was observed. Upon the addition of glucose oxidase, (final concentration 570 U/ml) a current of 0.48 μA was recorded, suggesting electrochemical coupling with the enzyme. The same experiment, when repeated with $RuCl_6^{2-}$, produced no oxidation current upon addition of enzyme. It should be noted that ruthenium red is the larger molecule and therefore the failure of $RuCl_6^{2-}$ to mediate cannot be attributed to steric hindrance. It is more likely to be due to the difference in charge between the two complexes, as it has previously been shown using ferrocenes, that oxidases in general coupled more efficiently with positively charged derivatives (Green & Hill, 1986). The coupling of $RuCl_6^{2-}$ with NADH oxidase probably reflects the greater accessibility of FAD in this enzyme, owing to its lability.

Using each mediator, NADH was calibrated under both anaerobic and ambient conditions. As can be seen in Figs. 3.5 and 3.6, the removal of oxygen from the cell

caused an increase in sensitivity, suggesting that neither mediator had fully replaced oxygen as electron acceptor to the enzyme. It is known that for glucose oxidase, when oxygen functions as the electron acceptor, the enzyme is cycled between the fully oxidised and fully reduced forms, without the semiquinone intermediate being produced (Massey *et al.*, 1966). However, for the one electron-transfer mediators used here, it seems likely that reaction with NADH oxidase would proceed by a different mechanism, involving the formation of the semiquinone form and that this route is presumably less favourable. Clearly, another factor affecting the rate of the mediated reaction, will be the thermodynamic driving force provided by the electrode. That is, the difference between the redox potentials of enzyme bound FAD/$FADH_2$ and the electron acceptor couple. In this instance, the use of a relatively high electrode potential was precluded by the need to prevent direct NADH oxidation. Thus the main advantage of mediation here, is in the lowering of the electrode response to possible interferents, rather than the removal of O_2-dependency.

3.3.6 Electron Transfer from Interferents

When coupling an enzyme to an electron transfer mediator, it is important to consider the effect of that mediator on other species present in the sample matrix. Hence, the possible electrocatalytic oxidation of ascorbate and urate by the ruthenium red/FAD and $RuCl_6^{2-}$/FAD systems, was examined using amperometry. The extent of electrocatalysis, was compared to that observed when using mediators previously reported as electrocatalytic to NADH. These were, potassium ferricyanide (Cardosi *et al.*, 1988), Meldolas' blue (MB) (Gorton, 1986) and phenazine methosulphate (PMS) (Torstensson & Gorton, 1981).

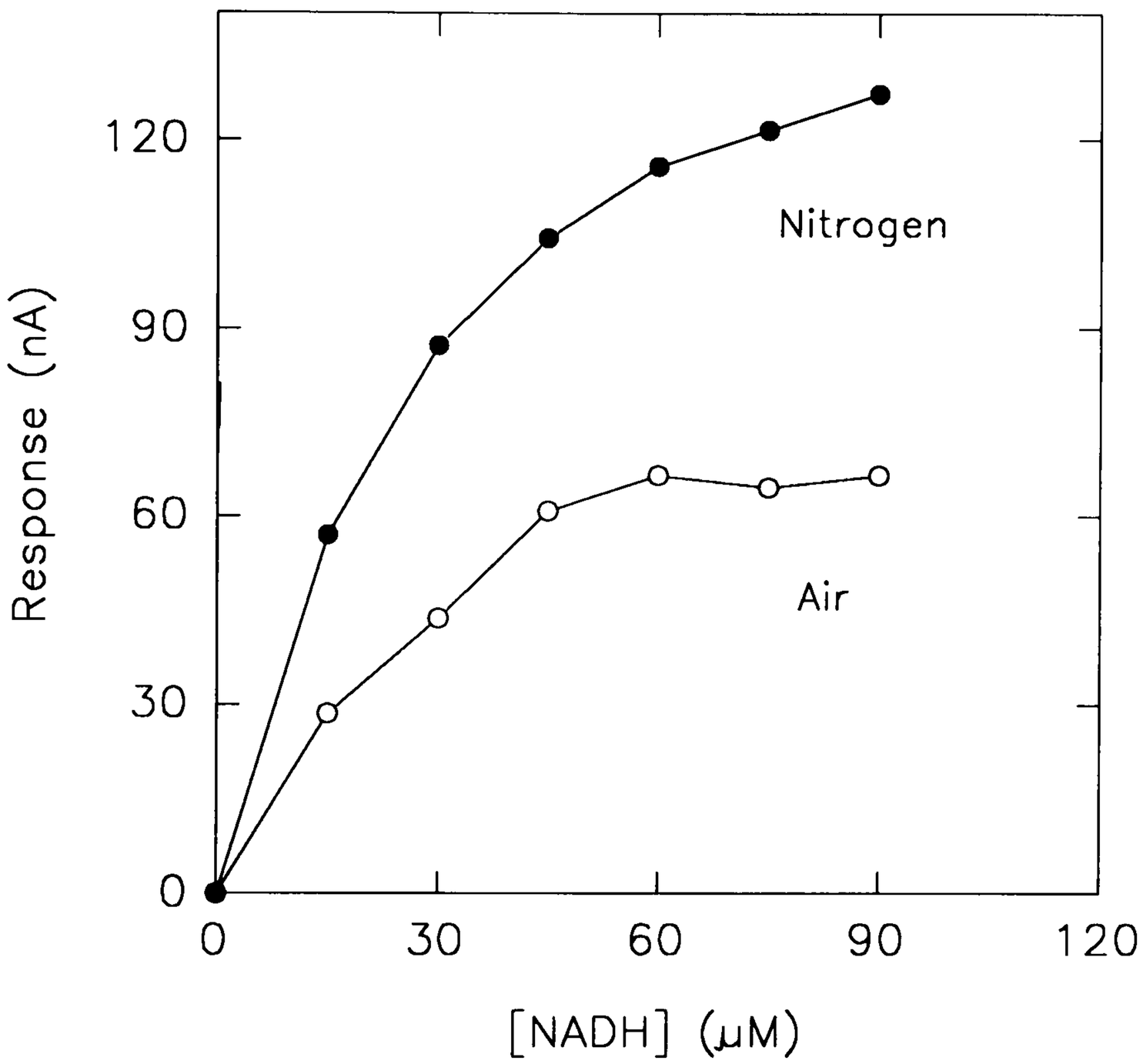

Fig. 3.5 Amperometric determination of NADH using the ruthenium red/brown redox couple. Electrode poised at 0 mV.

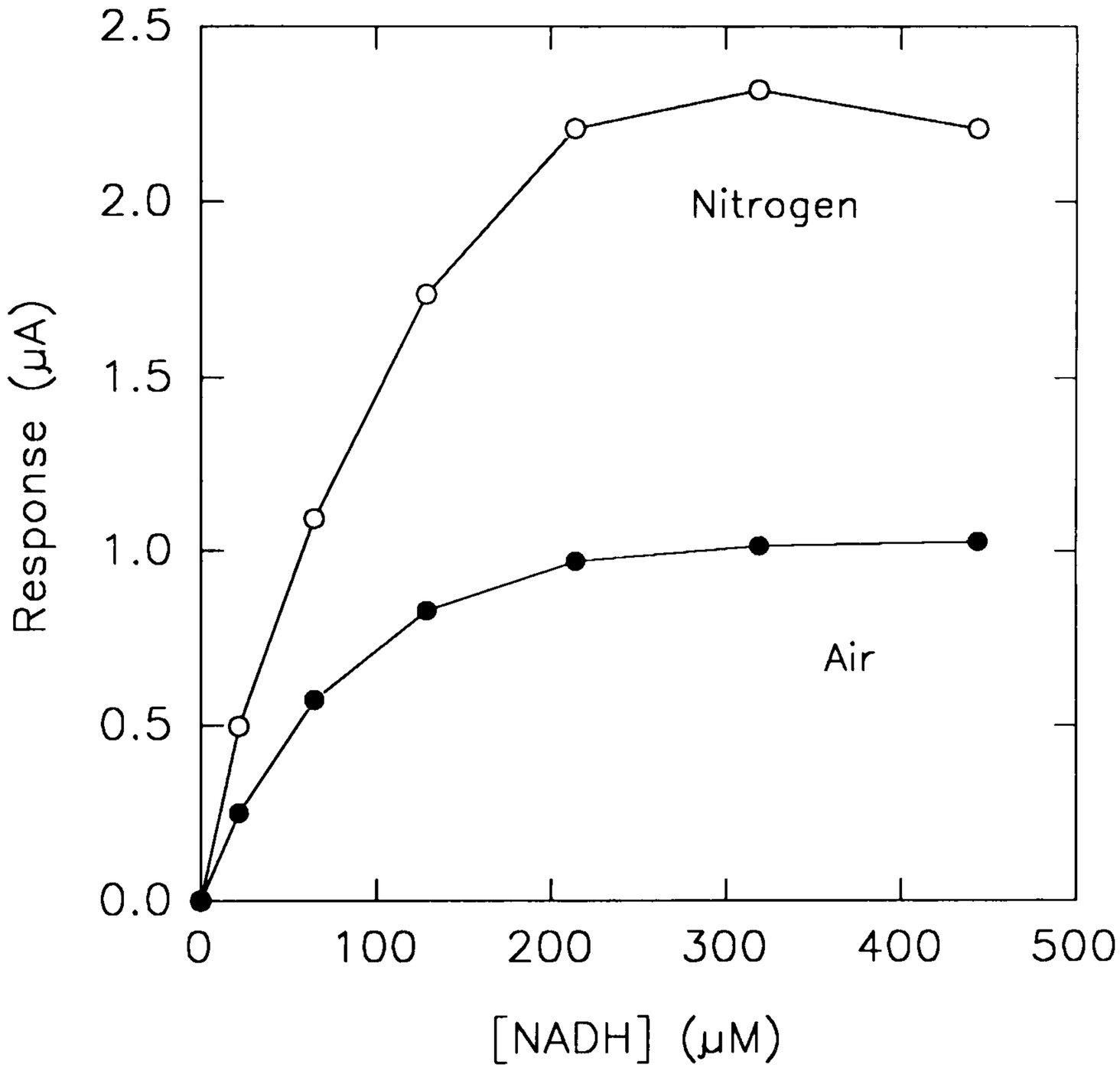

Fig. 3.6 Amperometric determination of NADH using the $RuCl_6^{2-}/RuCl_6^{3-}$ redox couple. Electrode poised at +150 mV.

The anodic peak potentials of $Fe(CN)_6^{3-}$, MB and PMS were measured by cyclic voltammetry (scan rate = 50 mV/s) and were found to be +240, -70 and -130 mV, respectively. Amperometric determinations were therefore made at 0 mV for MB and PMS, and at +300 mV for $Fe(CN)_6^{3-}$. For ruthenium red (RR) and $RuCl_6^{2-}$, the potentials were set at 0 and +150 mV respectively. At each potential, the response to ascorbate (0.044 mM) and urate (0.088 mM) was recorded in mediator-free buffer solution (pH 7.0), and in a buffer solution containing 0.67 mM mediator. When it was used, FAD was present at a final cell concentration of 0.44 mM. All measurements were made in duplicate.

The results are shown in Table 3.3. As can be seen, urate is less of an interference than ascorbate and at the concentrations used here, is only oxidised at the operating potential for $Fe(CN)_6^{3-}$ (+300 mV). When present in the cell, $Fe(CN)_6^{3-}$ caused a slight increase in the urate response (9.1 %) and a far greater increase in the ascorbate response (80.4%).

The other four mediator systems only gave responses to ascorbate. The least electrocatalytic of these was $RuCl_6^{2-}$/FAD, which left the ascorbate oxidative current virtually unchanged (0.14 % difference). However, it should be noted that the un-mediated current at +150 mV, was itself still relatively high (679 nA). The direct oxidation current at 0 mV was considerably lower (83 nA); although the three mediators working at this potential showed a greater electrocatalytic effect. Of these, the mediator system to exhibit least ascorbate interference was RR/FAD (i_c increased to 173 nA compared with 356 and 310 nA for MB and PMS respectively).

Table 3.3 The effect of some mediator systems on the oxidation of 44 μM ascorbate and 88 μM urate. Mediators were present at 0.67 mM, FAD at 0.44 mM. All determinations were made in duplicate. Bracketed values give the percentage increase in oxidative current, relative to the un-catalysed reaction.

Potential (mV)	Oxidant	Current (nA)	
		Ascorbate	Urate
0	none	82.8	-
150	none	679	-
300	none	726	800.8
0	RR/FAD	172.8 (109%)	-
"	MB	356.4 (330%)	-
"	PMS	310.2 (275%)	-
150	$RuCl_6^{2-}$/FAD	712.8 (0.14%)	-
300	$Fe(CN)_6^{3-}$	1310 (80.4%)	873.6 (9.1%)

Two observations can be made from this experiment: Firstly, if we note the un-mediated ascorbate response at +300 mV (726 nA), it is clear that the use of either RR or $RuCl_6^{2-}$ with NADH oxidase would give less interference than hydrogen peroxide detection at +650 mV. Secondly, using NADH oxidase via mediation through RR, still provides a more selective form of NADH measurement than electrocatalytic NADH oxidation by either MB or PMS.

3.3.6 NADH oxidase in Enzyme Amplification: Use of $RuCl_6^{2-}$

Enzyme amplification has been used successfully to improve the sensitivity of enzyme immunoassays (Cardosi *et al.*, 1988; Renneberg *et al.*, 1986; Stanley *et al.*, 1985). The principle, as described by Self (1985), is to increase the apparent activity of the enzyme label (the "preamplifier"), by coupling to a "power-amplifier" stage. Previous methods of amplification have included the use of alkaline phosphatase as the label; the catalytic dephosphorylation of $NADP^+$ allowing NAD^+ to enter the regenerative cycle. The NAD^+ response has been increased by using diaphorase with alcohol dehydrogenase and ferricyanide via either spectrophotometric (Stanley *et al.*, 1985) or electrochemical transduction (Cardosi *et al.*, 1988). However, this approach can lack sensitivity due to a difference of 3.0 pH units between the pH optima of the two enzymes. The broad pH insensitivity exhibited by NADH oxidase, therefore makes it a better choice for such an amplification scheme. Its potential has previously been illustrated in a two-site immunoassay for thyrotrophin (TSH), using the oxidation of hydrogen peroxide as the point of detection (McNeil & Athey, 1992). Here we report the construction of a more selective NADH oxidase-based amplification system; operating at a lower potential by mediating electron transfer through the $RuCl_6^{2-}/RuCl_6^{3-}$ redox couple.

The intended reaction scheme is shown in Fig. 3.7. The viability of the amplification sequence was tested in the absence of alkaline phosphatase, using NADH as the trigger molecule. This was to demonstrate the scale of any possible electrocatalytic effects. At the relatively low NADH concentrations used ($\leq$ 12 μM), no current was observed for the oxidation of NADH by either direct means or via its interaction with $RuCl_6^{2-}$ /FAD; nor did $RuCl_6^{2-}$ show any electrocatalytic activity toward the oxidation of ethanol. Hence, in the absence of the oxidase no current was observed. As shown in the inset to Fig. 3.8, in the absence of ADH, an NADH calibration gave a sensitivity of 8.7 nA μM^{-1}. This compares with a value of 350 nA μM^{-1} (Fig. 3.8 main graph) when the same mass of oxidase was used in the presence of the other amplifier components. This increase can be therefore be attributed to the regenerative sequence outlined.

3.3.7 Ethanol Determination via an ADH/NADH Oxidase Bilayer: Use of Ru Red

A second possible use for NADH oxidase, is in the detection of the substrate of a coupled NAD^+-dependent dehydrogenase. This was illustrated by producing an enzyme bilayer responsive to ethanol.

The immobilisation of NADH oxidase was examined using both carbodiimide activation of glassy carbon and physical adsorption following cross-linking with glutaraldehyde. Lineweaver-Burk plots were made for each electrode treatment, using $RuCl_6^{2-}$ in bulk solution to provide the analytical signal. As shown in Fig. 3.9, the values for the apparent K_M (K'_M) and V_{max} were 172 μM, 0.77 μA and 66 μM, 0.22 μA, for glutaraldehyde and carbodiimide respectively.

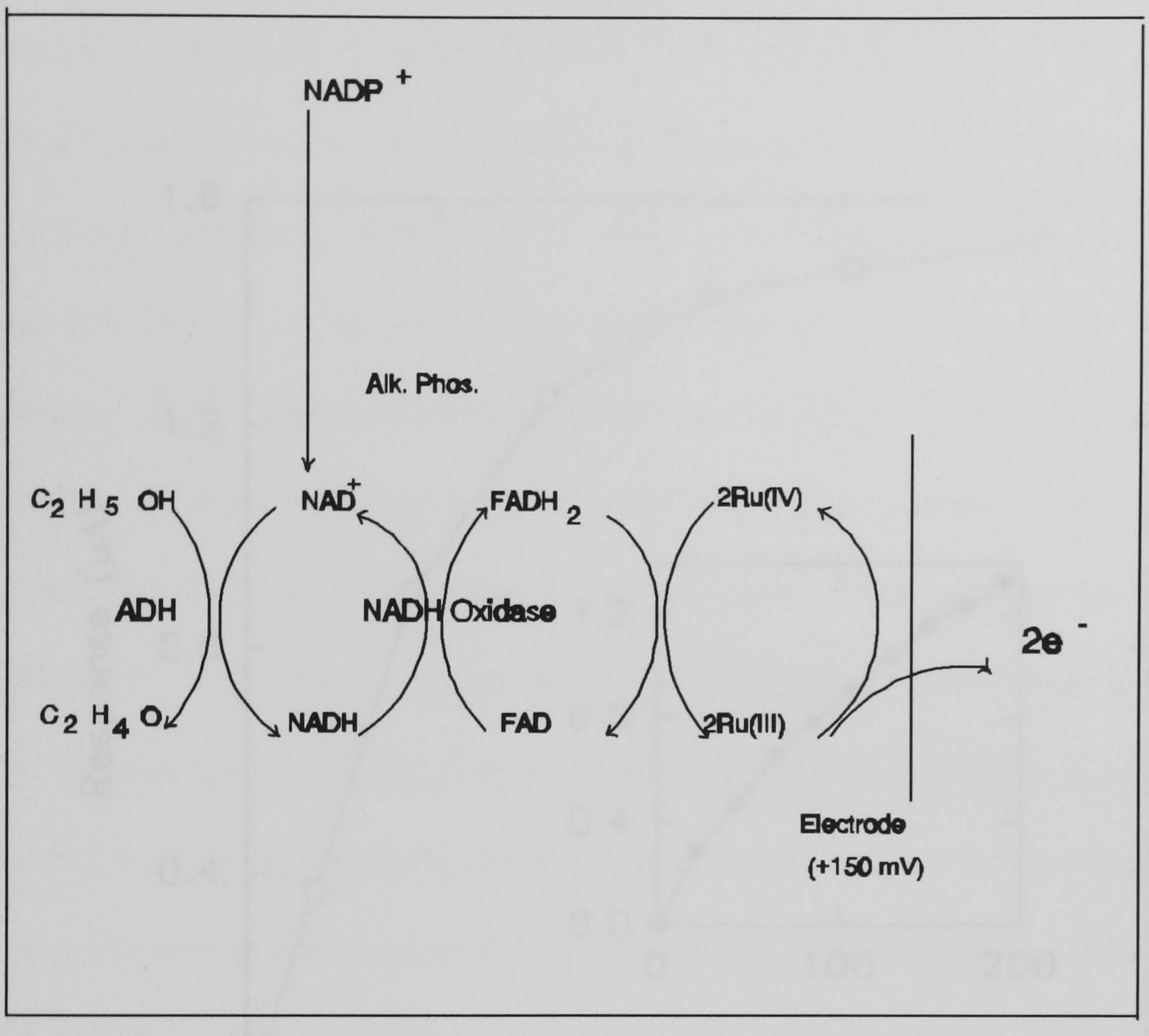

Fig. 3.7 Schematic representation of enzyme amplification. NAD^+ is produced by the enzyme label and is regenerated in the presence of excess ethanol. $RuCl_6^{3-}$ is re-oxidised at the electrode.

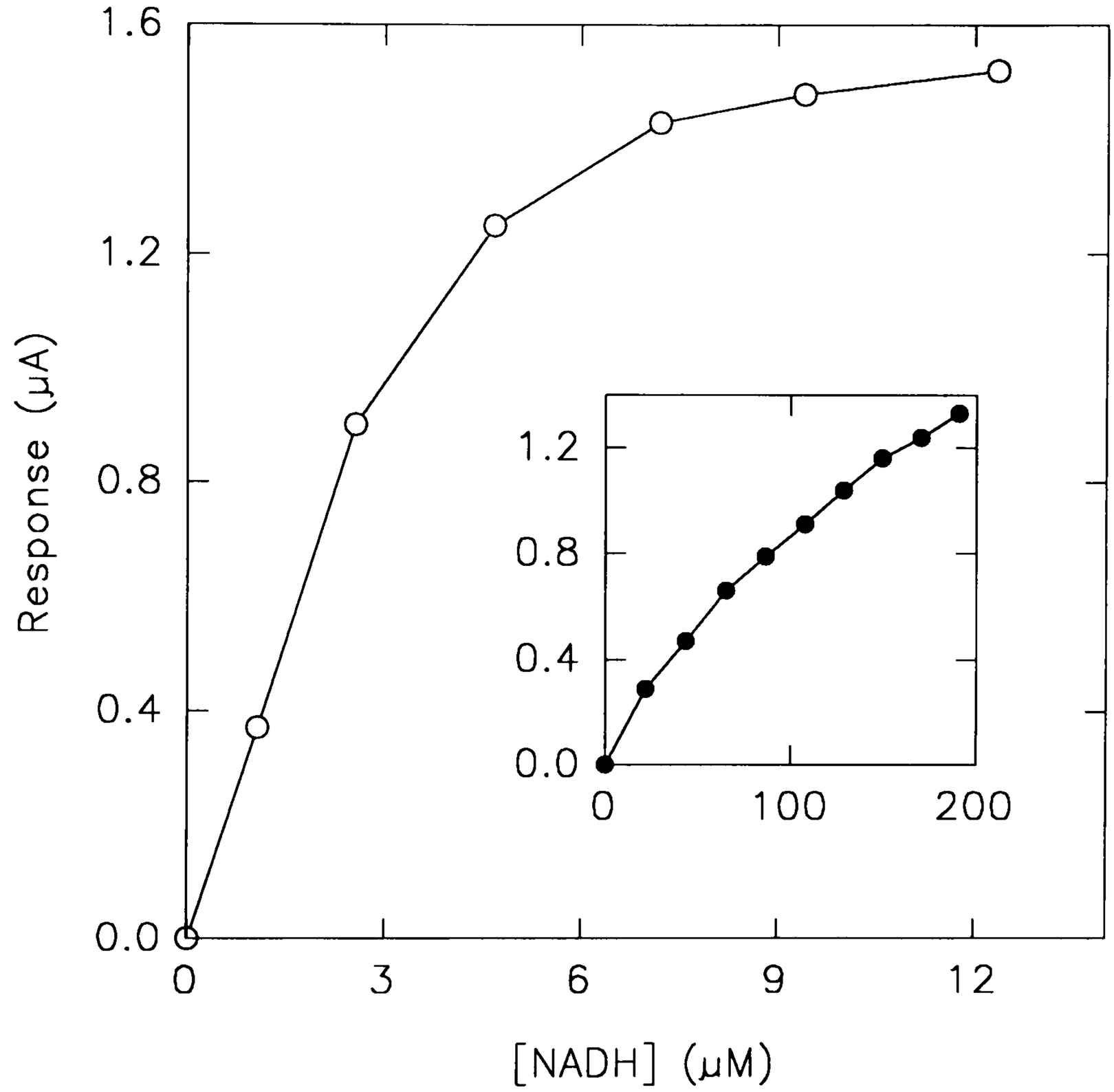

Fig. 3.8 Calibration of NADH at +150 mV using enzyme amplification. The signal is provided by the $RuCl_6^{2-}/RuCl_6^{3-}$ couple present in bulk solution. *Inset:* An unamplified NADH response using the same enzyme/mediator combination. Axis are the same as those given in the main figure.

Michaelis-Menten experiments have previously been performed for soluble NADH oxidase, using its natural electron acceptor, oxygen (McNeil *et al.*, 1989). Spectrophotometric and oxygen consumption data gave K'_M values of 40 and 43 μM respectively, while H_2O_2 oxidation produced a K'_M of 90 μM. This last value was thought to be higher due to the presence over the electrode, of a membrane to exclude direct NADH oxidation. Hence, the K'_M values reported here for the immobilised enzyme can be seen to be considerably higher than the solution value. This is as expected and can be attributed to the un-stirred Nernst diffusion layer at the electrode, the possible diffusion barrier presented by any immobilised, inactive enzyme and the lower rate constant for enzyme oxidation by the mediator. Comparison between the two immobilisation procedures, suggests that the glutaraldehyde method lead to a greater mass of enzyme present on the electrode, both in the active (leading to a greater V_{max}) and inactive state (leading to a higher K'_M). One possible source of inefficiency in the carbodiimide method, is that in addition to hydroxyl groups, the glassy carbon electrode surface will also contain functionalities such as quinones (Van der Linden & Dieker 1980), which will not form $-CO_2H$ groups upon electrochemical oxidation and will therefore not be available for binding with carbodiimide. In an attempt to improve the $-CO_2H$ coverage, carboxyl groups were generated on the electrode surface by the electropolymerisation of indole-5-carboxylic acid. However, control experiments showed that the polymer was itself electrocatalytic to NADH and therefore unsuitable as an enzyme support. The mechanism and implications of this electrocatalysis will be discussed in Chapter 3 Part III.

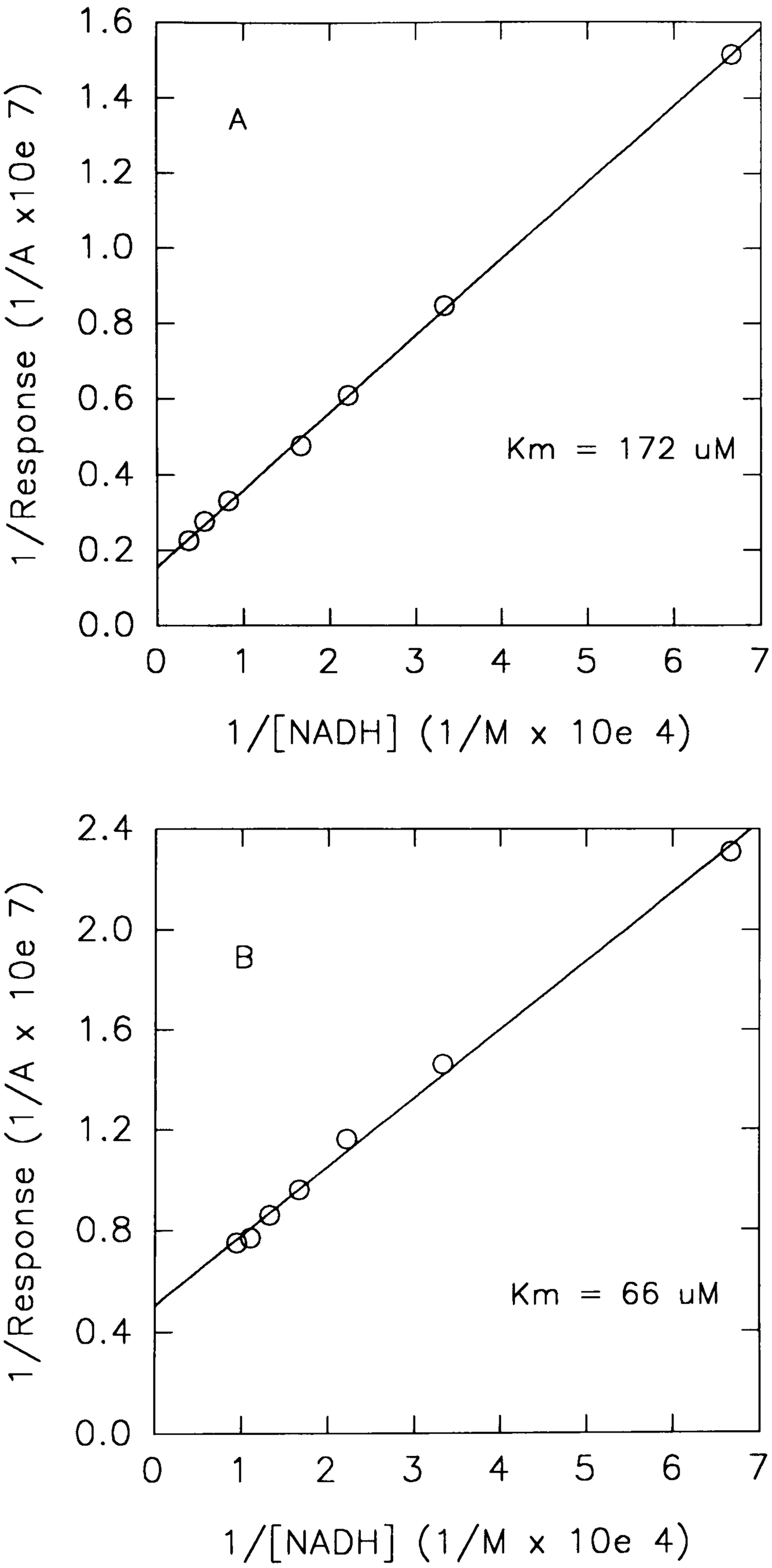

Fig. 3.9 Lineweaver-Burk plots for immobilised NADH oxidase. The enzyme was bound by physical adsorption following cross-linking with glutaraldehyde (A) and by covalent bonding, following activation of the electrode surface with carbodiimide (B).

Obviously, for the construction of a functioning enzyme bilayer, it is important that the activity toward NADH is higher than that toward ADH. Otherwise, changes in ethanol concentration would not be reflected in an increased response. Cross-linking was therefore chosen as the preferred form of immobilisation. To illustrate the use of the ruthenium red/brown couple, determinations were made at O mV with this mediator present in bulk solution.

After confirming the activity of an NADH oxidase layer, ADH was deposited and cross-linked. As shown in Fig. 3.10, ethanol responses were recorded across the range 20-200 μM. The electrode was stored in the working buffer at < 4 °C and was calibrated for ethanol once a day for six days. Over the same period of time, the activity of the oxidase alone was monitored by adding NADH directly to the cell. The results, given in Fig. 3.11, show very little change in the NADH response over this time period, suggesting that the drop in ethanol sensitivity was due chiefly to the decrease in ADH activity. This emphasises the utility of thermostable enzymes for immobilisation.

As indicated in Section 3.3.5, the response of this sensor would still exhibit some O_2-dependency. A possibility for improving on, or removing this characteristic, would be to immobilise the relevant sensor components behind a suitable membrane; thus providing a barrier to oxygen diffusion while leaving the interaction between the enzyme and mediator unaffected. Strategies for the immobilisation of water-soluble mediators will be examined in Chapter 3 Part II.

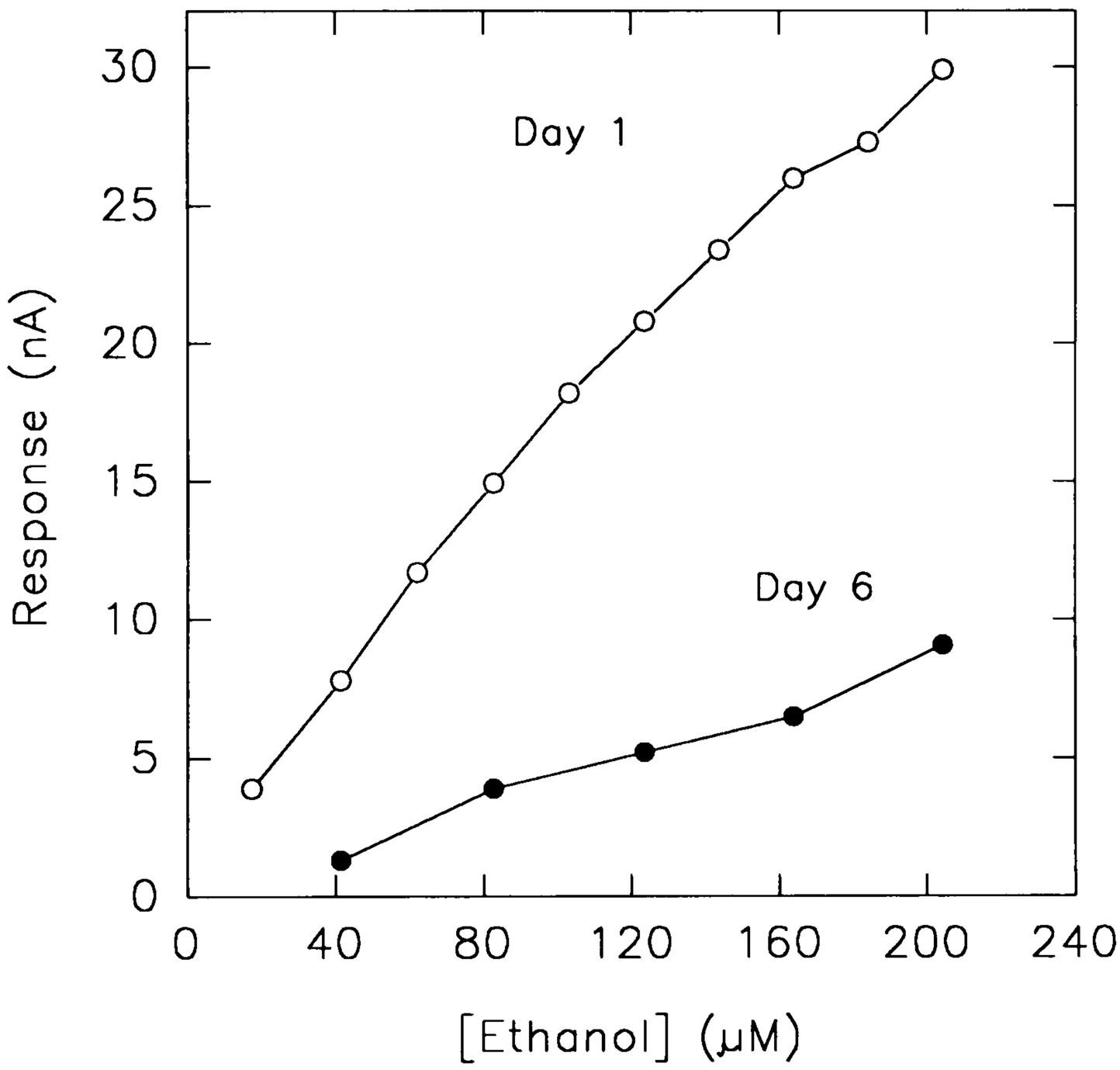

Fig. 3.10 Amperometric response to ethanol at 0 mV, using an immobilised ADH/NADH oxidase bilayer with ruthenium red present in bulk solution. Calibrations were performed once a day.

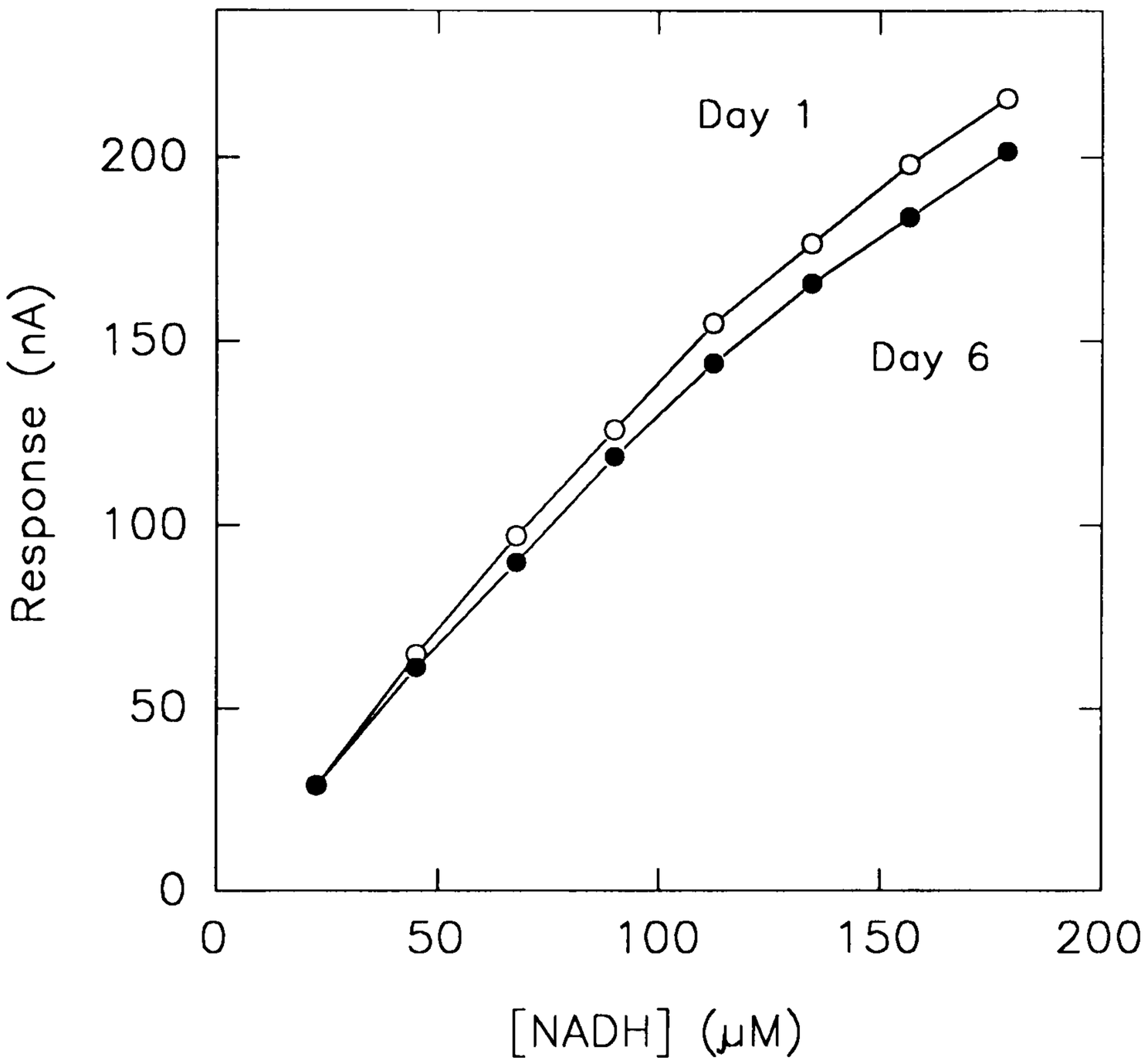

Fig. 3.11 Change in activity of NADH oxidase in enzyme bilayer. Monitored at 0 mV using ruthenium red in solution. Calibrations were performed once a day.

Chapter Four Using a Mediator Immobilised at the Electrode Surface: Study of an Ion-Exchange/Hydrogel Composite

4.1 Introduction

Part I of this chapter illustrated the use of electron-transfer mediators in bulk solution. Part II now considers the use of mediators immobilised at the electrode surface. The rationale for mediator immobilisation, is both to improve the operating characteristics of the resulting sensor and to provide greater convenience to the end user. The presence at the electrode of the electrocatalyst at high concentrations, can increase the magnitude of the sensor response and lower the response time. Additionally, mediator immobilisation is sometimes required if a membrane is to be used to screen interferents. From the point of view of convenience, the mediator can be re-used without the need for product/catalyst separation and the non-requirement of mediator in the analyte matrix can reduce the time for sample preparation.

Methods for mediator immobilisation can be divided into three categories: physical adsorption, ion-exchange and covalent binding. These three techniques were first illustrated by Lane and Hubbard (1973), Oyama and Anson (1980) and Moses *et al* (1975), respectively. All three procedures have since been extensively researched and have been reviewed recently by Murray (1992).

When immobilised, the mediator can either be present as a monolayer, or can be bound to a polymer for three-dimensional coverage. The second form is potentially better as it allows a greater quantity of catalytic sites to be held and therefore provides larger electrocatalytic reaction rates. However, multi-layer immobilisation can suffer from lower rates of charge transport, due to the diffusion (through the polymer) required for charge to reach the electrode.

The immobilisation method chosen for examination here, was that of ion-exchange. This was firstly because modification of an electrode with an ion-exchange polymer, is a relatively simple method of achieving multi-layer mediator coverage and secondly, because ion-exchange provides a general method which can be applied to a wide range of electrocatalysts.

To design an ion-exchange matrix for 3-dimensional mediator immobilisation, the following criteria should be considered: (1) The quantity of mediator which can be incorporated. (2) The long term stability of mediator retention. (3) The rate of charge transport within the matrix. (4) The permeability of the matrix to the analyte. An additional, often important factor, is the effect of the sample on the modified electrode. Electrode fouling may need to be prevented, if the analysis of real samples is to proceed without time-consuming pre-treatment steps.

One of the most extensively characterised ion-exchange materials, is the perfluorosulphonic polymer Nafion, which has been used to immobilise a large number of cations (Majda & Faulkner, 1982; Penner & Martin, 1985; White *et al.*, 1982). The most useful properties of Nafion, are the ability to incorporate relatively high concentrations of mediator and the fact that the mediator retention is extremely stable (Rubinstein & Bard, 1980; Yeager & Steck, 1981). However, drawbacks to its use for electrocatalysis are its impermeability to neutral and anionic analytes and the slow rates of electron transport exhibited by Nafion-immobilised cations (Majda & Faulkner, 1982; Rubinstein & Bard, 1980).

From the view-point of charge transport, some of the most promising immobilisation matrices currently available, are water-swollen polymer networks, known as hydrogels. The high aqueous content of hydrogels has often been shown to provide excellent diffusional characteristics for small molecules and ions (Ratner & Hoffman, 1976). The ion-exchange ability of the polysaccharide hydrogel carrageenan, has been used to immobilise cations such as $Ru(NH_3)_6^{3+}$ and $Ru(bpy)_3^{2+}$ (Crumbliss *et al.*, 1992). Alternatively, agarose has been used to improve the diffusional characteristics of methyl viologen in Nafion (Moran & Majda, 1986). However, neither of these approaches have progressed to sensor applications.

An additional quality of some hydrogels, is the ability to resist protein adsorption (Horbett, 1986) - an important criteria for sensors functioning in biological samples. One example of this, is poly(vinyl alcohol) (PVA). It has been shown that soluble PVA can form acetal linkages with glutaraldehyde as illustrated in Fig. 4.1, resulting in an insoluble, water swellable network (Higuchi & Iijima, 1985), which exhibits both good chemical stability (Aleyamma & Sharma, 1991) and good biocompatability (Ikada *et al.*, 1981). PVA has hence found applications in the biomedical field which include arteriovenous shunts for surgery, artificial skin and controlled release devices (Aleyamma & Sharma, 1991). The simplicity of producing PVA gels has also seen its use as an immobilisation matrix for enzymes in electrochemical biosensors (Kirstein *et al.*, 1985); while the availability of the -OH groups of the polymer for functionalisation, has enabled the immobilisation of indicators such as fluorescein, for use in fibre-optic chemical sensors (Zhujun *et al.*, 1989).

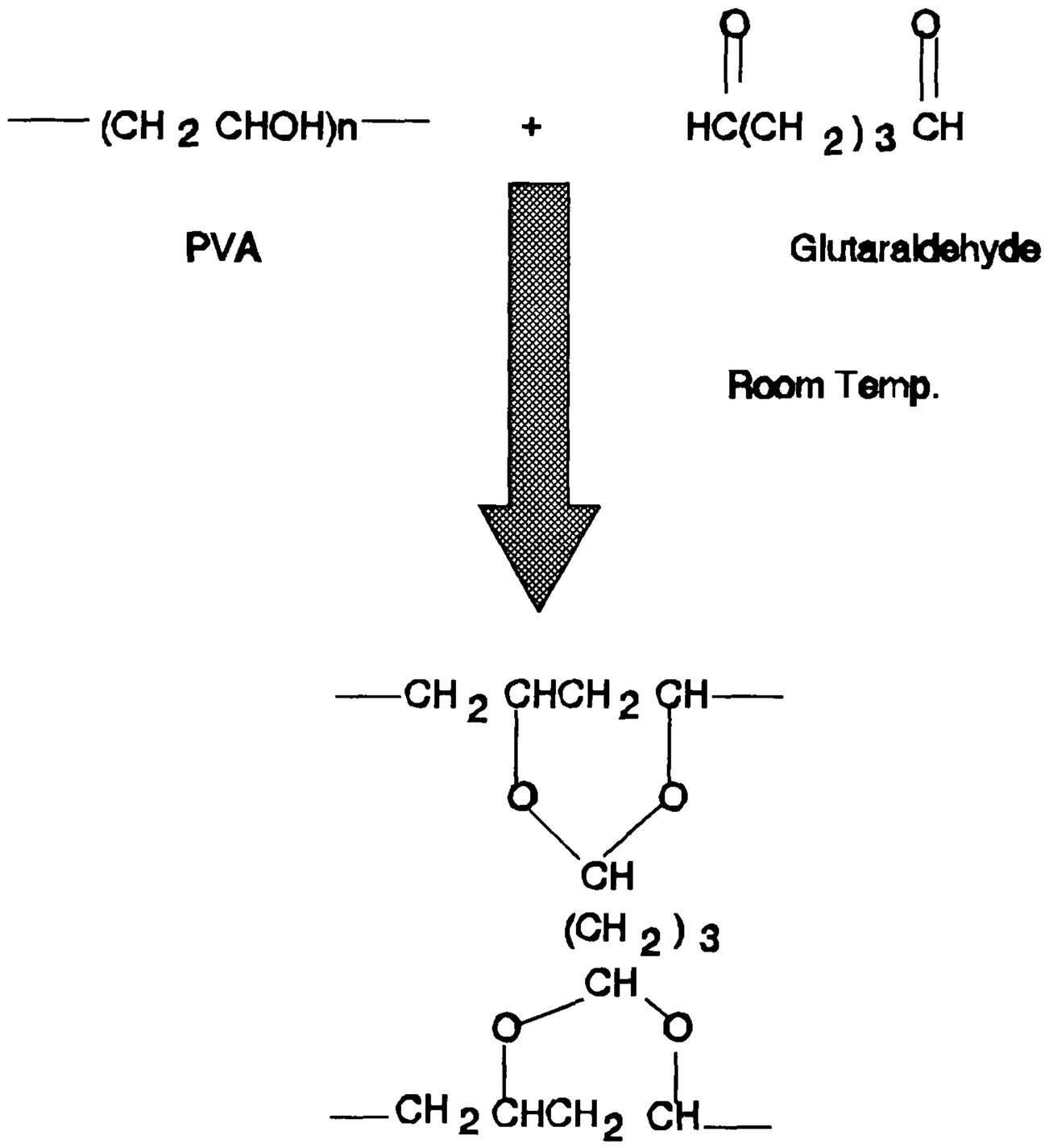

Fig. 4.1 Cross-linking of PVA by glutaraldehyde, as described by Higuchi and Iiyima (1985)

The object of Part II of this chapter was therefore to examine the possibility of producing a composite of Nafion and PVA, with the aim of constructing a mediator immobilisation matrix that would combine the attractive qualities of both materials.

4.2 Experimental

4.2.1 Reagents

All materials were reagent grade or better and were used as recieved. Methyl viologen was purchased from Johnson Matthey (Royston, UK). Albumin (bovine) was provided by Sigma Chemical Co. (Dorset, UK). Poly(vinyl alcohol) (mol. wt. 14,000) and D-glucose were obtained form BDH (Dorset, UK). Potassium hexacyanoruthenate (II) ($K_4[Ru(CN)_6]$) was obtained from ABCR (Karlsruhe, Germany). Nafion was purchased from Aldrich as a 5 % solution in water and lower aliphatic alcohols. Glucose oxidase from *Aspergillus niger* (57 U/mg) was provided by Rhone-Poulenc (Cheshire, UK). All other reagents were obtained from the suppliers given in previous chapters. All solutions were prepared using de-ionized water. The buffer used was 50 mM Tris-HCl, pH 7.0 containing 50 mM KCl as supporting electrolyte. Before use, D-glucose was left at 65 °C for two hours to mutarotate.

4.2.2 Apparatus

Electrochemical measurements were made in a single-compartment, water-jacketed cell, maintained at 25 °C by a circulating water-bath (Grant Instruments Ltd.). The working electrode unless otherwise stated, was a glassy carbon disk of 3 mm diameter.

Potentials were set relative to a saturated calomel electrode (SCE). The counter electrode was a platinum wire. Before each experiment the working electrode was polished, sonicated and rinsed as described in Section 3.2.2. Chronocoulometric experiments were made using an Autolab Electrochemical Analyser (Eco Chemie, Netherlands) interfaced to a DSL personal computer. Anson plots were made from the data using linear regression software supplied by the manufacturer (GPES3). Cyclic voltammograms were recorded as described in Section 2.2.2. Amperometric measurements were performed as described in Section 3.2.2. Where required, anaerobic conditions were created as described in Section 3.2.2.

4.2.3 Procedures

To prepare Nafion films, the Nafion stock solution was diluted with acetone to a concentration of 1 % (v/v). 40 µl of this solution was transferred to the electrode face in 20 µl increments. Each aliquot was left approximately 10 minutes for the solvent to evaporate.

Composite films were prepared from a solution containing 1 % Nafion and 1 % (wt/v) PVA in de-ionized water. For the immobilisation of glucose oxidase, the same Nf/PVA solution was made up in 100 mM citrate buffer, pH 4.0 and additionally contained 25 mg/ml of the enzyme. In both cases the film deposition remained the same and consisted of transferring two 20 µl aliquots of solution to the electrode face. Each aliquot was left for approximatley 30 minutes to allow partial evaporation of the solvent and then 10 µl of 2.5 % glutaraldehyde was deposited. At room temperature, the formation of a solid gel took between 40 minutes to 1 hour.

After modification, the electrodes were washed thoroughly with de-ionized water. The procedure for immobilisation of the redox couple was the same for both types of film and consisted of incubating the electrode in an aqueous solution of the cation (at a concentration of between 0.1 and 10 mM) for 20 minutes. Initial cyclic voltammetry measurements indicated inital, rapid leakage of mediator over the first 30 to 40 minutes following incorporation and hence all subsequent electrodes were incubated in de-ionized water for 1 hour prior to electrochemical experiments. When using phenazine methosulphate, immobilisation and equilibration of the cation were performed in the dark.

Cellulose acetate films were prepared by depositing 40 µl of a cellulose acetate solution (1 % wt/vol in acetone) onto the electrode in 20 µl aliquots, each aliquot being left 10 minutes for solvent to evaporate. Poly(carbonate) films were prepared by securing a commercial membrane (Nuclepore, 0.05 µm pore size) over the electrode using an "O"-ring.

4.3 Results and Discussion

4.3.1 Charge Transport by Methyl Viologen

To compare charge transport within the composite gel (Nf/PVA) to that within Nafion (Nf), the apparent diffusion coefficients (D_{exp}) were examined for both a hydrophobic and a hydrophilic redox couple. These were respectively, methyl viologen ($MV^{2+/.+}$) and ruthenium hexaamine ($Ru(NH_3)_6^{3+/2+}$). Both were chosen as compounds which, when incorporated into Nafion, are known to behave as true ionic diffusers (Gaudiello *et al.*,

1985; Martin & Dollard, 1983). Figs. 4.2 and 4.3 show cyclic voltammograms for electrodes modified with Nf and Nf/PVA, following the uptake of MV and $Ru(NH_3)_6$ respectively.

Values for the mediator relaxation rate (D_{exp}/L^2, s^{-1} where L = film thickness) across each type of film, were calculated from chronocoulometric measurements in mediator-free buffer solution. For MV^{2+} the potential was stepped from -0.3 to -0.8 V, while for $Ru(NH_3)_6^{3+}$ the potential step was from +0.1 to -0.5 V. The pulse width was 600 ms and charge-time data collected up to between 300 to 500 ms gave linear Anson plots ($r \geq 0.998$).

As described in the General Introduction (Section 1.3.3), when charge is measured against time for a redox reaction under diffusion control (an un-stirred solution containing a supporting electrolyte, with the electrode poised at a potential where the rate of electron transfer is considerably greater than the rate of mass transport), Q can be related to $t^{1/2}$ by the integrated Cottrell equation (Anson *et al.*, 1967):

$$Q = 2nFAD^{1/2}c^{b}t^{1/2}/\pi^{1/2} \qquad (4.1)$$

Hence a plot of Q as a function of $t^{1/2}$ gives a gradient of

$$\text{Grad.} = 2n\ FAD^{1/2}c^{b}/\pi^{1/2} = S \qquad (4.2)$$

Therefore for a reaction where n = 1, the apparent diffusion coefficient can be given by

$$D^{1/2}{}_{exp} = S\pi^{1/2}/2FAc^{b} \qquad (4.3)$$

For an immobilised mediator, the concentration of redox sites at the electrode surface can be given by

$$c = \Gamma/L \qquad (4.4)$$

Where Γ is the mediator coverage (mol cm^{-2}) and L is the film thickness (cm). Thus D_{exp} can be described by

$$D^{1/2} = S\pi^{1/2}L/2FA\Gamma \qquad (4.5)$$

Also, for the redox peak of a slow scan rate cyclic voltammogram (where the double layer charging current is minimal)

$$\Gamma = q/nFA \qquad (4.6)$$

Where q is the charge under the peak. Therefore for a reaction where n = 1, the mediator relaxation rate can be given by

$$D/L^2 = [S\pi^{1/2}/2q]^2 \qquad (4.7)$$

The concentration of the redox species in the film was varied by incubating the modified electrode in mediator solutions of varying concentration. In each case the coverage achieved (Γ) was calculated from a slow scan rate cyclic voltammogram (5 mV/s), as given in eq. 4.6. The electrochemical surface area in these calculations was determined by chronocoulometric measurements of a solution of $K_4Fe(CN)_6$ (1.0 mM) in KCl (1.0 M), the potential being stepped between 0 and +0.45 V for 400 ms and assuming a diffusion coefficient for the redox couple of 6.3 x 10^{-6} cm^2 s^{-1} (Adams,

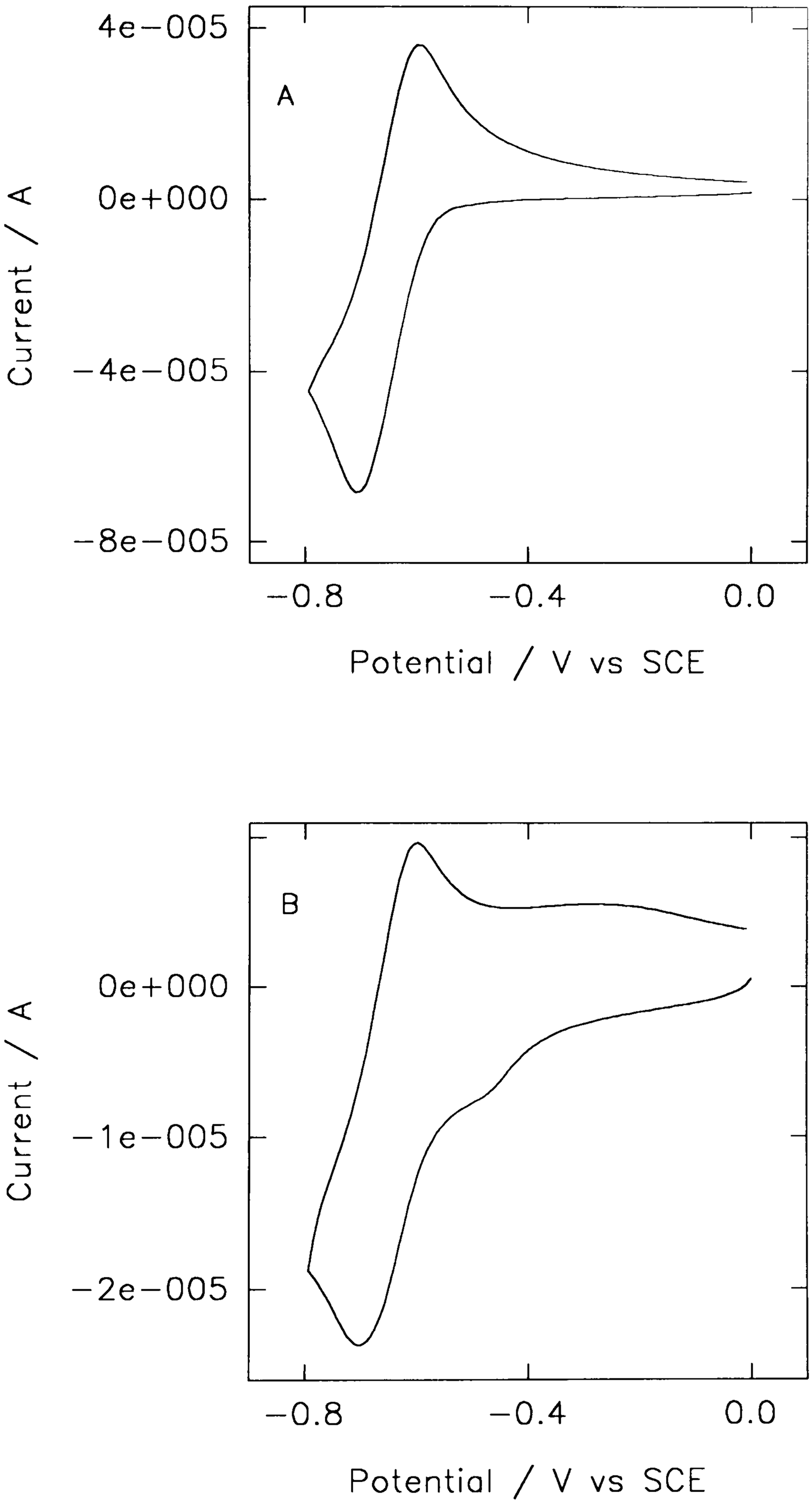

Fig. 4.2 Cyclic voltammogram of methyl viologen incorporated within a film of Nafion (A) and Nf/PVA (B). Both scans recorded in mediator-free buffer solution. Scan rate = 40 mV/s.

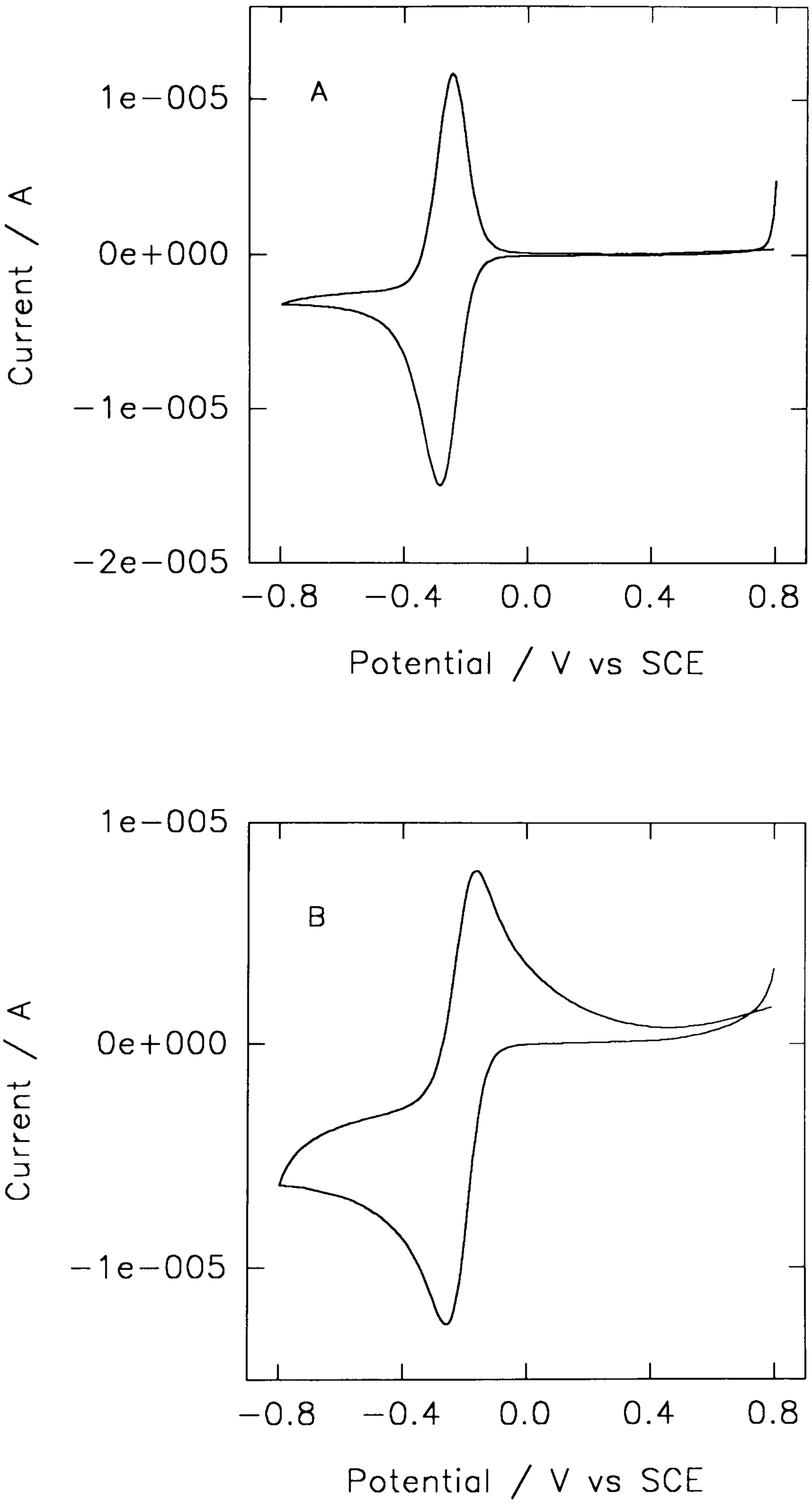

Fig. 4.3 Cyclic voltammogram of $Ru(NH_3)_6^{3+}$ incorporated within a film of Nafion (A) and Nf/PVA (B). Both scans recorded in mediator-free buffer solution. Scan rate = 5 mV/s.

1969). The resultant electrode area ($8.3 \pm 0.15 \times 10^{-2}$ cm^2 for three determinations) was in reasonable agreement with the geometrical value (7.07×10^{-2} cm^2).

From the data in Table 4.1, the mean value of D_{exp}/L^2 for MV^{2+} was found to be 0.52 s^{-1}, while the Nf/PVA films gave a mean value of 0.73 s^{-1}. These values were produced by incubation in stock solutions of the same concentration range (0.1 to 10 mM). To compare these values, the relative swelling of the films should be considered. As described in the introduction, hydrogels are by definition structures which include a high aqueous content and Zhujun *et al* (1989) have shown that gels of 10 % PVA, incubated over a 24 hr period, took up water to over 100 % of their inital weight. Thus it is likely that the Nf/PVA films are of a greater thickness. A relatively small change in L would give a noticeable difference in the value of D_{exp}/L^2 and therefore the increase in the value of D_{exp}/L^2 in spite of this, is likely to represent a significant increase in the MV^{2+} diffusion coefficient.

Also to be noted is the concentration dependence of D_{exp}/L^2 for the two films. If we make the assumption that for a given film deposition procedure, the values of film thickness (L) will remain reasonably constant, then the values of Γ can be taken as being proportional to the concentration of the immobilised mediator. The same assumption allows a comparison between values of D_{exp}/L^2 for a given type of film, predicting that changes in this value will be chiefly due to changes in D_{exp}. As can be seen from Table 4.1, when incorporated into Nafion, D_{exp}/L^2 for MV^{2+} decreases with increasing MV^{2+} concentration. This relationship has been observed previously (Moran & Majda, 1986) and has been ascribed to "single-file diffusion". That is, to the diffusing species having to move between effectively fixed sites within the polymer

matrix and therefore having their rate of motion reduced by the decreasing availability of the sites, as the concentration of the diffusing species increases (Buttry & Anson, 1983).

However, when immobilised within the composite membrane, MV^{2+} produces the opposite result, exhibiting increasing values of D_{exp}/L^2 with increasing mediator concentration. This result is obviously desirable for sensor applications, as it means a high concentration of redox sites will maintain a high rate of electron transport. To explain this difference in properties, we must first consider the structure of the composite films. Fig. 4.4 shows cyclic voltammograms for $Fe(CN)_6^{4-}$ and $Ru(CN)_6^{4-}$ (both at a concentration of 0.91 mM in bulk solution), at a bare glassy carbon electrode and at electrodes modified with Nf and with Nf/PVA. As can be seen, the electrochemistry of both anions is visible at the Nf/PVA-modified electrode, although the redox peak heights are lower than for the voltammograms obtained at bare glassy carbon. This difference is greater for $Fe(CN)_6^{4-}$, presumably because its higher charge density leads to greater repulsion from the $-SO_3^-$ sites of the polymer. When the same concentration of Nafion is present as a homogeneous film, the repulsion is sufficient to exclude both anions from the electrode completely. This would suggest that the Nf/PVA composite comprises of discrete regions of Nafion embedded within the porous structure of the hydrogel. This was also the structure proposed by Moran and Majda (1986) for films of Nafion/agarose.

It should also be noted that the incorporation of cations into the composite film is less permanent than into plain Nafion. Typically, 75 % of inital MV^{2+} redox activity remained in the Nf/PVA films after 30 minutes; compared with 95 % of initial activity

Table 4.1 Effect of MV^{2+} coverage on the value of D_{exp}/L^2 for mediator incorporated within films of Nafion (Nf) Nafion/poly(vinyl alcohol) (Nf/PVA).

Nafion		Nf/PVA	
Γ (mol cm^{-2} x 10^{-8})	D_{exp}/L^2 (s^{-1})	Γ (mol cm^{-2} x 10^{-8})	D_{exp}/L^2 (s^{-1})
0.37	0.99	0.77	0.26
0.60	0.57	0.86	0.54
1.35	0.54	0.93	0.79
3.20	0.30	1.39	0.85
5.10	0.21	1.45	1.22

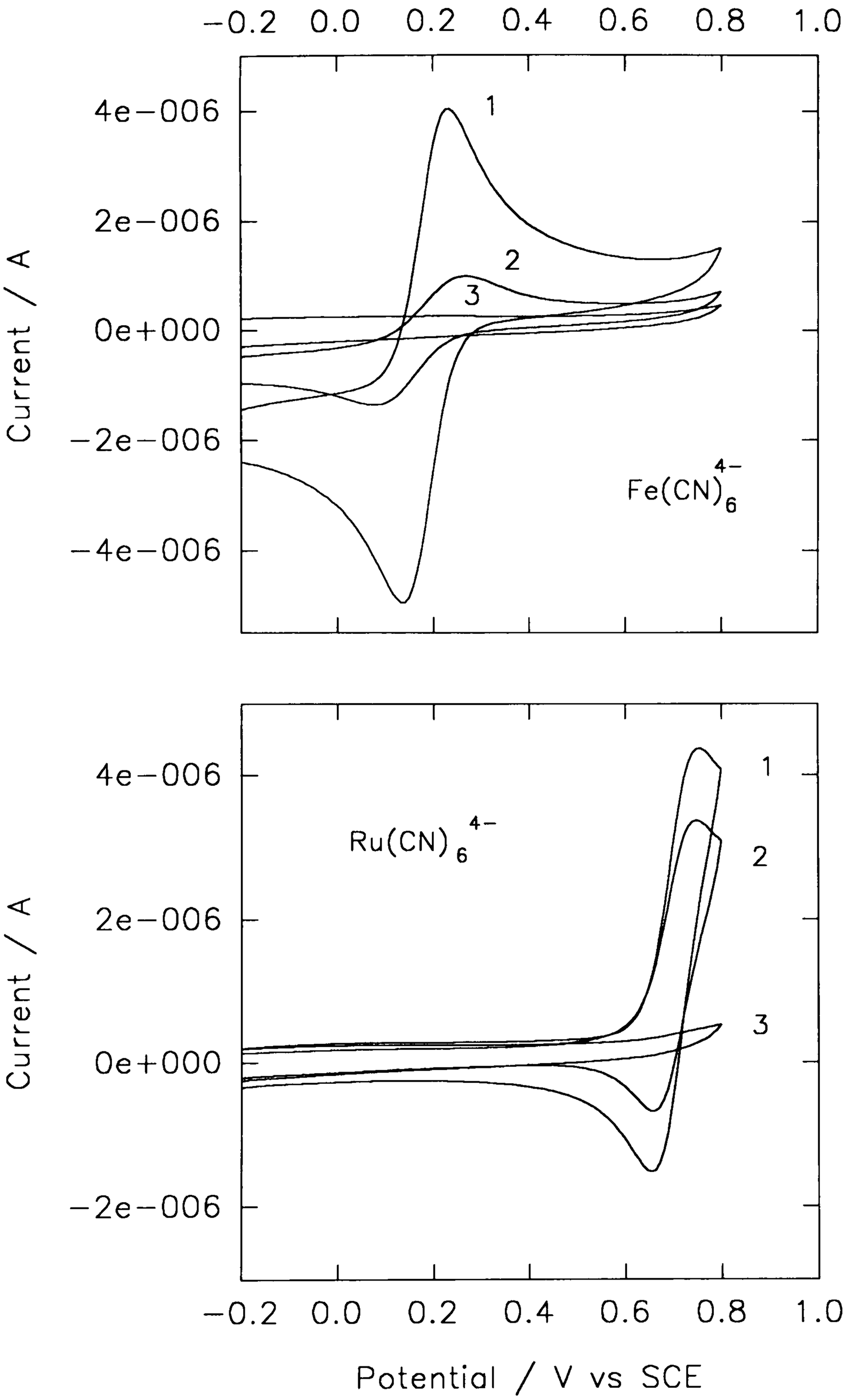

Fig. 4.4 Electrochemistry of $Fe(CN)_6^{4-}$ and $Ru(CN)_6^{4-}$ (both present at 0.91 mM in bulk solution) at bare glassy carbon (1) and glassy carbon coated with Nf/PVA (2) and Nafion (3). Scan rate = 20 mV/s.

retained by the Nafion films. This indicates that the MV^{2+} in the Nafion aggregates is in equilibrium with less tightly bound MV^{2+} present in the aqueous, porous regions of the film. It is to be expected that the MV^{2+} in these aqueous regions would exhibit a higher diffusion coefficient than the Nafion-bound component, as the value of D_{exp} for MV^{2+} in water is between three to four orders of magnitude greater than the D_{exp} value found in Nafion (Gaudiello *et al.*, 1985).

It should be remembered that the experimentally observed diffusion coefficient D_{exp} can be described by the following equation (Dahms, 1968; Ruff, 1970; Ruff & Friedrich, 1971):

$$D_{exp} = D_o + D_{et} \qquad (4.8)$$

Where D_o is the contribution from physical diffusion and D_{et} is the contribution from electron self-exchange (both in cm^2/s). For aqueous solutions $D_o >> D_{et}$; but in polymer films D_{et} can become significant. The value of D_{et} can be related to the electron self-exchange rate constant, k_{ex}, by the following equation (Andrieux & Saveant, 1980):

$$D_{et} = 10^3 \delta^2 k_{ex} C_T \qquad (4.9)$$

Where δ (cm) is the distance between species at reaction and C_T (mol cm^{-3}) is the redox site concentration. Hence, a possible explanation for the D_{exp} - concentration relationship observed in the composite films, is the coupling of the diffusional pathways of the two components by electron self-exchange. This effect has previously been discussed for homogeneous Nafion films (Buttry & Anson, 1983). These films have

been shown to exhibit separate hydrophilic and interfacial regions (Vining & Meyer, 1987; Yeager & Steck, 1981) as illustrated in Fig. 4.5, and cations in these regions with low values of k_{ex} will travel to the electrode via separate paths; the species in the interfacial phase diffusing more slowly (Yeager & Steck, 1981). However, where electron self-exchange is rapid, the diffusional processes occurring in each phase can be coupled, so that the apparent diffusion coefficient is governed by the motion of the ions through the hydrophilic phase. For example, Buttry and Anson (1983) showed that even when less than 0.1 % of $Ru(bpy)_3^{2+}$ is present in the hydrophilic phase, it carries most of the diffusional current. This is in agreement with the relatively high value of k_{ex} (10^9 $M^{-1}s^{-1}$) for this cation (Young *et al.*, 1977).

MV^{2+} will undergo hydrophobic interactions with Nafion (Martin & Dollard, 1983) and will therefore be found predominantly in the interfacial region of the polymer. However, the lower value of k_{ex} (8 x 10^5 $M^{-1}s^{-1}$) (Gaudiello *et al.*, 1985), prevents coupling with any MV^{2+} present in the more rapidly diffusing hydrophilic phase. The results given in Table 4.1 however, suggest that in Nf/PVA, electron exchange can occur between MV^{2+} in the Nafion aggregates and in the aqueous regions of the composite. As shown in eq. 4.9, when this takes place, an increase in the concentration of the redox species should increase the possibility of electron-hopping and therefore enhance D_{exp}.

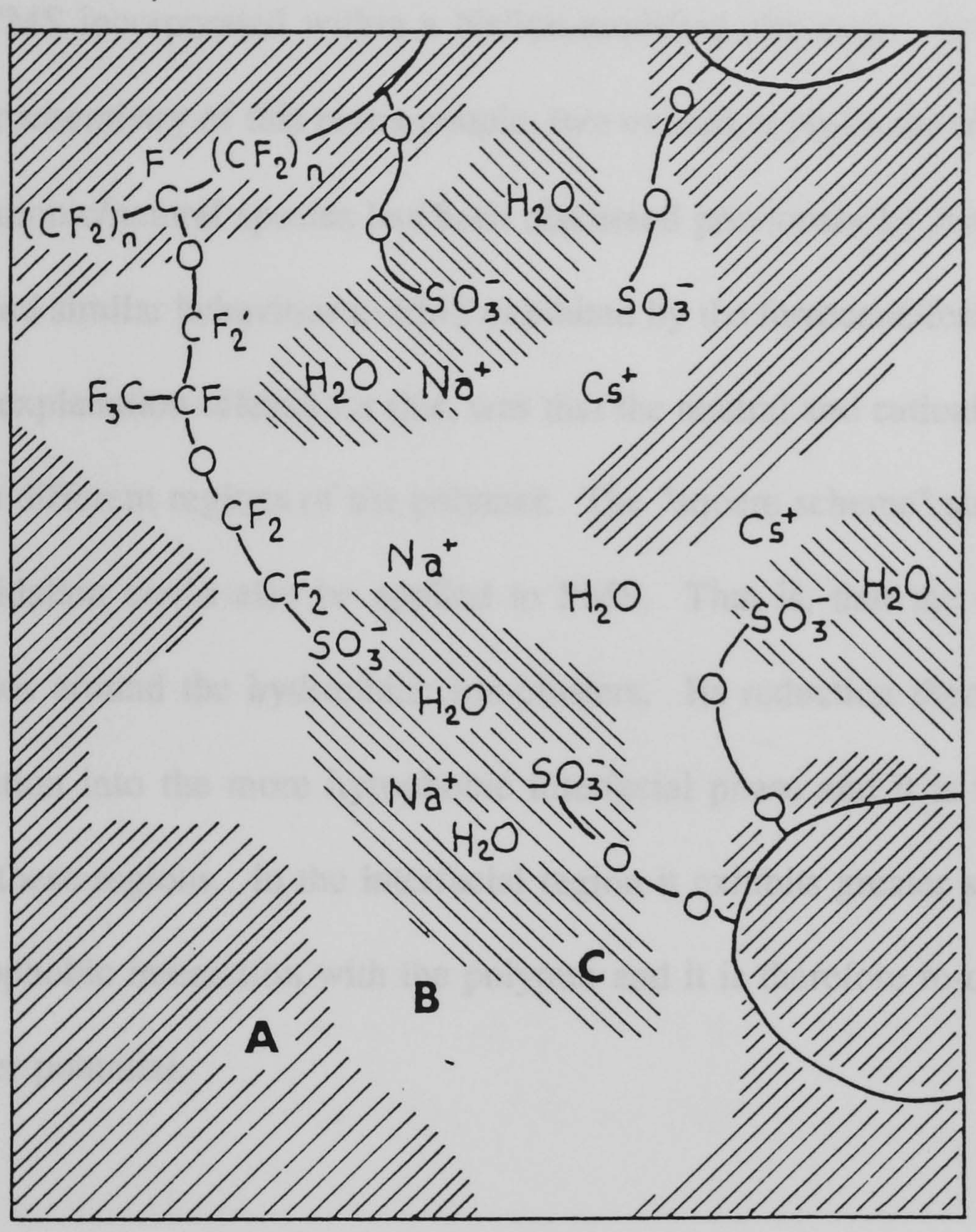

Fig. 4.5 Three-region structural model for Nafion as suggested by Yeager and Steck (1981). A, fluorocarbon; B, interfacial region; C, ion-clusters.

4.3.2 Electrochemistry of Phenazine Methosulphate

Qualitative evidence for the possibility of coupling these diffusional pathways, was provided by using phenazine methosulphate ($PMS^{+/0}$) as a probe. Fig.4.6 shows a cyclic voltammogram of PMS incorporated within a Nafion-modified electrode. In contrast to the solution electrochemistry of this redox couple, two oxidation peaks are observed. The behaviour of cationic/neutral species has been discussed previously by Rubinstein (1985), who has found similar behaviour to PMS exhibited by the ferrocene/ferricinium ($Fc^{+/0}$) couple. The explanation offered for this, was that the neutral and cationic forms of Fc resided within different regions of the polymer. The "square scheme" suggested for its reduction/oxidation could also be applied to PMS. That is, that the cationic PMS^{+} initially resides around the hydrophilic ion-clusters. Its reduction then causes some PMS^{0} to partition into the more hyrophobic interfacial phase and it is thus re-oxidised from both these regions. In the interfacial region it exhibits greater stability, due to greater hydrophobic interaction with the polymer and it is therefore re-oxidised from here at a higher potential.

Fig. 4.7 shows a voltammogram of PMS incorporated within the Nf/PVA composite. Here a single peak is observed for the re-oxidation of PMS^{0}, corresponding to the hydrophilic region of the film. Thus suggesting that PMS^{0} in these films travels to the electrode via a single pathway.

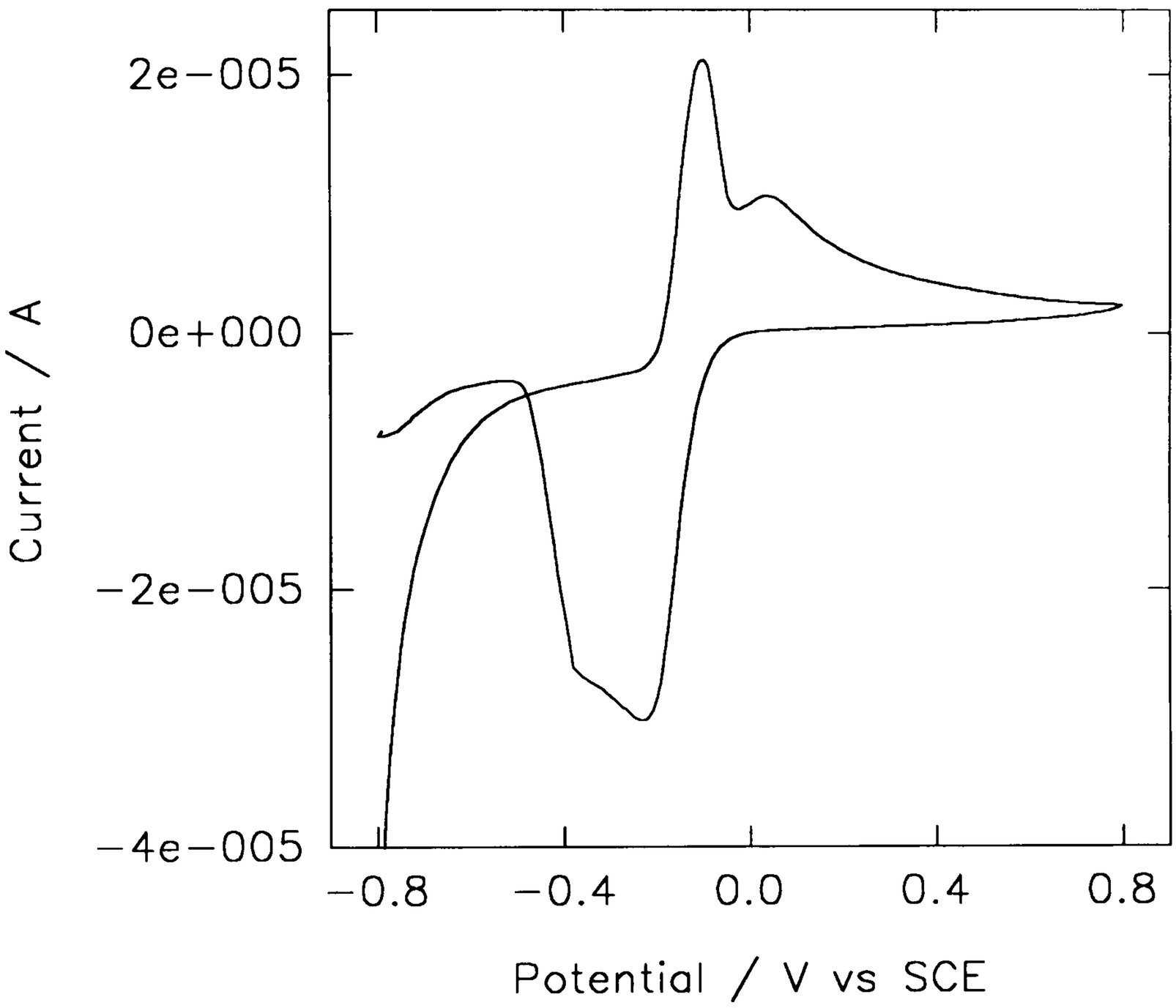

Fig. 4.6 Voltammogram of Nafion-modified electrode following the incorporation of PMS. Scan recorded in PMS-free buffer solution. Scan rate = 5 mV/s.

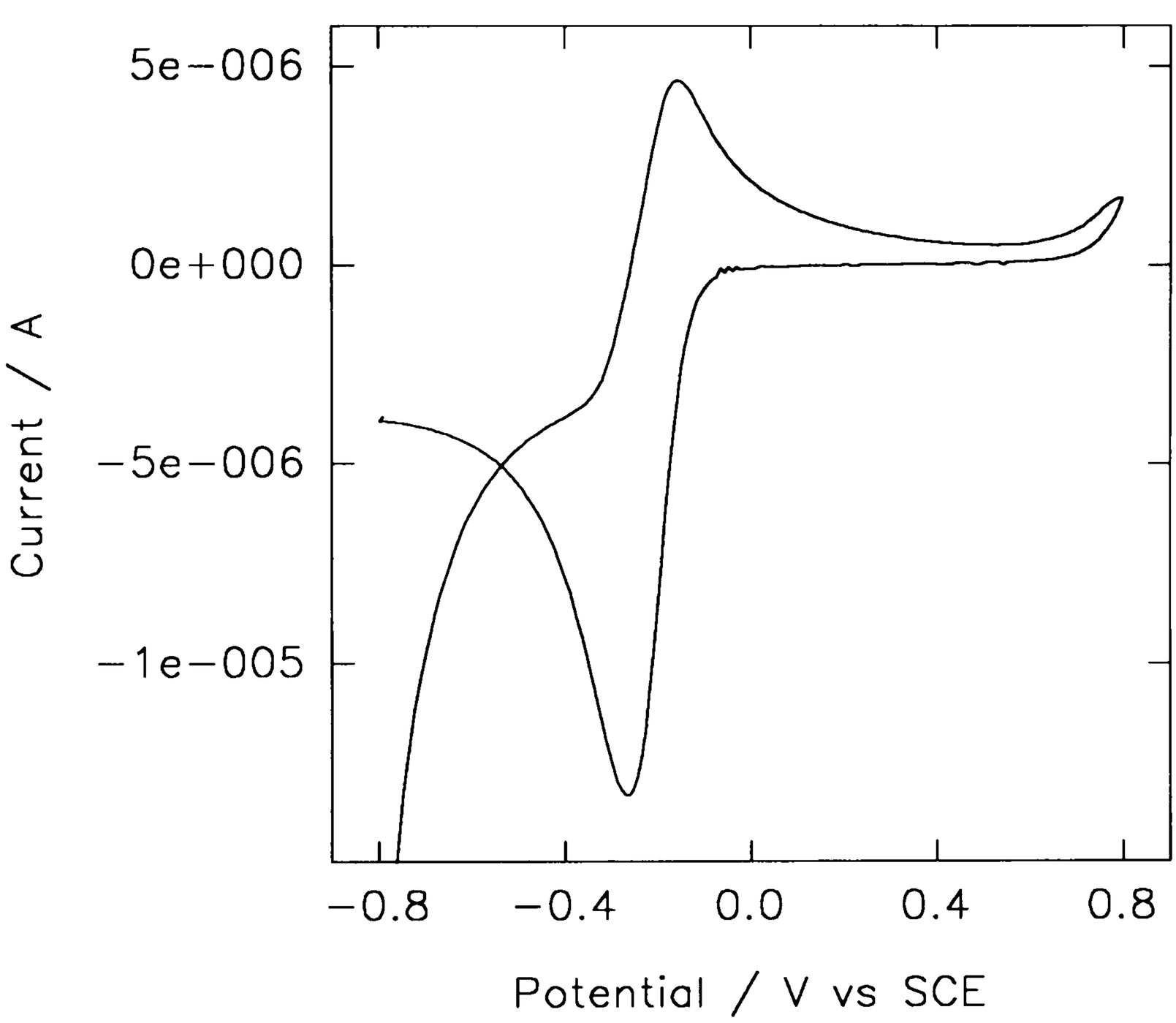

Fig. 4.7 Voltammogram of Nf/PVA-modified electrode following the incorporation of PMS. Scan recorded in PMS-free buffer solution. Scan rate = 5 mV/s.

4.3.3 Charge Transport by $Ru(NH_3)_6^{3+}$

Given this explanation for charge transport within the composite films, less of an increase would be expected in D_{exp} for a cation already present in the hydrophilic phase of Nafion, where the rate of diffusion is already notably more rapid. This is in agreement with the values of D_{exp}/L^2 recorded for $Ru(NH_3)_6^{3+}$ (0.03 ± 0.01 s^{-1} and 0.03 ± 0.02 s^{-1} for Nf and Nf/PVA respectively). It should also be noted that $Ru(NH_3)_6^{3+}$ has a lower value of k_{ex} (4×10^3 $M^{-1}s^{-1}$) (Meyer & Taube, 1968) than MV^{2+} and will therefore also be less able to couple with species present in the aqueous phase of the composite films.

For the range of $Ru(NH_3)_6^{3+}$ surface coverages achieved here (2.8 to 8.0 x 10^{-8} mol cm^{-2}), no concentration dependence for D_{exp}/L^2 was observed in either type of film. This could perhaps be because the changes in these values were within the experimental error of the measurements. Although it should also be noted that Crumbliss *et al* (1992) failed to find any concentration dependence for the D_{exp} values of $Ru(NH_3)_6^{3+}$ within films of a carageenan hydrogel.

4.3.4 Biocompatability

The resistance of the composite films to protein adsorption, was examined by following the change in electrochemistry of $Ru(CN)_6^{4-}$. An inital cyclic voltammogram (scan rate 20 mV/s) was recorded for 0.91 mM $Ru(CN)_6^{4-}$ in buffer solution at an Nf/PVA-modified electrode. An increasing concentration of albumin (bovine) was then added to the cell. After the addition of each aliquot, the solution was first stirred for 30 s to allow a uniform distribution of protein within the cell, and was then left to stand for

15s; a voltammogram was then recorded as before. Albumin has an iso-electric point of 4.7 (Johnson, 1991) and therefore at the pH of the working buffer (pH 7.0), will exhibit an overall negative charge. Thus, as the protein adsorbs onto the Nf/PVA film, it forms a barrier which can exclude the $Ru(CN)_6^{4-}$ anions by both charge and size. Hence, an attenuation of the $Ru(CN)_6^{4-}$ redox peaks is noted. Eventually, at high concentrations of protein, no redox activity is observed.

The same experiment was repeated for bare glassy carbon and bare platinum, and for a glassy carbon electrode coated with a cellulose acetate membrane and with a 0.05 μm poly(carbonate) membrane. The results given in Fig. 4.8, show the percentage decrease in the cathodic peak height of $Ru(CN)_6^{4-}$ for each membrane, as a function of the protein concentration. As can be seen, all three membranes give improved resistance to adsorption, when compared to the bare electrodes. However, the resistance provided by Nf/PVA was clearly superior to cellulose acetate and poly(carbonate). Obviously, these experiments involved a far less complex sample matrix than that provided by blood or serum. However, they never the less indicate that the composite films could perhaps be of use in the analysis of such materials. In general, the biocompatability exhibited by some hydrogels is thought to be due to their ability to simulate natural tissue due to their high water content and low interfacial tension. The possible biocompatability of the Nf/PVA films will be discussed in the General Discussion (Section 6.3).

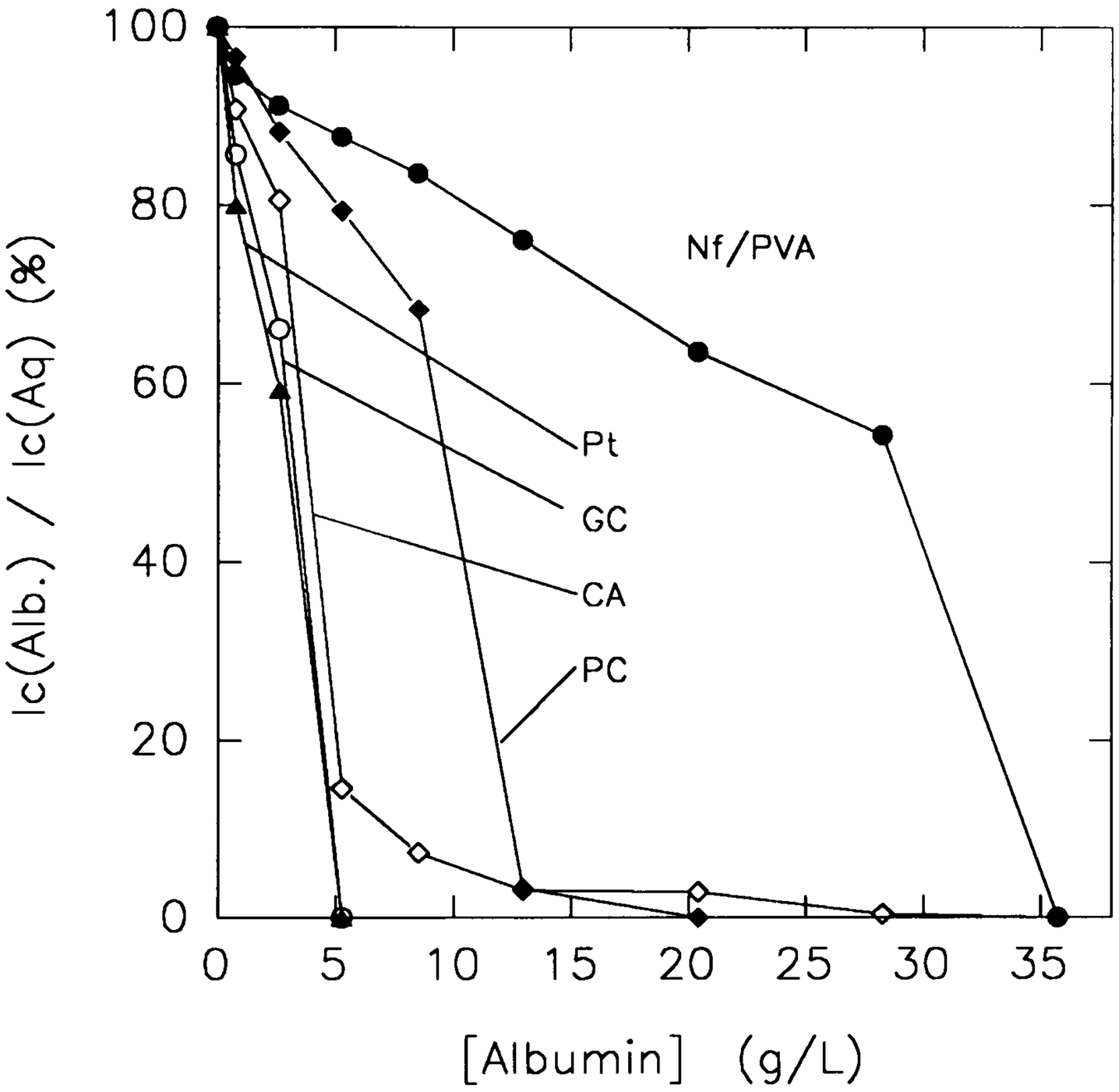

Fig. 4.8 Effect of albumin adsorption on the redox activity of a 0.91 mM $Ru(CN)_6^{4-}$ solution. The percentage decrease in the cathodic peak height is plotted as a function of the albumin concentration for bare glassy carbon (GC), bare platinum (Pt) and glassy carbon coated with cellulose acetate (CA), poly(carbonate) (PC) and the Nafion/PVA composite (Nf/PVA). Scan rate for all voltammograms = 20 mV/s.

4.3.5 Enzyme Immobilisation

To illustrate an analytical application for the Nf/PVA films, the immobilisation of glucose oxidase (GOD), by entrappment within the composite gel prior to cross-linking, was examined. In the first attempt to immobilise the enzyme, the Nf/PVA/GOD mixture was prepared in a buffer solution of pH 7.0. However, this produced a film with poor mechanical stability, which desorbed from the electrode after inital rinsing with de-ionized water. Previous work in this laboratory has shown that Nafion films also exhibit poor adhesion when cast over $Fe(CN)_6^{4-}$ (Jaffari, 1993) and therefore it seemed likely that the instability seen here was due to repulsion between the negatively charged enzyme and the $-SO_3^-$ sites of the polymer.

The iso-electric point of GOD is 4.2 (Swoboda & Massey, 1961) and hence a positive charge was induced in the enzyme by preparing the immobilisation solution in a buffer solution of pH 4.0. These films showed good mechanical stability. The enzyme is in this case entrapped by both physical adsorption and ion-exchange. It has been shown previously (Rubinstein, 1985) that exchanging Na^+ ions in Nafion with a bulky, weakly-hydrated cation, causes the ion-cluster region to become more hydrophobic, due to partial dehydration. Experiments with ruthenium red indicated that GOD had such an effect on the composite film. Fig. 4.9 (A) shows a voltammogram of ruthenium red within a Nf/PVA film, while Fig. 4.9 (B) shows the same cation within an Nf/PVA/GOD matrix. The addition of GOD causes the disapperence of the ruthenium red redox peaks, indicating immobility within the film, presumably due to the relatively large cation being held rigidly within constricted hydrophilic regions. This would suggest that the preferable choice of mediator for this system, would be a compound which could undergo hydrophobic interactions with Nafion, while coupling with species

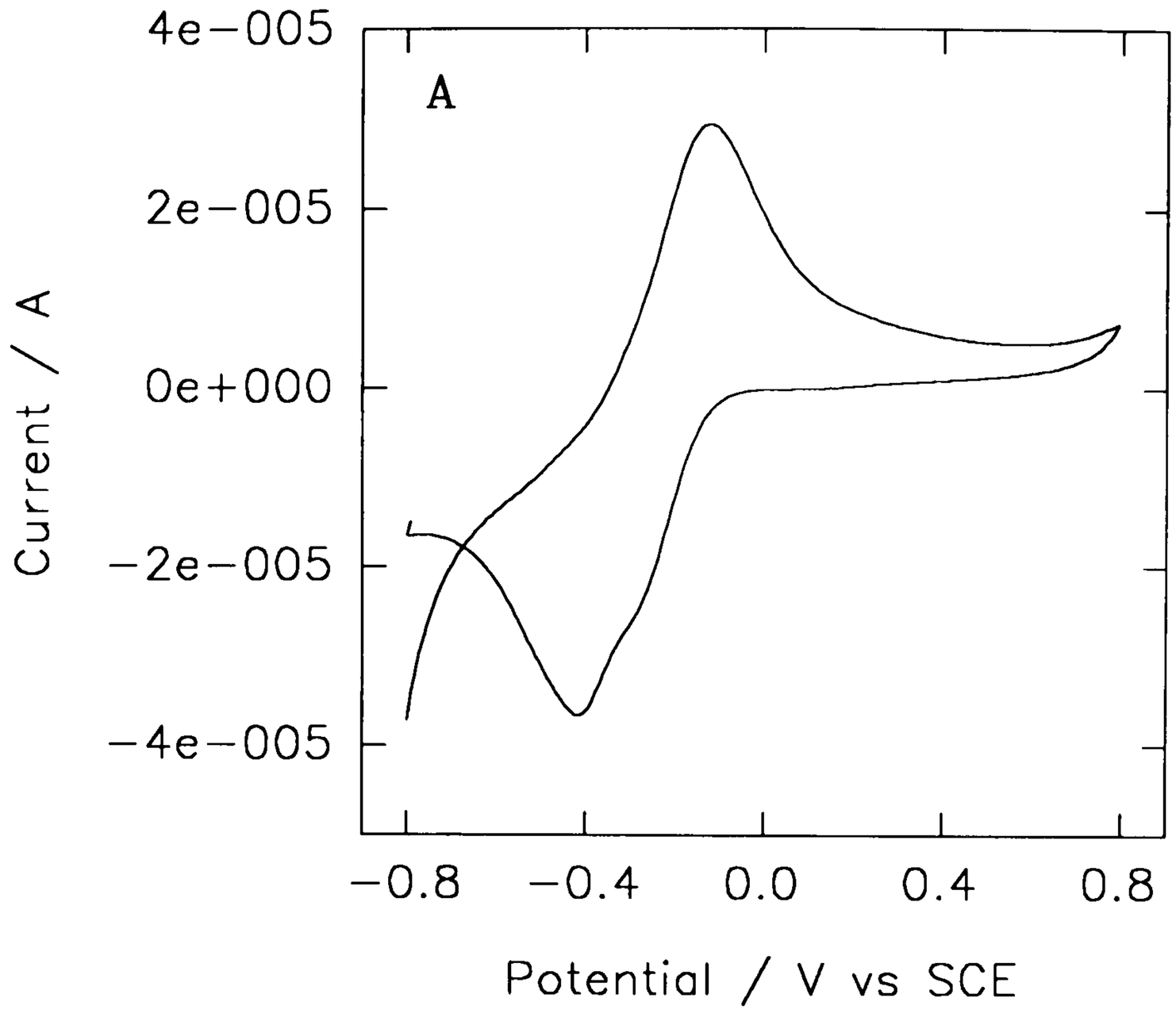

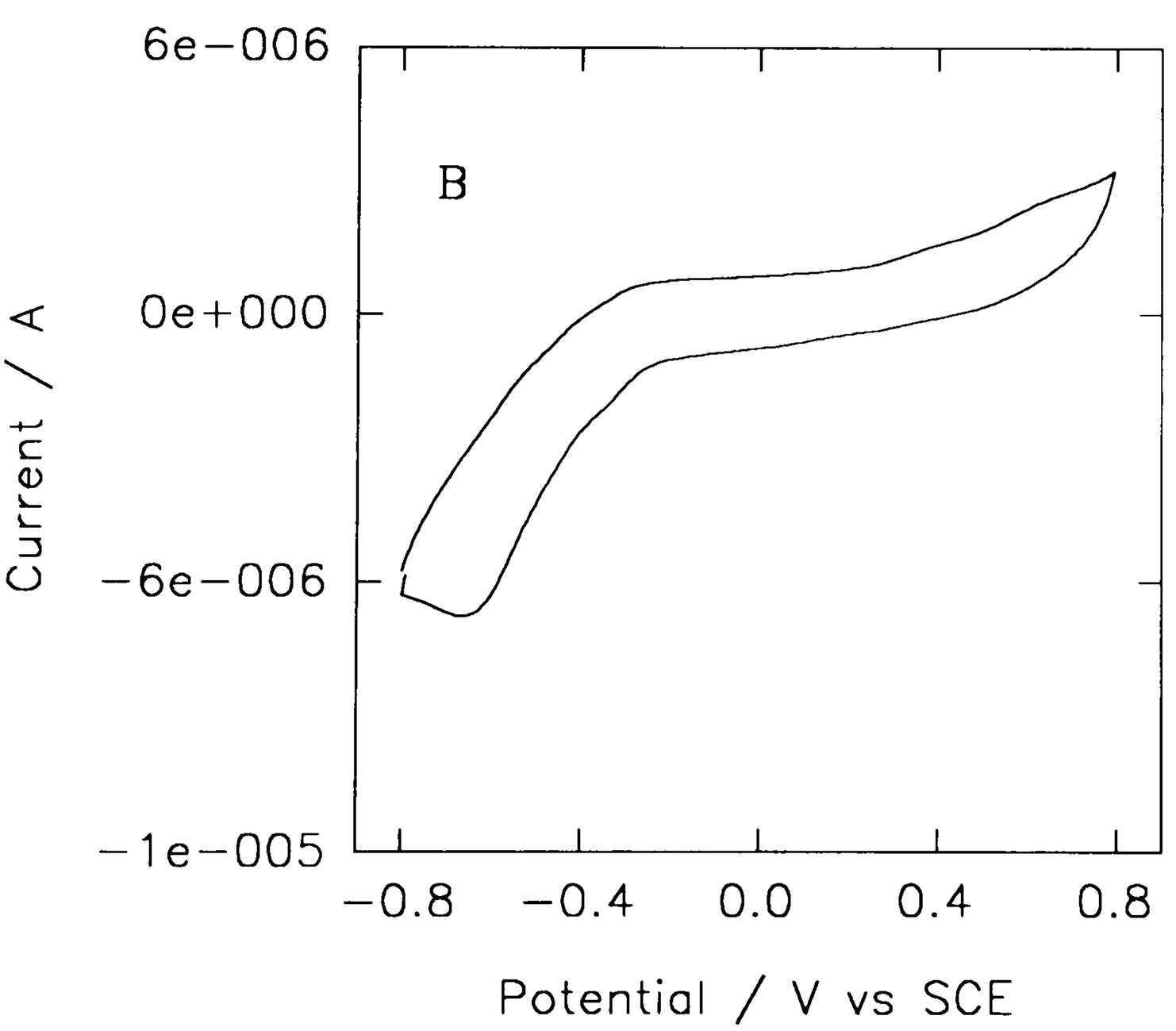

Fig. 4.9 Voltammogram of ruthenium red following its incorporation into a film of Nf/PVA (A) and Nf/PVA/GOD (B). Both voltammograms were recorded in ruthenium red-free buffer solution. Scan rate = 50 mV/s.

present in the solution phase of the composite. Hence PMS was chosen for co-immobilisation with the enzyme.

Fig. 4.10 (A) shows a slow scan rate cyclic voltammogram (2 mV/s) for an Nf/PVA/GOD film under anaerobic conditions, following the incorporation of PMS. It should be noted that PMS exhibits a single oxidation peak, corresponding to the species present in the aqueous phase of the composite. Figure 4.10 (B) shows the effect of adding D-glucose to the bulk solution at a concentration of 0.2 M. An increase in the PMS oxidation peak is observed, along with the disappearence of the peak corresponding to its reduction. When the same experiment was performed using an Nf/PVA film, no change in PMS electrochemistry was observed upon the addition of glucose. This suggests that Fig. 4.10 (B) represents the coupling of the enzymatic oxidation of glucose with the electrochemical re-oxidation of GOD, via mediated electron transfer through PMS.

Amperometric determination of glucose was performed at 0 mV in ambient conditions, using the electrode modification described above. As shown in Fig. 4.11, D-glucose was calibrated across the range 0.5 to 3.5 mM. The kinetics of membrane enzyme electrodes have previously been examined by Albery and Bartlett (1985), who have shown that if concentration polarisation is assumed to be negligable in both bulk solution and within the enzyme layer, and that there is no product inhibition, then the electrode response can be described by the following equation:

$$S/j = 1/k_{ME}' \, (1 + S/K_{ME} \, [1 - j/k_s'S]) \qquad (4.10)$$

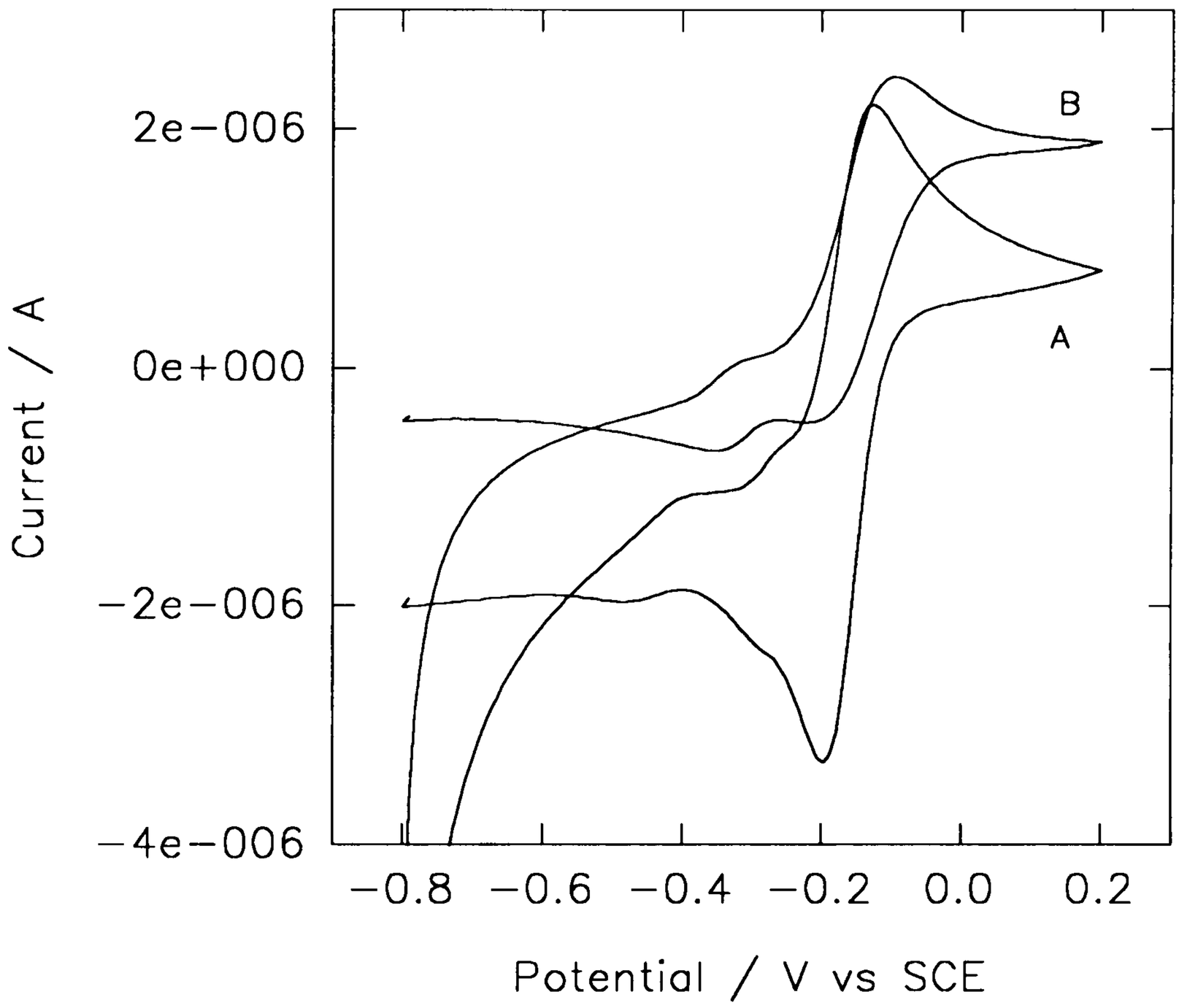

Fig. 4.10 (A) Voltammogram of an Nf/PVA/GOD film under anaerobic conditions, following the incorporation of PMS. (B) as for (A), but following the addition of D-glucose to the bulk solution at a concentration of 0.2 M. Scan rate = 2 mV/s.

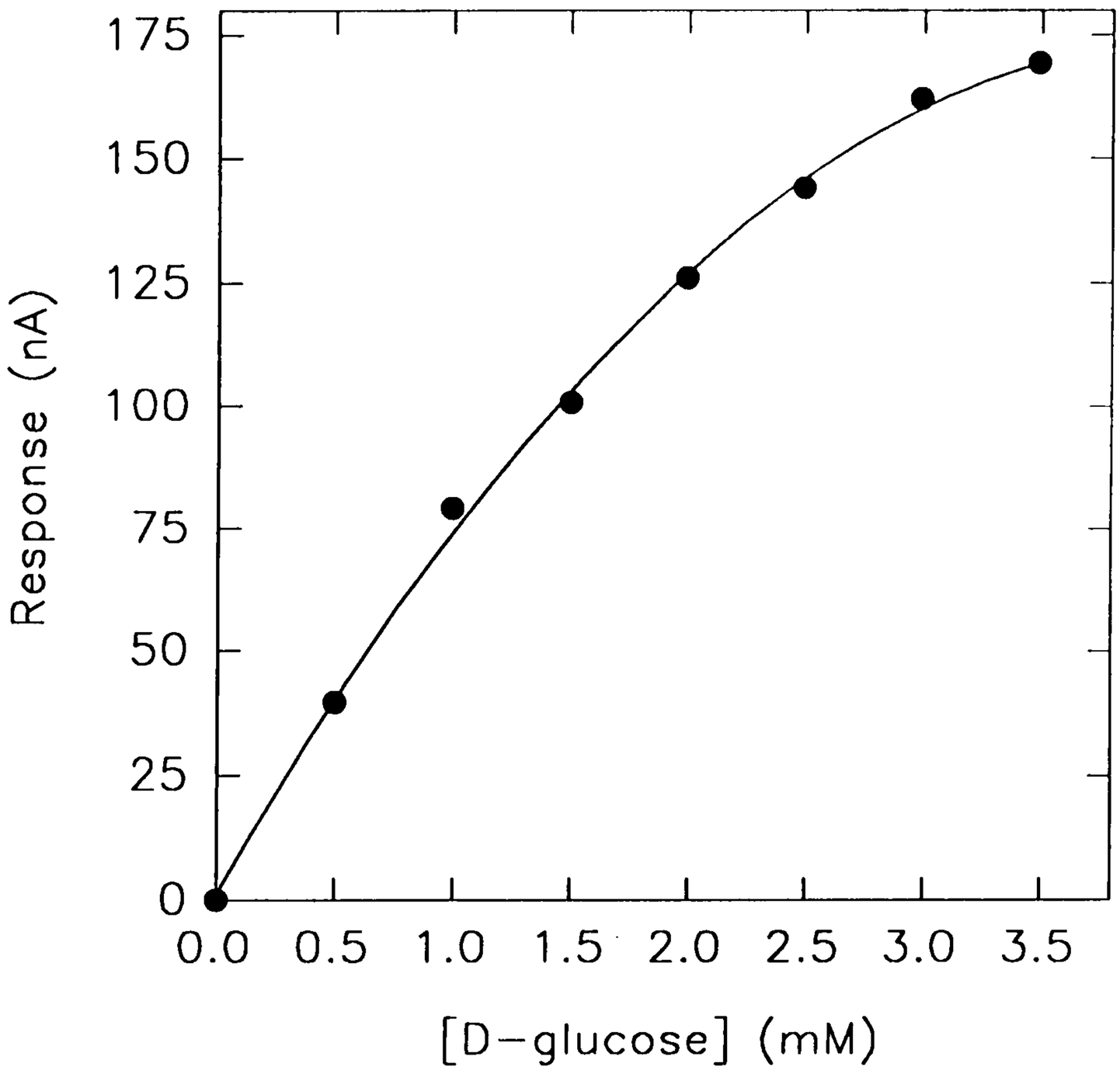

Fig. 4.11 Amperometric determination of D-glucose at 0 mV, using an Nf/PVA/GOD-modified electrode under ambient conditions, following the incorporation of PMS as electron-transfer mediator.

Where j (mol cm^{-2} s^{-1}) is the steady-state flux, k_{ME}' (cm s^{-1}) is the effective heterogeneous rate constant for the enzyme electrode, K_{ME} is the electrochemical Michaelis constant, k_s' (cm s^{-1}) is the rate of diffusion of substrate through the membrane and S is the concentration of substrate in bulk solution. The steady-state flux j, can also be described by

$$j = inF \qquad (4.11)$$

Where i is the current density (A cm^{-2}). Thus, a plot of S/i against S will give a *y*-intercept of $1/nFk_{ME}$'. This plot is shown in Fig. 4.12 (A), and leads to a value for k_{ME}' of 5.1×10^{-6} cm s^{-1}. Albery and Bartlett (1985) have also shown that the inverse of the *y*-intercept ($[i/S]_o$) enables calculation of the dimensionless ratio

$$\rho = [i/S] / [i/S]_0 \qquad (4.12)$$

which can be related to the kinetic terms in eq. 3 by

$$y = (\rho^{-1} - 1)/S = 1/K_{ME} (1 - \rho k_{ME}'/k_s') \qquad (4.13)$$

Figure 4.12 (B) shows a plot of y (mM^{-1}) against ρ. From this a value for K_{ME} of 3.2 mM can be calculated and a value for k_s' of 9.0×10^{-6} cm s^{-1}. These values suggest a mixture of kinetic and diffusional control for the overall electrode response. A purely diffusion limited response would be more preferable as this would produce insensitivity to slight changes in enzyme activity. A higher value of K_{ME} would also be required to measure glucose across the full clinical range (4-30 mM) (Tietz, 1987). Both requirements could perhaps be supplied by an additional membrane, such as a further PVA layer or by changes in the concentration

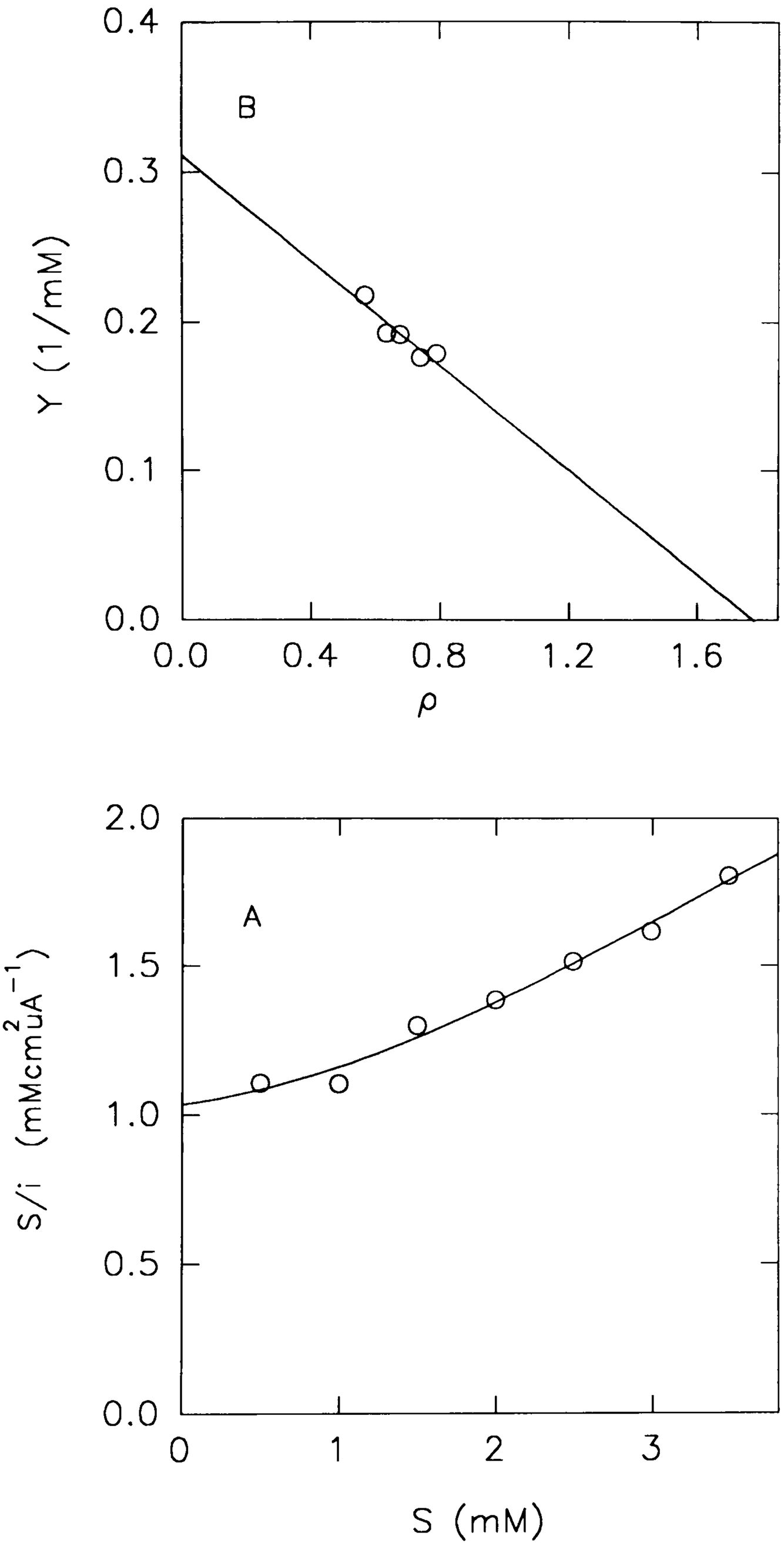

Fig. 4.12 (A) Plot of [substrate]/current density (S/i) as a function of current density (i), enabling calculation of k_{ME}' and the dimensionless ratio ρ ($[i/S]/[i/S]_0$). (B) Plot of $(\rho^{-1} -1)/S$ (Y) as a function of ρ, enabling calculation of K_{ME} and k_s'.

of either Nafion or PVA in the composite layer.

The long-term stability of the electrode was not examined, as PMS is neutral in its reduced state and would therefore not be expected to be retained over long periods. Also, the light sensitivity of the compound would further reduce electrode stability. However, these experiments served to illustrate that an enzyme could remain active within the composite film and could communicate with an electron transfer mediator. The obvious next step for this work would be to examine hydrophobic mediators which would both couple with an enzyme and remain cationic in their reduced form. Ferrocene derivatives of varying hydrophobicity have been shown to accept electrons from GOD (Cass *et al.*, 1984), and the synthesis of ferrocenes with positively charged pendent groups has previously been described (Schlogl & Falk, 1976). This area will be discussed further in the General Discussion (Section 6.3).

Chapter Five Alternatives to Mediation : Mediatorless Electrocatalysis by a Conducting Polymer

5.1 Introduction

In Parts I and II of Chapter 3 the possibility of electrocatalysis by electron transfer mediators was examined. The use of mediators entails either their presence in bulk solution, or the construction of an appropriate immobilisation matrix, enabling binding of the mediator by either adsorption, ion-exchange or the formation of covalent bonds. In this section an alternative strategy of modifying the electrode with a polymer which is itself inherently electrocatalytic, thus obviating the need for the co-immobilisation of a redox mediating species, is examined.

One of the most extensively studied treatment of electrodes in recent years, has been the synthesis of conducting polymers by electro-deposition (Imisides *et al.*, 1991). This is a procedure which has been shown to produce adherent polymer films and has the advantage of producing a precise coverage of virtually any electrode geometry, whilst allowing control over the thickness of the resulting film, by monitoring the current density of the reaction.

The electrochemical synthesis of a conducting polymer was first described by Dall'Olio (1968) for poly(pyrrole) and has since been reported for a variety of analogous monomers which include thiophene, furan, carbazole, indole, azulene, pyrene, fluorene, thianapthene and fluoranthene. A thorough review is given by Waltman and Bargon (1986). The mechanism for polymerisation in these cases is the same and consists of the following steps:

1) The electrode is poised positive of the oxidation potential of the monomer (R) and hence R is oxidised to give a radical cation ($R^{\cdot +}$), which adsorbs to the electrode.

2) This then reacts with another monomer unit (in preference to other nucleophiles which may be present in the solution) to form a dimer.

3) The adsorbed dimer is again oxidised to a radical cation, enabling binding with a further monomer. Hence a conjugated polymer film is built up on the electrode. Overall, the reaction can be described as follows:

$$(n + 2)R \quad \text{----->} \quad R\text{-}(\text{-}R\text{-})_n\text{-}R \quad + \quad (2n + 2)H^+ \quad + \quad (2n + 2)e^- \qquad (5.1)$$

All the monomers described above contain double bonds and when polymerised form an extended π-system. Conductivity in these films is achieved by driving the polymer into an oxidised state:

$$R\text{-}(\text{-}R\text{-})_n\text{-}R \quad \rightleftharpoons \quad R\text{-}(\text{-}R\text{-})_n\text{-}R^+ \quad + \quad e^- \qquad (5.2)$$

The removal of an electron facilitates electron hopping across the overlapping π-orbitals, effectively the movement of a positive hole in the opposite direction. It should be noted that because the film remains on the electrode as it is generated, the ability of the material to conduct is important for the continuation of the reaction. Hence, the oxidation potential of the polymer must be lower than that of the monomer, for it to form as a conducting film.

To provide electrical neutrality during the film growth, anions are incorporated from the electrolyte solution. Elemental analysis performed on poly(pyrrole) grown from dilute H_2SO_4 (Diaz, 1981), gave 0.15 SO_4^- ions present per pyrrole molecule, implying that when oxidised the polymer possessed a positive charge on every 3-4 monomer units.

Experiments have shown that the degree of oxidation is an intrinsic characteristic of the polymer rather than the counter-ion (Skotherm, 1986).

The ability to incorporate anions is an important feature of conducting polymers. The nature of the counter-ion can affect physical properties of the polymer such as morphology, conductivity, adhesion and mechanical strength (Skotherm, 1986). Additionally, counter-ion incorporation can be used to immobilse electrocatalysts. Examples of redox species immobilised in this manner include ferrocenecarboxylate (Iwakura *et al.*, 1988), ferrocyanide (Schuhmann *et al.*, 1991), *o*-naphthoquinone-sulphonate (Schuhmann *et al.*, 1991), Meldola blue (Yabuki *et al.*, 1990), FMN (Matsue *et al.*, 1991), N-methyl phenazinium (Foulds & Lowe, 1986) and benzoquinone (Janda & Weber, 1991).

An extension to this approach is the entrapment of a negatively charged enzyme. This was first illustrated by Foulds and Lowe (1986) for glucose oxidase. The process has since been demonstrated for dehydrogenases such as fructose (Khan *et al.*, 1992), alcohol (Yabuki *et al.*, 1990), glutamate (Yabuki *et al.*, 1991) and NADH (Matsue *et al.*, 1991). Mediator-based biosensors have thus been constructed by the entrapment of both enzyme and redox couple (Yabuki *et al.*, 1990).

However, a drawback to this approach is the leakage of the anionic mediator. Polymers such as poly(pyrrole) have been shown to exhibit ion-exchange properties (Beck *et al.*, 1989) and hence mediator located just below the polymer/solution interface will exchange with electrolyte ions. For example, Schuhmann *et al* (1991) have shown that

for an electrode stored in buffer solution, the redox activity of incorporated $Fe(CN)_6^{4-}$ disappeared over 24 hrs.

A more preferable, but as yet little examined alternative, is the use of a polymer which is electrocatalytic without requiring the action of an entrapped mediator. Thus far, only one such polymer, poly(3-methylthiophene) has been reported (Atta *et al.*, 1990). Inital experiments on NADH oxidation led to the development of a second such material. This is described in this Chapter.

5.2 Experimental

5.2.1 Reagents

Indole and indole-5-carboxylic acid were provided by Sigma Chemical Co. (Dorset, UK) and were used as received. Pyrrole (Sigma) was re-distilled with a short vigreiux column to give a clear liquid, which was stored in the dark at < 4 °C and was used, at most, within 12 hrs of its purification. All stock solutions were prepared in 50 mM Tris-HCl buffer at the pH stated in the text. Where solutions were used in electrochemical measurements, KCl was added as supporting electrolyte at a concentration of 50 mM unless otherwise stated. All other reagents were supplied and used as described in previous chapters. All solutions were prepared freshly prior to the start of each experiment.

5.2.2 Apparatus

The working electrode was a glassy carbon disc of 3 mm diameter or a platinum disc of 1.5 mm diameter. The reference and counter electrodes were as described in Chapter 3 Part I. The apparatus for cyclic voltammetric and amperometric experiments was as described in Chapter 2 (Section 2.2.2) and Chapter 3 Part I (Section 3.2.2) respectively. Before use the working electrode was polished, sonicated and rinsed according to the procedure described in Chapter 3 Part I (Section 3.2.2). All experiments were performed at room temperature, under ambient conditions unless otherwise stated. Where anaerobic conditions were required they were created as described in Chapter 3 Part I (Section 3.2.2).

5.2.3 Procedures

Enzyme immobilisation: Alcohol dehydrogenase (ADH) was immobilised on PICA films by physical adsorption, following cross-linking with glutaraldehyde. 40 µl of ADH solution (1700 U/ml in Tris-HCl buffer, pH 8.8) was transferred to the electrode face in 20 µl aliquots; each aliquot was left for 50 mins for partial evaporation of the solvent. 10 µl of 2.5 % glutaraldehyde solution was the deposited on the electrode and left for 40 mins at room temperature for cross-linking to occur. The electrode was stored in buffer (pH 8.8) below 4 °C.

5.3 Results and Discussion

5.3.1 Polymerisation

The electro-deposition of poly(indole-5-carboxylic acid) (PICA) by cyclic voltammetry, was examined in both organic and aqueous media. Films were grown onto both platinum and glassy carbon electrodes. PICA forms as a conducting layer and hence polymerisation was observed by noting the increase in redox peak heights for subsequent scans. Where films were grown from acetonitrile, the supporting electrolyte and polymer counter-ion was 0.1 M tetraethylammonium fluoroborate (TEAFB). When grown from aqueous media, this function was provided by 0.1 M potassium chloride.

Aqueous polymerisation solutions contained 5 mM monomer and were made up in Tris-HCl buffer (pH 8.8). Sonication of the polymerisation solution for 2 mins gave full dissolution of the monomer. The role of the buffer was to enhance the solubility of the monomer and also to provide pH control for the reaction (which as shown in eq. 5.1, will inject protons into the solution). The electrode potential was driven between -0.8 and 2.5 V at 0.2 V/s.

For polymerisation from acetonitrile, the potential was cycled from -0.8 to 1.5 V at 0.2 V/s. Indole-5-carboxylic acid exhibited greater solubility in acetonitrile and the monomer concentration was varied from 5 to 100 mM. Although pH control was not provided, polymerisation was still observed (from the increase in redox peak heights for subsequent scans).

A typical set of scans for the growth of PICA from acetonitrile is shown in Fig. 5.1. The increase in redox peak heights was similar for both glassy carbon and platinum electrodes. However, even when relatively thin films (from 5 mM monomer) were produced, they showed poor adhesion to the electrode and would desorb within 24 hrs of storage in buffer solution.

When grown from aqueous solution, PICA also desorbed from platinum relatively easily, but exhibited good adhesion to glassy carbon. A typical set of scans is shown in Fig. 5.2. Maximum coverage for these films was achieved by six to seven cycles, which corresponded on average to accumulating a charge density of approximately 0.2 C cm^{-2}.

It should be noted that for both types of film growth, the first scan, corresponding to the oxidation of only monomer units, reaches a higher potential before the onset of conductivity. Thus indicating that the polymer can be oxidised at a lower potential than the monomer. The difference in adhesion between polymers grown from aqueous and organic solutions was perhaps due to the different counter-ion. This feature of PICA was not investigated further as the films grown from buffer onto glassy carbon gave adequate stability for our purposes. The synthesis of substituted poly(indoles) has been studied previously by Waltman *et al* (1984), who found that polymers could be grown containing fairly bulky substituents on the benzene ring, but that substitution of the 3-position of the pyrrole ring made polymerisation impossible. Hence they suggested Fig. 5.3 as the likely structure for the indole polymers.

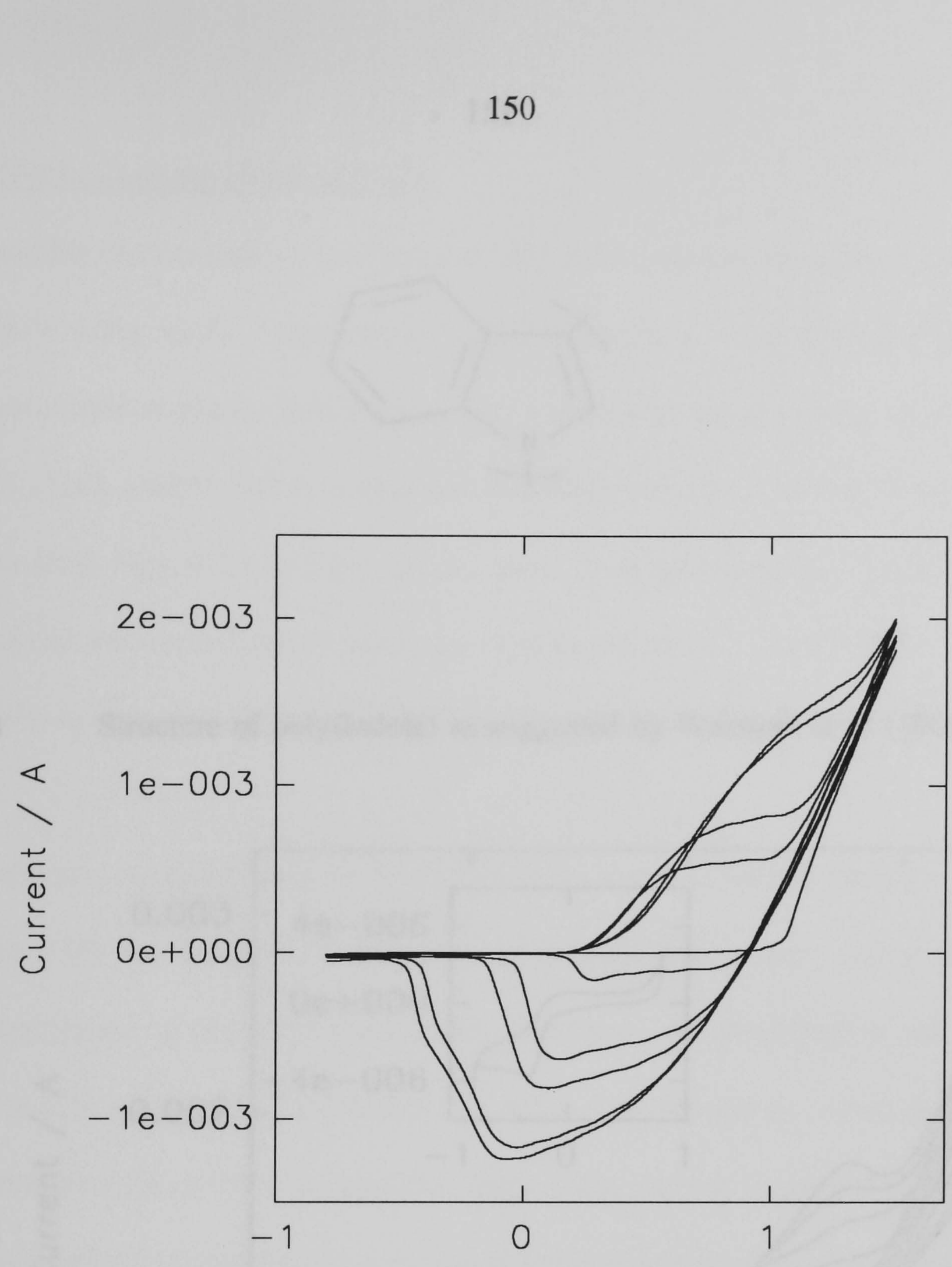

Fig. 5.1 Polymerisation of poly(indole-5-carboxylic acid) from 0.1 M monomer solution in acetonitrile containing 0.1 M TEAFB. Film growth is observed from the increase in peak heights for subsequent scans. Voltammograms 1,3,4,6 and 7 are shown. Scan rate = 200 mV/s.

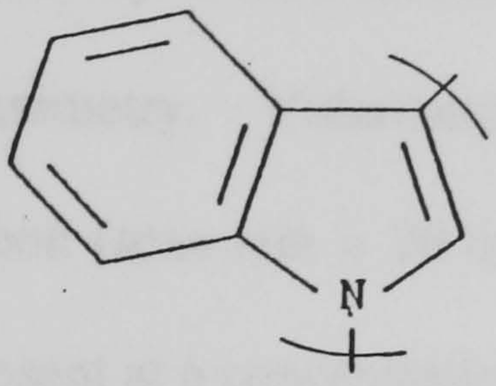

Fig. 5.3 Structure of poly(indole) as suggested by Waltman *et al* (1984).

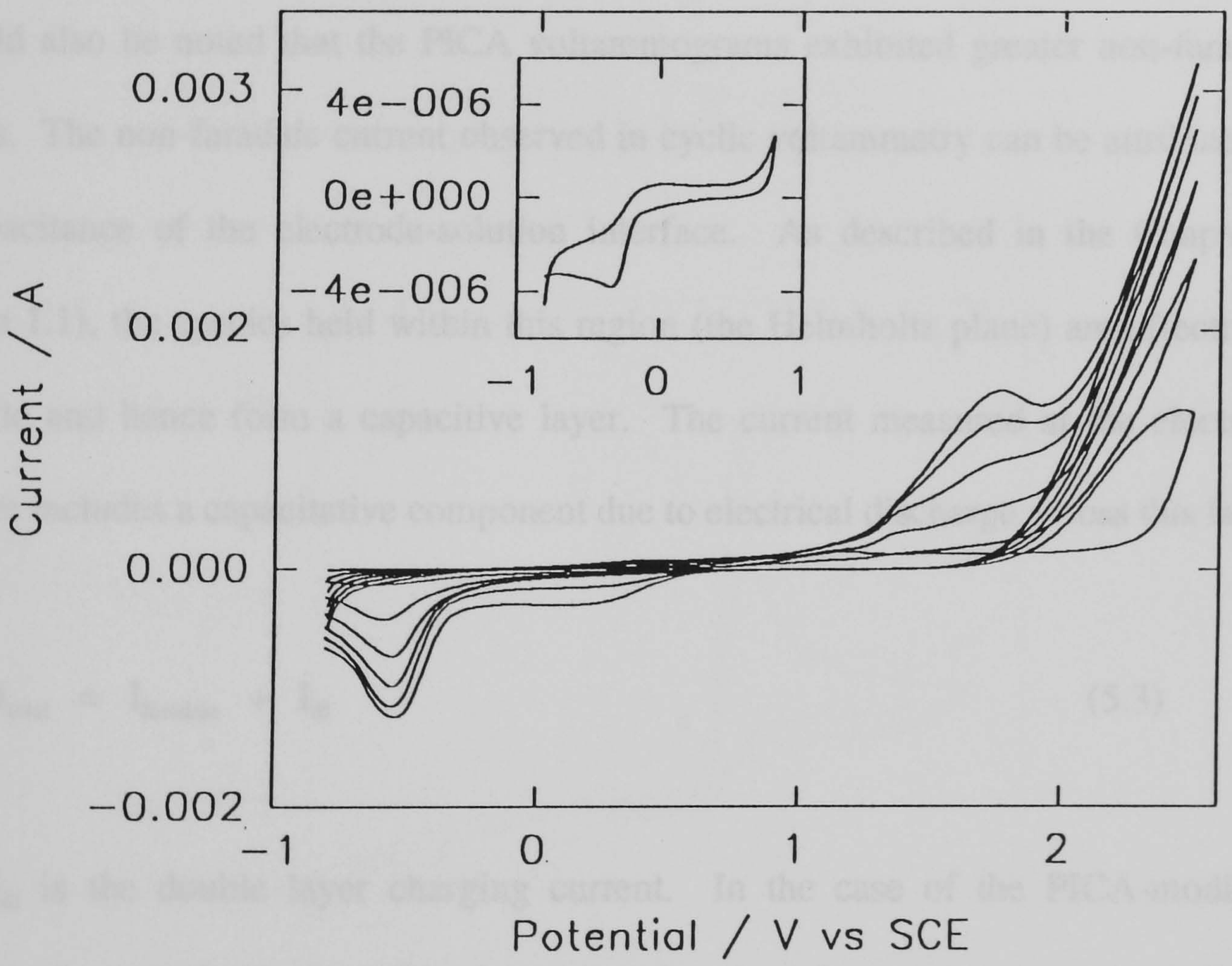

Fig. 5.2 Polymerisation of poly(indole-5-carboxylic acid) from 5 mM monomer solution in 50 mM Tris-HCl buffer, pH 8.8 containing 0.1 M KCl. Scan rate = 200 mV/s. *Inset:* Electrochemistry of PICA film in buffer solution. Scan rate = 20 mV/s.

5.3.2 Electrocatalytic Effect of PICA

The possible electrocatalytic activity of the PICA films grown from buffer solution, was examined using cyclic voltammetry. Voltammograms were recorded at bare and polymer-modified glassy carbon (scan rate = 20 mV/s) for ascorbate, urate, FAD and NADH. Each analyte was present at a concentration of 2 mM in bulk solution. As can be seen from Figs. 5.4.1 to 5.4.4, the oxidation peak potential (E_{pk}) for both ascorbate and NADH was shifted significantly in a negative direction. For ascorbate E_{pk} dropped from 300 to -90 mV, while for NADH the decrease in E_{pk} was from 500 to 390 mV.

It should also be noted that the PICA voltammograms exhibited greater non-faradaic currents. The non-faradaic current observed in cyclic voltammetry can be attributed to the capacitance of the electrode-solution interface. As described in the Chapter 1 (Section 1.1), the species held within this region (the Helmholtz plane) are effectively immobile and hence form a capacitive layer. The current measured at the electrode therefore includes a capacitative component due to electrical discharge across this layer:

$$I_{total} = I_{faradaic} + I_{dl} \qquad (5.3)$$

where I_{dl} is the double layer charging current. In the case of the PICA-modified electrode, the polymer in its reduced state can be viewed as a p-type semi-conductor from whose surface region, positive holes have been withdrawn. Thus a depletion region (alternatively known as the space charge region) is formed within the body of the polymer. This provides an added capacitive component, so that the total capacitance of the system becomes (Khan & Bockris, 1986):

$$1/C_{obs} = 1/C_{sc} + 1/C_{hl} \qquad (5.4)$$

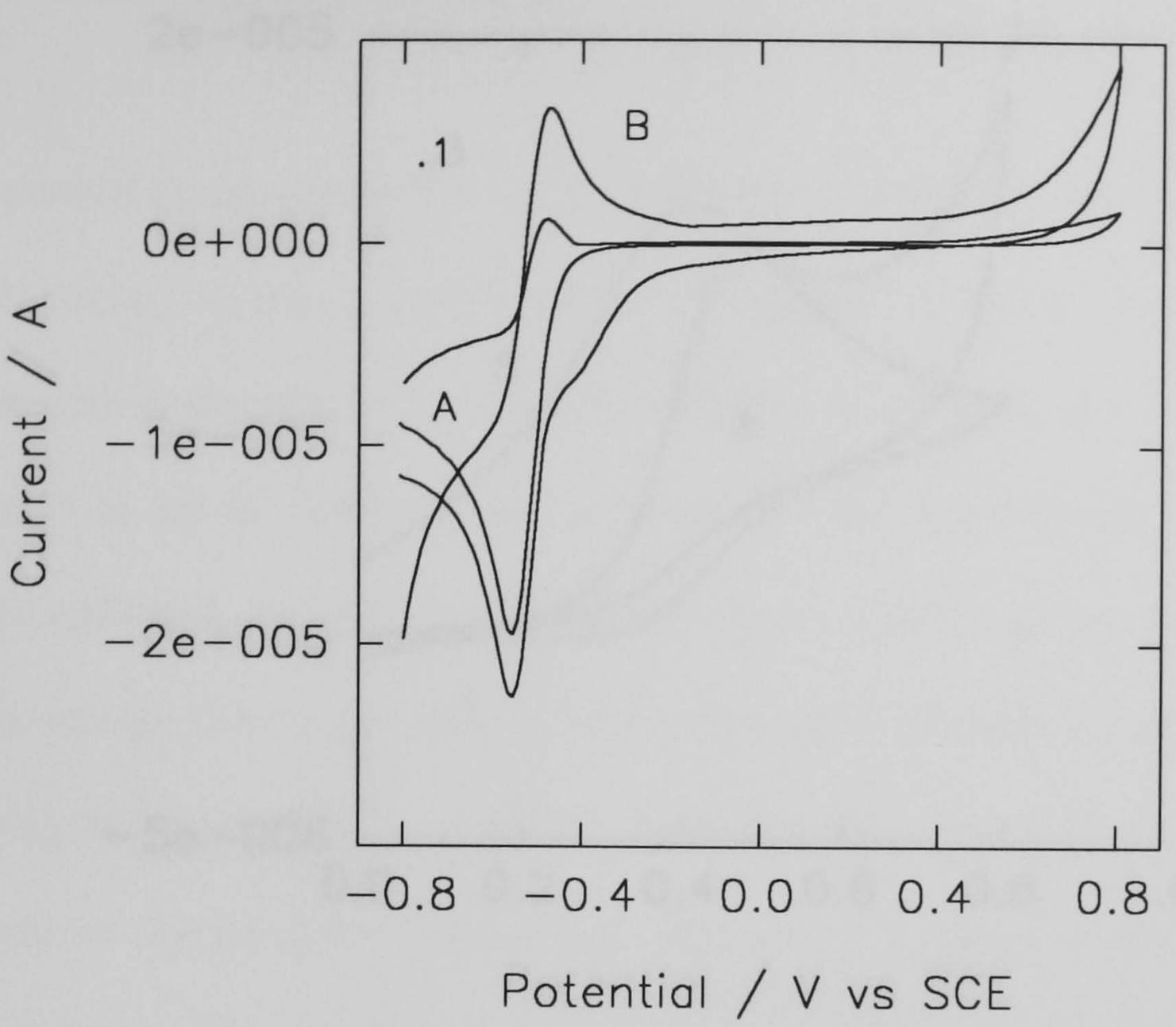

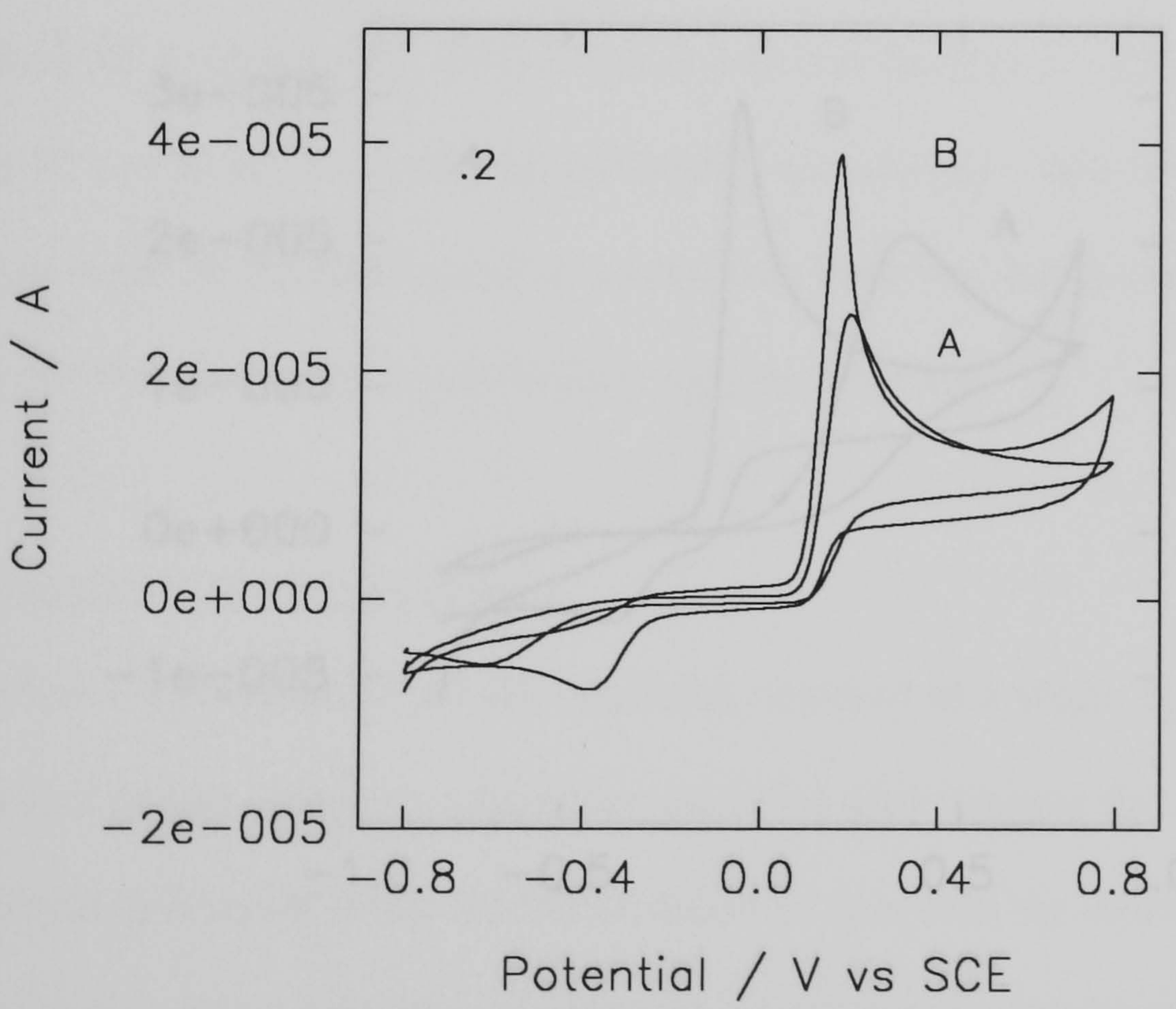

Fig. 5.4 (.1) Cyclic voltammogram of 2 mM FAD and (.2) 2 mM uric acid at (A) bare glassy carbon and (B) PICA-modified electrode.

Scan rate = 20 mV/s.

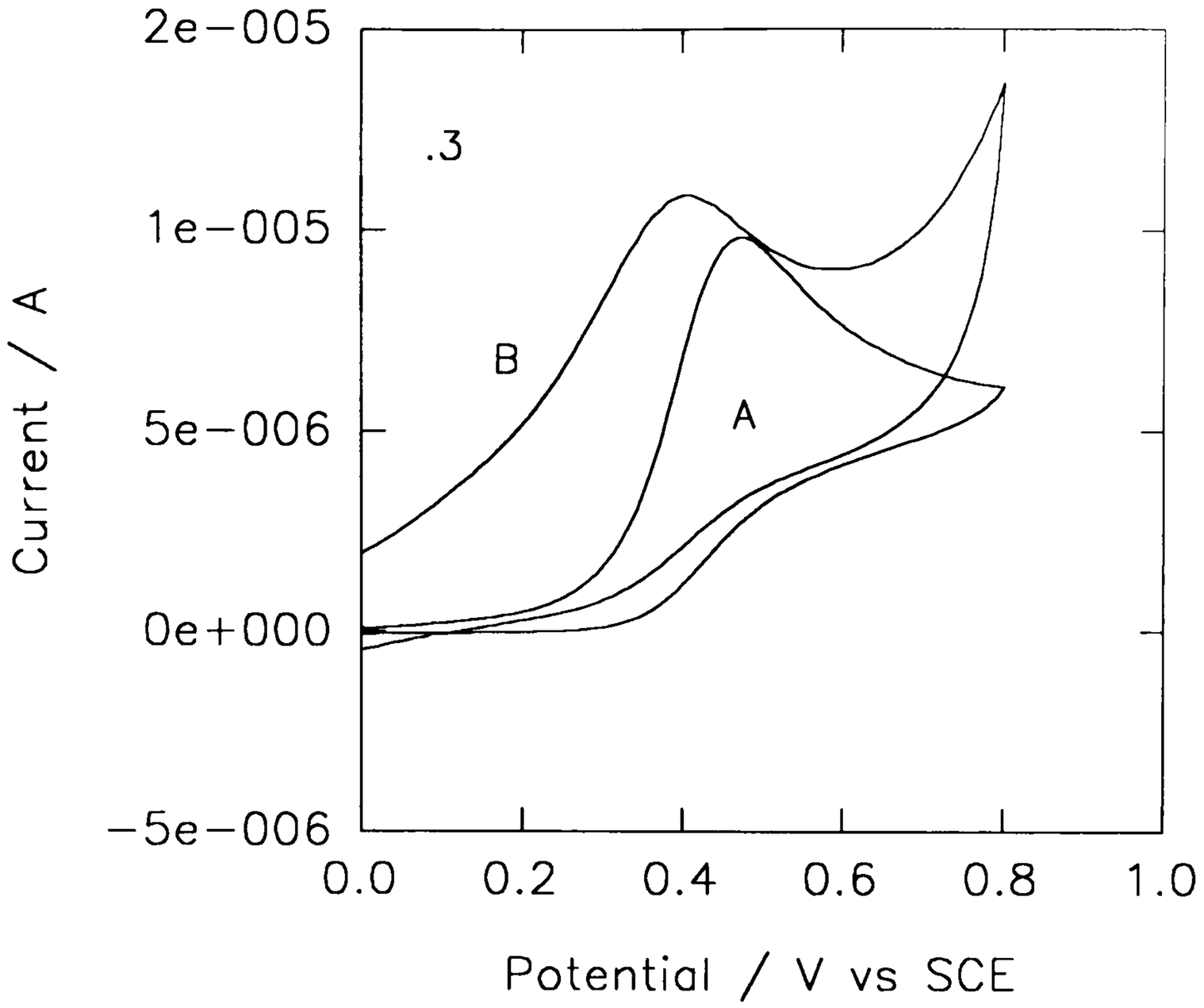

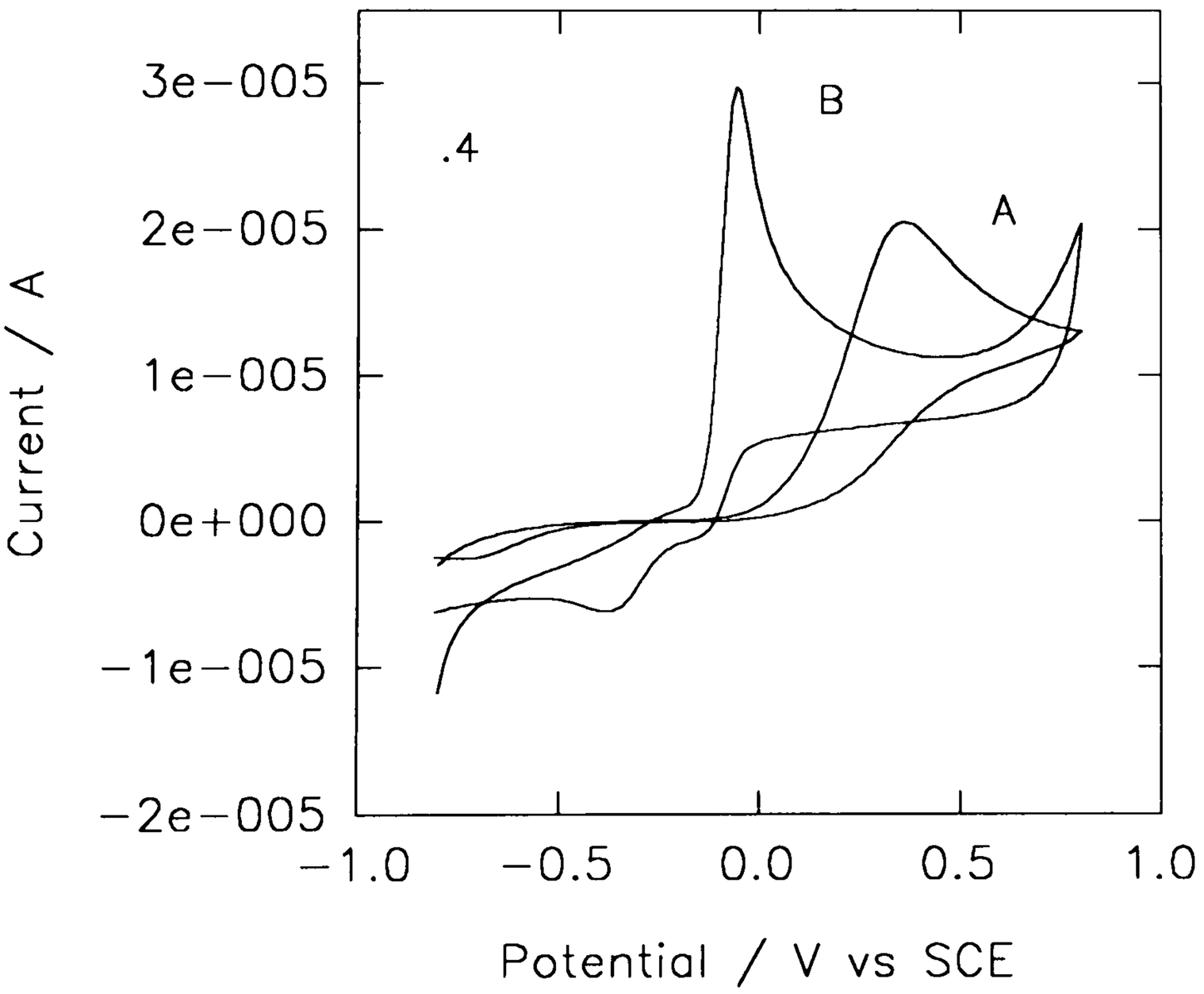

Fig. 5.4 (.3) Cyclic voltammogram of 2 mM NADH and (.4) 2 mM ascorbate at bare (A) and PICA-modified electrode (B). Scan rate = 20 mV/s.

thus resulting in a greater value of I_{dl}.

It has been shown previously that some electrochemical pretreatment schemes can create catalytic activity on glassy carbon surfaces (Cenas *et al.*, 1983). For example, Wang and Gonzalez-Romero (1993) showed that holding an electrode at + 1.2 V vs Ag/AgCl for 6 mins in 1.0 M NaOH, would lower the overpotential for NADH oxidation by approximately 340 mV. This was thought to be due to the introduction on the surface of redox groups such as quinones, as well as the effect of removing contaminants, thus improving the adsorption of NADH. Therefore, the effect of the polymerisation procedure on the electrode surface was examined. A glassy carbon electrode was cycled between -0.8 and 2.5 V as before, in monomer-free buffer solution. The electrochemistry of 2 mM ascorbate and 2 mM NADH was examined both before and after electrode treatment. E_{pk} for the voltammograms (scan rate = 20 mV/s) decreased by only 70 and 20 mV for ascorbate and NADH respectively. This result suggests that the major cause of the electrocatalytic effect seen here, was the presence of the PICA film, rather than activation of the underlying glassy carbon.

5.3.3 Mechanism of Electrocatalysis

The oxidation of both ascorbate and NADH is observed as a single peak and involves the removal of two electrons. Ascorbate oxidation also requires the cleavage of two oxygen-hydrogen bonds, while NADH oxidation proceeds via the cleavage of a carbon-hydrogen bond. The mechanism of ascorbate oxidation has not been elucidated. At an electrode NADH oxidation is thought to proceed as follows (Elving *et al.*, 1982):

$$NADH \text{ ----> } NADH^{\cdot +} + e^- \rightleftharpoons NAD^{\cdot} + H^+ + e^- \rightleftharpoons NAD^+ + 2e^- + H^+ \qquad (5.5)$$

The irreversible first electron transfer is the major cause of the high overpotential relative to the enzymatically determined value (-0.561 V sv SCE; Lehninger, 1975) and therefore a catalyst would need to provide an easier pathway for this first step, (mediation by an outer-sphere reaction) or to proceed by an alternate route. This could include mediation by an inner-sphere reaction. For example, it is thought (Carlson & Miller, 1985) that mediators such as quinones (Q) provide catalysis by either facilitating hydride transfer

$$NADH + Q \text{ -----> } NAD^{+} + QH^{-} \qquad (5.6)$$

or hydrogen transfer followed by electron transfer

$$NADH + Q \text{ -----> } NAD^{\cdot} + QH^{\cdot} \text{ -----> } NAD^{+} + QH^{-} \qquad (5.7)$$

As can be seen from the inset to Fig. 5.2, in the PICA film shows only an irreversible reduction peak in buffer solution. This would suggest that the polymer provides electrocatalysis without acting as an electron-transfer mediator, since to mediate oxidation of the analyte, the polymer would need to be re-oxidised at the electrode. Additionally, the catalytic oxidation peaks for ascorbate and NADH occur at different potentials, where as the re-oxidation of a mediating species would occur at a fixed potential, irrespective of the analyte.

Hence, this catalytic effect can perhaps be viewed simply as a form of surface catalysis; where the polymer provides sites for the analyte molecules to adsorb, in such a way that the activation energy for their oxidation is lowered. This adsorption could be due either

to forces similar to van der Waals forces (physisorption), or to the formation of bonds between analyte and polymer (chemisorption). The later type is the more common for surface catalysis (Moore, 1983).

Electrode treatments which facilitate surface catalysis by using transition metals such as platinum or rhodium have previously been described (Kao & Kuwana, 1984). These methods have been shown to lower the overpotential for the oxidation of compounds such as hydrogen peroxide. The mechanism for this form of catalysis has not been outlined. However, in general transition metals such as platinum are thought to function as catalysts through their possession of unpaired d-electrons and unfilled d-orbitals, which enable the formation of bonds with the adsorbate (Greef *et al.*, 1993). This function could perhaps also be provided by the conjugated π-system present in the PICA film

Surface catalysis can be considered as a sequence of five steps: (1) diffusion of substrate to the solid surface, (2) adsorption ,(3) chemical/electrochemical reaction (4) desorption of products and (5) diffusion of products away from the support. Steps (1) and (5) are usually much more rapid than the rest of the sequence (Moore, 1983). When using poly(3-methylthiophene) as an electrocatalyst, Atta *et al* (1990) recorded evidence of the required NADH adsorption from spectrochemical measurements on a SnO_x-coated glass electrode. Using PICA, the oxidative current at a modified electrode incubated in a 2 mM NADH solution (20 mV/s), was found to increase with time (from 13.85 to 16.93 μA in 1 hr), again suggesting uptake into the polymer film. Also, as shown in Fig. 5.5., cyclic voltammograms of a modified electrode in NADH-free buffer solution, following longer incubation times (1.5 to 2 hrs), showed the presence of

adsorbed NADH on the electrode. As seen in the inset to Fig. 5.5., the peak currents of the voltammograms show a linear dependence with scan rate, suggesting that NADH was adsorbed as a relatively thin layer resulting in the electrochemical reaction rather than in diffusional transport, being the rate limiting step for oxidation (Albery *et al.*, 1987).

There are three possible boundaries where electron transfer for this oxidation can take place. These are, at the electrode-polymer, electrode-solution or polymer-solution interface. For reaction to occur at the polymer-solution interface, the PICA film would need to either be in a conducting state (above approx. 1.7 V, from Fig. 5.2) or contain a species capable of mediating electron transfer. As neither of these criteria were fulfilled, the only possibility for this scheme would be that PICA has a structure similar to poly(3-methylthiophene). That is, a thin non-porous layer adjacent to the electrode, followed by a more permeable fibrillar region (Levi *et al.*, 1993). Electron-transfer could then occur via analyte diffusion through the fibrillar region, followed by electron-tunnelling across the thin, non-porous layer. This possibility is discussed later. Electron-tunnelling was the mechanism suggested by Atta *et al* (1990) for catalysis by poly(3-methylthiophene).

Electron transfer across the electrode-solution interface would imply that the films contained cracks or pinholes, enabling analyte molecules to reach the electrode without diffusion through the PICA matrix. Inspection of the electrodes after polymerisation showed that this was not the case, with PICA (visible as a yellow film) giving complete coverage of the glassy carbon.

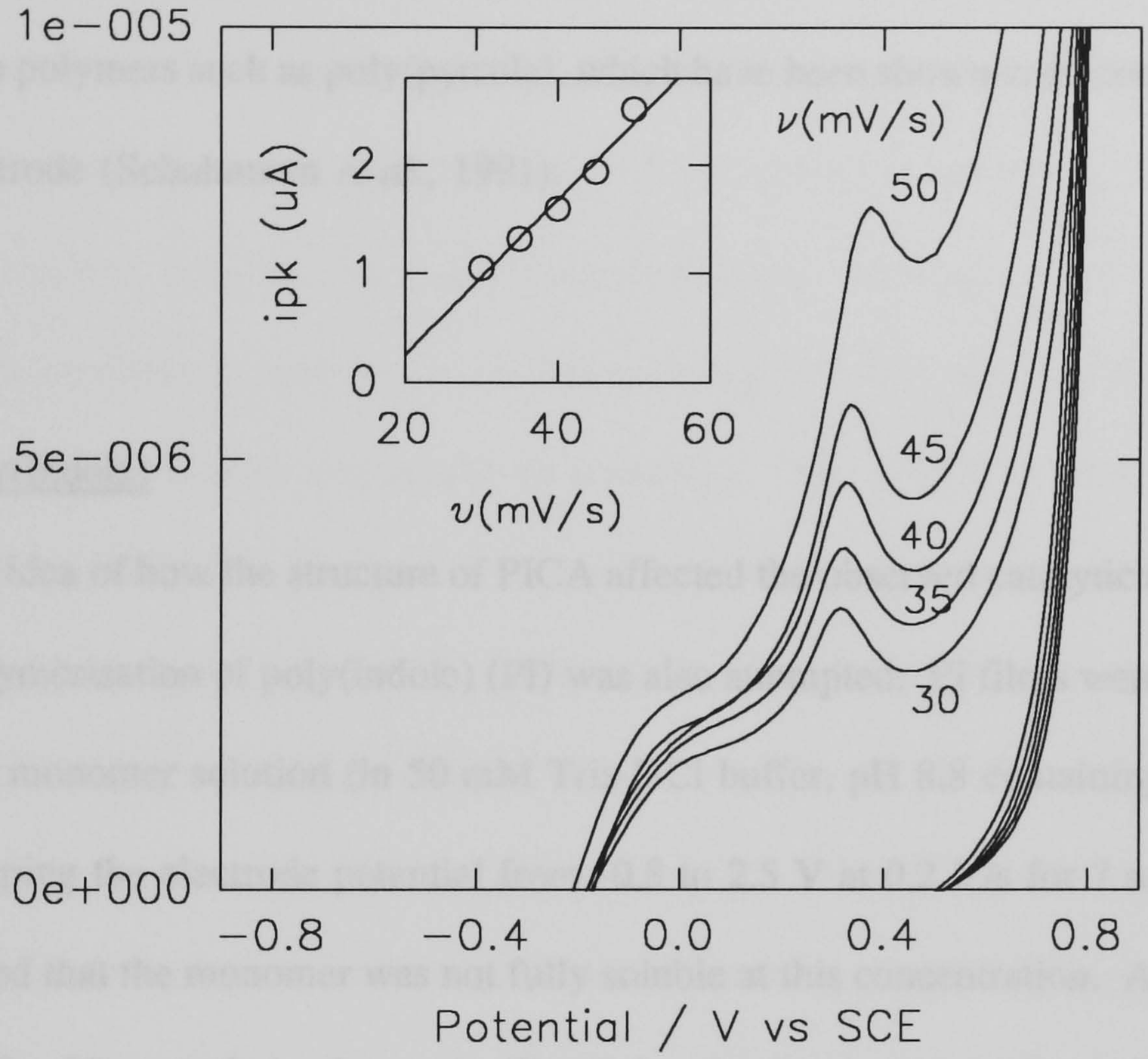

Fig. 5.5 Voltammograms taken at PICA-modified electrode in NADH-free buffer solution, following 2 hr incubation in 2 mM NADH solution. *Inset:* Plot of anodic peak height against scan rate for voltammograms in main figure.

Electron transfer across the electrode-polymer interface, would proceed following membrane-type diffusion of the analyte through the PICA matrix. Diffusion through conducting polymers is a well established phenomenon (Shinohara *et al.*, 1986) and has been used to construct conducting polymer-based ISEs (Dong *et al.*, 1988). The oxidation of NADH suggests a relatively open structure for the PICA matrix, with comparison to polymers such as poly(pyrrole), which have been shown to screen NADH from the electrode (Schuhmann *et al.*, 1991).

Effect of Poly(Indole)

To gain some idea of how the structure of PICA affected the observed catalytic activity, the electropolymerisation of poly(indole) (PI) was also attempted. PI films were grown from a 5 mM monomer solution (in 50 mM Tris-HCl buffer, pH 8.8 containing 0.1 M KCl) by sweeping the electrode potential from -0.8 to 2.5 V at 0.2 V/s for 7 scans. It should be noted that the monomer was not fully soluble at this concentration. A typical set of scans for PI growth is shown in Fig. 5.6. As can be seen, the polymer is oxidised at a lower potential than the monomer unit and hence forms as an insulating film.

The electrochemistry of ascorbate and NADH (both at a concentration of 2 mM) was examined at a PI-modified electrode (scan rate = 50 mV/s). As can be seen in Fig. 5.7, the oxidation potential for ascorbate was shifted by approximately the same amount as when exposed to a PICA electrode. However, the peak current was significantly lower than at either PICA or bare glassy carbon. As shown in Fig. 5.8, NADH was not oxidised at the PI electrode. Two conclusions can be drawn from this: first, the fact

that the ascorbate overpotential was shifted, suggests that the indole backbone of the polymer, rather than the pendant -COOH group, is responsible for catalytic activity. This would agree with the idea that the conjugated π-system of the polymer is responsible for electrocatalysis; second, it would appear that in PI the monomer units form a tighter, less porous matrix relative to PICA, resulting in some exclusion of ascorbate from the electrode and complete exclusion of the larger NADH. However, if electron-tunnelling was responsible for the NADH oxidation current in PICA (as required for electron transfer across the polymer-solution interface), then it would theoretically be possible to measure an NADH response across a very thin PI film, as this should have been equally susceptible to tunnelling. The growth of thin PI films was attempted by subjecting an electrode in the same monomer solution as before, to a single potential sweep (-0.8 to 2.5 V). Slow scan rates (1-10 mV/s) were chosen, so that complete coverage of the electrode could be achieved, while accumulating relatively low charge densities (0.1 C cm^{-2} at 1 mV/s). NADH oxidation was not observed in any of these cases. Although far from providing proof, this suggests that perhaps electron-tunnelling was not apparent across the PICA film. Hence, the most likely mechanism for catalysis is that the analyte molecules diffuse through the PICA matrix and adsorb to the inner polymer film, enabling electron transfer across the electrode-polymer interface. The activation energy for this reaction is apparently lowered by the nature of the adsorption to the polymer and perhaps involves the formation of bonds between analyte and the conjugated π-system of the support.

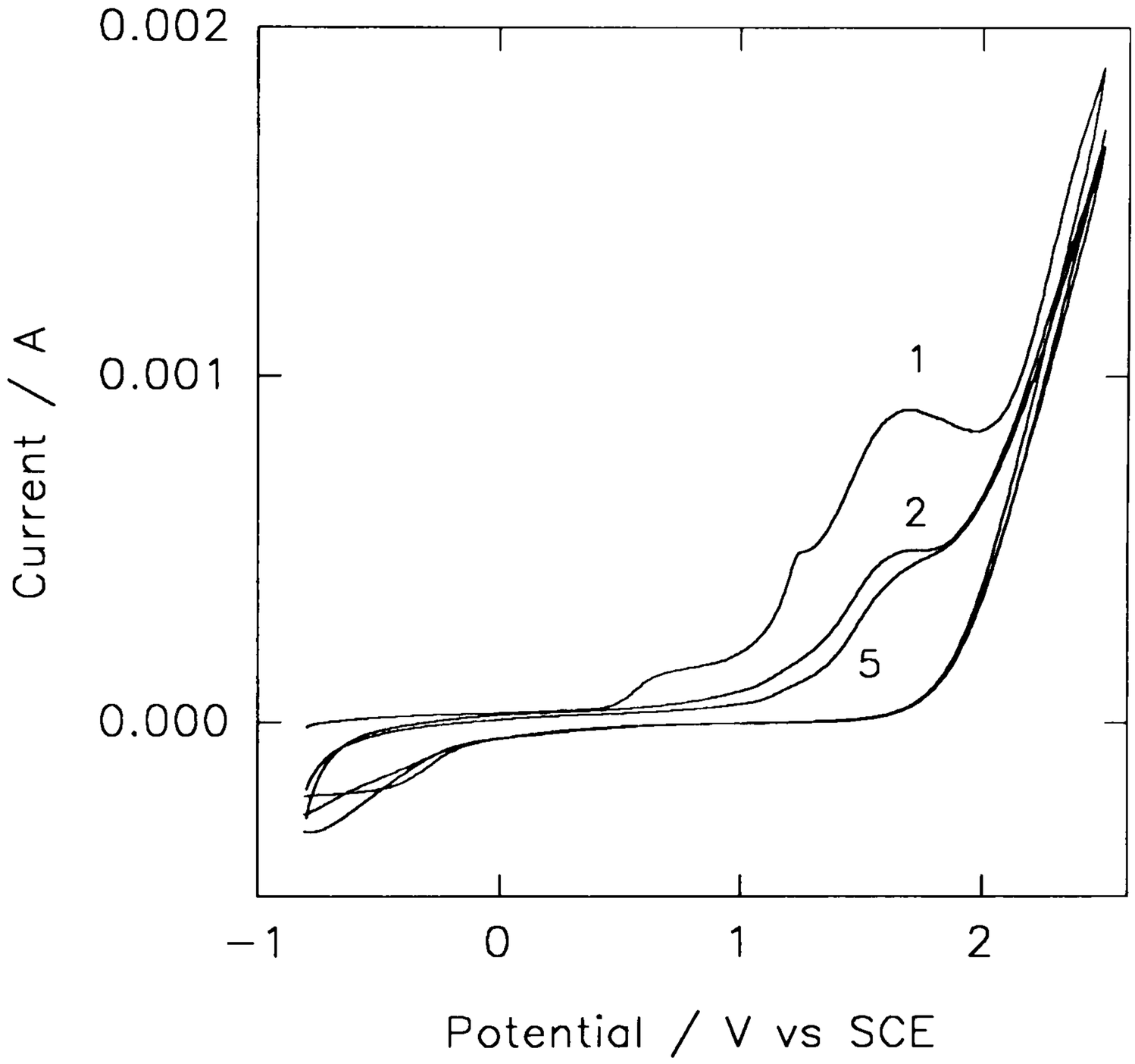

Fig. 5.6 Polymerisation of poly(indole) from 5 mM monomer solution in 50 mM Tris-HCl buffer, pH 8.8 containing 0.1 M KCl. First, second and fifth scans are shown. Scan rate = 200 mV/s.

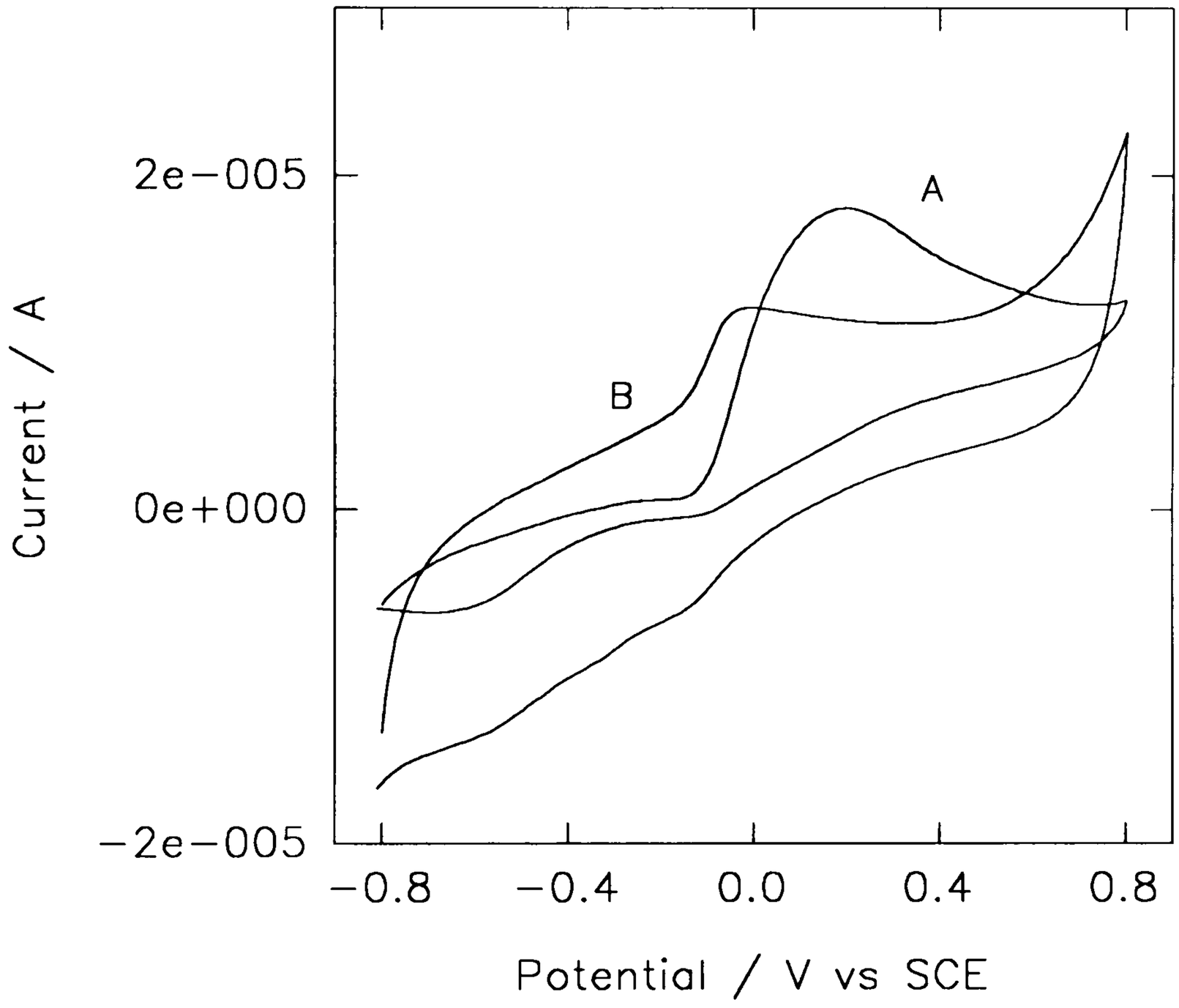

Fig. 5.7 Cyclic voltammogram of 2 mM ascorbate at (A) bare glassy carbon and (B) PI-modified electrode. Scan rate = 50 mV/s.

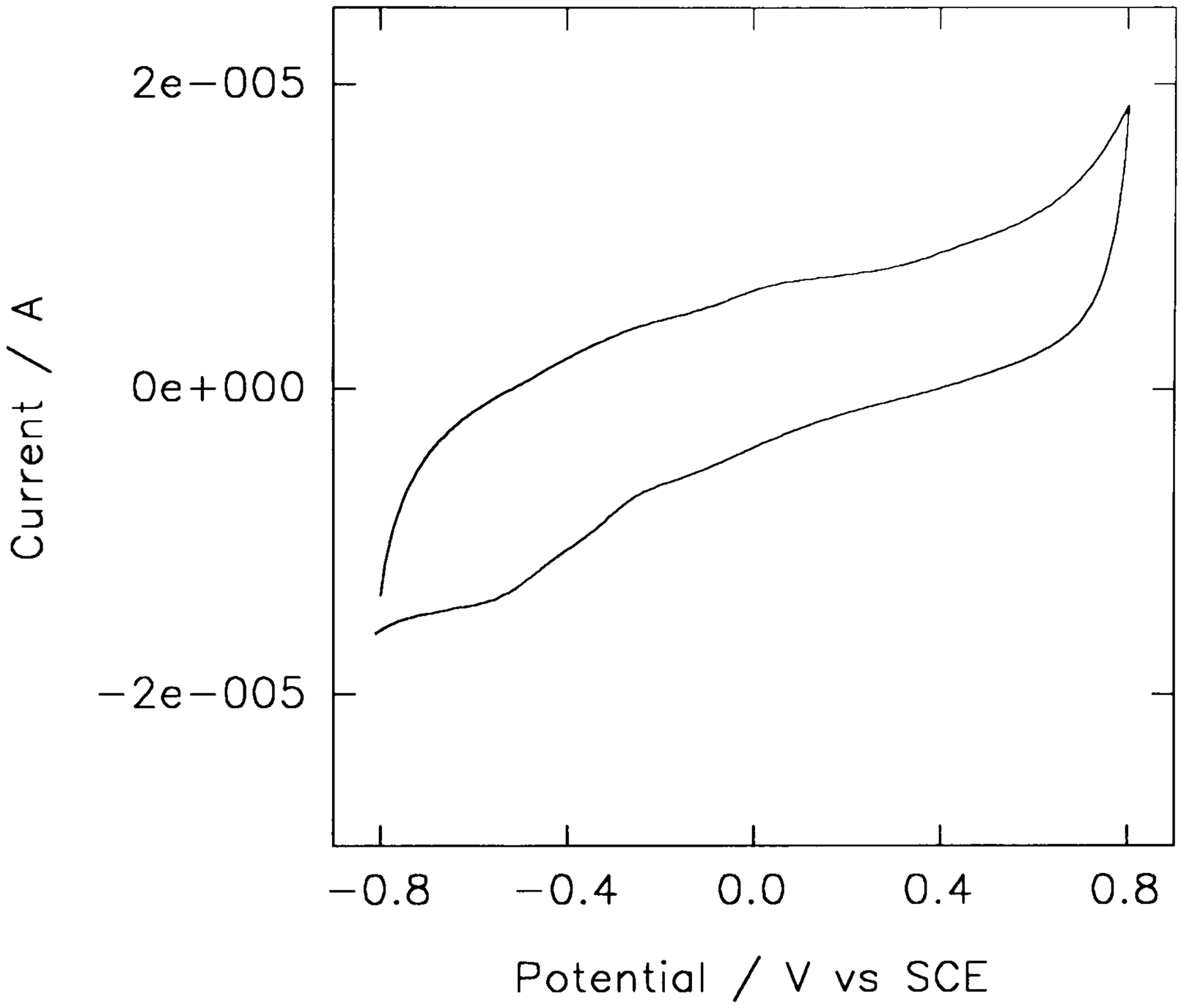

Fig. 5.8 Cyclic voltammogram of 2 mM NADH at PI-modified electrode. Scan rate = 50 mV/s.

5.3.4 Determination of Ascorbate and NADH

Ascorbate and NADH were determined by amperometry at 0 and +450 mV respectively. In each case calibrations were performed before and after electrode modification. As can be seen from Figs. 5.9 and 5.10, the increase in sensitivity for both analytes was similar (approximately six-fold), with the ascorbate response exhibiting higher actual values both before (5 compared to 2.5 nA μM^{-1} for ascorbate and NADH respectively) and after (28 compared to 16 nA μM^{-1} for ascorbate and NADH respectively) deposition of PICA. It should also be noted that PICA-modification of the electrode reduced the effect of passivation during NADH oxidation. This can be evidenced from the amperometric traces shown in Fig. 5.11, where the peak-shaped NADH-responses at a bare glassy carbon electrode can be contrasted with the steady-state currents recorded at the modified electrode. The effect of passivation can also be seen in the inset to Fig. 5.10, which illustrates how the un-modified glassy carbon electrode showed a much lower linear range, due to adsorption sites for NADH rapidly becoming blocked. The reduction in passivation for the PICA-modified electrode is interesting to note, in light of the evidence for the adsorption of NADH. Experiments on NADH oxidation by *o*-quinones, led Jaegfeldt *et al* (1983) to suggest that deactivation of the electrode was due to $NAD^{\cdot}$ radicals forming bonds with the mediator. NAD^{+} is known to adsorb more strongly to glassy carbon than NADH (Samec & Elving, 1983) and as the formation of $(NAD)_2$ dimers is known to occur during NADH oxidation (Jaegfeldt, 1980), it seems likely that passivation at glassy carbon electrodes occurs via strongly adsorbed NAD^{+} reacting with $NAD^{\cdot}$ radicals to form passivating dimers. Hence, the preferential adsorption of NADH over NAD^{+}, on PICA would be likely to prevent passivation to some extent.

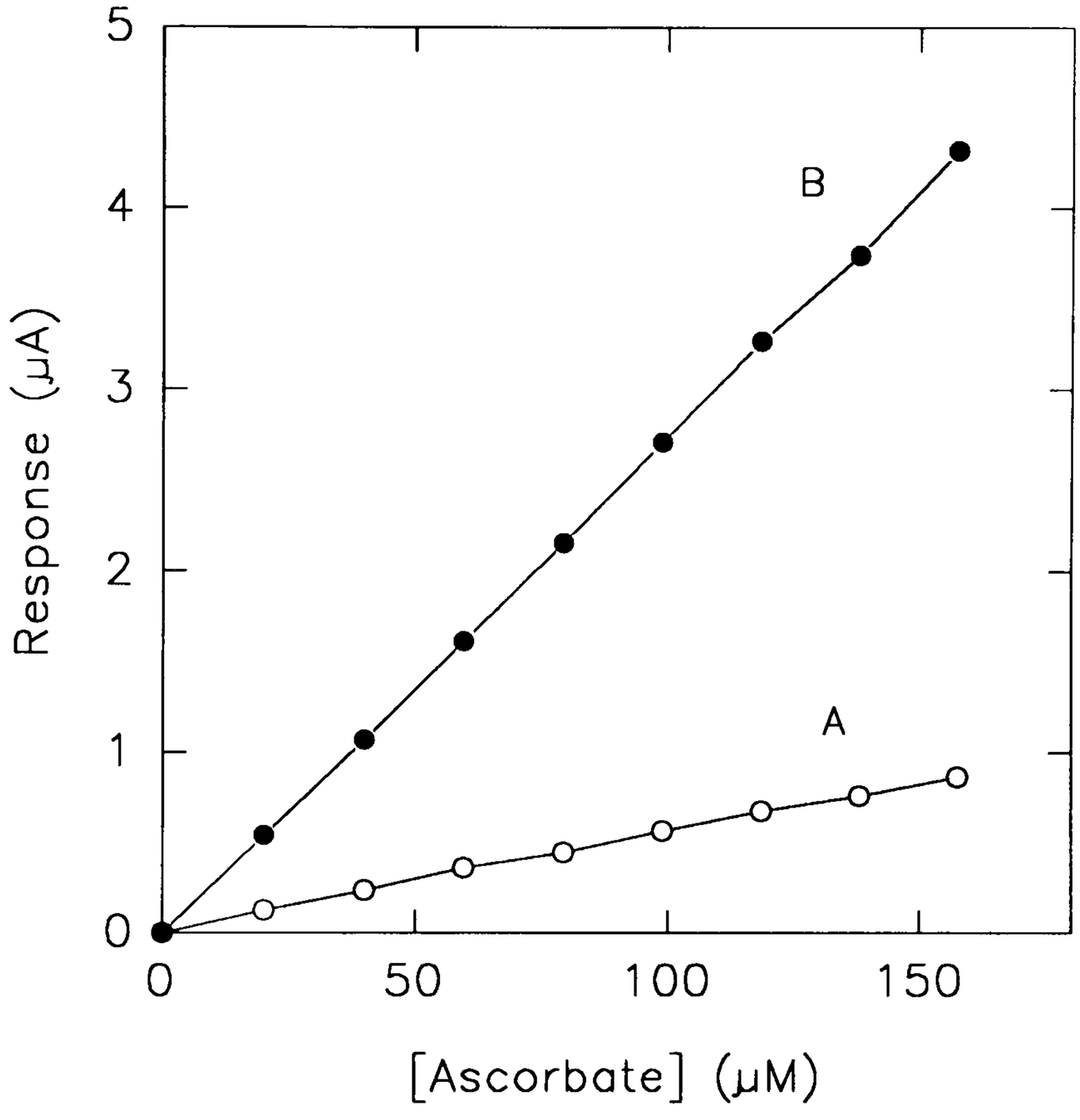

Fig. 5.9 Calibration of ascorbate at 0 mV at bare (A) and PICA-modified (B) glassy carbon electrode.

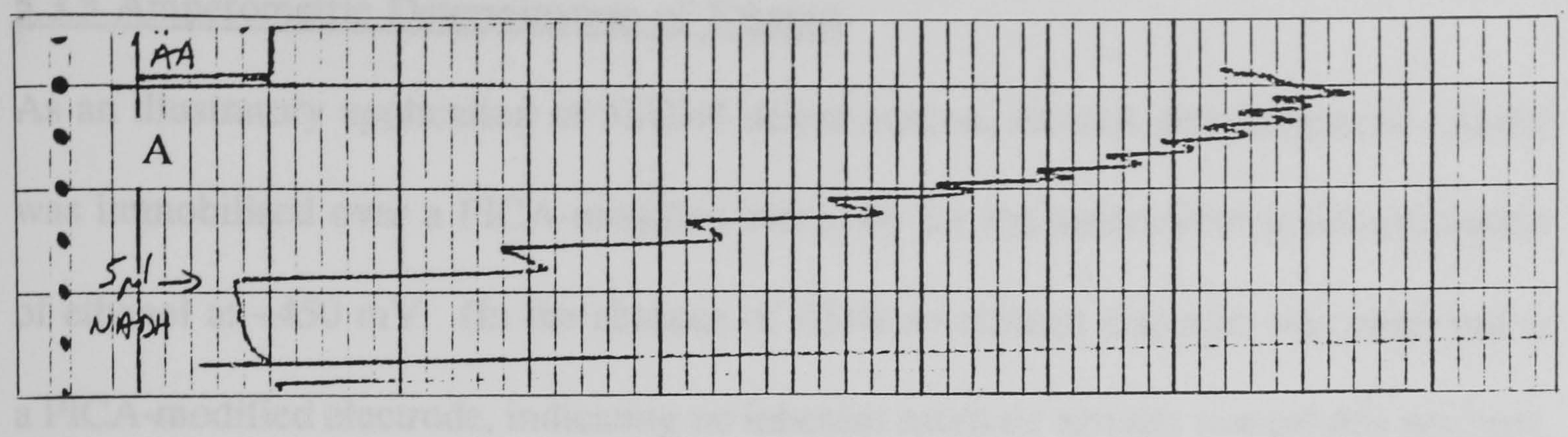

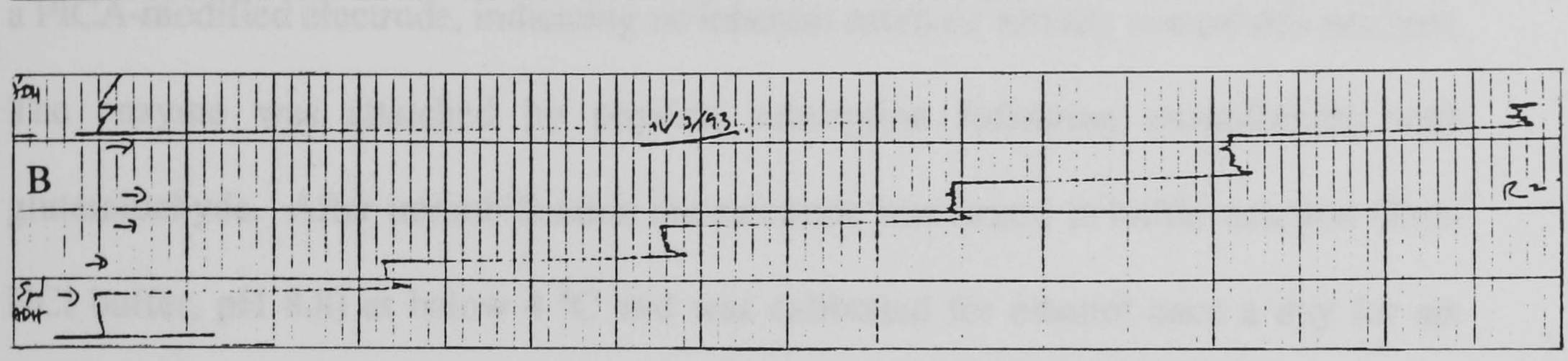

Fig. 5.11 Amperometric traces for the oxidation of NADH at bare (A) and PICA-modified (B) glassy carbon, at +450 mV.

Fig. 5.10 Calibration of NADH at +450 mV at bare (A) and PICA-modified (B) glassy carbon electrode. *Inset:* Calibration at bare electrode shown with expanded scale.

5.3.5 Amperometric Determination of Ethanol

As an illustratory application of NADH determination, alcohol dehydrogenase (ADH) was immobilised over a PICA-modified electrode for the amperometric determination of ethanol at +450 mV. (In the absence of ADH no ethanol response was observed at a PICA-modified electrode, indicating no inherent catalytic activity toward this analyte). The enzyme was attatched by physical adsorption following cross-linking with glutaraldehyde. After immobilisation the electrode was stored in buffer solution (Tris-HCl buffer, pH 8.8) at below 4 °C and was calibrated for ethanol once a day for six days (with NAD^+ present in bulk solution at 1.6 mM). As shown in Fig. 5.12, the ethanol response had a dynamic range of approximately 3 to 30 mM. As discussed in the General Introduction (Chapter 1, Section 1.5.2), the clinically relevant range for ethanol in toxicology diagnosis is 10 to 90 mM and therefore the concentration range obtained here would need to be extended. This could be achieved by the use of an outer membrane over the enzyme, as will be discussed later. In Chapter 3 (Section 3.3.7), when ADH was immobilised over an NADH oxidase layer, the electrode exhibited much poorer stability over the same time period. This was shown to be due mainly to the decrease in activity of the dehydrogenase. One possible reason for this is that in the bi-enzyme system a lower quantity of ADH was immobilised (51 U with respect to 68 U), to ensure that the dehydrogenase activity was rate limiting. However, when comparing the large difference in response between the two systems, it seems likely that this also reflects greater stability of ADH when immobilised on PICA. It should be noted that the addition of glutaraldehyde to ADH on PICA produced a white coloration in the solution covering the electrode; where as ADH immobilised on bare glassy carbon remained as a clear liquid after cross-linking. This suggests the formation of bonds between glutaraldehyde and the polymer and could perhaps have led to

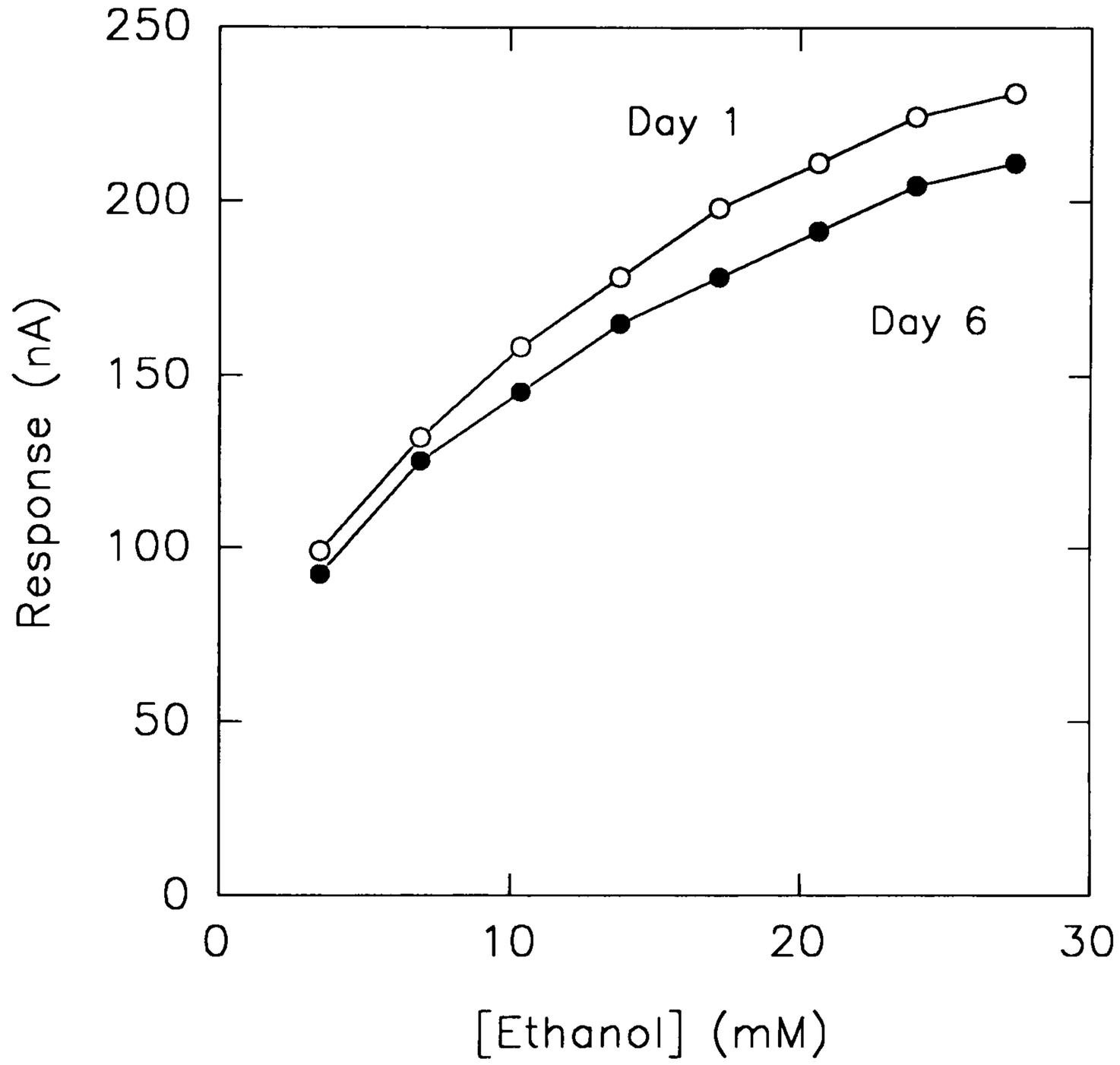

Fig. 5.12 Determination of ethanol at +450 mV using ADH immobilised on PICA-modified electrode. Sensor stored < 4 °C and calibrated once a day.

improvement of ADH stability by either improved entrapment of ADH within the immoblisation matrix, or because ADH was itself involved in the bond formation.

Michaelis-Menten experiments were performed for the immobilised enzyme using NAD^+ and ethanol in bulk solution. It has been shown (Michal, 1978) that for a multisubstrate reaction of the type

$$E + A \rightleftharpoons EA + B \rightleftharpoons EAB \dashrightarrow E + Products \qquad (5.8)$$

the inital velocity of the reaction V_o, can be described by

$$V_o = V_{max} / \{ 1 + K_{M(A)}/[A] + K_{M(B)}/[B] + K_{M(AB)}/[AB] \} \qquad (5.9)$$

Where V_{max} is the saturation velocity and $K_{M(\ )}$ refers to the Michaelis constant of the relevant species. Under conditions where one substrate is present at a concentration much higher than its Michaelis constant, eq. 5.9 can be reduced to

$$V_o = V_{max}/\{1 + K_{M(B)}/B\} = V_{max}/\{1 + K_{M(A)}/A\} \qquad (5.10)$$

Hence enabling calculation of the apparent K_M (K'_M) from standard Lineweaver-Burk plots. As shown in Fig. 5.13, with ethanol present at a concentration of 506 mM (~ 50 Km), the K'_M for NAD^+ was determined at 3.2 mM; while for an NAD^+ concentration of 38 mM, (10 Km), K'_M for ethanol was found to be 10.7 mM. Both values are significantly higher than previously reported data taken at this pH using dissolved ADH, with solution phase $Fe(CN)_6^{3-}$ as oxidant to NADH (3.2 mM for ethanol, 0.08 mM for NAD^+; Ciolkosz, 1993). In general, higher K'_M values are expected for immobilised

enzymes due to the unstirred Nernst diffusion layer at the electrode and the resulting concentration gradient across it (Zaborsky, 1973). However, the increase in K'_M for NAD^+ observed here (approx. 48 times), is much greater than that for ethanol (approx. 3 times). This is likely to be due to the additional effect of adsorbed NADH lowering the rate of formation at the electrode surface, of the ADH-NAD^+ complex.

Effect on Ascorbate Response

Where ethanol determination is envisaged in clinical sample matrices such as blood or urine, the possible interference of an ascorbate signal should be considered. Ascorbate was calibrated at a PICA-modified electrode poised at +450 mV, both before and after the immobilisation of 68 U of ADH. The presence of ADH on the electrode reduced the ascorbate sensitivity from 42 to 5 nA μM^{-1}. This is likely to be due to the diffusional barrier presented by the cross-linked enzyme and also to the fact that ADH from yeast has an iso-electric point of pH 5.4 (Sund & Theorell, 1963) and therefore at the pH of working buffer (pH 8.8) would present an overall negative charge to the ascorbate anions. The ascorbate sensitivity of the PICA enzyme electrode was still relatively high with comparison to the NADH sensitivities recorded at PICA-modified electrodes (16 nA μM^{-1}). Further reduction of the ascorbate response would require the use of either charge or size selective membranes. However, as NAD^+ is a considerably larger molecule than ascorbate (RMM = 663 and 176 for NAD^+ and ascorbate respectively), the use of a screening membrane for ascorbate would preclude the use of NAD^+ in bulk solution. Hence the immobilisation of NAD^+ would need to be achieved before attempting to remove the ascorbate signal.

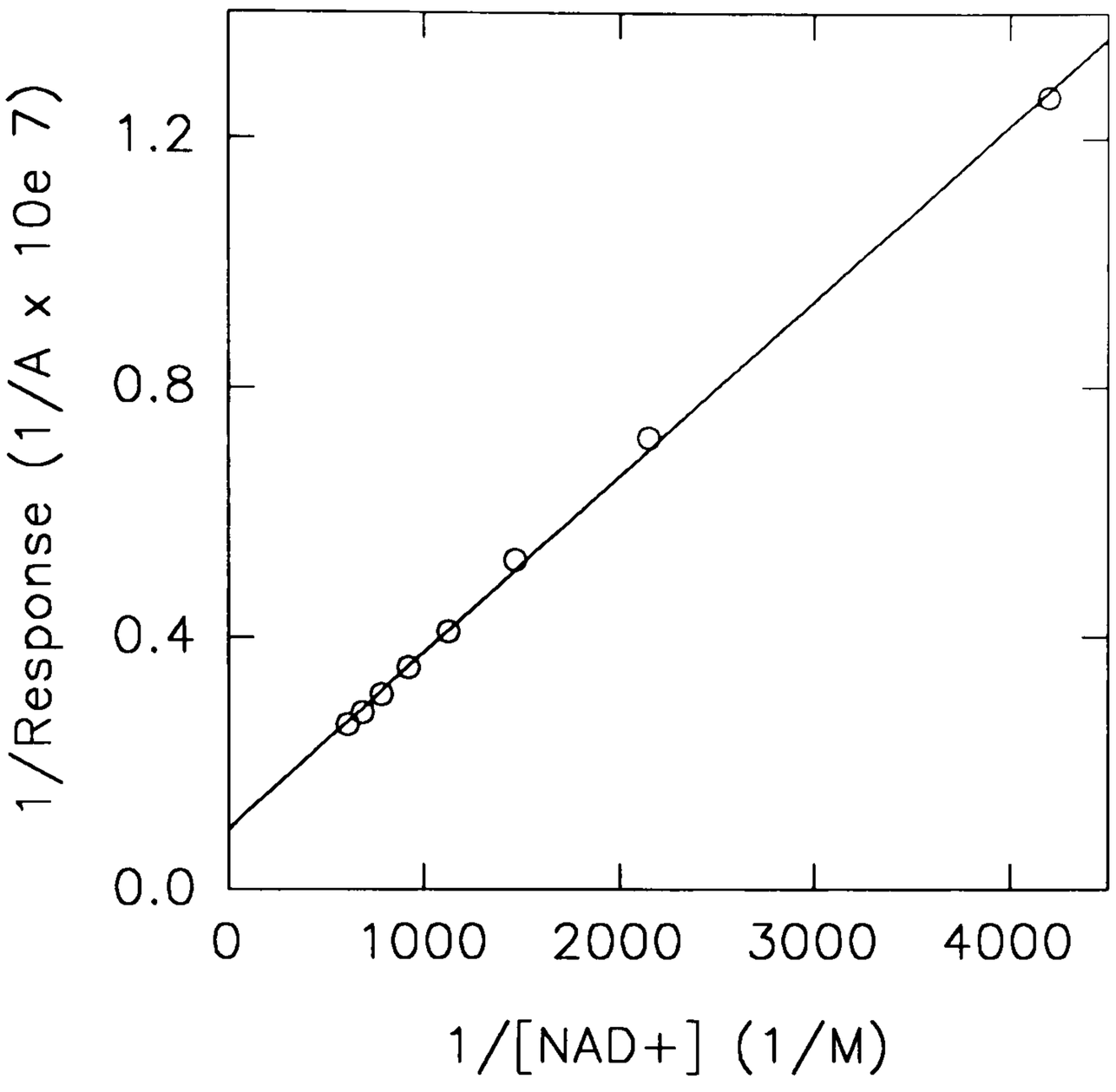

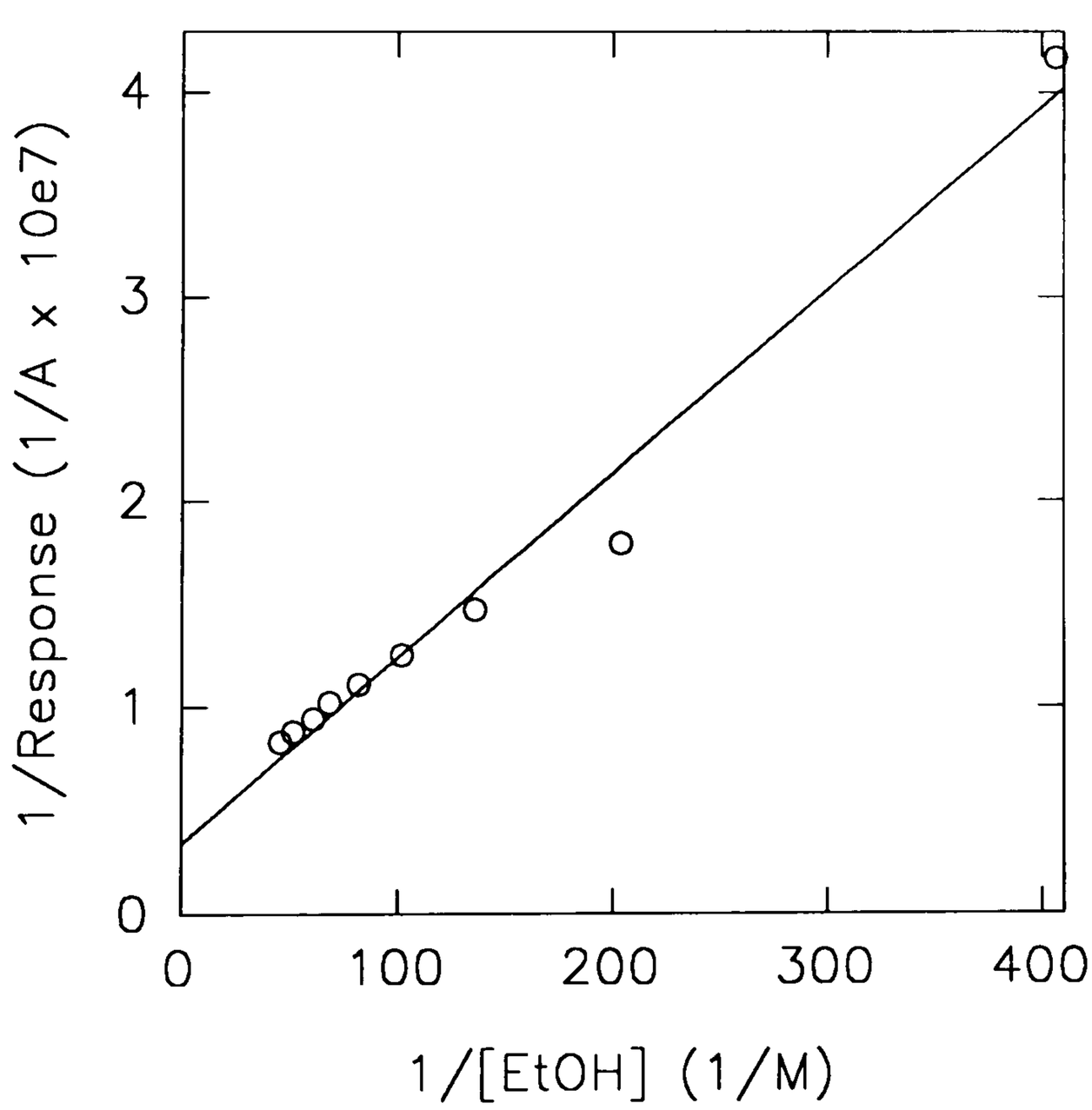

Fig. 5.13 Lineweaver-Burk plots for determination for K'_M for ethanol and NAD^+.

K'_M (ethanol) = 10.7 mM (NAD^+ present at 38 mM).

K'_M (NAD^+) = 3.2 mM (ethanol present at 506 mM).

NAD$^+$ Immobilisation

Up to now, only two general methods of NAD$^+$ entrapment (without modifying its structure) have been reported. These are, its incorporation within either the body of a carbon paste electrode (Bremle *et al.*, 1991), or within a film of poly(pyrrole) (PPy), following its uptake from bulk solution during the growth of the polymer (Yabuki *et al.*, 1990). Variations of both these methods were attempted, as well as the retention of NAD$^+$ within an appropriate membrane.

Carbon paste electrodes incorporating indole-5-carboxylic acid (ICA) were fabricated as described in Chapter 2 Section 2.2.3, using a graphite : monomer ratio of 2:1. However, these electrodes showed no catalytic activity to either NADH or ascorbate, suggesting that ICA would only be catalytic in the form of a polymer film.

Hence, the electro-deposition of the polymer was performed as before in the presence of ADH (1700 U/ml) and NAD$^+$ (10 mM). However, the resulting films showed no activity towards ethanol, perhaps because of little or no entrapment of enzyme and co-factor within the PICA. As PPy had previously been reported as an immobilisation matrix for these components, the fabrication of a PPy/PICA bilayer was examined.

PICA films were grown as before and following their deposition, PPy was polymerised from a 0.1 M monomer solution in 25 mM Tris-HCl buffer, pH 8.8 containing 0.05 M KCl, 0.025 M NAD$^+$ and ADH at a concentration of either 1700, 3400 or 5100 U/ml. Polymerisation was performed under anaerobic conditions, with solid ADH being added to the cell and dissolved after the N_2 purge had been completed. The growth of PPy would require PICA to be in its conducting form and therefore the PICA electrode was

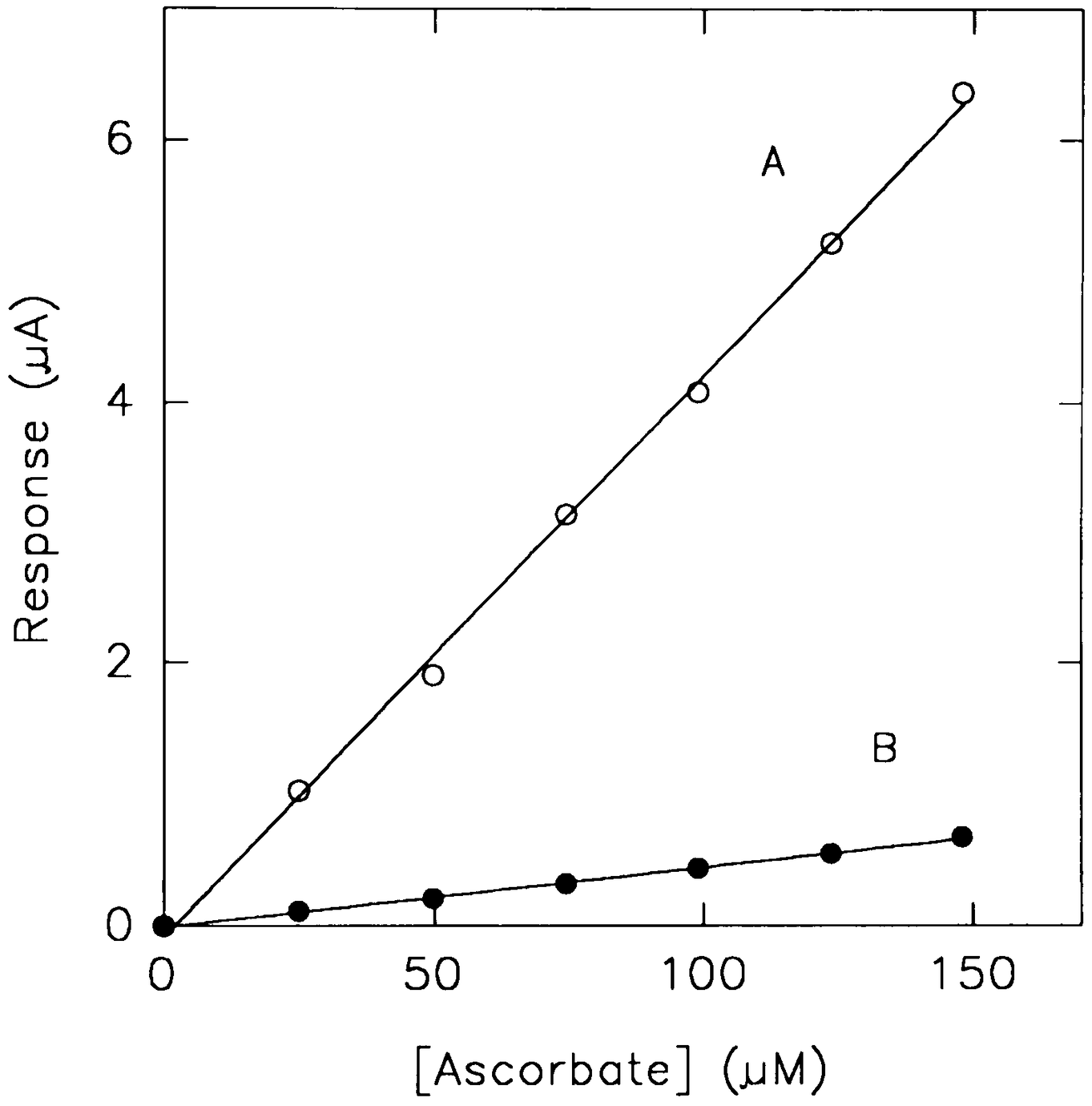

Fig. 5.14 Calibration of ascorbate at +450 mV at PICA-modified electrode in the absence (A) and presence (B) of immobilised ADH (68 U deposited).

cycled between -0.8 and 2.5 V (0.2 V/s) for 12 scans.

The electrode response to ethanol was examined at +450 mV. The PICA/PPy electrodes required relatively long time periods (approx. 30 mins) for the background current to decay to a stable value. This was probably due to the large capacitance produced by the polymer bilayer. As can be seen from Fig. 5.15, even when produced from 5100 U/ml ADH solutions, the electrodes exhibited very low current responses to high ethanol concentrations. Significant responses were produced from control experiments in which PPy was grown from a polymerisation solution containing no ADH; indicating that the current recorded was due partly to the exchange of NAD^+ and Cl^- ions across the polymer-solution interface and the changes in electrode conductivity associated with this. The loss of ADH activity was likely to be due to the detrimental effect of the high electric field required for polymerisation across PICA.

The covalent binding of NAD^+ to PICA was examined, using carbodiimide to activate the -COOH groups of the polymer. Two approaches were used: A PICA film was grown as before and the modified electrode was then incubated in carbodiimide (20 mg/ml in 200 mM citrate buffer, pH 5.5) for 90 mins, followed by incubation in 20 mM NAD^+ for 90 mins (both at room temperature). The electrode failed to respond to ethanol in the presence of dissolved ADH (1700 U/ml), suggesting either no binding of NAD^+, or its immobilisation in a form that made it enzymatically inactive. Alternatively, the synthesis of an ICA-NAD^+ conjugate was attempted prior to polymerisation. The ICA monomer (10 mg/ml) was incubated in a 0.1 M KCl solution containing carbodiimide and NAD^+ (both at 30 mg/ml), for six hours at room temperature. However, no polymerisation of this solution was observed upon sweeping

the electrode potential.

The entrappment and use of NAD^+ within PPy, as previously reported by Yabuki *et al* (1990), suggests that under the conditions described (0.1 M potassium chloride for entrappment, 0.1 M phosphate buffer, pH 7.5 for storage an use), NAD^+, despite its nominal structure, exhibited an overall negative charge, presumably due to the dissociation of protons. Therefore, at the pH used in these experiments (pH 8.8), NAD would also be expected to carry a negative charge. Hence, electrostatic repulsion by Nafion was examined as a method for immobilising NAD^+.

Initially, cyclic voltammetry was used to detect membrane permeability. The peak for the reduction of NAD^+ (E_{red} = -1.6 V vs SCE; Elving, 1982) would under ambient conditions, have been likely to have been obscured by O_2 reduction and therefore for reasons of convienience, the oxidation of NADH was examined instead.

40 µl of a Nafion solution (diluted to 1 % with acetone) was deposited onto a poly(carbonate) membrane (pore size 0.05 µm, diameter 13 mm) in 10 µl aliquots. Following this, the membrane was fastened across the face of a glassy carbon electrode, using strips of Parafilm to seal the edge of the membrane to the electrode body. The Nafion layer was set facing the external solution. Fig. 5.16 scan (a) shows a voltammogram taken with this electrode (50 mV/s) of a 1.9 mM NADH solution containing 128 mM ethanol, following incubation in the solution for 1 hr. Scan (b) shows the effect of replacing the membrane with an untreated poly(carbonate) layer and scan (c) shows the electrochemistry of the same solution at bare glassy carbon. Comparison of scans (b) and (c) suggest some size exclusion of NADH by

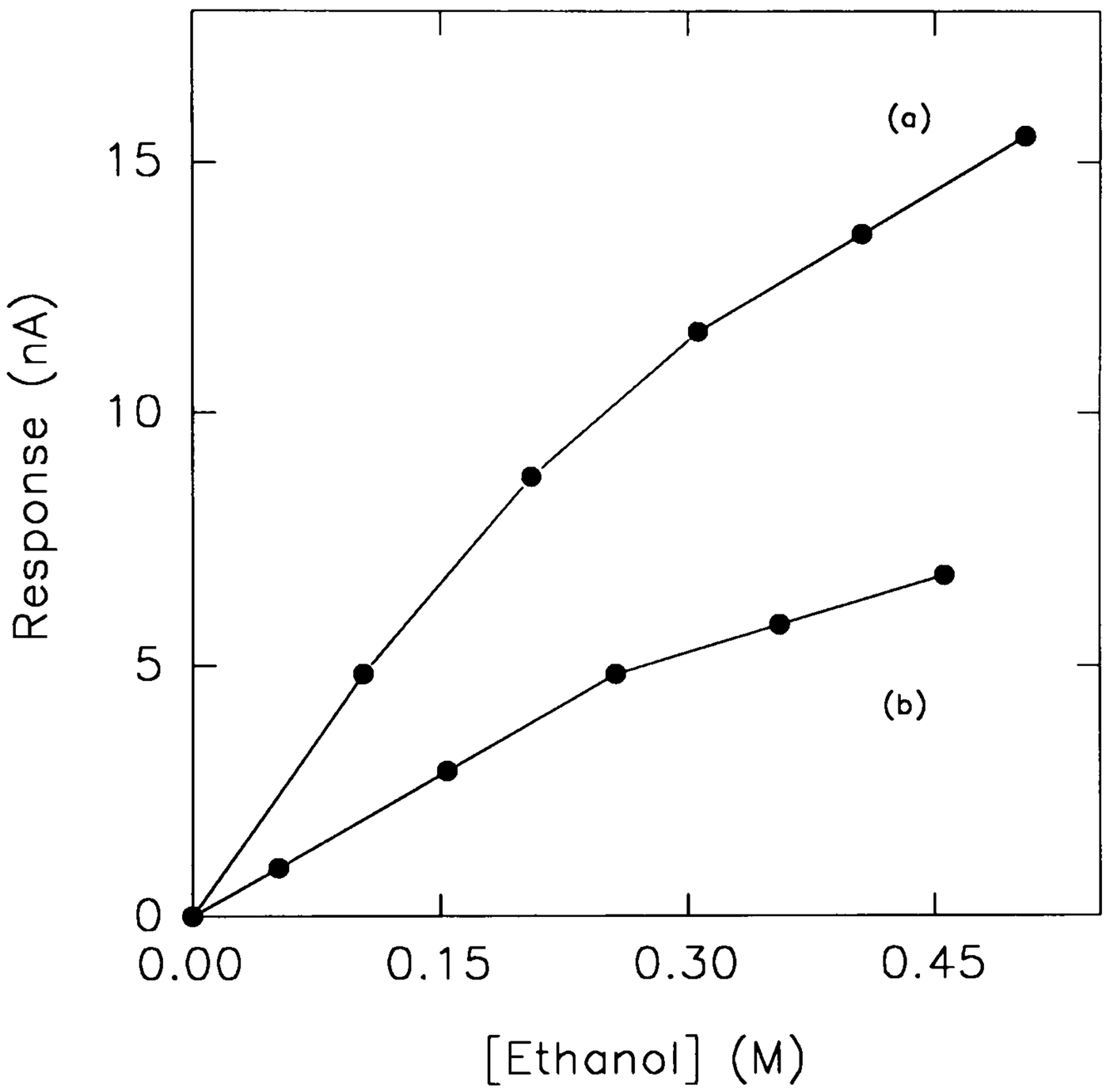

Fig. 5.15 Calibration of ethanol at +450 mV using PPy/PICA bilayer. Polymer grown (a) in the presence of 5100 U/ml ADH and (b) in the absence of ADH.

poly(carbonate). Comparison between scans (a) and (b) suggests both a further exclusion of NADH from the electrode, owing to the presence of Nafion and that the Nafion layer had thus remained adsorbed over this period of time in the presence of ethanol at above its clinically relevant concentration. This is interesting to note in light of the solubility of Nafion in ethanol and is probably due to hydrophobic interactions between the Nafion and poly(carbonate).

These results indicate that this system could be used for NAD^+ immobilisation and hence further studies were performed using amperometry. A PICA electrode was modified with 68 U of ADH as described previously (Section 5.2.3) and following amperometric confirmation of ADH activity (using 0.48 mM NAD^+ in bulk solution), a 20 µl aliquot of NAD^+ (10 mM at pH 8.8) was deposited on the electrode and left for 75 mins for partial evaporation of the solvent. A Nafion-treated poly(carbonate) membrane was then fixed over the electrode as before, with the Nafion layer facing the immobilised ADH/NAD^+. The electrode was calibrated for ethanol and then stored in buffer at < 4 °C. Fig. 5.16, curve (a) shows the initial ethanol response of the electrode. Curve (b) shows the electrode response after storage for 48 hrs. As can be seen, there is a significant decrease in sensitivity over this period. The same electrode gave no response to 0.44 mM ascorbate either initially or after storage. As a relatively small molecule, ascorbate would be expected to permeate un-treated poly(carbonate) and the absence of a response therefore suggests that a substantial proportion of the Nafion layer had remained in place over this length of time. The poor electrode stability is likely to indicate that either the membrane is significantly more permeable to NAD^+ than NADH, or that the relatively slow kinetics for NADH oxidation on glassy carbon, meant that the cyclic voltammetry experiments did not adequately reflect its movement

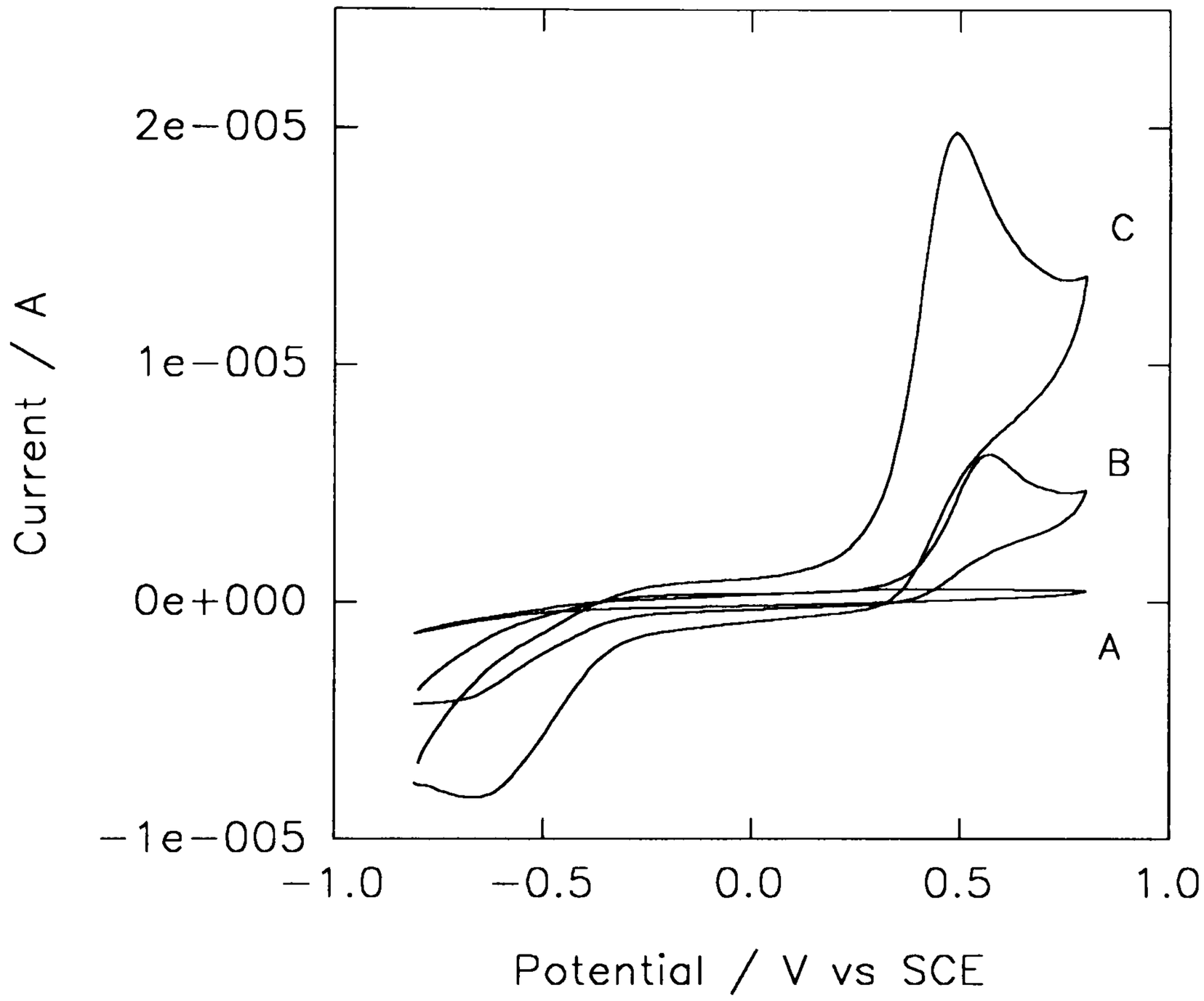

Fig. 5.16 NADH permeation of poly(carbonate) (PC) examined by cyclic voltammetry. Solution in cell = 1.9 mM NADH + 128 mM ethanol. (A) Electrode modified with Nafion/PC membrane, scan taken after incubation in cell for 1 hr. (B) Electrode modified with PC membrane. (C) Bare glassy carbon. Scan rate = 50 mV/s.

through the membrane.

Hence this work did not finally achieve the long term immobilisation of NAD^+. Further possible approaches to NAD^+ immobilisation will be considered in the General Discussion (Section 6.4).

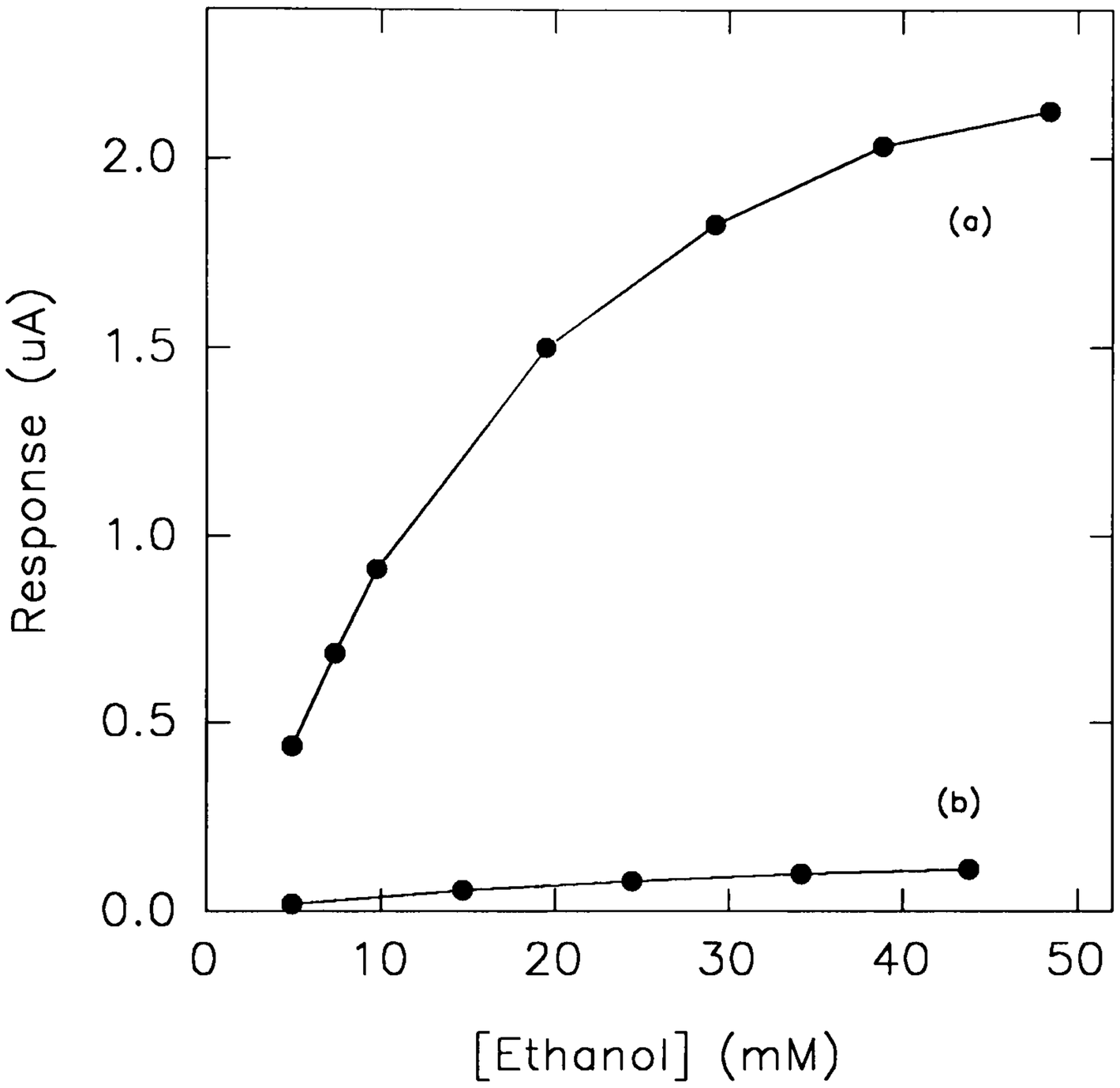

Fig. 5.17 Calibration of ethanol at +450 mV with ADH/NAD^+ immobilised behind Nafion/poly(carbonate) membrane. (a) Initial response of electrode; (b) electrode response after storage in buffer < 4 °C for 48 hrs.

Chapter Six

General Discussion

6.1 Sensors Utilizing the Formation of a Metal Complex

The first experimental chapter of this thesis (2.0), examined the viability of using metal complexation as a method of metal ion detection. The electrochemistry of a series of ligands was monitored by cyclic voltammetry, both before and after binding to a particular metal. The ligands were chosen for their ability to complex the relevant metal ion with a degree of selectivity. Summarized in Table 6.1 are the observed electrochemical changes. As can be seen, of the fifteen ligands examined, seven gave no change in redox activity upon complexation. Of the remaining eight ligands, six showed changes which proved to be non-specific. In the case of the ligands which were incorporated into carbon paste, this is likely to be due to leakage from the modified electrode over time; with the electrochemistry of the ligand changing as it moved from the essentially organic environment of the liquid paraffin/graphite mixture, to the aqueous environment of the bulk solution.

Non-specific changes were also observed for some of the ligands used in solution. These experiments were performed in the absence of a supporting electrolyte, to better simulate analysis of real samples and hence the changes in redox activity observed on addition of de-ionized water, could perhaps have been due to alterations in the solution conductivity.

Two ligands, desferrioxamine and bis-cyclohexanone oxaldihydrazone (BCO), gave voltammograms whose redox characteristics were altered solely by complexation with a metal. Desferrioxamine, when used in solution exhibited an oxidation peak at +430 mV. The anodic peak current lowered upon the binding of increasing amounts of iron(III). As described in Section 2.3.4, this result agrees with previous work in this

Table 6.1 Summary of redox characteristics for the ligands examined in Chapter 2. Letters in brackets refer to the use of the relevant ligand either in solution (S) or incorporated within carbon paste (mcp).

Analyte	Ligand	Initial Redox (mV)	Effect of Metal ion	Specificity
Ca^{2+}	Hydroxy Napthol Blue (S)	E_p^C -100 E_p^A 0	No change	-
	Calcein Blue (S)	none	No change	-
	Fura 2 AM (S)	none	No change	-
	Glyoxal-bis(2-hydroxyanil) (S)	E_p^A 600	I_p^A reduced	Non-specific
	Arsenazo III (mcp)	E_p^C 100 E_p^A 600	I_p^A increased I_p^C "	Non-specific
	Calcion (S)	none	no change	-
	Murexide (S)	E_p^C -500 E_p^A 450	I_p^A increased	Non-specific
Cr^{3+}	Orcinol Monohydrate (S)	E_p^A 100	I_p^A increased	Non-specific
Fe^{3+}	Ferrozine (mcp)	none	E_p^C -600	Red$^{n.}$ of metal
	Desferrioxamine (S)	E_p^A 430	I_p^A reduced	Due to complexation
Ni^{2+}	α-Furildioxime (mcp)	E_p^A 600	No change	-
Al^{3+}	Eriochrome Cyanine (S)	E_p^A 400	I_p^A increased	Non-specific
Cd^{2+}	Rhodamine B (S)	none	no change	-
PO_4^{2-}	Alizarin Red (S)	none	no change	-
Cu^{2+}	Bis-cyclohexanone oxaldihydrazone (mcp)	none	E_p^A 235 & -100	E_p^A at 235 due to complexation

field (Beer *et al.*, 1990a), which predicts that the attractive force of the metal ion will hinder the removal of the ligand electrons. When incorporated into carbon paste, the electrochemistry of desferrioxamine proved unstable, with the oxidative current decreasing over time. This was likely to have been due to the highly water soluble compound leaching from the carbon paste and thus lowering the concentration of ligand influenced by the electrode.

The relatively low solubility of BCO made incorporation of the ligand into carbon paste possible and the modified electrodes thus produced, exhibited an oxidation peak of +235 mV upon complexation with copper(II).

The technique of quantifying a metal by measuring the change in ligand electrochemistry, has previously only been used in a method analogous to ASV (Picon *et al.*, 1987) (preconcentration followed by sweeping the potential). Hence, this thesis has described for the first time the adaption of the technique to amperometry. Screen printing was used to produce disposable, 'one-shot' BCO-modified electrodes, responsive to copper(II) at +235 mV. At this potential relatively little interference would be expected from most biological or environmental sample matrices. Where a comparison is possible (NH_4^+, Ba^{2+}, Ca^{2+}, Mg^{2+}, Co^{2+}, Fe^{3+}), the degree of interference from competing cations was, in all cases, less than that experienced by Peterson and Bollier (1955) when using the same ligand for spectrophotometric copper measurement. Apart from transportation and ease of use, the application of 'one-shot' sensors has the advantage of not making great demands on electrode stability. It is recommended by the manufacturer (Sigma) that BCO be stored at below 4 °C. However, for single measurement purposes, the modified electrodes could be used at temperatures of up to

75 °C. Measurement at physiological temperatures would therefore not be problematic.

The limit of detection for this study (30 μM) is notably higher than that reported for copper determinations using ASV (3.8 μM) (Hoyer & Florence, 1987). However, the greater sensitivity of ASV can be weighed against the convenience of the technique reported here. Hence, this work suggests the possibility of a complementary scheme to the conventional methods of electroanalysis; enabling the preferred technique to be chosen by regarding its particular application.

Regarding electrode fabrication, the next step for this work would be to screen-print Ag/AgCl strips alongside the BCO-modified layers, providing the system with a self-contained reference and counter electrode. Electrode designs of this type have previously been described (Kulys & D'Costa, 1991) and would enable a portable detection system of the type used for glucose (Hill & Sanghera, 1990). The electrodes described could function without the use of a supporting electrolyte, as would be required for the analysis of environmental samples. Also required for such analysis, is a pH-independent response. This could perhaps be achieved by incorporating Tris-HCl into the BCO-modified layer.

The reason for the electrochemical change in BCO upon binding copper (the ligand is more readily oxidised), is unclear and is in contradiction to previous work in this field (Beer *et al.*, 1990a). The first step in explaining this effect would be to elucidate the structure of the BCO-copper complex. This could perhaps be achieved by X-ray crystallography.

6.2 Metal Complexes as Mediators

In the second experimental chapter of this thesis (3.0), the study of metal complexes progressed to their use as electron-transfer mediators. The purpose of a mediator is to lower the activation energy of a particular redox reaction, by providing an easier route for electron transfer. This can be required either because an analyte exhibits slow kinetics at a bare electrode, or because as in the case of some enzymes, the redox centre is inaccessible to the electrode. In contrast to the previous chapter, this required the use of complexes in which the ligands were electrochemically inert, leaving redox activity to be provided by the changing oxidation state of the metal. As discussed in Section 3.1, the advantage of utilizing such outer sphere reactions, is that they provide redox characteristics which are pH-independent; where as the peak potentials exhibited by organic mediators correspond to inner sphere reactions usually involving the loss or gain of protons and are therefore usually shifted by changes in pH.

Part I of Chapter 3 concerned the use of homogeneous mediators in a biosensor. NADH oxidase from *Thermus aquaticus* YT-1 was chosen as the enzyme for study. This was because of both the analytical relevance of NADH (as described in Section 1.5.2) and because the oxidase from *T. aquaticus* had previously been shown to possess useful qualities for biosensor construction, including thermostability and a wide pH range (McNeil *et al.*, 1989). Also, although it had previously been shown that electron transfer could be mediated from the enzyme (McNeil *et al.*, 1989), mediated coupling with a dehydrogenase had not been illustrated for this, or any other NADH oxidase. Nine metal complexes were examined for coupling with the enzyme. All were chosen as possessing low enough oxidation potentials (<+200 mV) to keep the direct NADH oxidation current to a negligible value. Mediation with the enzyme was achieved from

two compounds containing the Ru(III/IV) redox couple, $RuCl_6^{2-/3-}$ and ruthenium red/brown. This was the first reported use of either compound with an enzyme. When tested, $RuCl_6^{2-}$ failed to couple with glucose oxidase. This suggests another useful aspect of NADH oxidase; namely that the lability of its prosthetic group (as illustrated in Section 3.3.2) enables coupling with a wider range of compounds.

NADH oxidase was coupled with alcohol dehydrogenase for an enzyme amplified NADH response, detected at +150 mV through the use of $RuCl_6^{2-}$. Also described, was an immobilised enzyme bilayer responsive to ethanol at 0 mV, through the use of ruthenium red. Although both these mediators enabled a reduction in interference (as seen in Table 3.3), experiments suggested that the second order rate constant for the mediated reactions was not high enough to fully remove the oxygen dependency of the sensor response (Section 3.3.5). A possible improvement to this could be to immobilise the sensor components behind a suitable membrane, as discussed in Section 3.3.7, hence providing a barrier to oxygen diffusion. However, the detection system used here was a relatively complex one (FAD, NAD^+, the mediator and two enzymes) and its full immobilisation proved to be beyond the scope of this thesis. Instead, the requirements for the immobilisation of a single mediator and enzyme were considered in Part II of the chapter, while the possibilities for immobilising NAD^+ were considered in Part III.

6.3 Mediator Immobilisation

As discussed in Chapter 3 Part I, mediator immobilisation is often a prerequisite for the use of interference-screening membranes. Additionally, immobilisation can provide a convenient way of generating high concentrations of mediator at the electrode surface.

With these considerations in mind, Part II of Chapter 3 concerned the development of a new mediator immobilisation matrix.

Ion-exchange by Nafion was chosen as the technique for study, as it provided a simple method of electrode modification, applicable to a wide range of electrocatalysts. In order to reduce the detrimental qualities of Nafion (slow rates of electron transport within the polymer and impermeability to anions), a composite of Nafion and poly(vinyl alcohol) (Nf/PVA) was formed. The structure of the composite was investigated by following the electrochemistry of anions at Nf/PVA-modified electrodes and by examining the diffusional characteristics of both organic and inorganic mediators within the composite films. The results indicated discrete regions of Nafion embedded within the more porous poly(vinyl alcohol). It appeared that for an organic mediator present mainly in the hydrophobic region of Nafion, the observed diffusion coefficient (D_{exp}) was increased within the composite, due to electron exchange with mediator diffusing through the more hydrophilic poly(vinyl alcohol) region of the film. Quantitative evidence for this was provided by measurements of D_{exp}/L^2 for methyl viologen, while qualitative evidence for this was seen in cyclic voltammograms of phenazine methosulphate (PMS). For an inorganic mediator present in the hydrophilic phase of Nafion ($Ru(NH_3)_6^{3+}$), no change in D_{exp} was observed.

To illustrate an analytical application for the composite, the Nf/PVA solution was prepared at an acidic pH, enabling the entrapment of glucose oxidase by a combination of ion-exchange and cross-linking. D-glucose was calibrated across the range 0.5 - 3.5 mM. A kinetic analysis of the sensor response, indicated that the rate of the electrochemical processes within the film (ie. the enzyme/substrate and enzyme/mediator

reactions) were significantly slower than rate of substrate diffusion into the composite layer. Studies on sensor stability were not thought to be meaningful, owing to the light sensitivity of PMS. As discussed in Section 4.3.5, a hydrophobic metal complex would be the best choice of mediator for this system and therefore the next logical step for this work would be the synthesis and incorporation of a positively charged ferrocene.

In Section 4.3.4, albumin adsorption to the composite was examined by following the change in redox behavior of $Ru(CN)_6^{4-}$ at Nf/PVA-modified electrode. The results indicated superior resistance to adsorption compared to either cellulose acetate or poly(carbonate). When considering the possible causes of adsorption resistance, it should be noted that the negatively charged Nafion centers in the composite would to some extent have repelled the negatively charged protein. However, it should be remembered that the less resistant cellulose acetate membrane would also have exhibited an overall negative charge (from the presence of residual carboxyl groups; Wilson & Thevenot, 1990) and therefore the adsorption resistance of the composite was probably not due to electrostatic repulsion alone, but was likely to have been aided by the hydrogel nature of the film.

It has been shown previously, both that many hydrogels exhibit resistance to protein adsorption and that when proteins do adsorb they are often bound far less tightly (Horbett, 1986). As described in Section 4.3.4, this is thought to be due to their similarity to natural tissue. The next step for this work would therefore be to examine the effect of blood or plasma on the Nf/PVA films. Obviously such protein mixtures would present far more demanding sample matrices than albumin alone and it should be borne in mind that some hydrogels have occasionally been shown to increase the

adsorption of a particular protein (eg. albumin on NVP; Boffa *et al.*, 1977). Also, the reduction in the adsorption of some proteins can sometimes lead to the increased adsorption of others, that do not usually compete as successfully.

One possible method of improving the general adsorption resistance of a hydrogel, is to increase the chain mobility of the polymer, as it has previously been shown that increased mobility reduces the likelihood of the multipoint attachment thought to be necessary for protein adsorption (Horbett, 1986). This could perhaps be achieved for the Nf/PVA films by increasing the incubation time following gelation, since the results of Zhujun *et al* (1989) suggest the films used in this thesis were not fully swollen. Also, the glutaraldehyde concentration could perhaps be lowered to produce less cross-linking. In this case the advantage of increased chain mobility would have to be weighed against the effect of lower mechanical strength.

Another method of improving PVA biocompatability, is that of heparinization. Heparin has previously been irreversibly immobilised on PVA by reaction with glutaraldehyde (Sefton *et al.*, 1984). Binding is predominantly through the terminal serine group of the molecule and its attachment at only one end is thought to be responsible for heparin retaining its native conformation and biological activity (Cholakis & Sefton, 1983). Heparin-PVA gels have been shown to posses increased thromboresistance relative to un-modified PVA, due to the formation of a surface bound inactive thrombin-antithrombin III complex (Sefton *et al.*, 1984). Hence, heparinization of the Nf/PVA gels could perhaps provide a further improvement to their biocompatability.

6.4 Mediatorless Electrocatalysis

The final part of Chapter 3 considered a possible alternative to catalysis by an electron-transfer mediator. As seen in Parts I and II of Chapter 3, the use of a mediator often requires its immobilisation at the electrode surface. In the case of water-soluble mediators this can often prove problematic, with some consideration required as to how efficient charge transport may be maintained (Part II). Additionally, for applications such as *in-vivo* analysis, the issue of mediator leakage can be critical. In such cases, a better alternative is perhaps a form of electrode treatment which enables surface catalysis to occur without needing a mobile, mediating species. In Part III of Chapter 3, such catalytic activity was described for a film of poly(indole-5-carboxylic acid) (PICA) electrodeposited onto glassy carbon. The overpotential for the oxidation of both ascorbate and NADH was lowered; with the amount of electrode passivation during NADH oxidation also being reduced.

This form of catalysis at a conducting polymer-modified electrode has been described once before, using poly(3-methylthiophene) for the oxidation of NADH (Atta *et al.*, 1990) and acetaminophen (Wang & Li, 1989). The possible mechanism for such catalysis has not so far been examined, although as described in Section 5.3.3, it can perhaps be seen as analogous to transition metal modifications of electrodes, such as platinization to improve hydrogen peroxide oxidation (Kao & Kuwana, 1984).

Transition metals are thought to be electrocatalytic because of their ability to facilitate chemisorption, due to the possession of un-paired d-electrons (Moore, 1983). Additionally, in the case of platinized carbon, a synergistic effect is thought to exist due to electron donation from platinum to carbon and it has been argued that this also

affects the observed electrocatalytic activity (Jalan, 1979). Techniques such as ESR and photoelectron spectroscopy could perhaps be used to see whether similar interactions exist between PICA and glassy carbon. The extent of platinum dispersion on carbon electrodes has also been shown to have an effect on catalytic activity (Mukerjee, 1990) and hence the morphology of PICA films is also likely to be important.

Voltammograms recorded at PICA-modified electrodes, indicated greater non-faradaic currents due to the added capacitive component provided by the polymer (as described in Section 5.3.2). This effect could perhaps be somewhat counteracted by the use of micro-electrodes (which would reduce the double-layer charging current).

As seen in Section 5.3.4, the oxidation of ascorbate would provide interference to an NADH response and therefore the immobilisation of NAD^+ was attempted as a precursor to screening ascorbate by charge repulsion. A Nafion/poly(carbonate) membrane was used, as well as the entrapment of ADH and NAD^+ within poly(pyrrole), but neither method gave successful long-term retention. However, during the writing of this thesis a patent application (Goto, 1992) described the immobilisation of NAD^+ behind poly(vinyl chloride). If suitable to long-term retention, this method could perhaps provide the means for adapting PICA films to the construction of dehydrogenase-based biosensors capable of functioning without the addition of external reagents.

7.0 References

Adams, R.N. (1969). Electrochemistry of Solid Electrodes. New York, Marcel Dekker, p 220.

Aizawa, M., Morioka, A., Suzuki, S. & Nagamura, Y. (1979). Enzyme immunosensor, III. Amperometric determination of human chorionic gonadotropin by membrane bound antibody. *Anal. Biochem.* **94**: 22-28.

Albery, W.J. & Bartlett, P.N. (1985). Amperometric enzyme electrodes, Part I. Theory. *J. Electroanal. Chem.* **194**: 211-222.

Albery, W.J., Bartlett, P.N. & Cass, A.E.G. (1987). Amperometric enzyme electrodes. *Phil. Trans. R. Soc. Lond.* . **B 316**: 107-119.

Aleksandrovskii, Y.A., Bezhikina, L.V. & Rodionov, Y.V. (1981). Comparative-study of reactions catalysed by glucose-oxidase in the presence of different electron-acceptors. *Biochem.-USSR.* **46**: 593-599.

Aleyamma, A.J. & Sharma, C.P. (1991). *Poly(vinyl alcohol) as a biomaterial.* C. P. Sharma and M. Szycher. Blood Compatable Materials and Devices. Pennsylvania, USA, Technomic Pub. Comp. Inc. pp 123-130.

Andrieux, C.P. & Saveant, J.M. (1980). Electron transfer through redox polymer films. *J. Electroanal. Chem.* **111**: 377-381.

Anson, F.C., Christie, J.H. & Osteryoung, R.A. (1967). A study of the adsorption of cadmium(II) on mercury from thiocyanate solutions by double potential step chronocoulometry. *J. Electroanal. Chem.* **13**: 343-345.

Atta, N.F., Galal, A., Karagozler, A.E., Zimmer, H., Rubinson, J.F. & Jr., H.B.M. (1990). Voltammetric studies of the oxidation of reduced nicotinamide adenine dinucleotide at a conducting polymer electrode. *J. Chem. Soc., Chem. Commun.* : 1347-1349.

Baldwin, R.P., Christensen, J.K. & Kryger, L. (1986). Voltammetric determination of traces of nickel (II) at a chemically modified electrode based on dimethylglyoxime-containing carbon paste. *Anal. Chem.* **58**: 1790-1798.

Balistreri, W.F. & Shaw, L.M. (1987). *Liver Function.* N. W. Tietz. Fundamentals of Clinical Chemistry. Philadelphia, W.B. Saunders Co. pp 729-758.

Bartlett, P.N., Tebbutt, P. & Whitaker, R.G. (1991). Kinetic aspects of the use of modified electrodes in bioelectrochemistry. *Prog. Reaction Kinetics.* **16**: 55-155.

Beck, F., Braun, P. & Schloten, F. (1989). Anodic release of anions from polypyrrole. *J. Electroanal. Chem.* **267**: 141-148.

Beer, P.D. (1989a). Redox responsive macrocyclic recceptor molecules containing transition metal redox centres. *Chem. Soc. Rev.* **18**: 409-450.

Beer, P.D., Blackburn, C., McAleer, J.F. & Sikanyika, H. (1990a). Redox-responsive crown ethers containing a conjugated link between the ferrocene moiety and a benzo crown ether. *Inorg. Chem.* **29**: 378-381.

Beer, P.D., Sikanyika, H., Blackburn, C. & McAleer, J.F. (1989b). Selective electrochemical recognition of the potassium guest cation in the presence of sodium and magnesium ions by a new ferrocenyl ionophore. *J. Chem. Soc., Chem. Commun.* : 1831-1833.

Beer, P.D., Kocian, O., Mortimer, R.J. (1990b). Novel mono-and di-ferrocenyl bipyridyl ligands: Syntheses, electrochemistry and electropolymerisation studies of their ruthenium complexes. *J. Chem. Soc. Dalton Trans.*: 3283-3288.

Bertine, K.K. & Goldberg, E.D. (1971). Fossil fuel combustion and the major sedimentary cycle. *Science*. **178**: 233-235.

Blanke, R.V. & Deker, W.J. (1987). *Analysis of Toxic Substances*. N. W. Tietz. Fundamentals of Clinical Chemistry. Philadelphia, W.B. Saunders Co. pp 869-902.

Boffa, G.A., Lucien, N., Faure, A., Boffa, M.C., Jozefonviz, J., Szubarga, A. & Larrieu, M. (1977). Polytetrafluoroethylene-N-vinylpyrrolidone graft copolymers: affinity with plasma proteins. *J. Biomed. Mater. Res.* **11**: 317-.

Bourdillon, C., Bourgeois, J.P. & Thomas, J.P. (1980). Covalent linkage of glucose oxidase on modified glassy carbon electrodes. Kinetic phenomena. *J. Am. Chem. Soc.* **102**: 4231-4235.

Bremle, G., Persson, B. & Gorton, L. (1991). An amperometric glucose electrode based on carbon paste, chemically modified with glucose dehydrogenase, nicotinamide adenine dinucleotide, and a phenoxine mediator, coated with a poly(ester sulphonic acid) cation exchanger. *Electroanalysis*. **3**: 77-86.

Brooks, S.L., Higgins, I.J., Newman, J.D. & Turner, A.P.F. (1991). Biosensors for process control. *Enzyme Microb. Technol.* **13**: 946-955.

Butler, J.A.V. (1924). Studies in heterogeneous equilibria. Part III. A kinetic theory of reversible oxidation potentials at inert electrodes. *Trans. Faraday Soc.* **19**: 734-739.

Buttry, D.A. & Anson, F.C. (1983). Effects of electron exchange and single-file diffusion on charge propagation in Nafion films containing redox couples. *J. Am. Chem. Soc.* **105**: 685-689.

Caraway, W.T. & Watts, N.B. (1987). *Carbohydrates*. N. W. Tietz. Fundamentals of Clinical Chemistry. Philadelphia, W.B. Saunders Co. pp 422-445.

Cardosi, M.F., Stanley, C.J., Cox, R.B. & Turner, A.P.F. (1988). Amperometric enzyme-amplified immunoassays. *J. Immunol. Meth.* **112**: 153-161.

Carlson, B.W. & Miller, L.L. (1985). Mechanism of the oxidation of NADH by quinones - energetics of one-electron and hydride routes. *J. Am. Chem. Soc.* **107**: 479-485.

Cass, A.E.G. (1990). Biosensors, A Practical Approach. Oxford. Oxford University Press.

Cass, A.E.G., Francis, D.G., Hill, H.A.O., Aston, W.J., Higgins, I.J., Plotkin, E.V., Scott, L.D.L. & Turner, A.P.F. (1984). Ferrocene-mediated enzyme electrode for amperometric determination of glucose. *Anal. Chem.* **56**: 667-671.

Cenas, N., Rozgaite, J., Pocius, A. & Kulys, J. (1983). Electrocatalytic oxidation of NADH and ascorbic-acid on electrochemically pretreated glassy-carbon electrodes. *J. Electroanal. Chem.* **154**: 121-128.

Cha, S.K., Kasem, K.K. & Abruna, H.D. (1991). Effects of competitive binding on the amperometric determination of copper with electrodes modified with chromotrope 2B. *Talanta.* **38**: 89-93.

Cheek, G.T. & Nelson, R.F. (1978). Applications of chemically modified electrodes to analysis of metal ions. *Anal. Lett.* **A11**: 393-402.

Cholakis, C.H. & Sefton, M.V. (1983). Chemical characterization of an immobilized heparin: heparin-PVA. *Abs. Am. Chem. Soc.* **185**: 140.

Ciolkosz, M.K. & Jordan, J. (1993). Comparison of spectrophotometric rate parameters of enzymatic reactions. *Anal. Chem.* **65**: 164-168.

Clark, L.C. Jr. & Lyons, C. (1962). Electrode systems for continuous monitoring in cardiovascular surgery. *Ann. NY Acad. Sci.* **102**: 29-45.

Cocco, D., Rinaldi, A., Savini, I., Cooper, J.M. & Bannister, J.V. (1988). NADH oxidase from the extreme thermophile *thermus aquaticus* YT-1. *Eur. J. Biochem.* **174**: 267-271.

Coleman, J.E. & Vallee, B.L. (1961). Metallocarboxypeptidases: Stability constants and enzymatic characteristic. *J. Biol. Chem.* **236**: 2244-2249.

Compagnone, D., Bannister, J.V. & Federici, G. (1992). Electrochemical sensors for the determination of metal ions. *Sens. Actuators B.* **7**: 549-552.

Compagnone, D., Bannister, J.V., Federici, G. & McNeil, C.J. (1991). Electrochemical determination of iron with desferrioxamine B. *Clin. Chem. Enzym. Comms.* **4**: 167-172.

Cotton, F.A. & Wilkinson, G. (1980). Advanced Inorganic Chemistry. New York, John Wiley & Sons. pp 917-919.

Cottrell, F.G. (1902). Der reststrom bei galvanischer polarisation, betrachtet als ein diffusionsproblem. *Z. Physik. Chem.* **42**: 385-430.

Coury, L.A., Oliver, B.N., Egekeze, J.O., Sosnoff, C.S., Brumfield, J.C., Buck, R.P. & Murray, R.W. (1990). Mediated anaerobic voltammetry of sulphite oxidase. *Anal. Chem.* **62**: 452-458.

Cox, J.A. & Majda, M. (1980). Modification of a platinum electrode surface by irreversible adsorption of adenosine-5'-monophosphate and metallation by iron. *Anal. Chem.* . **52**: 861-864.

Crumbliss, A.L., Hill, H.A.O. & Page, D.J. (1986). The electrochemistry of hexacyanoruthenate at carbon elecrodes and the use of ruthenium compounds as mediators in the glucose oxidase system. *J. Electroanal. Chem.* **206**: 327-331.

Crumbliss, A.L., Perine, S.C., Edwards, A.K. & Rillema, D.P. (1992). Characterization of carrageenan hydrogel electrode coatings with immobilized cationic metal complex redox couples. *J. Phys. Chem.* **96**: 1388-1394.

Dahms, H. (1968). Electronic conduction in aqueous solution. *J. Phys. Chem.* **72**: 362-364.

Dall'Olio, A., Dascola, G., Varacca, V. & Bocchi, V. (1968). Résonance paramagnétique électronique et conductivité d'un noir d'oxypyrrol électrolytique. *C.R. Acad. Sc. Paris.* **C 267**: 433-435.

Daniel, R.M., Cowan, D.A., Morgan, H.W. & Curran, M.P. (1982). A correlation between protein thermostability and resistance to proteolysis. *Biochem. J.* **207**: 641-644.

Dean, J.G., Bosqui, F.L. & Lanouette, V.H. (1972). Removing heavy metals from waste water. *Environ. Sci. Technol.* **6**: 518-522.

Diaz, A. (1981). Electrochemical preparation and characterisation of conducting polymers. *Chemica Scripta.* **17**: 145-148.

Dong, S. & Kuwana, T. (1984). Activation of glassy-carbon electrodes by dispersed metal-oxide particles. 1. Ascorbic acid oxidation. *J. Electrochem. Soc.* **131**: 813-819.

Dong, S.J., Sun, Z.S. & Lu, Z.L. (1988). Chloride chemical sensor based on an organic conducting polypyrrole polymer. *Analyst.* **113**: 1525-1528.

Dong, S. & Wang, Y. (1989). The application of chemically modified electrodes in analytical chemistry. *Electroanalysis.* **1**: 99-106.

Elvehjem, C.A. & Sherman, W.C. (1932). The action of copper in iron metabolism. *J. Biol. Chem.* **98**: 309-319.

Elving, P.J., Bresnahan, W.T., Moiroux, J. & Samec, Z. (1982). NAD/NADH as a model redox system : mechanism, mediation, modification by the environment. *Bioelectrochem. Bioenerg.* **9**: 365-378.

Erdey-Gruz, T & Volmer, M. (1930). Zur theorie der wasserstoffüberspannung. *Z. Physik. Chem.* **150A**: 203-213.

Forstner, U. & Wittmann, G.T.W. (Eds.). (1979). Metal Pollution in the Aquatic Environment. Berlin, Heidelberg, New York, Springer-Verlag.

Flores, A., Leon, L.E. & Clavo, A. (1987). Cyclic voltammetric studies of the R-nitroso salt. Application to the indirect determination of iron(II). *Anal. Lett.* **19**: 1913-1919.

Forster, R.J. & Vos, J.G. (1992). *Theory and analytical applications of modified electrodes*. Smyth, M.R. & Vos, J.G. Analytical Voltammetry. New York. Elsevier Science Publishing Co. Inc. pp 465-529.

Foulds, N.C. & Lowe, C.R. (1986). Enzyme entrapment in electrically conducting polymers. *J. Chem. Soc. Faraday Trans. 1.* **82**: 1259-1264.

Frew, J.E., Harmer, M.A., Hill, H.A.O. & Libor, S.I. (1986). A method for estimation of H_2O_2 based on mediated electron-transfer reactions of peroxidases at electrodes. *J. Electroanal. Chem.* **201**: 1-10.

Galvani, L. (1791). De Viribus Electricitatis in Motu Musculari Commentarius. Bologna.

Gaudiello, J.G., Ghosh, P.K. & Bard, A.J. (1985). Polymer films on electrodes. 17. The application of simultaneous electrochemical and electron spin resonance techniques for the study of two viologen-based chemically modified electrodes. *J. Am. Chem. Soc.* **107**: 3027-3032.

Gorton, L. (1986). Chemically modified electrodes for the electrocatalytic oxidation of nicotinamide coenzymes. *J. Chem. Soc., Farady Trans., 1.* **82**: 1245-1258.

Goto, M. (1992) Ethanol biosensor. *Jap. Pat.* 04,370756 [92,370,756] (Cl. G01N27/327).

Greef, R., Peat, R., Peter, L.M., Pletcher, D. & Robinson, J. (1993). Instrumental Methods in Electrochemistry. London, Ellis Horwood Ltd.

Green, M.J. & Hill, H.A.O. (1986). Amperometric enzyme electrodes. *J. Chem. Soc. Faraday Trans.* **182**: 1237-1243.

Guilbault, G.G. & Montalvo J.G. Jr. (1969). A urea-specific enzyme electrode. *J. Am. Chem. Soc.* **91**: 2164-2165.

Hajizadeh, K., Tang, H.T., Halsall, H.B. & Heineman, W.R. (1991). Chemical cross-linking of a redox mediator thionin for electrocatalytic oxidation of reduced nicotinamide adenine dinucleotide. *Anal. Lett.* **24**: 1453-1469.

Hartley, F.R., Burgess, C. & Alcock, R.M. (1980). Solution Equilibria. West Sussex, Ellis Horwood Ltd., England. pp 44-51.

Heyrovsky, J. (1960). Trends in polarography. Nobel laureate lecture. *Science*. **132**: 123-130.

Higuchi, A. & Iijima, T. (1985). DSC investigation of the states of water in poly(vinyl alcohol) membranes. *Polymer*. **26**: 1207-1211.

Hill, H.A.O. & Sanghera, G.S. (1990). *Mediated amperometric enzyme electrodes*. A. E. G. Cass. Biosensors, A Practical Approach. Oxford, Oxford University Press. pp 19-46.

Horbett, T.A. (1986). *Protein adsorption to hydrogels*. N. A. Peppas. Hydrogels in Medicine and Pharmacy, Fundamentals. Boca Raton, FL, CRC Press. Section. pp 127-171.

Hoskins, D.D., Whiteley, H.R. & Mackler, B. (1962). The reduced diphosphopyridine nucleotide oxidase of *Streptococcus faecalis*: purification and properties. *J. Biol. Chem.* **237**: 1647-2651.

Hoyer, B. & Florence, T.M. (1987). Application of polymer-coated glassy carbon electrodes to the direct determination of trace metals in body fluids by anodic stripping voltammetry. *Anal. Chem.* **59**: 2839-2842.

Hurrell, H.C. & Abruna, H.D. (1988). Polymer-modified microelectrodes for metal ion determination and the development of a calcium amperometric probe based on surface-immobilised Antipyrylazo III. *Anal. Chem.* **60**: 254-258.

Ikada, Y., Iwata, H., Horii, F., Matsunaga, T., Taniguchi, M., Suzuki, M., Taki, W., Yamagata, S., Yonekawa, Y. & Handa, H. (1981). Blood compatibility of hydrophilic polymers. *J. Biomed. Mat. Res.* **15**: 697-718.

Imisides, M.D., John, R., Riley, P.J. & Wallace, G.G. (1991). The use of electropolymerization to produce new sensing surfaces: A review emphasizing electrodeposition of heteroaromatic compounds. *Electroanalysis*. **3**: 879-889.

Iwakura, C., Kajiya, Y. & Yoneyama, H. (1988). Simultaneous immobilization of glucose oxidase and a mediator in conducting polymer films. *J. Chem. Soc. Chem. Commun.* : 1019-1020.

Jacob, R.A. (1987). *Trace Elements*. N. W. Tietz. Fundamentals of Clinical Chemistry. Philadelphia, W.B. Saunders Co. pp 517-532.

Jaegfeldt, H. (1980). Adsorption and electrochemical oxidation behaviour of NADH at a clean platinum electrode. *J. Electroanal. Chem.* **110**: 295-302.

Jaegfeldt, H., Kuwana, T & Johansson G. (1983). Electrochemical stability of catechols with a pyrine side chain strongly adsorbed on graphite electrodes for catalytic-oxidation of dihydronicotinamide adenine-dinucleotide. *J. Am. Chem. Soc.* **105**: 1805-1814.

Jaffari, S. (1993). Cranfield University. Personal Communication.

Jalan, V.M. (1979). *Microstructure of highly dispersed Pt catalyst and its interaction with carbon supports*. Workshop on Oxygen Electrochemistry. Quail Hollow, Painesville, Ohio.

Janda, P. & Weber, J. (1991). Quinone-mediated glucose-oxidase electrode with the enzyme immobilised in polypyrrole. *J. Electroanal. Chem.* **300**: 119-127.

Johnson, K.W. (1991). Reproducible electrodeposition of biomolecules for the fabrication of miniature electroenzymatic biosensors. *Sensors and Actuators B.* **5**: 85-89.

Kalcher, K. (1985). Voltammetric determination of trace amounts of gold with a chemically modified carbon paste electrode. *Anal. Chim. Acta.* **177**: 175-182.

Kalcher, K. (1987). Extraktive anreicherung von gold an mit phosphororganischen verbindungen modifizierten kohlepasteelektroden. *Fresenius Z Anal. Chem.* **327**: 513-517.

Kao, W.-H. & Kuwana, T. (1984). Electrocatalysis by electrodeposited spherical Pt microparticles dispersed in a polymeric film electrode. *J. Am. Chem. Soc.* **106**: 473-476.

Karube, I., Mitsuda, S. & Suzuki, S. (1979). Glucose sensor using immobilised whole cells of *Pseudomas fluorescens*. *Eur. J. Appl. Microbiol. Biotechnol.* **7**: 343-350.

Khan, G.F., Kobatake, E., Shinohara, H., Ikariyama, Y. & Aizawa, M. (1992). Molecular interface for an activity controlled enzyme electrode and it's application for the determination of fructose. *Anal. Chem.* **64**: 1254-1258.

Khan, S.U.M. & Bockris, J.O'M. (1986). *Fundamental Aspects of Electron Transfer at Interfaces*. F. Gutmann and H. Keyzer. Modern Bioelectrochemistry. New York, Plenum Press. pp 1-43.

Kirchgessner, M., Schwarz, F.J. & Schnegg, A. (1982). *Interactions of essential metals in human physiology*. A. S. Prasad. Clinical, Biochemical and Nutritional Aspects of Trace Elements. New York, Alan R. Liss, Inc. pp 477-512.

Kirstein, D., Scheller, F., Olsson, B. & Johansson, G. (1985). Enzyme electrode for urea with amperometric indication - Electrode with diffusional limitation. *Anal. Chim. Acta.* **171**: 345-350.

Kulys, J. & D'Costa, E.J. (1991). Printed electrochemical sensor for ascorbic acid determination. *Anal. Chim. Acta.* **243**: 173-178.

Kulys, J.J. (1986). Enzyme electrodes based on organic metals. *Biosensors.* **2**: 1-13.

Kuriyama, S. & Rechnitz, G. (1981). Plant tissue-based biocatalytic membrane electrode for glutamate. *Anal. Chim. Acta.* **131**: 91-96.

Lafis, S. (1992). Rapid Microbial Detection. *PhD Thesis*. Cranfield Institute of Technology.

Lane, R.F. & Hubbard, A.T. (1973). Electrochemistry of chemisorbed molecules. I. Reactants connected to electrodes through olefinic substituents. *J. Phys. Chem.* **77**: 1401-1410.

Lehninger, A.L. (1975). Biochemistry. New York, Worth Publishers. p 479.

Levi, M.D., Alpatova, N.M., Ovsyannikova, E.V. & Vorotyntsev, M.A. (1993). Mechanism of cathodic reactions at electron-conducting polymer films: electroreduction of chloranil and tetracyanoquinodimethane at a poly-3-methylthiophene-coated glassy carbon electrode. *J. Electroanal. Chem.* **351**: 271-284.

Lubert, K.-H., Schnurrbusch, M. & Thomas, A. (1982). Preconcentration and determination of uranyl ions on electrodes modified by tri-n-octylphosphine oxide. *Anal. Chim. Acta.* **144**: 123-136.

Majda, M. & Faulkner, L.R. (1982). A luminescence probe for measurements of electron-exchange rates in polymer-films on electrodes. *J. Electroanal. Chem.* **137**: 149-156.

Martin, C.R. & Dollard, K.A. (1983). Effect of hydrophobic interactions om the rates of ionic diffusion in Nafion films at electrode surfaces. *J. Electroanal. Chem.* **159**: 127-135.

Massey, V., Palmer, G., Williams, C.H., Swoboda, B.E.P. & Sands, R.H. (1966). E. C. Slater. Flavins and Flavoproteins. Amsterdam, Elsevier. p 133.

Matsue, T., Kasai, N., Narumi, M., Nishizawa, M., Yamada, H. & Uchida, I. (1991). Electron-transfer from NADH dehydrogenase to polypyrrole and its applicability to electrochemical oxidation of NADH. *J. Electroanal. Chem.* **300**: 111-118.

Matsue, T., Suda, M., Uchida, I., Kato, T., Akiba, U. & Osa, T. (1987). Electocatalytic oxidation of NADH by ferrocene derivatives and the influence of cyclodextrin complexation. *J. Electroanal. Chem.* **234**: 163-173.

McCracken, L.L., Wier, L.M. & Abruna, H.D. (1987). Determination of Ni with electrodes modified with mordant violet 5. *Anal. Lett.* **20**: 1521-1539.

McNeil, C.J. & Athey, D. (1992). *Amplified enzyme immunoassay using thermophilic β-NADH oxidase*. Biosensors '92. The Second World Congress on Biosensors. Geneva, Switzerland. Elsevier Advanced Technology. p 384.

McNeil, C.J., Spoors, J.A., Cocco, D., Cooper, J.M. & Bannister, J.V. (1989). Thermostable reduced nicotinamide adenine dinucleotide oxidase: application to amperometric enzyme assay. *Anal. Chem.* **61**: 25-29.

Mertz, W. (1979). The newer trace elements. *Biol. Trace Elem. Res.* **1**: 259-270.

Meyer, T.J. & Taube, H. (1968). Electron-transfer reactions of ruthenium ammines. *Inorg. Chem.* **7**: 2369-2379.

Michal, G. (1978). H. U. Bergmeyer. Principles of Enzymatic Analysis. New York, Verlag Chemie. pp 29-34.

Miller, S.R., Gustowski, D.A., Chen, Z.-H., Gokel, G.W., Echegoyen, L. & Kaifer, A.E. (1988). Rationalization of the unusual electrochemical behaviour observed in lariat ethers and other reducible macrocyclic systems. *Anal. Chem.* **60**: 2021-2024.

Miyawaki, O. & Wingard L.B. Jr. (1985). Electrochemical and glucose oxidase coenzyme activity of flavin adenine dinucleotide covalently attached to glassy carbon at the adenine amino group. *Biochim. Biophys. Acta.* **838**: 60-68.

Mizutani, F., Yabuki, S. & Katsura, T. (1991). Amperometric enzyme electrode based on dehydrogenase and NADH oxidase. *Anal. Sci.* **7**: 871-874.

Moore, W.J. (1983). Basic Physical Chemistry. New Jersey, Prentice Hall International, Inc. pp 318-319.

Moran, K.D. & Majda, M. (1986). Electrode films of porous agarose impregnated with Nafion. Structural heterogeneity and its effects on electron transport. *J. Electroanal. Chem.* **207**: 73-86.

Morris, N.A., Cardosi, M.F., Birch, B.J. & Turner, A.P.F. (1992). An electrochemical capillary fill device for the analysis of glucose incorporating glucose oxidase and ruthenium(III) hexamine as mediator. *Electroanalysis.* **4**: 1-9.

Moses, P.R., Wier, L. & Murray, R.W. (1975). Chemically modified tin oxide electrode. *Anal. Chem.* **47**: 1882-1886.

Mukerjee, S. (1990). Particle size and structural effects in platinum electrocatalysis. *J. App. Electrochem.* **20**: 537-548.

Murray, R.W. (1992). Molecular Design of Electrode Surfaces. Techniques of Chemistry. New York, John Wiley & Sons, Inc.

National Diabetes Data Group. (1979). Classification and diagnosis of diabetes mellitus and other categories of glucose intolerance. *Diabetes*. **28**: 1039-1057.

Nicholls, D. (1974). Complexes and First-Row Transition Elements. London, MacMillan Education Ltd. pp 48-72.

Nicholson, R.S. & Shain, I. (1964). Theory of stationary electrode polarography. Single scan and cyclic methods applied to reversible, irreversible and kinetic systems. *Anal. Chem.* **36**: 706-723.

Oyama, N., Shimomura, T., Shigehara, K. & Anson, F.C. (1980). Electrochemical responses of multiply-charged transition metal complexes bound electrostatically to graphite electrode surfaces coated with polyelectrolytes. *J. Electroanal. Chem.* **112**: 271-280.

Park, H.-J., Reiser, C.O.A., Kondruweit, S., Erdmann, H., Schmid, R.D. & Sprinzl, M. (1992). Purification and characterisation of a NADH oxidase from the thermophile *Thermus thermophilus* HB8. *Eur. J. Biochem.* **205**: 881-885.

Penner, R.M. & Martin, C.R. (1985). Ion transporting composite membranes 1. Nafion-impregnated Gore-Tex. *J. Electrochem. Soc.* **132**: 514-515.

Peterson, R.E & Bollier, M.E. (1955). Spectrophotometric determination of serum copper with biscyclohexanoneoxaldihydrazone. *Anal. Chem.* **27**: 1195-1197.

Picon, A.R., Alonso, R.G., Leon, L.E. & Calvo, A. (1987). Indirect voltammetric determination of iron. *Anal. Lett.* **19**: 65-75.

Prabhu, S.V., Baldwin, R.P. & Kryger, L. (1987). Chemical preconcentration and determination of copper at a chemically modified carbon-paste electrode containing 2,9-dimethyl-1,10-phenanthroline. *Anal. Chem.* **59**: 1074-1078.

Ramaraj, R. & Kaneko, M. (1993). In situ spectrocyclic voltammetric studies on Ru-red and Ru-brown complexes for water oxidation catalyst in homogeneous aqueous solution and in heterogeneous Nafion membrane. *J. Mol. Cat.* **81**: 319-332.

Ramaraj, R., Kira, A. & Kaneko, M. (1987). Oxygen evolution by water oxidation with polynuclear ruthenium complexes. *J. Chem. Soc., Faraday Trans. 1.* **83**: 1537-1551.

Randles, J.E.B. (1948). A cathode ray polarograph. Part II - The current-voltage curves. *Trans. Faraday Soc.* **44**: 327-338.

Ratner, B.D. & Hoffman, A.S. (1976). J. D. Andrade. Hydrogels for Medical and Related Applications. Washington DC, American Chemical Society. p 1.

Renneberg, R., Schubert, F. & Scheller, F. (1986). Coupled enzyme reactions for novel biosensors. *Trends Biochem. Sci.* **11**: 216-220.

Rubinstein, I & Bard, A.J. (1980). Polymer films on electrodes. 4. Nafion-coated electrodes and electrogenerated chemiluminescence of surface attached $Ru(bpy)_3^{2+}$. *J. Am. Chem. Soc.* **102**: 6641-6642.

Rubinstein, I. (1985). The influence of the polymer structure on electrochemical properties of uncharged molecules in Nafion films on electrodes. *J. Electroanal. Chem.* **188**: 227-244.

Ruff, I. (1970). Experimental evidence of electronic conduction in aqueous solutions. *Electrochim. Acta.* **15**: 1059-1061.

Ruff, I. & Friedrich, V.J. (1971). Transfer diffusion. I. Theoretical. *J. Phys. Chem.* **75**: 3297-3302.

Saeki, Y., Nozaki, M. & Matsumoto, K. (1985). Purification and properties of NADH oxidase from *Bacillus-magaterium. J. Biochem.* **98**: 1433-1440.

Saini, S., Hall, G.F, Downs, M.E.A. & Turner, A.P.F. (1991). Organic phase enzyme electrodes. *Anal. Chim. Acta.* **249**: 1-15.

Samec, Z. & Elving, P.J. (1983). Anodic-oxidation of dihydronicotinamide adenine dinucleotide at solid electrodes - mediation by surface species. *J. Electroanal. Chem.* **144**: 217-234.

Schlogl, K. & Falk, H. (1976). *Ferrocenes*. F. Korte. Methodicum Chimicum. New York, Academic Press. pp 470-498.

Schuhmann, W., Lammert, R., Hammerle, M. & Schmidt, H.-L. (1991). Electrocatalytic properties of polypyrrole in amperometric electrodes. *Biosens. Bioelectron.* **6**: 689-697.

Sefton, M.V., Ip, W.F., Rollason, G., Hatton, M.W.C. & Zingg, W. (1984). The thromboresistance of a heparin-polyvinyl alcohol hydrogel. *Chem. Eng. Commun.* **30**: 141-154.

Self, C.H. (1985). Enzyme amplification - a general method applied to provide an immunoassisted method for placental alkaline phosphatase. *J. Immunol. Methods.* **76**: 389-393.

Sevčik, A. (1958). Oscillographic polarography with periodical triangular voltage. *Coll. Czech. Chem. Commun.* **13**: 349-377.

Shinohara, H., Aizawa, M. & Shirakawa, H. (1986). Ion-sieving of electrosynthesized polypyrrole films. *J. Chem. Soc., Chem. Commun.* : 87-88.

Skoog, D.A. & West, D.M. (1982). Fundamentals of Analytical Chemistry. New York, CBS College Publishing. pp 478-503.

Skotheim, T.A. (1986). Handbook of Conducting Polymers (Vol. 1). New York, Marcel Dekker.

Stanley, C.J., Johannsson, A. & Self, C.H. (1985). Enzyme amplification can enhance both the speed and the sensitivity of immunoassays. *J. Immunol. Meth.* **83**: 89-95.

Sund, H. & Theorell, H. (1963). *Alcohol Dehydrogenases*. P. D. Boyer, H. Lardy and K. Myrback. The Enzymes. New York, Academic Press. Section. p 25.

Swoboda, B.E.P. & Massey, V. (1961). On the reaction of glucose oxidase from *Aspergillus niger* with bisulphite. *J. Biol. Chem.* **241**: 3409-3416.

Tafel, J. (1905). Über die polarisation bei kathodischer wasserstoffentwicklung. *Z. Physik. Chem.* **50**: 641-712.

Taniguchi, I., Miyamoto, S., Tomimura, S. & Hawkridge, F.M. (1988). Mediated electron-transfer of lactate oxidase and sarcosine oxidase with octacyanotungstate (IV) and octacyanomolybdate (IV). *J. Electroanal. Chem.* **240**: 333-339.

Tietz, N.W. (1987). Fundamentals of Clinical Chemistry. *Fundamentals of Clinical Chemistry.* Philadelphia. W.B. Saunders Co. p 954.

Tolbert, A.M. & Baldwin, R.P. (1989). Liquid-chromatography and electrochemical detection of alditols and acidic sugars at a cobalt phthalocyanine-containing chemically modified electrode. *Electroanalysis.* **1**: 389-395.

Torstensson, A. & Gorton, L. (1981). Catalytic oxidation of NADH by surface-modified graphite electrodes. *J. Electroanal. Chem.* **130**: 199-207.

Tse, D.C.-S. & Kuwana, T. (1978). Electrocatalysis of dihyronicotinamide adenosine diphosphate with quinones and modified quinone electrodes. *Anal. Chem.* **50**: 1315-1318.

Turner, A.P.F., Karube, I. & Wilson, G.S. (1987). *Biosensors, Fundamentals and Applications.* Oxford. Oxford University Press.

Updike, S.J. & Hicks, G.P. (1967). The enzyme electrode. *Nature*. **214**: 986-988.

Van der Linden, W.E. & Dieker, J.W. (1980). Glassy carbon as electrode material in electroanalytical chemistry. *Anal. Chim. Acta.* **119**: 1-24.

Vining, W.J. & Meyer, T.J. (1987). Direct evidence for chemically distinct regions within Nafion films on electrodes. *J. Electroanal. Chem.* **237**: 191-208.

Vydra, F., Stulik, K. & Julakova, E. (1976). Electrochemical Stripping Analysis. Sussex, England, Ellis Horwood Ltd.

Waltman, R.J., Diaz, A.F. & Bargon, J. (1984). Substituent effects in the electropolymerisation of aromatic heterocyclic compounds. *J. Phys. Chem.* **88**: 4343-4346.

Waltman, R.J. & Bargon, J. (1986). Electrically conducting polymers: a review of the electropolymerisation reaction, of the effects of chemical structure on polymer film properties, and of applications towards technology. *Can. J. Chem.* **64**: 76-95.

Wang, E. & Liu, A. (1991). Eastman-AQ/Ni(II) modified electrode characterisation and application in flow injection determination of carbohydrates and amino acids. *J. Electroanal. Chem.* **319**: 217-225.

Wang, J., Greene, B. & Morgan, C. (1984). Carbon paste electrodes modified with cation-exchange resin in differential pulse voltammetry. *Anal. Chim. Acta.* **158**: 15-22.

Wang, J. & Li, R.L. (1989). Highly stable voltammetric measurements of phenolic compounds at poly(3-methylthiophene)-coated glassy carbon electrodes. *Anal. Chem.* **61**: 2809-2811.

Wang, J & Gonzalez-Romero, E. (1993). Amperometric biosensing of alcohols at electrochemically pretreated glassy-carbon enzyme electrodes. *Electroanalysis.* **5**: 427-430.

Watkins, B.F., Behling, J.R., Kariv, E. & Miller, L.L. (1975). A chiral electrode. *J. Am. Chem. Soc.* **97**: 3549-3550.

Whipple, W., Hunter, J.V. & Yu, S.L. (1977). Effects of storm frequency on pollution from urban runoff. *J.W.P.C.F.* **49**: 2243-2248.

White, H.S., Leddy, J. & Bard, A.J. (1982). Polymer films on electrodes. 8. Investigation of charge-transport mechanisms in Nafion polymer modified electrodes. *J. Am. Chem. Soc.* **104**: 4811-4817.

Wilson, G.S. & Thevenot, D.R. (1990). *Unmediated amperometric enzyme electrodes.* Cass, A.E.G. Biosensors, A Practical Approach. Oxford. Oxford University Press. p 8.

Wood, J.M. (1974). Biological cycles for toxic elements in the environment. *Science.* **183**: 1049-1052.

Yabuki, S., Mizutani, F., Katsura, T. & Asai, M. (1991). Electrical control of the glutamate dehydrogenase reaction in polypyrrole membranes. *Bioelectrochem. Bioenerg.* **28**: 489-493.

Yabuki, S., Shinohara, H., Ikariyama, Y. & Aizawa, M. (1990). Electrical activity controlling system for a mediator-coexisting alcohol dehydrogenase-NAD conductive membrane. *J. Electroanal. Chem.* **277**: 179-187.

Yeager, H.L. & Steck, A. (1981). Cation and water diffusion in Nafion ion-exchange membranes - influence of polymer structure. *J. Electrochem. Soc.* **128**: 1880-1884.

Young, R.C., Keene, F.R. & Meyer, T.J. (1977). Measurement of rates of electron transfer between $Ru(bpy)_3^{3+}$ and $Fe(phen)_3^{2+}$ and between $Ru(phen)_3^{3+}$ and $Ru(bpy)_3^{2+}$ by differential excitation flash photolysis. *J. Am. Chem. Soc.* **99**: 2468-2473.

Zaborsky, O. (1973). Immobilized Enzymes. Cleveland, CRC Press. pp 54-56.

Zhujun, Z., Zhang, Y., Wangbai, M., Russell, R., Shakhsher, Z.M., Grant, C.L., Seitz, W.R. & Sundberg, D.C. (1989). Poly(vinyl alcohol) as a substrate for indicator immobilization for fiber-optic chemical sensors. *Anal. Chem.* **61**: 202-205.

8.0 Publications

Work from this thesis has been reported in the following papers:

Somasundrum, M. & Bannister, J.V. (1993). Amperometric determination of copper using screen-printed electrodes. *Sens. Actuators B.* **15**: 203-208.

Somasundrum, M. & Bannister, J.V. (1993). Mediatorless electrocatalysis at a conducting polymer-modified electrode: Application to ascorbate and NADH measurement. *J. Chem. Soc., Chem. Commun.* 1629-1631.

Somasundrum, M. & Bannister, J.V. (1994). Electrocatalysis in the presence of a Nafion/poly(vinyl alcohol) composite film. *J. Electroanal. Chem.* Submitted.

Somasundrum, M., Hall, J. & Bannister, J.V. (1994). Amperometric NADH determination via both direct and mediated electron transfer by NADH oxidase from *Thermus aquaticus* YT-1. *Anal. Chim. Acta.* Submitted.